The Role of the Lupus Autoantigen La in the Human MicroRNA Pathway

DISSERTATION

ZUR ERLANGUNG DES
DOKTORGRADES DER NATURWISSENSCHAFTEN (DR. RER. NAT.)
DER FAKULTÄT FÜR BIOLOGIE UND VORKLINISCHE MEDIZIN
DER UNIVERSITÄT REGENSBURG

Vorgelegt von
Daniele Hasler

aus
Rom (Italien)

Im Jahr 2018

Das Promotionsgesuch wurde eingereicht am: 01. März 2018

Die Arbeit wurde angeleitet von: Prof. Dr. Gunter Meister

Unterschrift:

“Mi manderete a scuola?” chiese Peter Pan.

“Sì”

“E poi in ufficio?”

“Credo di sì”

“E presto sarò un uomo?”

“Molto presto”

“Ma io non voglio andare a scuola e imparare cose serie…

non voglio diventare un uomo.

Oh,… pensa se un giorno dovessi svegliarmi e accorgermi di avere la barba!”

Peter Pan

Contents

Abstract

The Lupus autoantigen La is an RNA-binding protein that stabilizes RNA polymerase III (Pol III) transcripts and supports correct RNA folding. In addition, La was shown to affect the biogenesis of mammalian microRNAs (miRNAs).

In this study, we have analyzed the consequences of La depletion on the Argonaute (Ago)-bound small RNA (sRNA) population in human cells. We find that in the absence of La, distinct tRNA fragments are loaded into Ago proteins. Thus, La functions as gatekeeper ensuring correct tRNA maturation and thereby protects the cell from tRNA fragments, which might be potentially harmful by acting as unintended miRNAs.

We further provide evidences, that viral non-coding RNAs (ncRNAs) perturb La's gatekeeper function and induce the production of Ago-loaded tRNA fragments, mimicking the effects observed under La depletion.

Interestingly, one specific isoleucine precursor tRNA (pre-tRNA) produces both, a tRNA and a functional miRNA, even when La is present. We demonstrate that this specific pre-tRNA is able to partially escape from La binding due to its fully complementary 5' leader and 3' trailer sequences. The double-stranded RNA structure of this specific isoleucine pre-tRNA reduces the affinity to La and allows processing by components of the miRNA biogenesis machinery.

In sum, our study unraveled a novel aspect of La biology, showing that it supports correct pathway selection and, by that, maturation of primary Pol III transcripts. Furthermore, we characterized in molecular detail the biogenesis of a non-canonical, pre-tRNA-derived miRNA.

Zusammenfassung

Das Protein Lupus Autoantigen La bindet an das 3’ Ende von primären RNA Polymerase III (Pol III) Transkripten und schützt sie somit vor exonukleolytischem Abbau. Zudem fördert La die korrekte Faltung der gebundenen Transkripte. Des Weiteren wurde La als ein Faktor beschrieben, der die Biogenese einiger mikroRNAs (miRNAs) reguliert.

In dieser Arbeit wurde der Einfluss von La auf die Population von kurzen RNAs untersucht, die mit Argonaut (Ago) Proteinen interagiert. Daraus ergab sich, dass La die Entstehung von einigen kurzen tRNA Fragmenten verhindert. In Abwesenheit von La akkumulieren diese tRNA Fragmente in Ago Protein-Komplexen und könnten daher fälschlicherweise als miRNAs wirken, was mögliche negativen Konsequenzen birgt.

Zusätzlich liefert unsere Studie Hinweise dafür, dass diese Kontroll-Funktion von La durch virale, nicht-kodierende RNAs beeinträchtigt wird. Die Expression solch viraler RNAs führte zur Produktion von Ago-interagierenden tRNA Fragmenten. Somit ähnelte dieser Effekt den Auswirkungen einer La Depletion.

Interessanterweise kann aus einer bestimmten Isoleucin Vorläufer-tRNA (pre-tRNA) sogar in Anwesenheit von La eine tRNA oder auch eine funktionelle miRNA entstehen. Wir konnten zeigen, dass die strukturellen Besonderheiten dieser pre-tRNA eine effiziente Bindung durch La verhindern. Dies beruht darauf, dass die 5’ und 3’ Überhänge der Isoleucin pre-tRNA stark komplementär zueinander sind. Die dadurch entstehende doppelsträngige Struktur verursacht zwar eine verminderte Affinität zu La, ermöglicht jedoch gleichzeitig die Prozessierung durch Komponenten der miRNA Biogenese Maschinerie.

Zusammengefasst hat unsere Studie eine bis dahin unbekannte Funktion des Proteins La aufgeklärt. La besitzt eine wegweisende Rolle in der Reifung von primären Pol III Transkripten und verhindert dadurch, dass pre-tRNAs durch konkurrierende Prozesse fehlgeleitet werden, z.B. in den miRNA-Biogeneseweg. Zudem wurde der molekulare Mechanismus aufgeklärt, der dazu führt, dass eine nicht-kanonische miRNA aus einer pre-tRNA entstehen kann.

1. Introduction

1.1. TRNA Biology: Ancient But Still Attractive

The fundamental role of tRNAs in protein translation was unravelled very early in the history of molecular biology (Hoagland et al., 1958). By translating the code of nucleic acids into the code of proteins, tRNAs act as the Rosetta Stone of the cell, allowing genetic information to be expressed. In order to fulfil this central role, tRNA functionality needs to be guaranteed. Although the final mode of action of tRNAs within translation is conserved among all domains of life, it is striking how frequently convergent evolution resulted in different mechanisms to ensure that the requirement of functional tRNAs is satisfied. This aspect of tRNA biology, in particular, still leaves many open questions. Are some molecular mechanisms described in specific model organisms peculiar for them or are they shared as well by other species?

Not only do the details in tRNAs' life cycle remain partially elusive but also the plethora of RNA base modifications and the responsible enzymes are detected and characterized in only a few organisms (El Yacoubi et al., 2012). Furthermore, the extent of tRNA modification dynamics and the resulting regulatory potential have been addressed by a handful of studies, but still require broader investigations (Emilsson et al., 1992; Noon et al., 2003; Chan et al., 2010; Yi and Pan, 2011).

In addition to their well-known function in translation, tRNAs fascinate also by their many non-translational activities (reviewed in Schimmel, 2017), starting from the chromatin insulator role of tRNA genes as shown for different eukaryotes (Kuhn et al., 1991; Raab et al., 2012). Mature, aminoacylated tRNAs are involved as well in several pathways, for example, tRNA-Arg and the arginyl-tRNA-protein transferase act in a specific protein degradation pathway (Kaji, 1968; Balzi et al., 1990). Furthermore, aminoacylated tRNA-Glu has been shown to serve as a substrate for the biosynthesis of tetrapyrroles (i.e., chlorophyll and heme) in green plants, archaebacteria and many eubacteria (Huang et al., 1984; Schön et al., 1986; Jahn et al., 1992). Recently it has been reported that tRNA binding to cytochrome c leads to inhibition of caspase activation and

therefore blocks apoptosis (Mei et al., 2010). Intriguingly, mature tRNAs can be hijacked by retroviruses and long terminal repeat (LTR) retrotransposons during their replication cycles, and are thereby used as primers for reverse transcription (Rosenthal and Zamecnik, 1973; Mak and Kleiman, 1997).

In the past decade a new aspect of tRNA biology has emerged, namely, the occurrence of tRNA-derived fragments. They seem to excerpt diverse biological roles and several modes of actions have been proposed. However, published data are not always satisfying and are often contradictory. In this regard, the elusive nature of tRNA-derived fragments is probably the most prominent challenge to tackle next within the tRNA field.

1.1.1. Structure and Nucleotide Modifications Guarantee tRNA Functionality

TRNAs are highly transcribed and represent one of the most abundant transcript class within a cell. It has been estimated that a single yeast cell contains three million tRNAs (Waldron and Lacroute, 1975). This tremendous amount of molecules is transcribed by RNA polymerase III (Pol III). The following sections aim to describe several processing steps tRNAs undergo before being loaded with the correct amino acid (Figure 1.1).

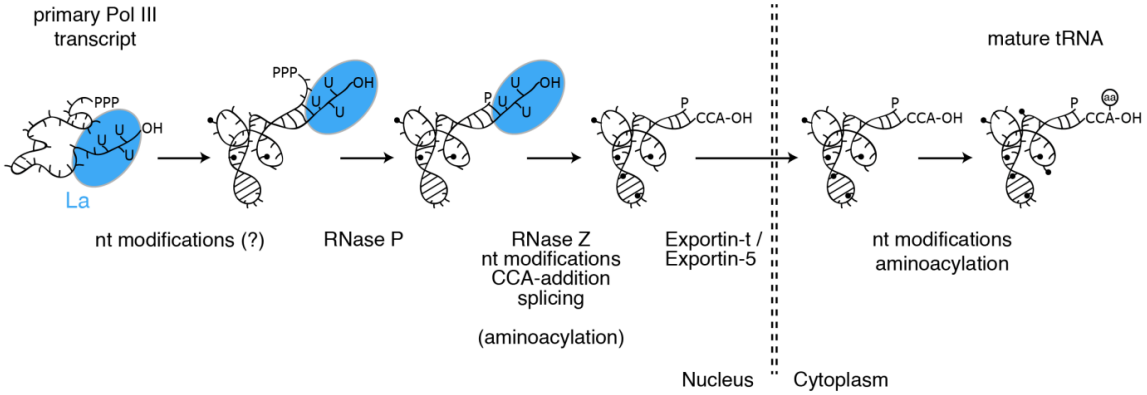

Figure 1.1: TRNA Maturation is a Multistep Process. Schematic representation of processing events and key enzymes required during the biogenesis of tRNAs. The La protein (blue) binds and protects the 3' end of pre-tRNA transcripts supporting their correct folding. The order of the reactions, enzymes as well as cellular localization of the steps might vary under certain conditions and between different organisms.

The outcome of tRNA biogenesis are structurally highly conserved molecules which have co-evolved with the ribosome to match the requirements for protein synthesis (reviewed in Tamura, 2015; Zhang and Ferré-D'Amaré, 2016). Importantly, the folding of tRNAs is not only relevant for its fundamental role during translation, but its acquisition during the maturation of tRNAs also governs several subsequent reactions (e.g., removal of the 5'

leader sequence from pre-tRNAs by RNase P) and structural determinants are continuously interrogated for quality control (e.g., by the tRNA nucleotidyltransferase).

The typical secondary structure of tRNAs resembles a cloverleaf and according to distinguishing attributes the different stem-loops have been named D-arm, T-arm and anticodon arm (Figure 1.2A). The loop of the D-arm contains several dihydrouridine modified nucleosides, while the loop of the T-arm almost universally starts with a ribothymidine, which is uncommon in RNAs. It is followed by a pseudouridine (Ψ) and a cytidine, whereby the T-arm is alternatively also referred to as TΨC-arm. The anticodon itself, consisting of three nucleotides pairing with the codon triplet on the mRNA, is located at the center of the anticodon loop. Between the anticodon arm and the T-arm a segment of variable length can occur (variable arm).

The first crystal structure of a tRNA was solved in the 70's (Kim et al., 1973) and revealed the L-shape of this molecule. The acceptor stem and the T-arm form one segment, which is also called minihelix, while the D-arm together with the anticodon arm form the second part of the L-shape. These two branches are joined by the elbow which consists of the loops of the D- and T-arms (Figure 1.2B). Importantly, several Watson-Crick interactions as well as extensive unconventional base pairings occur within this region and are essential for stabilizing the overall tertiary structure of the tRNA (reviewed in Zhang and Ferré-D'Amaré, 2016).

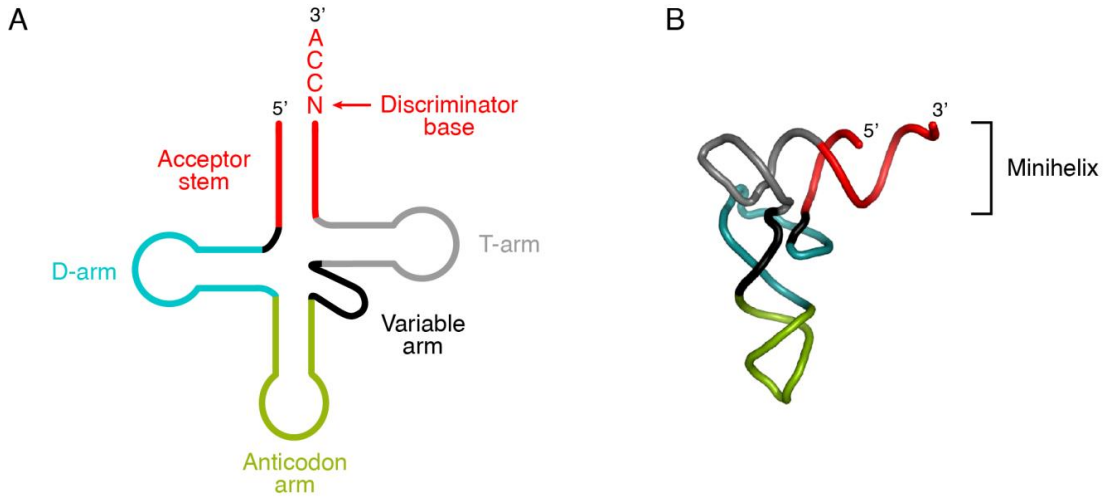

Figure 1.2: Structural Characteristics of Mature tRNAs. (A) The secondary structure of tRNAs resembles a cloverleaf. D-arm, anticodon arm, variable arm, T-arm and the acceptor stem are depicted in different colors. The last four nucleotides at the 3' end of the acceptor stem are indicated. They form a single-stranded overhang, whereby the terminal CCA is added post-transcriptionally. The preceding nucleotide (N) is termed discriminator base. (B) TRNAs adopt an L-shaped tertiary structure. The corresponding colors as in (A) are used. Figure adapted from Tamura (2015).

A multitude of tRNA structures have been obtained meanwhile and some of them depict the tRNA bound by some processing and maturation enzymes or engaged at the ribosome during different translation steps (reviewed in Giegé et al., 2012). These data highlight the intrinsic flexibility of tRNAs, especially of the elbow, which accounts for the variability in the positioning of the two L-shaped segments relative to each other (Giegé, 2008; Giegé et al., 2012).

Important for the correct folding (Helm et al., 1999) as well as for the structural stabilization of tRNAs (Anderson et al., 1998, see also sections 1.1.4.3 and 1.1.9) is their amazing repertoire of posttranscriptional modifications. Approximately 100 different nucleoside variants have been identified. Their generation requires the activities of an astonishing amount of highly specialized enzymes, which are very often responsible for position-specific modification of certain bases (Figure 1.3).

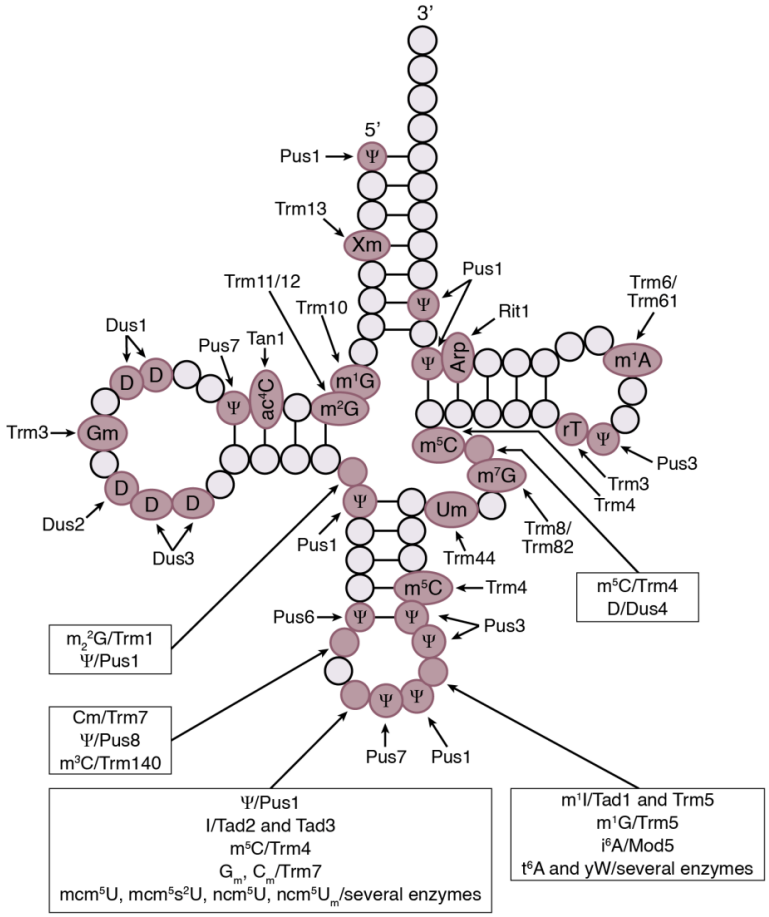

Figure 1.3: Frequent Modifications and Responsible Enzymes for Yeast Cytoplasmic tRNAs. Schematic representation of a tRNA with circles indicating nucleotides and lines indicating base pairings. Positions which are unmodified in all tRNAs are depicted with lighter circles, positions where modifications can occur are shown with darker circles. Figure adapted from El Yacoubi et al. (2012); abbreviations used as listed therein.

Due to the complex chemical properties of some of these nucleotide variants it is frequent that they are obtained in multi-step reactions through the action of several proteins (reviewed in El Yacoubi et al., 2012; Hori, 2014). Despite all the efforts life has dedicated to the evolution of these elaborated modifications, only few of them are strictly essential or are related to severe phenotypes. These are mostly located within the anticodon loop (Björk et al., 2001; Wolf et al., 2002; El Yacoubi et al., 2009) and the lack of specific modification has been implicated in different human diseases as well (Kirino et al., 2004; Wei et al., 2011; reviewed in Torres et al., 2014). TRNA modifications within the anticodon loop contribute in several ways to the accuracy of protein translation. First of all, modified nucleoside behave as identity determinants for the enzyme, specifically charging tRNAs with the correct amino (reviewed in El Yacoubi et al., 2012). Most importantly, tRNA modifications within the anticodon loop impact translation rates (Nedialkova and Leidel, 2015) and contribute to decoding accuracy by stabilizing codon-anticodon interactions. In this context they are required either for allowing wobble interactions or for ensuring stringent discrimination of closely related codons. This is particularly relevant for so-called split codon boxes whereby different amino acids (or a stop codon) are decoded depending only on the last nucleotide of the codon (Björk et al., 2007; Johansson et al., 2008).

1.1.2. Organisation of tRNA Genes

Currently, 610 tRNA genes are annotated at the genomic tRNA database (gtRNAdb) 2.0 for the human genome (Chan and Lowe, 2015). According to the amino acid they carry, tRNA genes are grouped into different isotypes. Due to the degeneracy of the genetic code, one specific amino acid can be encoded by several codons, which are recognized by distinct tRNA isoacceptors. For the nomenclature of different tRNA isoacceptors, the sequence of the anticodon is used (e.g., tRNA-Ile-TAT and tRNA-Ile-AAT). A specific isoacceptor group consists of so-called isodecoders, i.e., tRNAs sharing a common anticodon. Although originating from different genomic loci, some mature tRNA isodecoders might have identical sequences. However, isodecoders can also slightly differ in their tRNA body sequence. The hierarchical grouping of tRNA genes is exemplarily shown in Figure 1.4 for the tRNA-Ile isotype.

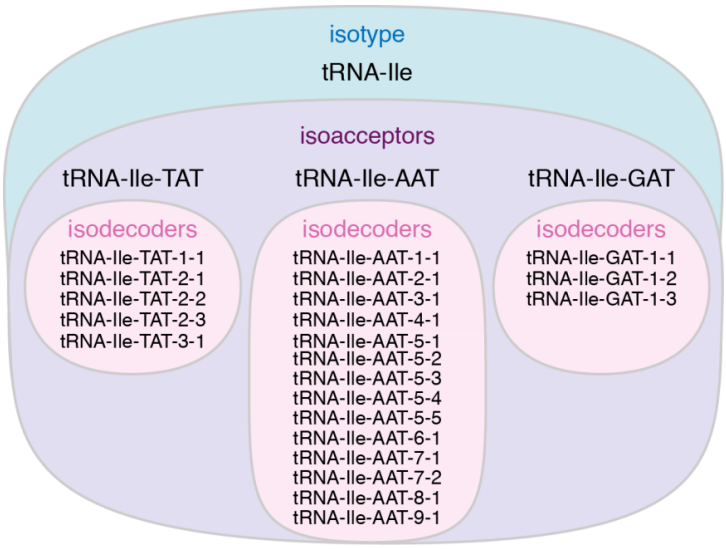

Figure 1.4: TRNAs Are Hierarchically Grouped into Isotypes (blue), Isoacceptors (violet) and Isodecoders (pink). Illustration of the different terms used to categorize tRNAs. See main text for details. Please note in the numbering of tRNA isodecoders that those sharing the same first number (e.g., tRNA-Ile-TAT-2-1, tRNA-Ile-TAT-2-2 and tRNA-Ile-TAT-2-3) have identical mature tRNA sequences. Nevertheless, they can originate from distinct genomic loci which are unambiguously indicated by the second number.

Of note, not all possible tRNA isoacceptors are encoded in the genome (Figure 1.5). This is possible because wobble interactions (i.e., non-standard Watson-Crick pairings) can occur at the third base within a codon with the first base of a tRNA's anticodon. Thus, a smaller set of tRNA isoacceptors allows decoding of all 64 possible codon sequences. Figure 1.5 also shows, that the number of certain tRNA isodecoder genes is over-represented for certain isoacceptors, e.g., for tRNA-Cys-GCA (38), compared to others, e.g, to tRNA-Ser-GGA (1). The reasons for this fact remain elusive, since tRNA copy numbers do not always correlate with the codon usage rates.

Regarding their distribution, tRNA genes are in general dispersed throughout the human genome, differing from the strictly clustered localization of rRNA repetitive units. Still, small clusters especially on chromosomes 1, 6 and 17 are present as well (Raab et al., 2012). In the fission yeast *Schizosaccharomyces pombe* clustering is more pronounced and tRNA genes are found at centromeric DNA sequences (Kuhn et al., 1991). It has been shown that binding of Pol III-specific transcription factors to these tRNA genes is sufficient to hinder spreading of repressive chromatin marks to distal regions. Interestingly, the insulator function of tRNA genes is conserved in humans as well, although the small clusters are not present at centromeres (Raab et al., 2012).

six box tRNA sets

Isotype	tRNA count by anticodon (corresponding codon usage)										Total
Ser	AGA 12 (1.52%)	GGA 1 (1.77%)	CGA 4 (0.44%)	TGA 6 (1.22%)	ACT 1 (1.21%)	GCT 8 (1.95%)					32 (8.11%)
Arg	ACG 7 (0.45%)	GCG - (1.04%)	CCG 4 (1.14%)	TCG 6 (0.62%)			CCT 5 (1.2%)	TCT 7 (1.22%)			29 (5.67%)
Leu	AAG 12 (1.32%)	GAG - (1.96%)	CAG 11 (3.96%)	TAG 4 (0.72%)			CAA 12 (1.29%)	TAA 9 (0.77%)			48 (10.02%)

four box tRNA sets

Isotype	tRNA count by anticodon (corresponding codon usage)				Total
Ala	AGC 31 (1.84%)	GGC 1 (2.77%)	CGC 5 (0.74%)	TGC 10 (1.58%)	47 (6.93%)
Gly	ACC - (1.08%)	GCC 15 (2.22%)	CCC 13 (1.65%)	TCC 9 (1.65%)	37 (6.6%)
Pro	AGG 10 (1.75%)	GGG 1 (1.98%)	CGG 4 (0.69%)	CCA 8 (1.69%)	23 (6.11%)
Thr	AGT 10 (1.31%)	GGT - (1.89%)	CGT 7 (0.61%)	TGT 6 (1.51%)	23 (5.32%)
Val	AAC 12 (1.1%)	GAC 1 (1.45%)	CAC 17 (2.81%)	TAC 8 (0.71%)	38 (6.07%)

other tRNA sets

Isotype	tRNA count by anticodon (corresponding codon usage)				Total
Ile	AAT 18 (1.6%)	GAT 6 (2.08%)		TAT 5 (0.75%)	29 (4.43%)
Met			CAT 20 (2.2%)		20 (2.2%)
Trp			CCA 8 (1.32%)		8 (1.32%)
SeC				TCA 3	3
Sup			CTA 2	TTA 2	4

two box tRNA sets

Isotype	tRNA count by anticodon (corresponding codon usage)				Total
Phe	AAA - (1.76%)	GAA 15 (2.03%)			15 (3.79%)
Asn	ATT 2 (1.7%)	GTT 34 (1.91%)			36 (3.61%)
Lys			CTT 24 (3.19%)	TTT 20 (2.44%)	44 (5.63%)
Asp	ATC 1 (2.18%)	GTC 17 (2.51%)			18 (4.69%)
Glu			CTC 10 (3.96%)	TTC 14 (2.9%)	24 (6.86%)
His	ATG - (1.09%)	GTG 10 (1.51%)			10 (2.6%)
Gln			CTG 22 (3.42%)	TTG 18 (1.23%)	40 (4.65%)
Tyr	ATA 5 (1.22%)	GTA 32 (1.53%)			37 (2.75%)
Cys	ACA 1 (1.06%)	GCA 38 (1.26%)			39 (2.32%)

Figure 1.5: Overview of Predicted Human tRNA Genes and Corresponding Codon Usage. The tRNA isotypes are grouped in different sets according to the number of anticodons used to decode the same amino acid. Potential suppressor tRNAs are shown in grey as no experimental evidence exists for their functionality in humans. Consider that the codons TGA, TAA and TAG are recognized as stop codons under normal conditions. Data obtained from the gtRNAdb 2.0 (Chan and Lowe, 2015).

The proximity of tRNA loci to each other is not only visible in regard to their position on the genomic DNA but is also evident from their spatial localization within the nucleus. The three-dimensional organization of tRNA genes has been studied in great detail in the budding yeast *Saccharomyces cerevisiae* and actively transcribed tRNA genes were detected in nucleoli (Thompson et al., 2003). TRNA genes were shown also in human cells to be enriched in nucleolus-associated chromatin domains (Németh et al., 2010), however, not many analyses have been performed in the human system.

1.1.3. Transcription by Pol III

1.1.3.1. Pol III Transcription Is Driven by Different Promoter Types

Pol III is the largest of the three RNA polymerases and, yet, it is structurally the least characterized. Only recently, structures at ~4 Å resolution have been achieved by cryo-electron microscopy (EM) (Hoffmann et al., 2015; Abascal-Palacios et al., 2018), although a first low resolution structure at 17 Å was published almost ten years before applying cryo-EM as well (Fernández-Tornero et al., 2007). The Pol III holoenzyme consists of 17 subunits, of which ten are unique to Pol III, while the other seven subunits are either shared by Pol I and Pol III or are present in all three RNA polymerases.

Transcription by Pol III is directed by three distinct promoter types (I, II and III) which differ in regard to *cis* regulatory elements; consequently, the composition of transcription factors involved varies among the different promoters (Figure 1.6). Common to all promoters is the requirement of the general transcription factor TFIIIB. This complex consists of the TATA box-binding protein (TBP), the Pol III-specific transcription factors TFIIIB component B" homolog (BDP), and TFIIB-related factor 1 (BRF1) or TFIIB-related factor 2 (BRF2). While the binding of TBP to a TATA-box or TATA-like sequence is required for type III promoters, the presence of such sequence elements is not mandatory for the other two promoter types, but has been shown to increase transcription efficiency (Giuliodori et al., 2003). In addition, activity of type III promoters is facilitated by the binding of the small nuclear RNA-activating protein complex ($SNAP_c$) to a proximal sequence element (PSE) and by the binding of OCT1 and STAF to the distal sequence element (DSE) (reviewed in Schramm and Hernandez, 2002). Of note, the promoter type III is found only in multicellular organisms.

In contrast, the main characteristic of promoter type I and II is that the sequence elements driving transcription are located within the transcribed sequence. These so called A-box,

B-box, C-box and intermediate elements (IE) are therefore very often embedded in the mature transcripts (e.g., in tRNAs). In the case of type II promoters, which drive the expression of all tRNA genes with a minor exception, the A-box and B-box form together a specific binding site for positioning the multisubunit complex TFIIIC (Figure 1.6).

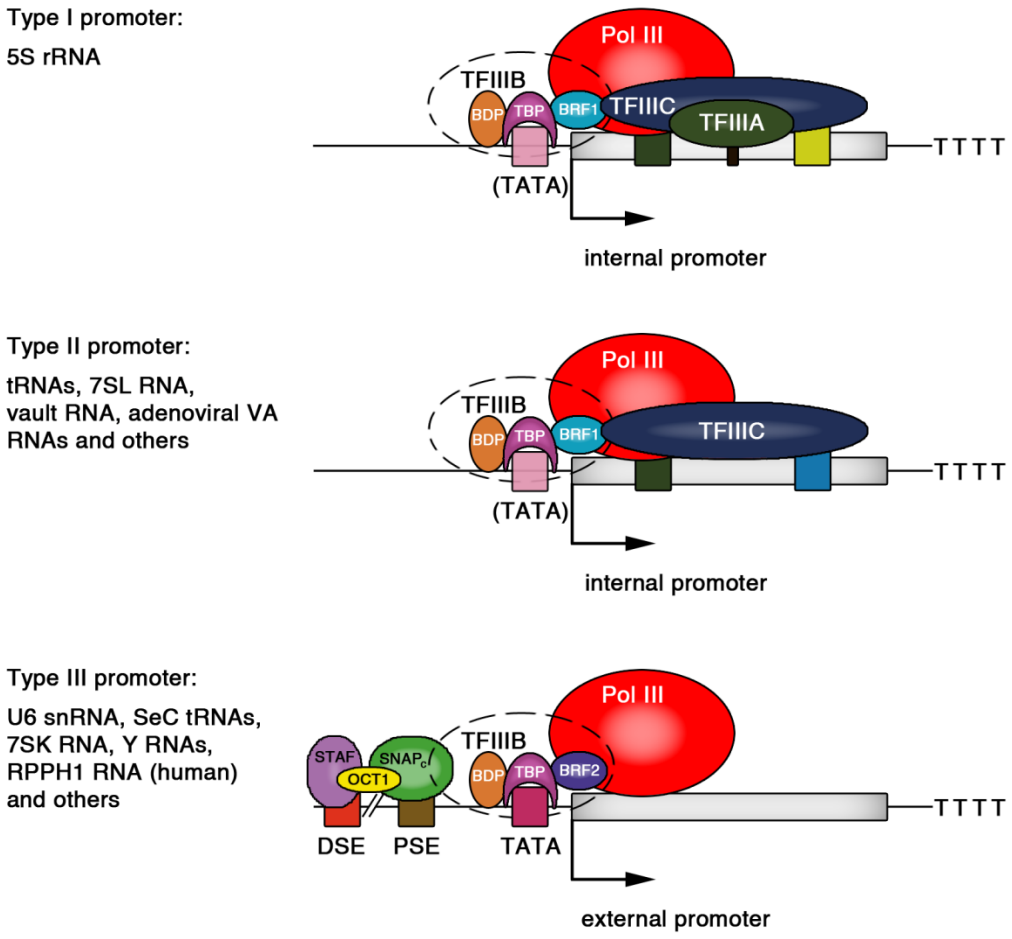

Figure 1.6: Type I, II and III of Pol III Promoter Differ in Sequence Elements and Required Transcription Factors. See main text for details. IE, intermediate element; DSE, distal sequence element; PSE, proximal sequence element; TTTT transcription termination signal; TATA, TATA box or TATA-like sequence, parentheses indicate that not all type I and type II promoters contain a TATA element. Adapted from Dieci et al. (2007) and Oler et al. (2010).

1.1.3.2. Regulation of Pol III Transcript Levels

As mentioned before, TFIIIB consists of three different proteins (TBP, BDP and BRF1 or BRF2), where the exact composition depends on the promoter type. BRF1 is required for transcription from internal promoters (type I and II), while it is replaced by the vertebrate-specific BRF2 at type III gene-external promoters. This variance might account for the potential to regulate specifically gene expression of promoter type III genes

independently from the other promoter types. In fact, recent X-ray crystallographic structures of BRF2-TBP complexes bound to different natural promoter sequences shed light on a fascinating feature of BRF2: the presence of a redox-sensing regulatory module wherein a conserved cysteine residue (C361) can cycle through reduced and oxidized states. In case C361 is oxidized, assembly of the complex on DNA is severely compromised (Gouge et al., 2015). Consequently, BRF2-dependent transcription of promoter type III genes is reduced during oxidative stress. Of note, the only tRNAs possessing such promoters are tRNA-SeC gene loci, while all the other tRNAs are transcribed from type II promoters (Oler et al., 2010). Selenocystein is especially required for the synthesis of several proteins directly involved in the oxidative stress response. However, the BRF2-dependent down regulation of tRNA-SeC levels during prolonged oxidative stress conditions and the resulting decrease of selenoproteins expression, lead to the induction of apoptosis (Gouge et al., 2015). This protective mechanism seems to be overcome in several types of cancers, where oncogenic BRF2 overexpression is observed (Cabarcas and Schramm, 2011).

The regulation of tRNA-SeC expression by the BRF2 redox-sensor is probably the only known mechanism explaining how tRNA levels can be modulated at the transcriptional level. Indeed, several pieces of evidence emerged during the past years suggest that the protein synthesis machinery is not fuelled by a constant tRNA pool (reviewed in Kirchner and Ignatova, 2014; Orioli, 2017). First indications came from microarray-based analyses of different tissues, demonstrating remarked levels of tRNA heterogeneity among the tested samples (Dittmar et al., 2006). Furthermore, chromatin immunoprecipitation (ChIP) experiments revealed considerable variance in the tRNA loci occupied by Pol III. Also, the total amount of *in silico* predicted tRNA genes bound by Pol III varied between four different cell lines, ranging from ~30% to ~60% (Oler et al., 2010). Finally, a broad microarray-based study extensively demonstrated changes in the tRNA pool among proliferative, differentiating and senescent cells (Gingold et al., 2014). The tRNA content of several cancer types and cancer stages was also characterized recently, providing first evidences for the relevance of differing tRNA levels. These changes correlated with a shift in the codon-usage signature of genes involved in the driving processes of the analyzed conditions (Gingold et al., 2014; Goodarzi et al., 2016). A similar adaptive dynamic in tRNA supply and codon-usage demand has been proposed as well for cell cycle-regulated genes (Frenkel-Morgenstern et al., 2012). All these findings depict the coordinated adaptation of the expressed tRNA subset and the codon-usage requested

under specific situations. According to such a system, the translation of the requested proteins will be favoured in contrast to unintended gene products (Gingold et al., 2014; Quax et al., 2015). Still, the chicken or the egg question remains, regarding the driving force for this co-evolution process: did the tRNA pool adapt to a varying demand or did the bias in codon-usage of important genes react to the altered tRNA composition? In both cases, the molecular mechanisms resulting in the differential tRNA expression remain largely elusive. The core elements of tRNA genes are very similar to each other and motif analyses of Pol III bound versus non-bound tRNA genes did not reveal any differences in A-box and B-box sequence composition (Oler et al., 2010) or only modest variances (Canella et al., 2010). However, when similar analyses were performed with tRNAs enriched during differentiation or proliferation, the sequence motif of the B-box differed between the two subsets and therefore might be a first indication of the underlying regulatory mechanism (Gingold et al., 2014).

1.1.3.3. Transcription Termination by Pol III

Similarly to the relatively unsophisticated organisation of Pol III promoters, transcription termination by Pol III is driven by a direct mechanism, simply requiring a short oligo(dT) tract on the non-template strand (Arimbasseri and Maraia, 2015). Neither post-translational modification of the polymerase nor the activity of *trans*-acting factors is required for Pol III termination unlike for Pol II (Arimbasseri et al., 2013). Although the short oligo(dT) tract is the universal terminator for Pol III, the minimum length for efficient termination varies among different species. The yeast *S. cerevisiae* requires six or more Ts for efficient termination (Allison and Hall, 1985), while in vertebrates four Ts are generally sufficient (Bogenhagen and Brown, 1981; Cozzarelli et al., 1983). At the same time, sequence analyses of human tRNA loci revealed the presence of strong terminator sequences (i.e., having more than four Ts) more downstream than observed in *S. cerevisiae* (Orioli et al., 2011). The more proximal terminator sequences instead appear to be weaker in humans. This, together with other findings, suggests that transcription of tRNA genes in vertebrates is more prone to read-through events resulting in 3’ extended transcripts. The strong secondary terminators ensure thereby stringent termination (Arimbasseri et al., 2013).

The context surrounding the stretch of four Ts influences the ability of Pol III to terminate transcription, at least in some situations (Gunnery et al., 1999). The ability of Pol III to

discriminate permissive oligo(dT) tracts is fundamental for the production of Lys-TTT tRNAs. Beside the required three Us in the anticodon, an invariant U immediately upstream of them is present, resulting in four consecutive Ts on the non-template strand (Mazabraud et al., 1987). On the other side, termination at non-canonical oligo(dT)-stretches has been observed as well (Orioli et al., 2011).

The underlying principle of transcription termination is based on two distinct processes, namely pausing of the polymerase and transcript release. The intrinsic nature of the oligo(dT) tract already accounts for slowing down Pol III, as the base pairing of the nascent oligo(rU) on the RNA with the oligo(dA) tract on the template DNA strand is the weakest possible interaction compared to other RNA:DNA hybrids (Arimbasseri et al., 2013). This characteristic leads to the destabilization of the elongating polymerase complex. However, it is not sufficient to release the transcript and the requirement of the Pol III endonucleolytic cleavage activity (Huang et al., 2005; Arimbasseri and Maraia, 2013) and the role of proximal RNA secondary structures (Nielsen et al., 2013; Arimbasseri et al., 2014; Nielsen and Zenkin, 2014; Gogakos et al., 2017) are still a matter of debate.

As more and more details are being unravelled regarding the potent properties of Pol III transcript termination, it should still be considered that the 3’ ends of the transcripts are heterogeneous and differ in the number of Us incorporated before being released (Arimbasseri et al., 2013).

1.1.4. Maturation of tRNA Ends

1.1.4.1. 5’ End Processing of Pre-tRNAs by RNase P

As described above, the primary Pol III transcripts all terminate on a stretch of Us, which is immediately bound by the Lupus autoantigen La protein at the transcription site (Fairley et al., 2005). This interaction is not only fundamental for protecting the 3’ end from exonucleolytic degradation but is also required for the efficient processing of Pol III transcript, in particular of tRNAs. RNA chaperone activities have been attributed to the La protein and it therefore facilitates correct folding of the bound pre-tRNAs (Pannone et al., 1998; Chakshusmathi et al., 2003; Belisova et al., 2005; Kucera et al., 2011; Naeeni et al., 2012). In addition, the interaction with La governs the hierarchy of the different tRNA processing events. Upon phosphorylation of La the 5’ end of the pre-tRNA becomes

accessible for the RNase P complex which removes the 5’ leader sequence by endonucleolytic cleavage (Fan et al., 1998; Intine et al., 2000).

The human RNase P is a ribonucleoprotein (RNP) complex composed of ten protein subunits and the catalytic (Kikovska et al., 2007) RNA H1 (or RPPH1), which is transcribed as well by Pol III and localizes at least in part in the nucleoli and in the nucleoplasm (Jarrous et al., 1999). First studies performed with the RNA moiety of bacterial RNase P clearly demonstrated that the RNA is endonucleolytically active on its own, and was therefore the first true ribozyme being characterized (Guerrier-Takada et al., 1983). Of note, bacterial RNase P consists of the catalytic RNA and one single protein, while the number of protein components increased during evolution (Lai et al., 2010). Studies performed in yeast demonstrated that the protein subunits of RNase P are required for cell viability, and that RNase P activity was decreased *in vivo* upon conditional depletion of single subunits (Lygerou et al., 1994; Chu et al., 1997; Dichtl and Tollervey, 1997; Stolc and Altman, 1997; Chamberlain et al., 1998). Still, the exact role of the protein components and the reason for the increased complexity of the eukaryotic complexes remain an open question, although the protein subunits might be involved in stabilization and folding of the RNA H1 (Esakova et al., 2008), and might increase the binding affinity of the RNase P for its substrates (Esakova and Krasilnikov, 2010). In addition, eukaryotic RNase P has acquired novel regulatory functions which might depend at least in part on the protein subunits (Reiner et al., 2006). Interestingly, the 5’ ends of mitochondrial tRNAs are cleaved by a protein only heterotrimeric complex which thus represents the only known exception to the ubiquitous RNA-catalysed RNase P enzymes (Holzmann et al., 2008).

1.1.4.2. 3’ End Processing of Pre-tRNAs by RNase Z

The canonical processing of the 3’ end of pre-tRNAs requires the endonucleolytic cleavage activity of a single protein termed RNase Z. However, the characterization of this endoribonuclease lags behind the deeper knowledge about the multisubunit RNase P complex. In particular, most studies regarding RNase Z activity and substrate specificity have been conducted *in vitro* and only in spare cases the *in vivo* requirement of RNase Z for the removal of the 3’ trailer from pre-tRNAs has been demonstrated (Pellegrini et al., 2003; Dubrovsky et al., 2004; Brzezniak et al., 2011; Skowronek et al., 2014; Xie and Dubrovsky, 2015; Reinhard et al., 2017).

Two forms of RNAse Z exist, a short version composed of 280-360 amino acids (referred to as RNase Z^S) and a long version composed of 750-930 amino acids (referred to as RNase Z^L) (Späth et al., 2007). RNase Z^S is found in representatives from all three domains of life, while RNase Z^L is present only in eukaryotes. The latter very likely originated from gene duplication of RNase Z^S, since sequence similarities to RNase Z^S are found in the N- as well as in the C-terminal part of RNase Z^L (Takaku et al., 2004). Remarkably, the genomes of eukaryotic organisms in general encode at least one RNase Z^L protein (e.g., in *S. cerevisiae* and *D. melanogaster*), while distribution of the short RNase Z^S form varies among eukaryotes. In humans, for example, both forms of RNase Z are present, whereby RNase Z^S is encoded by the *ELAC1* gene and RNase Z^L by *ELAC2*. Localization studies showed that RNase Z^S is found in the cytosol, while RNase Z^L in the nucleus and in mitochondria. Interestingly, the dual localization of the latter protein is achieved by the alternative use of two translation initiation sites. This results in an RNase Z^L variant containing a mitochondrial targeting sequence and a slightly shortened RNase Z^L variant lacking 15 N-terminal amino acids and, therefore, most of the mitochondrial targeting sequence (Rossmanith, 2011). Since RNase Z^L is the only RNase Z form found in some eukaryotes, it has been speculated that RNase Z^L is sufficient for the biogenesis of nuclear- and mitochondrial-encoded tRNAs. However, it has been not clarified whether both RNase Z forms might have redundant functions at least under certain conditions, or if the RNase Z^S encoded in some eukaryotic genomes has acquired a completely different specialization. Although these two proteins still remain largely uncharacterized *in vivo*, recent biochemical evidences confirmed the role of RNase Z^L in the processing of mitochondrial tRNAs (Brzezniak et al., 2011; Reinhard et al., 2017). Furthermore, mutations in *ELAC2* have been identified to occur in prostate cancer (Tavtigian et al., 2001) and in other diseases (Haack et al., 2013; Akawi et al., 2016).

An important aspect of 3’ processing of pre-tRNAs is the fact that eukaryotic tRNA genes do not encode the 3’ terminal CCA which is mandatory for aminoacylation of mature tRNAs. Hence, eukaryotic RNase Z enzymes are required to cleave pre-tRNAs immediately after the discriminator base, which is the unpaired nucleotide 3’ to the last base pair (bp) of the acceptor stem. The tRNA nucleotidyltransferase successively proceeds with the non-templated addition of the 3’ CCA end. The situation is different in archea and bacteria: some organisms encode only CCA-containing tRNA genes, others encode CCA-containing and CCA-less genes. Those organisms which do not encode any RNase Z only possess tRNAs with the CCA end already encoded in the genome. The 3’

processing of such tRNAs relies on the action of 3'→5' exoribonucleases. Although some other bacteria like, for example, *Escherichia coli* also encode the CCA end within all tRNAs genes, they still possess RNase Z proteins. They have been shown to be catalytically active *in vitro* and can cleave off the trailer of CCA-less pre-tRNA substrates. However, some evidence suggests that their physiological substrates are other RNA transcripts, unrelated to tRNAs (Perwez and Kushner, 2006). In those organisms encoding CCA-containing and CCA-less pre-tRNAs, the action of RNase Z is restricted, with some minor exceptions, to the CCA-less pre-tRNA subpopulation alone. In this way it has been demonstrated that the presence of the CCA motif downstream of the discriminator base inhibits RNase Z activity (Pellegrini et al., 2003; Dutta et al., 2013). A similar anti-determinant property of the terminal CCA sequence has been observed as well for several eukaryotic RNase Z enzymes and might therefore prevent mature tRNAs from being pinched at the acceptor stem (Nashimoto, 1997; Mohan et al., 1999).

From the structural point of view, RNase Z enzymes are quite exotic endoribonucleases, as they are characterized by a metallo-hydrolase domain of the β-lactamase family. Such a domain is found in only one other RNA processing enzyme, namely, in the cleavage and polyadenylation specificity factor 73 (CPSF-73) protein which is the endoribonuclease cleaving the mRNA 3' ends and allowing subsequent polyadenylation (Mandel et al., 2006). These proteins exhibit zinc-dependent phosphodiesterase activity.

A peculiarity of RNase Z is the so-called exosite, which is a flexible arm that protrudes from the main protein body as elucidated by the crystal structures of the RNase Z^S from different organisms (de la Sierra-Gallay et al., 2005; Ishii et al., 2005; Kostelecky et al., 2006). Although this element does not participate in the catalytic reaction, it was later shown to clamp the pre-tRNA by several hydrogen bond contacts (de la Sierra-Gallay et al., 2006).

RNase Z^S forms homodimers, whereby the one subunit might account for substrate recognition and the other for cleavage (de la Sierra-Gallay et al., 2005, 2006). Instead, the longer RNase Z^L acts as a monomer but has sequence similarities to RNase Z^S in its N- and C-terminal parts. This fact suggests that RNase Z^L has lost the necessity to form homodimers by linking the two components within the same protein. It further seems that the two halves of RNase Z^L have acquired specialization, as the N-terminal part has lost catalytic activity but still possesses the exosite, and, on the contrary, the C-terminal part is functionally active but does not contain the exosite (Takaku et al., 2003, 2004; Ma et al., 2017).

1.1.4.3. Alternative Processing of Pre-tRNA Ends

Most of the experimental evidence corroborates a model whereby pre-tRNA 5' end processing precedes 3' end processing (O'Connor and Peebles, 1991). In particular, the interaction of La with the newly synthesized pre-tRNAs buries their 3' ends hindering removal of the trailer (Teplova et al., 2006), while it is conceivable with the recruitment of RNase P (Fan et al., 1998; Intine et al., 2003). In addition, a decrease of RNase Z processivity has been reported for substrates with 5' extensions, suggesting that the removal of the leader sequence is preferred before cleavage of the trailer (Pellegrini et al., 2003).

Still, some exceptions to this 5'-before-3' processing rule have been reported. In particular, studies conducted in *S. cerevisiae* wild type and mutant strains revealed that pre-tRNA-Trp transcripts undergo first maturation of the 3' end, but still interact with the La homologous protein 1 (Lhp1), the budding yeast ortholog of the human La protein (Kufel and Tollervey, 2003).

Not surprising instead is the more substantial effect manifested by yeast Lhp1 depletion strains concerning the general tRNA maturation process. Due to the loss of the Lhp1's protective function, the 3' ends of pre-tRNAs are readily trimmed by exonucleases, while the 5' leader is removed only subsequently (Yoo and Wolin, 1997). Thus, reversal of the 5'-before-3' order in favor of the 3'-before-5' processing can be observed in the absence of Lhp1 and acts as a backup mechanism to keep tRNA biogenesis running.

However, 3'-before-5' processing might not only intervene for rescuing the perturbed function of Lhp1. Some evidence indicates that a fraction of pre-tRNAs is processed on a Lhp1-independent manner even under normal growth conditions, but this alternative processing pathway is overshadowed by the canonical 5'-before-3' order (reviewed in Maraia and Lamichhane, 2011). Such a situation could originate from the intrinsic property of Pol III transcription, namely the length heterogeneity of the terminal oligo(U) tail of pre-tRNAs. Analyses of pre-tRNAs from wild type *S. pombe* cells indicated in fact that these transcripts terminate on shorter U-stretches than noticed in yeast strain encoding a mutated Pol III subunit. The mutant strain exhibited reduced Pol III 3' cleavage activity resulting in abnormal transcription termination characterized by longer terminal oligo(U) tracts. These particular pre-tRNAs showed strong association with the yeast La ortholog and their maturation obeyed the 5'-before-3' hierarchy (Huang et al., 2005). Contrarily, in the wild type condition a larger fraction of pre-tRNAs with few 3'

terminal Us might exist and might escape binding by La proteins, whose availability appears to be a limiting factor (Huang et al., 2005; Maraia and Lamichhane, 2011). The maturation of such pre-tRNAs would consequently also be independent of RNase Z and rely on the action of diverse exoribonucleases as shown for pre-tRNAs with particularly short 3' trailers (Skowronek et al., 2014). As suggested also by others, pre-tRNAs would thus be subject to a permanent competition between binding by La and exonucleolytic processing (Copela et al., 2008).

The knowledge about the exoribunucleases involved in the 3' trimming of pre-tRNAs is still relatively spare, and their identification required elaborated experimental strategies. All studies performed so far have been carried out in yeast due to the versatility of genetic tools available for monitoring tRNA 3' end formation (Rijal et al., 2015). A major issue consists in the occurrence of several closely related exoribonucleases and which might therefore be able to adopt redundant functions. In this context, Rex1 was the first 3'→5' exoribonuclease experimentally linked to the processing of selected pre-tRNAs (van Hoof et al., 2000; Copela et al., 2008; Ozanick et al., 2009; Skowronek et al., 2014), while the contribution of its homolog Rex2 seems to play a minor role (Skowronek et al., 2014).

Of note, in Rex1 deletion strains the accumulation of polyadenylated pre-tRNA intermediates was observed (Copela et al., 2008; Ozanick et al., 2009; Skowronek et al., 2014), similar to previous findings indicating that hypomodified initiator pre-tRNA-Met gets polyadenylated by Trf4, a subunit of the Trf4/Air2/Mtr4 polyadenylation (TRAMP) complex (Kadaba et al., 2004). In the latter case, it has been shown that the structural instability caused by the lacking modification activates the nuclear surveillance machinery, and that the polyadenylated initiator pre-tRNA-Met is degraded by the nuclear exosome (Kadaba et al., 2004). It has been therefore speculated that in Rex1 deletion strains, some pre-tRNA transcripts would accumulate unprocessed 3' ends, and that this feature is recognized as well by the nuclear surveillance machinery (Ozanick et al., 2009). Alternatively, Trf4-mediated polyadenylation of some pre-tRNAs and subsequent trimming by Rex1 might be not related to degradation processes but might be the initial steps during the maturation of the 3' end (Ozanick et al., 2009). In such a scenario polyadenylation might be a prerequisite for Rex1 exonucleolytic activity, but this aspect has not been well addressed so far.

It is evident that a caveat for studying the role of exonucleases in tRNA maturation processes is to discern these activities from the effects directed to degrade tRNAs within quality control pathways (Copela et al., 2008; Ozanick et al., 2009; Hopper and Huang,

2015). In this regard, it is challenging to interpret the observation that yeast strains depleted for the nuclear exosome specific Rrp6 subunit accumulate different pre-tRNA precursors (Copela et al., 2008; Skowronek et al., 2014) as well as a structurally aberrant initiator pre-tRNA-Met (Kadaba et al., 2004). For more detail regarding the quality control pathway of tRNAs see section 1.1.9.

1.1.5. CCA Addition by the tRNA Nucleotidyltransferase

The eukaryotic end-processed tRNAs acquire their 3' CCA end post-transcriptionally by the action of the tRNA nucleotidyltransferase (Hecht et al., 1958; Deutscher, 1972). This process has been shown to take place in the nucleus (Solari and Deutscher, 1982; Lund and Dahlberg, 1998). However, the enzyme resides as well in the cytoplasm where it is able to heal damaged tRNAs, similar to its bacterial counterpart (Mukerji and Deutscher, 1972). Indeed, those prokaryotes which encode the terminal CCA within the tRNA genes also possess tRNA nucleotidyltransferase for repairing the tRNA 3' ends (Zhu and Deutscher, 1987). Furthermore, a third isoform of the tRNA nucleotidyltransferase is imported into mitochondria accounting for CCA addition to the tRNAs encoded in the genome of these organelles (Mukerji and Deutscher, 1972; Chen et al., 1992).

An intriguing characteristic of tRNA nucleotidyltransferases is their ability to specifically and exactly add the CCA overhang in a stepwise reaction without the requirement of any nucleic acid template. Interestingly, this property is shared by two distinct classes of tRNA nucleotidyltransferases which seem to have evolved independently from each other (Aravind and Koonin, 1999). Class I tRNA nucleotidyltransferases are found in archea and they share similarities to the eukaryotic poly(A) polymerases. Class II enzymes, instead, are found in bacteria and eukaryotes. The crystal structures of representatives from both classes have been solved (reviewed in Xiong and Steitz, 2006 and Betat and Mörl, 2015), unraveling extensive structural and mechanistic differences. Nevertheless, both enzyme types generate an environment which mimics Watson-Crick base pairing for selecting the correct nucleotide to incorporate; however, they exploit different strategies. The active site of class II enzymes forms a selectivity filter only via the side chains of its own amino acids. This mechanism is therefore referred to as "protein templating" (Li et al., 2002; Tomita et al., 2004). Contrarily, in class I enzymes the side chain of a specific amino acid as well as interactions with the phosphate backbone of the bound tRNA substrate contribute to the correct nucleotide selection (Xiong and Steitz, 2004).

During polymerization, tRNA nucleotidyltransferases undergo a specificity switch after the incorporation of the second C nucleotide and are prompted for the addition of the terminal A nucleotide. This exceptional feature distinguishes tRNA nucleotidyltransferases from the other template-independent polymerases, namely poly(A) polymerases, terminal RNA uridylyltransferases (TUTase) and the terminal deoxynucleotidyl transferase, as these enzymes simply add homopolymeric sequences to their targets. Mechanistically, this process has been unraveled thanks to the structural information acquired from class I tRNA nucleotidyltransferases. It has been described that the nucleotide binding pocket of the enzymes is subjected to changes in size and shape consequent to the progressive extension of the tRNA 3' end in such a manner that only an ATP molecule can be accommodated in the active site for the final reaction. This conformational resetting is supported by the intrinsic flexibility of the so-called head domain which bears the catalytic center. Thus, during CCA addition the tRNA substrate is maintained in the same position (Shi et al., 1998a), while the head domain is repositioned progressively on the extending tRNA end (Xiong and Steitz, 2004).

Of note, although the overall structure of class I and class II tRNA nucleotidyltransferases exhibits great differences, both enzymes are able to recognize their substrates on a similar way. TRNA nucleotidyltransferases are obligated to recognize their substrates independently of their sequences in order to attach the invariant CCA overhang to the 3' ends of all tRNAs. Thus, it is not surprising that both enzyme classes almost exclusively interact with the sugar-phosphate backbone of the tRNAs and that their peculiar shape is the main determinant for substrate binding. TRNAs have an L shaped tertiary structure, whereby the acceptor stem together with the T-arm form the so-called minihelix, while the other edge is formed by the anticodon stem-loop and the D-arm. In this regard, tRNA nucleotidyltransferases have developed an extended cleft which is perfectly suited to accommodate the minihelix structure in such a manner, that the 3' end of the tRNA is positioned within the active site of the head domain (Tomita et al., 2004; Xiong and Steitz, 2004). However, an interesting finding was done when *in vitro* CCA-addition assays were performed with an excess of the enzyme in respect to the RNA substrates. This condition ensured single-turnover kinetics and revealed that constructs consisting only of the minihelix portion were not suitable substrates for tRNA nucleotidyltransferases (Dupasquier et al., 2008), despite previous observations achieved under different experimental setups (Shi et al., 1998b). Even more intriguing is the fact that a full-length tRNA with a nick in the anticodon loop turned out as well to be an

unsuited substrate, although the anticodon loop is not contacted at all by the tRNA nucleotidyltransferases. Thus, it has been postulated that these enzymes possess the innate ability to sense structural stability of the tRNAs and are therefore involved in quality control mechanisms (Dupasquier et al., 2008).

This hypothesis has been confirmed by the discovery of a tRNA nucleotidyltransferase-dependent tRNA degradation pathway, whereby structurally unstable tRNAs and unfunctional tRNA-like sRNAs are marked by a second CCA-addition cycle. The resulting CCACCA 3' end behaves like a degradation tag which might recruit several exonucleases (Wilusz et al., 2011). Recent and comprehensive crystallographic studies have revealed how tRNA nucleotidyltransferases are able to prevent damaged and therefore potentially harmful tRNAs from becoming available for protein synthesis. Once the first CCA has been added, the head domain of the tRNA nucleotidyltransferase adopts a conformation which is competent for a second CCA-addition cycle and a new nucleotide for the polymerization reaction is bound. By doing so, the head domain generates a clockwise screw motion leading to the overwinding and compression of the bound substrate. A stable tRNA is resistant to this tension and is released without further consequences. Instead, the torque force applied on defective tRNAs causes the on-enzyme refolding of the bound RNA, whereby a small bulge is ejected in proximity of the 3' end. If the substrate adopts such a conformation the tRNA nucleotidyltransferase is consequently able to catalyze a second CCA-addition cycle. The enzyme therefore employs a strategy resembling the action of a vise for interrogating the structural property of the bound tRNA (Kuhn et al., 2015).

1.1.6. Extravagant Splicing Mechanism for tRNA Introns

1.1.6.1. A Specialized Splicing Machinery Removes tRNA Introns

Of the 606 annotated human tRNAs, 34 contain an intron sequence (Chan and Lowe, 2015). The proportion of intron-containing to intron-less tRNA genes varies substantially across different organisms. In *S. cerevisiae* for example, 21.5% of the tRNAs harbor introns, compared to 5.6% of the human genome (Chan and Lowe, 2015). Also the length of the embedded introns differs and usually ranges between 6 and 133 nucleotides, whereby extraordinary long introns of about 200 nucleotides have been predicted in some insects (Chan and Lowe, 2015; Lu et al., 2015). The position within the body of eukaryotic tRNAs instead is extremely conserved and introns mostly start at the second

nucleotide 3' to the anticodon sequence. Some particular exceptions have been found instead in archea, whereby the most extreme case is represented by the so-called "split tRNA genes". Here, mature tRNAs are produced by the ligation of two halves originating from completely independent transcripts (Randau et al., 2005a, 2005b).

Apart from such exotic tRNA precursors, it has been shown by chemical and enzymatic probing of several yeast pre-tRNAs that the presence of the introns does not significantly affect their secondary and tertiary structure compared to their mature species. The intron sequence generates a double-stranded segment by base-pairing with elements of the anticodon loop and thereby forms a helix just extending the anticodon stem (Swerdlow and Guthrie, 1984; Lee and Knapp, 1985). While archeal pre-tRNA introns are characterized by a bulge-helix-bulge motifs present at both splice sites (Daniels et al., 1985; Thompson and Daniels, 1990; Marck and Grosjean, 2003), the structural features of eukaryotic intron-containing pre-tRNAs are less sophisticated. In this regard, the presence of a so-called A-I (for anticodon-intron) interaction upstream of the 5' splice sites is required, as well as the typical tRNA folding (Mattoccia et al., 1988; Reyes and Abelson, 1988; Baldi et al., 1992). It is therefore not surprising that splicing of pre-tRNA introns in archea and in eukaryotes exhibits some mechanistic differences, for example in the positioning of the splicing enzymes on their substrates (reviewed in Belfort and Weiner, 1997). The rest of this section will focus on the molecular aspects of tRNA splicing in eukaryotes.

In these organisms, removal of pre-tRNA introns relies on the function of a dedicated tRNA splicing endonuclease (TSEN) complex, which is not related to the spliceosome required for pre-mRNA processing. First described in yeast (Rauhut et al., 1990; Trotta et al., 1997) and later in humans (Paushkin et al., 2004), the eukaryotic TSEN complex is a heterotetramer composed of Sen2, Sen34, Sen54 and Sen15 subunits, whereof Sen2 and Sen34 are catalytically active. Each of these two subunits catalyzes a phosphoester transfer reaction, resulting in the cleaved intron and in the 5' and 3' tRNA halfes. These bear respectively at the resected ends a 2',3'-cyclic phosphate and a 5'-OH (Peebles et al., 1983). Studies conducted in yeast mutant strains argued that Sen2 is responsible for the cleavage reaction at the 5' site (Ho et al., 1990), while Sen34 is designated to cut at the 3' site (Trotta et al., 1997). In addition, it has been proposed that Sen34 is involved in positioning the RNA within the active site of Sen2, therefore supporting cleavage at the 5' site as well (Trotta et al., 2006).

The two structural subunits, Sen54 and Sen15, have been shown to interact, respectively, with Sen2 and Sen34 (Trotta et al., 1997; Li et al., 1998). Unfortunately, the structure of the eukaryotic TSEN complex has not been solved yet, and the only information available is a model based on the crystal structure of a dimeric archeal splicing endonuclease bound to an RNA substrate (Xue et al., 2006). These data corroborate the hypothesis formulated almost two decades in advance that the TSEN complex acts as a molecular ruler for the correct positioning of the enzyme on the intron-containing pre-tRNA (Reyes and Abelson, 1988). In particular, it has been proposed that the Sen54 subunits contact the characteristic structures present also in mature tRNAs which are required as well for correct splicing (Di Nicola Negri et al., 1997; Li et al., 1998; Xue et al., 2006).

A major issue to be considered regarding splicing in eukaryotes is that although the molecular components of the TSEN complex are conserved across evolution, the localization of tRNA splicing is totally different between yeast and vertebrates. As mentioned previously, the first steps in tRNA maturation occur in the nucleus, where RNase P and RNase Z are localized (reviewed in Hopper et al., 2010). This also applies for the vertebrate's TSEN complex (Melton et al., 1980; Paushkin et al., 2004) but not for the yeast's complex which localizes in the cytoplasm and associates with the mitochondrial outer membrane. This finding implies that end-processed, intron-containing pre-tRNA intermediates are exported from the nucleus, spliced at the mitochondrial surface and re-imported into the nucleus where the final steps of maturation take place. The reason for such a laborious process is not well understood. It has been found that the depletion of TSEN complex components results in impaired rRNA processing (Volta et al., 2005). This phenotype could not be complemented by exogenous, nuclear-targeted TSEN complex, while pre-tRNA splicing and further maturation occurred normally (Dhungel and Hopper, 2012). Thus, it is tempting to speculate that in yeast the localization of the TSEN complex at the mitochondrial membrane has acquired novel functions unrelated to tRNA splicing. The TSEN complex has been shown additionally to cleave the mRNA encoding the cytochrome b mRNA processing 1 (Cbp1) protein, which co-translationally localizes at the mitochondrial surface (Tsuboi et al., 2015). Of note, the nuclear localized human TSEN complex has been related to pre-mRNA processing (Paushkin et al., 2004). All together, the distinct localization of the tRNA splicing machinery in yeast and humans might result from the necessity to adapt the function of the endonucleases to novel requirements unrelated to tRNA biogenesis.

1.1.6.2. Diverse Strategies for Joining the tRNA-Splicing Intermediates

Following the endonucleolytic cleavage of the pre-tRNA intron, the resulting two tRNA halves need to be ligated. In the past years several studies have contributed to shed light on this process, which has been, and to some extent still is, enigmatic. Two different strategies have been reported and the text-book knowledge is that fungi and plants rely on the so-called 5'-phosphate ligation pathway, while other organisms like vertebrates use the 3'-phosphate ligation pathway. However, since extracts from mammalian cell lines are able *in vitro* to catalyze the same reactions of the 5'-phosphate ligation pathway (reviewed in Yoshihisa, 2014) and some mutations in the corresponding genes have been implicated in tRNA splicing abnormalities and severe diseases (Hanada et al., 2013; Karaca et al., 2014; Schaffer et al., 2014), the 5'-phosphate ligation pathway might be active also in vertebrates, at least to a minor extent (see also section 1.1.10.1).

The 5'-phosphate ligation pathway requires two enzymes, the multi-domain protein tRNA ligase 1 (Trl1) (Greer et al., 1983; Xu et al., 1990) and the tRNA 2'-phosphotransferase 1 (Tpt1) (McCraith and Phizicky, 1990). The former enzyme catalyzes three distinct reactions which finally yield the ligated tRNA with a 2'-phosphate left at the splice site. To this end, the cyclic phosphodiesterase domain of Trl1 first opens the 2',3'-cyclic phosphate at the 3' terminus of the 5' tRNA half generating a 2'-phosphate. Next, the 5' end of the 3' tRNA half is phosphorylated by the NTP-dependent polynucleotide kinase domain of Trl1. The actual ligation reaction is subsequently carried out by a third domain, whereby the phosphorylated 5' end of the 3' tRNA half is first activated by transfer of AMP from an adenylated Trl1 intermediate and then joined to the 5' tRNA half (Greer et al., 1983). Finally, Tpt1 removes the 2'-phosphate still present at the splice junction (McCraith and Phizicky, 1990) by transferring it onto a nicotinamide adenine dinucleotide (NAD^+) molecule generating ADP-ribose 1"-2" cyclic phosphate (McCraith and Phizicky, 1991; Culver et al., 1993).

The characterization of the 3'-phosphate ligation pathway largely benefited from recent studies performed in the human system. It has been known for several years that the phosphate at the newly formed phosphodiester bond joining the two tRNA halves is derived from the 3'-phosphate resulting at the 5' tRNA half after splicing (Filipowicz and Shatkin, 1983; Filipowicz et al., 1983; Laski et al., 1983). This differs from the situation in fungi and plants, where the phosphate at the splice junction originates from the *de novo* phosphorylation of the 5' end of the 3' tRNA half as mentioned above. Isolation of the

vertebrate's enzyme which directly ligates the 2',3'-cyclic phosphate and the 5'-OH termini had been achieved already in the past (Perkins et al., 1985). However, molecular characterization of this RNA ligase occurred almost three decades later (Popow et al., 2011). The enzyme has been named RTCB (previously also known as HSPC117) and was shown to form a multimeric protein complex together with ASW, RTRAF, FAM98B and the DEAD-helicase DDX1. Further studies revealed that the ATPase activity of the latter protein is required for RTCB-mediated ligation reactions (Popow et al., 2014). Even more intriguing is the fact that an additional protein, ZBTB8O (also known as archease), drastically stimulates the multiple turnover activity of the ligase in a GTP-dependent manner. Thus, ZBTB8O supports the formation of a guanylated RTCB intermediate. It has been proposed that the GMP moiety would be then transferred to the 3' end of the 5' tRNA half (Popow et al., 2014). However, in vertebrates neither has the activation of the 3' end by this GMP transfer been experimentally proven, nor has the activity which opens the 2',3'-cyclic phosphate at the 3' end been identified.

Interestingly, Trl1 in yeast and the RTCB ligase in metazoa, although differing in their molecular mode of action, share an additional function which is not related to tRNA splicing. It has been specifically shown that they participate in the unfolded protein response pathway which is triggered by the non-canonical splicing of the relevant *HAC1/XBP1* mRNA. In this context, Trl1/RTCB join the resulting two exons allowing translation of the transcription factor encoded by the spliced mRNA (Sidrauski et al., 1996; Jurkin et al., 2014; Kosmaczewski et al., 2014; Lu et al., 2014).

1.1.7. Mechanisms of tRNA Export from the Nucleus

As illustrated by the biogenesis of intron-containing tRNAs in yeast (see section 1.1.6.1), the movement of tRNAs between the nucleus and the cytoplasm is neither unidirectional nor dependent on a single mechanism. Kinetic measurements after nuclear microinjections provided the first piece of the complex mosaic depicting the subcellular trafficking of tRNAs. It was shown that export of tRNAs was not driven by diffusion despite their small molecular size, but was likely to be mediated by some carrier (Zasloff, 1983). As more studies identified the factors required for the nuclear-cytoplasmic transport of proteins, their influence on tRNA localization was investigated. It was thus found that tRNA transport depends on the nuclear pool of RanGTP (Izaurralde et al., 1997). Soon after the responsible export factor was identified in vertebrates, and on

account of its role in tRNA metabolism it was termed Exportin-t (Xpo-t) (Arts et al., 1998a; Kutay et al., 1998). Sequence comparisons revealed that Xpo-t is a homolog of the yeast protein Los1 (Kutay et al., 1998), which was previously shown to affect processing of intron-containing tRNAs (Hopper et al., 1980; Hurt et al., 1987; Sharma et al., 1996; Simos et al., 1996). It is now clear that Xpo-t is a member of the karyopherin-β family which is regulated by the GTPase Ran. Xpo-t directly binds tRNAs in the nucleus by the cooperative interaction with RanGTP and it mediates the export through the nuclear pore complexes. In the cytoplasm, hydrolysis of RanGTP occurs by the action of the Ran GTPase-activating protein which leads to the release of the tRNA cargo.

Chemical and enzymatic footprinting assays (Arts et al., 1998b) and later the crystal structure of a RanGTP-Xpo-t-tRNA complex (Cook et al., 2009) demonstrated that Xpo-t contacts the phosphate backbone of tRNAs mainly at the acceptor stem and the T-arm which together form the so-called minihelix portion. In addition, the 5' end of the tRNA is buried in a binding pocket and its 3' end lies within a groove on the protein's surface. It is thus evident that Xpo-t binding *per se* subjects tRNAs to a quality control as it requires the structural elements of correctly processed and folded tRNAs. Because the anticodon stem is not contacted at all, the presence of a tRNA intron (which always occurs at this site) does not hinder binding of the export complex. This property is important since in yeast, end-matured, intron-containing tRNA intermediates need to be delivered to the tRNA splicing machinery which is localized in the cytoplasm. Until recently, only Los1/Xpo-t was experimentally shown to fulfil this task, however, the existence of at least one additional factor exporting intron-containing tRNAs was assumed (reviewed in Hopper, 2013). In this regard, a genome-wide screen of vast yeast mutant collections provided first evidence that Crm1, known in vertebrates as Exportin-1 (Xpo1) might have such an overlapping function (Wu et al., 2015). Crm1/Xpo1 is as well a member of the karyopherin-β family and is the major export factor of nuclear proteins and of several RNP complexes (Fornerod et al., 1997; Stade et al., 1997). In addition, the two components of the general mRNA export machinery, namely, Mex67 and Mtr2, known in vertebrates as NXF1 and NXT1, respectively, might also contribute to the export of intron-containing tRNAs (Wu et al., 2015). However, it is not yet clear to what extent and under which conditions this export pathway might be exploited.

As it will be described in more detail within section 1.1.8.2, tRNAs can be aminoacylated already within the nucleus for quality control purpose. In addition, cytoplasmic tRNAs are imported into the nucleus not only in response to stress conditions but also

constitutively (Grosshans et al., 2000; Shaheen and Hopper, 2005; Takano et al., 2005). Importantly, the positioning of the terminal nucleotide of the tRNA within the crystal structure of the ternary RanGTP-Xpo-t-tRNA complex does not preclude the presence of an amino acid (Cook et al., 2009). In fact, a recent study demonstrated that Los1, the yeast homolog of Xpo-t, interacts with uncharged, as well as with aminoacylated, tRNAs (Huang and Hopper, 2015). Therefore, experimental evidence suggests that at least for certain tRNA Los1/Xpo-t is involved in the primary export of intron-containing tRNAs as well as in the export of mature tRNAs either in their aminoacylated or in the deacylated form.

Although Xpo-t/Los1 has been extensively shown to play the major role in trafficking tRNAs to the cytoplasm, the fact that Los1 yeast deletion strains have a normal growth phenotype (Hurt et al., 1987) suggests that other overlapping export and re-export pathways of mature tRNAs exist. Indeed, even before being identified as the canonical export factor of precursor miRNAs (pre-miRNAs) (Lund et al., 2004), it was found that Exportin-5 (Xpo5) is involved in tRNA export processes in a RanGTP-dependent manner (Bohnsack et al., 2002; Calado et al., 2002). In contrast to the Los1 deletion strain, the primary export of intron-containing tRNA intermediates is not impaired in yeasts lacking Msn5, the ortholog of Xpo5. Instead, mature tRNAs originating from intron-containing as well as intron-less tRNA genes accumulate in their nuclei (Murthi et al., 2010). It has been therefore proposed that Xpo5/Msn5 might be dedicated to the general export and re-export of charged tRNAs (Murthi et al., 2010; Huang and Hopper, 2015). Supporting this hypothesis is the fact that Xpo5 transfers the tRNA to the cytoplasm in a quaternary complex together with eEF1A, which is the eukaryotic elongation factor delivering aminoacylated tRNAs to the ribosome (Bohnsack et al., 2002; Calado et al., 2002; Huang and Hopper, 2015). It had been proven already in previous studies that the reduction of eEF1A levels leads to nuclear accumulation of mature tRNAs (Grosshans et al., 2000), but at the time of these investigations the dependency on Xpo5/Msn5 was unknown. Still nowadays some properties of the aminacyl-tRNA-eEF1A-Xpo5-RanGTP complex remain puzzling. For example, first *in vitro* analyses indicated that Xpo5/Msn5 binds directly to the tRNA and, consequently, it interacts with eEF1A on a tRNA-dependent manner (Bohnsack et al., 2002; Calado et al., 2002). A recent *in vivo* study however opened the possibility that Xpo5/Msn5 might dimerize with eEF1A in the absence of tRNAs whereby eEF1A would be required to stabilize the binding to the tRNA (Huang and Hopper, 2015). This issue is very intriguing because structural studies of eEF1A (Andersen et al.,

2000) and of its prokaryotic ortholog EF-Tu (Nissen et al., 1995) demonstrate that they contact the aminoacylated tRNA at its 3’ end. Also the 3’ end of pre-miRNAs participates in the interaction with Xpo5 and is placed into a tunnel formed by the protein (Okada et al., 2009). All together, Xpo5/Msn5 and eEF1A should both be able to bind to the 3’ end of tRNAs. It remains a matter of speculation how this interaction, which at a first glance would seem to be mutually exclusive, looks like in the quaternary aminoacyl-tRNA-eEF1A-Xpo5-RanGTP complex. Interestingly, this export pathway not only ensures that mature tRNAs gain access to the cytoplasm and that eEF1A is constantly excluded from the nucleus (Bohnsack et al., 2002), but it seems also that specific transcription factors can be trapped on the aminoacyl-tRNA-eEF1A-Xpo5-RanGTP complex and are thereby transported out of the nucleus (Mingot et al., 2013).

1.1.8. Final Processing by Aminoacyl-tRNA Synthetases

1.1.8.1. Loading of the Cognate Amino Acid

In contrast to all biogenesis steps described so far, which rely on generalized recognition mechanisms, the enzymes involved in loading a given tRNA with its cognate amino acid are highly specialized and thus extremely accurate in order to avoid the deleterious potential of mischarged tRNAs. As a consequence, eukaryotes possess the complete set of 20 different ARS activities. Each of them is dedicated to the direct charging of a specific amino acid onto the same cytoplasmic tRNA isotypes, i.e., all those tRNA isoacceptors whose anticodon sequences decode the same amino acid. Of note, 18 ARSs are encoded by separate genes while a bifunctional ARS (EPRS) loads glutamic acid or proline on the cognate tRNAs using two distinct domains (Cerini et al., 1991). According to the standard nomenclature, all other cytoplasmic ARSs are named with the single-letter amino acid code followed by “ARS” (e.g., the alanyl-tRNA synthetase is reffered to as AARS).

The general aminoacylation reaction catalyzed by ARSs can be divided into two steps. First, the amino acid is activated at its carboxyl group by ATP generating an aminoacyl-adenylate intermediate. Successively, the amino acid is transferred to the 3’-terminal adenosine of the tRNA by which an ester bond is formed (reviewed in Ibba and Soll, 2000). Surprisingly, two different types of ARSs seem to have evolved independently from each other in order to fulfill this fundamental task. ARSs can therefore be divided into class I and class II types depending on the presence of specific sequence motifs. The active site of class I ARSs is characterized by a Rossmann fold, while class II ARSs

possess an anti-parallel β-fold. These structural domains do not only determine a different mode for binding the ATP and the tRNA substrate, but even more strikingly they affect the chemistry of the catalyzed reaction. Indeed, class I ARSs attach the amino acid to the 2' hydroxyl group of the tRNA adenosine end, while class II ARSs to the 3' hydroxyl group (reviewed in Sprinzl, 2006). In solution however, spontaneous transacylation occurs (Reese and Trentham, 1965; Griffin et al., 1966) resulting in a mixture of 2' and 3' aminoacylated tRNAs. Nevertheless, only tRNAs carrying the amino acid at the 3' position are able to accomplish all steps occurring during translation. Of particular note, the 2' hydroxyl group at the terminal adenosine has been shown to participate actively in the peptide bond formation (Weinger et al., 2004). It is therefore crucial that the tRNAs delivered to the ribosome are in the 3' aminoacyl configuration. Studies determining the kinetics of the transacylation reaction suggested that an enzymatic factor exists, which enhances this reaction and stabilizes the useful 3' aminoacylated tRNAs (Taiji et al., 1983). This 2'-3' isomerase activity has later been attributed to the elongation factor which binds aminoacylated tRNAs and delivers them to the A-site of the ribosomes (Taiji et al., 1985; Nissen et al., 1995; Safro and Klipcan, 2013).

It is plausible to assume that the aminoacylation of tRNAs is one of the most ancestral processes to have emerged during evolution and, consequently, these reactions would be expected also to be highly conserved. Instead, this is not at all the case (reviewed in Woese et al., 2000). As already mentioned, the charging of different tRNA isotypes is accomplished by two structurally unrelated classes of ARSs, suggesting that novel enzymes have evolved and ultimately have replaced, at least for some amino acids, the original ARSs. Even more stunning is the fact that archea and some bacteria exploit an indirect aminoacylation pathway to generate tRNA-Gln and in some cases also tRNA-Asn (reviewed in Tumbula et al., 1999). With some exceptions, these organisms lack the genes encoding the ARSs for direct aminoacylation. Instead, tRNAs charged with Gln (or Asn) are generated by tRNAs-Gln (or tRNAs-Asn) which are first misacylated by a non-discriminating glutamyl-ARS (or aspartyl-ARS) with Glu (or Asp). In a second reaction, the "precursor" amino acid is converted on the tRNA to Gln (or Asn) by an amidotransferase (Wilcox and Nirenberg, 1968). Importantly, this transamidase pathway is responsible for the generation of tRNA-Gln also in eukaryal organells, mitochondria and chloroplasts, which do not possess a Gln-ARS (Martin et al., 1977; Schön et al., 1988; Nagao et al., 2009). In general, human mitochondria possess a complete set of tRNAs (mt-tRNAs) which are transcribed from the mitochondrial genome, while most of

the mitochondrial ARSs are encoded by specialized genes on the nuclear DNA (reviewed in Diodato et al., 2014). An exception are Gly- and Lys-ARS which originate from one nuclear gene respectively encoding the cytoplamic as well as the mitochondrial protein isoforms (Shiba et al., 1994; Tolkunova et al., 2000).

It was realized quite early, that some cytoplasmic ARSs assemble together in a macromolecular multisynthetase complex (Bandyopadhyay and Deutscher, 1971), which encompasses at least nine ARS activities (Cirakoglu et al., 1985; Kerjan et al., 1994) together with three accessory proteins (Quevillon and Mirande, 1996; Quevillon et al., 1997, 1999). The latter have been termed aminoacyl tRNA synthetase complex-interacting multifunctional protein 1-3 (AIMP1-3), since they also exert diverse biological functions not related to the aminoacylation of tRNAs (Knies et al., 1998; Kim et al., 2003; Park et al., 2005).

The fact that different ARSs assemble together suggests that concentrating these enzymes in something which could be interpreted as “aminoacylation factories” might have some beneficial consequences. Indeed, it has been shown that tRNAs aminoacylated by the multisynthetase complex contribute mainly to protein synthesis, rather than those aminocylated by an ARS variant not present in high molecular mass complexes (Kyriacou and Deutscher, 2008). In addition, several ARSs, including the multisynthetase complex, have been found associated to the ribosome (Irvin and Hardesty, 1972; Ussery et al., 1977; Kaminska et al., 2009). These studies reinforced a hypothesis which was formulated in earlier times, namely, that for overcoming the great demand of aminoacylated tRNAs required during protein synthesis, tRNAs might be re-acylated immediately after supplying the amino acid for translation (Smith, 1975; Negrutskii and Deutscher, 1991, 1992; Stapulionis and Deutscher, 1995). In this regard, channeling tRNAs from the ribosome directly to ARSs and back might be an efficient strategy for maintaining adequate levels of charged tRNAs.

1.1.8.2. ARSs Safeguard Correct tRNA Maturation at Several Steps

The many sections of this introduction underline the great efforts spent by the cell in the production of functional tRNAs. It is thus fundamental to ensure that the final products are processed correctly whereby ARSs play an important proofreading role. Although their main function is exerted in the cytoplasm, ARSs are also present in the nucleus where they undertake the first aminoacylation reaction of the newly synthetized tRNAs. It

has been shown that those tRNAs which fail to be loaded with their cognate amino acids due to structural deficiencies are hindered from entering the cytoplasm and therefore do not join the translation cycle (Lund and Dahlberg, 1998; Sarkar et al., 1999).

Furthermore, ARSs safeguard the correct aminoacylation of tRNAs at several steps resulting in a great accuracy. First of all, each ARS is specialized in order to recognize its cognate tRNA by extensive interactions not only with the anticodon, but also with the acceptor stem and in particular with the discriminator base. Also, features which are characteristic for certain tRNA isoacceptors are efficiently recognized by these enzymes. In this regard, specific nucleotide modifications have been shown to signal the identity of the tRNA (reviewed in Ibba and Soll, 2000). ARSs are required to face an even greater challenge when discriminating between cognate and similar non-cognate amino acids, as these can differ in as little as a single methyl group. It was noticed quite early, that ARSs are able to hydrolyse non-cognate aminoacyl-adenylate intermediates avoiding the likely event of misacylating an incorrect tRNA (Baldwin and Berg, 1966). Studies performed over several years revealed that ARSs can be equipped with two intrinsic editing activities. The first is in fact directed against the aminoacyl-adenylate intermediate itself, so that the wrong amino acid is prevented from loading. This mechanism is referred to as “pre-transfer proofreading”. The “post-transfer proofreading” mechanism intervenes if a tRNA has been misacylated avoiding its release from the enzyme. Instead, it is transferred to the editing site which removes the incorrect amino acid (reviewed in Jakubowski, 2012). Only those aminoacyl-tRNAs passing all these checkpoints are finally used by the ribosomes to assemble the polypeptides which make up the proteomic landscape of the cell.

1.1.9. Quality Control and Turnover of tRNAs

Several enzymes involved in the biogenesis of tRNAs fulfill not only their actual task, they also monitor the quality of the tRNA intermediates with which they interact. As mentioned already, this is the case for the tRNA nucleotidyltransferase, Xpo-t and ARSs. The former protein adopts an ingenious strategy for actively interrogating the structure of its substrates. Instable tRNAs are thereby marked with a CCACCA end which finally leads to their degradation (see section 1.1.5 for more details).

Instead, Xpo-t (Cook et al., 2009) and ARSs (Lund and Dahlberg, 1998; Sarkar et al., 1999; and reviewed in Ibba and Soll, 2000) achieve a quality control function due merely

to their structural properties which allow stringent binding of correctly matured and folded tRNAs. The fate of those tRNAs that do not pass such checkpoints is still unclear. Do proteins exist that specifically recognize misprocessed tRNAs and channel them into degradation pathways? An alternative possibility might hold true, considering that newly synthesized transcripts are constantly threatened by degradation, for example through the nuclear surveillance pathway (reviewed in Wichtowska et al., 2013). In fact, it has been reported that ~50% of all newly transcribed tRNA precursors are degraded by the exosome (Gudipati et al., 2012; Schneider et al., 2012). From this perspective, aberrant tRNAs might be easy prey for exonucleases due to their inefficient protective interaction with processing enzymes (Copela et al., 2008). Indeed, experimental evidence revealed that pre-tRNAs are processed more slowly if they do not possess certain modifications resulting in degradation by the concerted action of the TRAMP and of the nuclear exosome complexes (see section 1.1.4.3 and Kadaba et al., 2004).

Importantly, tRNAs quality is not only controlled during their production, but also at their mature state. Although tRNAs are extremely stable with half-lives ranging from hours to days (Weber, 1972; Kanerva and Mäenpää, 1981) a pathway has been identified over the last decade that is dedicated to the degradation of aberrant, mature tRNAs (Alexandrov et al., 2006). Most of the studies have been performed in yeast strains lacking enzymes responsible for certain tRNA modifications which showed remarked growth phenotypes when they were shifted to higher temperatures (Alexandrov et al., 2006; Chernyakov et al., 2008; Whipple et al., 2011; Turowski et al., 2012). It was understood that under these conditions the aminoacylation levels as well as the steady-state levels of hypomodified mature tRNAs decreased very rapidly (reduction by 50% within 30 min). For this reason the newly identified pathway acting on mature tRNAs was termed rapid tRNA decay (RTD) and was shown to by independent from the genes involved in the nuclear surveillance, i.e., the TRAMP and the exosome complexes. Also, the degradation of tRNAs seemed to be uncoupled from translation since it occurred even during cycloheximide treatment (Alexandrov et al., 2006). Later analyses unraveled the molecular components involved in RTD, namely, the two 5'-3' exonucleases Xrn1 and Xrn2 (also known as Rat1 in yeast) which localize, respectively, in the cytoplasm and the nucleus (Chernyakov et al., 2008).

An important topic for deciphering the mechanistic details of RTD concerns its substrate specificity. It was clear that the lack of modifications itself is not sufficient to trigger RTD, as only a subset of tRNAs known to possess the missing modifications were

targeted by Xrn1/2 (Alexandrov et al., 2006; Chernyakov et al., 2008). Careful analyses revealed that those tRNA species with less stable acceptor and T-stems were preferred RTD substrates. In other words, the structural stability of such tRNAs relies more on certain modifications, and if these are lacking, the tRNAs are easily degraded, most likely because their 5' end is more accessible for the exonucleases (Whipple et al., 2011). These observations were later confirmed by a high-throughput mutation screening, which underscored the importance of the tRNA acceptor stem for conferring resistance to RTD. However, an unexpected result emerged, since mutations distributed all over the tRNA sequence, and not only within the acceptor and T-stem, affected the susceptibility to RTD-mediated degradation. The overall integrity of tRNAs seems therefore to be monitored. Still, it is not clear how this is detected in the case of mutations which apparently should not alter the tertiary structure of tRNAs (Guy et al., 2014).

Another intriguing aspect is that RTD might selectively act on aminoacylated tRNAs as this pool was affected under the different experimental setups, while the levels of deacylated tRNAs remained constant (Alexandrov et al., 2006; Chernyakov et al., 2008). Several observations support this hypothesis. First of all, RTD competes with eEF1A for binding of aminoacylated tRNAs, whereby overexpression of eEF1A inhibits tRNA degradation (Dewe et al., 2012). In addition, end-extended tRNA species, which are not charged with an amino acid, are not targeted by Xrn1 (Kramer and Hopper, 2013).

As mentioned previously, Xrn1 and Xrn2 are differentially localized within the cell. Xrn1 is involved mainly in the degradation of cytoplasmic mRNAs, while Xrn2 contributes in the nucleus to the processing of several RNAs, the removal of aberrant transcripts as well as Pol II transcription termination (reviewed in Houseley and Tollervey, 2009; Wolin et al., 2012). Deletion of both exonucleases has an additive effect in the context of RTD, suggesting that both contribute to tRNA degradation (Chernyakov et al., 2008). The reason for the requirement of exonucleases localizing in both cell compartments remains, nonetheless, largely elusive. Obviously, Xrn1 might be the last instance catching and removing aberrant tRNAs which passed all the previous quality control checkpoints as well as mature tRNAs which acquired destabilizing damages over time (Chernyakov et al., 2008; Kramer and Hopper, 2013). The implications for Xrn2 and nuclear tRNA turnover, instead, are more sophisticated. Retrograde tRNA import has been well documented during the last years. Although tRNAs have been suggested to be constitutively re-imported, nuclear tRNA accumulation is acquired during cellular stress conditions (Shaheen and Hopper, 2005; Shaheen et al., 2007; Murthi et al., 2010;

Miyagawa et al., 2012). To date, only spare evidence indicates that Xrn2 might specifically degrade the mature initiator tRNA-Met following its accumulation in the nuclei of heat-stressed HeLa cells (Watanabe et al., 2013). Additionally, some tRNAs might reach the cytoplasm before all required nuclear processing events were fulfilled. Retrograde transport would thus act as a backup mechanism to return tRNAs which were precociously exported. Back in the nucleus, such tRNAs might get a second chance for maturation or, alternatively, they might be eliminated (Kramer and Hopper, 2013). However, a direct role for Xrn2 in such a context has not been proven yet.

1.1.10. Many Faces of tRNA Fragments

The recent advances in the field of next generation sequencing significantly boosted knowledge regarding the widespread occurrence of stable tRNA-derived fragments (tRFs). They can be grouped into different categories according to the region from which they originate within the longer tRNA transcripts (Figure 1.7).

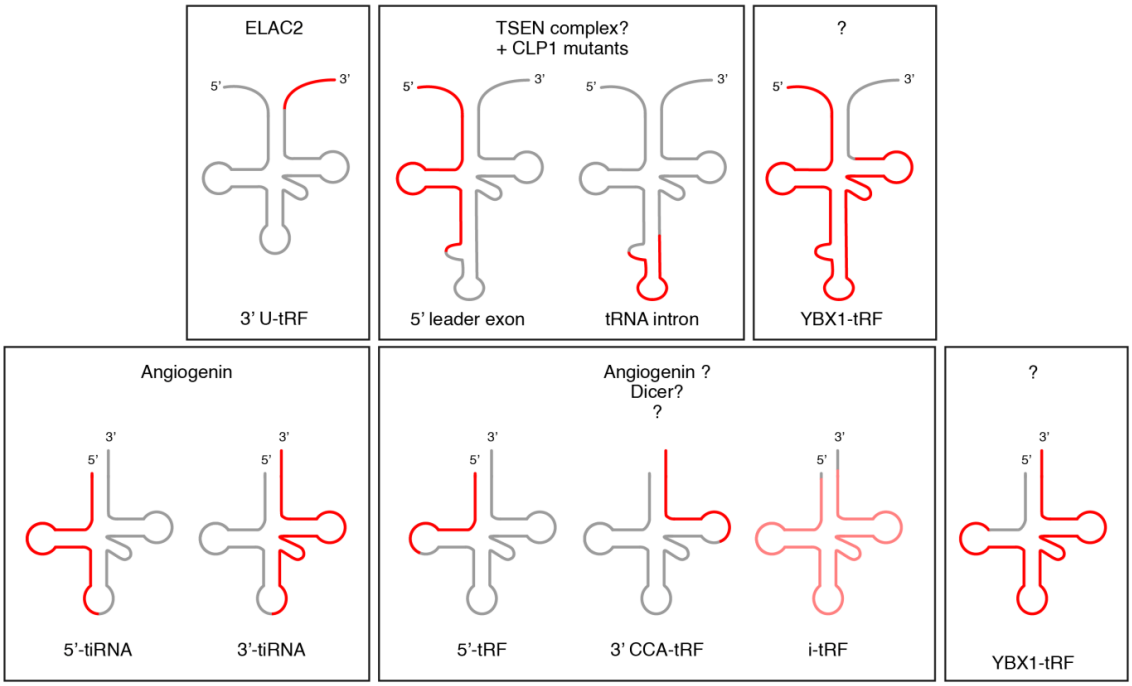

Figure 1.7: Different Types of Fragments Originate from Pre-tRNAs (upper panels) or Mature tRNAs (lower panels). Possible processing enzymes are indicated at the top of the panels. The regions of the tRNA from which the fragments derive is indicated in red. 3' U-tRF are trailers of pre-tRNAs terminating on a U-stretch. 5' leader exon fragments and tRNA introns accumulate if splicing is impaired. Some tRFs derived from intron-containing pre-tRNAs or mature tRNAs interact with YBX1 (YBX1-tRF). TRNA-derived stress-induced small RNAs (tiRNAs) are generated by cleavage within the anticodon loop. 5'-tRFs begin at the 5' end of mature tRNAs, 3' CCA-tRFs usually begin within the T-loop and all of them terminate with the CCA end. Internal tRF (i-tRF) can originate from several regions but per definition do not span the 5' and 3' CCA ends. This is represented by a pale red coloring. Figure adapted from Megel et al., (2015), nomenclature of most fragments according to Keam and Hutvagner (2015).

Several lines of evidence indicate that at least some tRFs are not just transient by-products of tRNA turnover, but are a distinct class of sRNAs with regulatory potential. In general, the processing of tRNAs into smaller fragments seems to be conserved across species (Kumar et al., 2015) and the expression levels of tRFs does not always correlate with the abundance of the tRNAs from which they originate. Their production exhibits site-specific patterns, and the resulting fragments have characteristic lengths suggesting the involvement of specialized enzymes (Figure 1.7) (Cole et al., 2009; Li et al., 2012; Telonis et al., 2015). Finally, the functionality of certain tRFs has been proven (Ivanov et al., 2011; Goodarzi et al., 2015; Sharma et al., 2016).

Nevertheless, the major challenge still consists in translating the vast amount of descriptive data into functional networks. 5'-tRFs and 3' CCA-tRFs, for example, are easily defined by sequence analysis; however, according to the current literature their biogenesis as well as their function seem a potpourri of distinct processes (reviewed in Gebetsberger and Polacek, 2013; Keam and Hutvagner, 2015). A critical examination of the published studies is therefore required to clarify the reliability of the proposed models. In particular, at the beginning, research on tRFs was driven by the discovery of several non-canonical miRNAs, and some of these studies were probably biased by assigning them miRNA-like characteristics (Cole et al., 2009; Haussecker et al., 2010).

1.1.10.1. Pre-tRNAs as an Early Source of tRFs

Some tRFs can promptly be generated from newly transcribed pre-tRNAs and are, to some extent, a physiological consequence of tRNA maturation (Figure 1.7). This is the case for 3' U-tRFs which have been detected in mammalian cell lines. They are the 3' trailers resulting from RNase Z cleavage and Pol III transcription termination. Hence, they end on the typical U-stretch. So far, evidence for the functionality of 3' U-tRFs has been achieved only for a fragment originating from a pre-tRNA-Ser, which was shown to positively affect cell proliferation rates (Lee et al., 2009). The molecular mechanisms underlying this effect are still unknown. Some indication exists that 3' U-tRFs might associate with Argonaute (Ago) proteins, the key players of miRNA-mediated post-transcriptional gene silencing. However, their relative preference for Ago3-4 compared to Ago1-2, as well as their inability to repress target constructs, clearly indicate that 3' U-tRFs act in a different way than miRNAs (Haussecker et al., 2010). Thus they might interact primarily with factors yet to be identified.

In addition, different types of fragments from intron-containing pre-tRNAs have been detected recently in cells with mutations in the *CLP1* gene (Hanada et al., 2013; Karaca et al., 2014). Human patients bearing such mutations, as well as related animal models, show severe phenotypes ranging from neuromuscular disorders to progressive and widespread neurodegeneration. CLP1 has been described as the first mammalian RNA kinase (Weitzer and Martinez, 2007) and was found to interact with the TSEN complex which cuts off the introns of pre-tRNAs (Paushkin et al., 2004). Even more importantly, different *CLP1* mutations turned out to affect the integrity of the TSEN complex and thereby resulted in impaired pre-tRNA cleavage. Although some debate exists concerning the effect of *CLP1* mutations on the steady-state levels of mature tRNAs (Karaca et al., 2014; Schaffer et al., 2014), it was proven that the accumulation of pre-tRNA fragments possesses cytotoxic potential. These harmful sequences were identified in a mouse model and consisted of the 5' tRNA exon half of some pre-tRNAs still containing the 5' leader (Hanada et al., 2013). Also, spliced introns were found to be enriched in fibroblasts derived from affected patients (Karaca et al., 2014).

As illustrated in section 1.1.6.2, the text-book knowledge concerning removal of tRNA introns in vertebrates implies that rejoining of the two tRNA parts is achieved via the 3'-phosphate ligation pathway (Filipowicz and Shatkin, 1983; Filipowicz et al., 1983; Laski et al., 1983). This strategy does not require the phosphorylation of the splicing intermediates, and thus it should not depend on the kinase activity of CLP1. Nevertheless, the mass of evidence provided in the studies mentioned above indicates that an alternative ligation strategy resembling the 5'-phosphate ligation pathway of fungi and plants might be present as well in vertebrates (Hanada et al., 2013; Karaca et al., 2014; Schaffer et al., 2014). Further investigations are required to unravel the interplay between these different splicing mechanisms and to clarify whether toxic fragments might also occur in *CLP1* wild type conditions.

1.1.10.2. Mature tRNA Halves

The most distinct class of tRNA-derived fragments consists of those generated by cleavage within the anticodon loop, resulting in two similarly long halves (Figure 1.7). Interestingly, tRNA halves have been observed already in the 70's appearing very rapidly in *E. coli* after infection by bacteriophage T4 (Yudelevich, 1971). Later works revealed that tRNA cleavage was mediated by a specific endoribonuclease and was part of an

antiviral response of the host leading to the suicide of infected cells (Levitz et al., 1990). It is not surprising that effective tRNA cleavage has a potent cytotoxic effect. This is exploited as well by some bacteria (Ogawa et al., 1999; Tomita et al., 2000) and yeast species (Lu et al., 2005; Klassen et al., 2008; Chakravarty et al., 2014) which secrete so-called ribotoxins to kill surrounding competitor cells.

TRNA halves have been identified in eukaryotes also under physiological conditions. This is the case for example for the recently described Sex HOrmone-dependent TRNA-derived RNAs (SHOTRNAs), which are expressed at high levels in sex hormone-dependent breast and prostate cancer cells (Honda et al., 2015). However, most of the studies performed so far focussed on tRNA halves induced in response to cellular stress, and the resulting fragments have been therefore termed tRNA-derived stress-induced small RNAs (tiRNAs) (Lee and Collins, 2005; Jöchl et al., 2008; Thompson et al., 2008).

The endonuclease Rny1, which is responsible for the production of tiRNAs in yeast, is a member of the RNase T2 family (Thompson and Parker, 2009). In humans, instead, tRNAs are sliced into halves by angiogenin (ANG), which is unrelated to Rny1 and is a member of the RNase A family (Saxena et al., 1992; Fu et al., 2009; Yamasaki et al., 2009). ANG has been long known as a secreted growth factor with potent angiogenic properties, and was first isolated from the supernatant of an adenocarcinoma cell line (Fett et al., 1985). In the following years, the broad spectrum of ANG functions started to be unravelled and its ribonucleolytic activity was discovered. However, ANG is considerably less active compared to other RNases of the same family (reviewed in Sheng and Xu, 2016) and in fact only a small proportion of the general tRNA pool, less than 5%, are targeted during stress responses (Thompson et al., 2008; Pang et al., 2014). Due to this rather moderate effect on tRNA levels, ANG-mediated cleavage does not exert the same harmful potential as ribotoxins. On the contrary, the production of tiRNAs turned out to be beneficial for the cell while coping with several kinds of stress. Interestingly, tiRNAs are involved in distinct mechanisms, which might reflect a specialization of the fragments originating from different tRNA isoacceptors.

One of these cytoprotective pathways was discovered following hyperosmotic stress of mouse embryonic fibroblasts or following excitotoxic stress of human motorneurons. Apoptosis is induced under these conditions and an early event triggered by the resulting signaling cascade is the release of cytochrome c from the mitochondria (Bevilacqua et al., 2010; Ivanov et al., 2014). Biochemical *in vivo* studies revealed that certain tiRNAs produced by ANG bind to cytochrome c in the cytoplasm, and on this account they halt

the further progression of apoptosis. Thus, tiRFs can function as anti-apoptotic molecules (Saikia et al., 2014).

Even more profound is the effect mediated by tRNA halves in the regulation of translation following induction of oxidative stress, heat shock, or ultraviolet irradiation. Indeed, certain 5'-tiRNAs, but not their 3' counterpart, were proven to promote phospho-eIF2-independent arrest of translation and assembly of stress granules (Yamasaki et al., 2009; Emara et al., 2010). Subsequent studies revealed that these 5'-tiRNAs are able to displace eIF4G, a component of the eIF4F translation initiation complex, from the 5' cap of mRNAs. It turned out that the inhibitory property of these 5'-tiRNAs, mainly derived from tRNA-Ala and tRNA-Cys, depends on the presence of the D-loop and on a common 5'-terminal oligoguanine motif (Ivanov et al., 2011). The latter has been shown to adopt a so-called G-quadruplex structure which is essential for the activity of 5'-tiRNAs (Ivanov et al., 2014). Also, the G- stretch was shown to allow specific interaction with YBX1, a well-known RNA-binding protein (RBP) (Ivanov et al., 2011, 2014). Recent findings suggest that the binding of 5'-tiRNAs to YBX1 is not required for displacement of eIF4F and therefore for translational repression. Instead, depletion of YBX1 results in the inability of cells to assemble 5'-tiRNAs-dependent stress granules (Lyons et al., 2016).

Interestingly, an independent study identified another class of tiRNAs interacting with YBX1 in breast cancer cells. These YBX1-interacting tRFs (YBX1-tRFs) were longer than conventional tRNA halves and were generated from an intron-containing pre-tRNA-Tyr as well as from the 3' part of several mature tRNAs (Figure 1.7). YBX1-tRFs were induced under hypoxic conditions in breast cancer cells, however not in highly metastatic subpopulations of the parental cell line. Although it has not been addressed whether their production depends on ANG-mediated cleavage, the consequences of their accumulation have been characterized. It appears that these rather unconventional tRNA-derivates compete, via a novel sequence motif, with the 3' UTRs of several mRNAs for binding to YBX1. The upregulation of YBX1-tRFs leads to the displacement of the RBP from its target transcripts which finally results in their destabilization. This regulation has been proposed to modulate oncogenesis in breast cancer and seems to be avoided by highly metastatic cells which do not boost YBX1-tRFs production (Goodarzi et al., 2015).

In summary, the ANG-tiRNA-axis might have evolved as a protective system to adapt and to fine-tune the cellular response to stress. As it is often the case, viruses are able to turn molecular pathways of the host to their own advantage and this was proven to occur also during infections by the respiratory syncytial virus (RSV) with ANG-dependent

tiRNAs. Initially, an increased production, in particular, of 5'-tiRNAs was described following RSV infection of a lung epithelial cell line (Wang et al., 2013). Later analyses demonstrated that a specific, RSV-induced 5'-tiRNA interacts by sequence complementarities with the mRNA of apolipoprotein E receptor 2 (APOER2). This finally results in the post-transcriptional repression of APOER2 which in turn promotes RSV replication (Deng et al., 2015). Although the underlying molecular mechanism is still unknown, it should be noted that several characteristics of 5'-tiRNA evidence that this regulation occurs in a different way than miRNA-mediated repression (Wang et al., 2013; Deng et al., 2015).

All the aforementioned examples of tRFs production rely on cleavage within the anticodon loop which thus seems to be favoured for endonucleolytic cutting. Interestingly, the tRNAs derived from cells lacking either NSun2 or TRDMT1 (also known as DNMT2), two tRNA methyltransferases, turned out to be more susceptible to ANG-mediated cleavage (Schaefer et al., 2010; Blanco et al., 2014). Methylation of specific nucleotides therefore has a protective effect which was said to depend on the influence of these modifications on the accessibility of the anticodon loop (Schaefer et al., 2010). In addition, substrate specificity of ANG does not depend on the tRNA structure *per se*, but is restricted to single-stranded RNA. Cutting occurs preferentially after pyrimidine bases which are followed by adenine. The highest ribonucleolytic activity is thereby directed toward a CA substrate sequence (Russo et al., 1996). These characteristics pointed attention towards the universal, single-stranded, 3' CCA end of tRNAs. It was shown in fact that it is cut by ANG very rapidly after induction of oxidative stress resulting in general translational repression (Czech et al., 2013). Finally, ANG might also be involved in the generation of other tRFs beside tiRNAs, since *in vitro* assays performed with the recombinant protein revealed its ability to cleave as well within the loop of the T-arm (Li et al., 2012).

1.1.10.3. Puzzling Diversity of tRFs

The majority of tRFs expressed under normal conditions probably arose from what previously was engaged as functional tRNAs. Supporting this hypothesis is the fact that the 5' and 3' ends, respectively, of 5'-tRFs and 3' CCA-tRFs, are identical to those of mature tRNAs. In addition, a study performed in the ciliate *Tetrahymena thermophila* demonstrated, by two-dimensional thin-layer chromatography, that a particular fraction of

3’ CCA-tRFs possesses base modifications which are also present in the corresponding region of the full-length tRNAs (Couvillion et al., 2012). Finally, in human breast cancer cells the 3’ half of the aforementioned SHOTRNAs carry an amino acid at their 3’ end (Honda et al., 2015). Still, the trait which triggers the production of the different tRFs from, to all appearances, functional tRNAs is unknown, while the majority of these molecules remains intact. One possibility could be that, under certain conditions, a subpopulation of tRNAs acquires damages which cause severe conformational changes. These would consequently provoke ribonucleolytic processing but through a pathway unrelated to the total degradation achieved by the RTD (Mishima et al., 2014).

This point leads to another matter of debate, namely, the identification of the enzymes involved in the biogenesis of 5’-tRFs, 3’ CCA-tRFs and the recently described internal tRFs (i-tRFs) (Telonis et al., 2015). As already mentioned in section 1.1.10.2, various recombinant RNases including ANG, were able to fragment a tRNA substrate *in vitro*, and they gave rise to a processing pattern resembling the endogenous tRF content of a cell (Li et al., 2012). Unfortunately, the physiological role of these ribonucleases in the generation of 5’-tRFs, 3’ CCA-tRFs or i-tRFs requires further confirmation.

Early studies dedicated to the global profiling of sRNAs have pointed attention towards another protein which might be involved in the biogenesis of tRFs, i.e., the RNase III enzyme Dicer, the same endonuclease that finalizes the maturation of miRNAs (Cole et al., 2009; Haussecker et al., 2010; Maute et al., 2013). However, an aspect which has not been well addressed in these reports is that tRNAs fold in the typical cloverleaf structure which does not correspond to a canonical double-stranded Dicer substrate (Zhang et al., 2002). Although it is conceivable that pre-tRNAs might adopt alternative secondary structures (Babiarz et al., 2008), it is not clear how tRNAs, which have undergone all maturation events, should refold into double-stranded hairpins to enable cleavage by Dicer. Indeed, other reports clearly indicate that at least some tRFs are not generated by the endonucleases involved in miRNA biogenesis since they can be detected in Drosha and/or Dicer knockout cell lines (Li et al., 2012; Kumar et al., 2014).

Despite their mysterious production, tRFs were reported by several groups to associate with members of the AGO clade (Cole et al., 2009; Haussecker et al., 2010; Burroughs et al., 2011; Li et al., 2012; Maute et al., 2013; Keam et al., 2014; and reviewed in Shigematsu and Kirino, 2015). To some extent, their potential to behave like miRNAs was demonstrated by different artificial assays (Haussecker et al., 2010; Li et al., 2012) but, also in this regard, contradictory results were obtained (Thomson et al., 2014).

Nevertheless, the 3’ CCA-tRFs termed CU1276, which is derived from a tRNA-Gly, is expressed in human B cells and some lines of evidence indicate that CU1276 is a *bona fide* miRNA. It associates with Ago proteins and is able to repress an endogenous target mRNA thereby modulating proliferation and DNA damage responses. Interestingly, when comparing the enrichment of CU1276 with overexpressed Ago1-4 proteins, interaction with Ago2 seemed to be less favored compared to Ago1, Ago3 and Ago4 (Maute et al., 2013). Similar observations were done by different groups analyzing other tRFs (Haussecker et al., 2010; Kumar et al., 2014). Also, it emerged that Ago proteins tend to enrich tRFs which are shorter than canonical miRNAs, i.e., ≤ 21 nucleotides long (Haussecker et al., 2010; Telonis et al., 2015). Of note, interaction of Ago2 with certain full-length tRNAs or nascent tRNA transcripts was reported as well (Maniataki and Mourelatos, 2005; Woolnough et al., 2015).

Altogether, it is indisputable that some tRFs are loaded into Ago proteins, though this interaction displays many differences compared to miRNAs. Further investigations are required to clarify to what extent Ago-tRF associations are dedicated to the sequence-specific regulation of gene expression or, alternatively, might participate to pathways unrelated to miRNA-like functions.

In fact, several findings emerged during the last years which corroborate the idea that tRFs also act independently of the miRNA machinery. One of these examples resembles the inhibitory effect on translation achieved by 5’-tiRNAs during stress responses (see section 1.1.10.2). In this case, translational repression is mediated by 5’-tRFs via a distinct mechanism that does not require any complementarity to the regulated mRNAs (Sobala and Hutvagner, 2013) and probably depends on the association of such 5’-tRFs with the multisynthetase complex (Keam et al., 2017). In contrast, a specific 3’ CCA-tRF originating from tRNA-Leu-CAG was recently shown to positively affect the translation of two ribosomal proteins, i.e., RPS15 and RPS28. Although the exact mechanisms leading to the enhanced translation are still elusive, the 3’ CCA-tRF excerpts its function in virtue of the sequence complementarity to the mRNAs encoding for the two ribosomal proteins (Kim et al., 2017).

TRFs are also able to influence gene expression at the transcriptional level. Following the identification of several 5’-tRFs in mammalian sperm, their functional role was analyzed in embryonic stem cells and in zygotes. It turned out that inhibition of a specific tRF derived from tRNA-Gly resulted in the direct upregulation of certain genes (Sharma et al., 2016). Thus, the tRF content of sperms might be markedly involved in the regulation of

early developmental processes (Chen et al., 2016; Sharma et al., 2016). The expression of these derepressed transcripts was previously shown in pre-implantation embryos to be driven by activation of endogenous MuERV-L retroelements (Macfarlan et al., 2012). No mechanistic information is available at the moment that might explain the effect of the tRNA-Gly-derived tRF, but an intriguing finding was reported some years ago. It was noticed that 3' CCA-tRFs are often complementary to endogenous retroviral LTR elements (Li et al., 2012), and recent findings confirmed that 3' CCA-tRFs inhibit the replication of endogenous retroviral sequences (Schorn et al., 2017).

Another important insight revealed in the study by Sharma et al. (2016) is the fact that the tRFs present in the mature sperm are probably derived from an external source only at a late stage of spermatogenesis. Indeed, it is long known that, while travelling through the epididymis, sperms fuse with extracellular vesicles called epididymosomes (reviewed in Sullivan, 2015). These are likely to deliver their high tRF-content to the sperm cells (Sharma et al., 2016). Secretion of tRFs is certainly not restricted to the reproductive tract, as they were already detected in different kind of vesicles (Guzman et al., 2015; Li et al., 2015), as well as circulating in serum (Dhahbi et al., 2013) and in urine (Speer et al., 1979; Zhao et al., 1999). In addition, the vast amount of RNA profiling data sets indicates that, compared to healthful samples, tRFs are differentially expressed in several cancer types as well as during viral infections (Speer et al., 1979; Maute et al., 2013; Wang et al., 2013; Goodarzi et al., 2015; Guo et al., 2015; Guzman et al., 2015; Selitsky et al., 2015; Telonis et al., 2015; Pekarsky et al., 2016). Owing to this information and to the recent progress in unraveling their molecular functions, tRFs are becoming more and more the focus of clinical research. These fascinating molecules could soon be used as biomarkers or possibly as drug targets for cancer therapy. Also in this regard, our knowledge will benefit from getting a deeper view into this new and puzzling field of tRNA biology.

1.2. The miRNA Pathway

MiRNAs are sRNAs that guide post-transcriptional regulation of gene expression by targeting miRNA-induced silencing complexes (miRISCs) to specific mRNAs. This is achieved by sequence complementarity between the miRNA and, in most cases, the 3' UTR of the target mRNA. Subsequently, miRISC mediates translational repression as well as destabilization of the bound transcripts. By doing so, miRNAs are important regulators of developmental processes and cellular homeostasis. Their function is frequently perturbed in cancer and in several human pathologies contributing to the progression of these diseases.

1.2.1. The Nuclear Part of MiRNA Biogenesis

Canonical miRNAs are transcribed by Pol II (Lee et al., 2004) and they can originate from independent gene units but very often they are embedded within intronic regions of protein-coding mRNAs as well as ncRNAs. Also, in latter cases transcription can be either coupled to host gene expression or can be driven by independent promoters (reviewed in Finnegan and Pasquinelli, 2013). Different miRNAs tend to cluster together within the genome and, consequently, some primary-miRNAs (pri-miRNAs) are expressed as polycistronic transcripts. In any case, miRNAs are embedded within hairpin structures of the pri-miRNA. A multi-step processing pathway consisting of two endonucleolytic cleavage events is therefore required to liberate the ~22 nt long mature miRNAs (Bartel, 2004; Kim, 2005; Kim et al., 2009) (Figure 1.8).

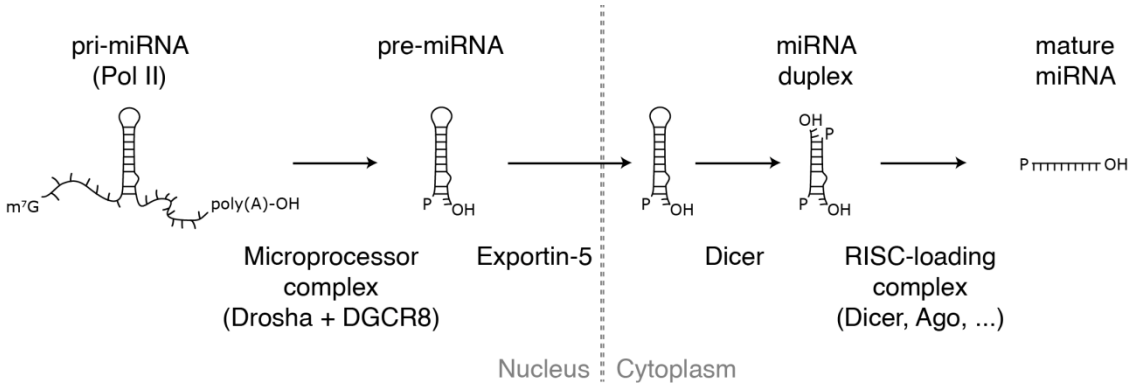

Figure 1.8: The Biogenesis of Canonical MiRNAs Occurs via Several Processing Steps. Schematic representation of the events and of the proteins which are required for the maturation of miRNAs. The key characteristics of the secondary structure of the different miRNA processing intermediates are indicated as well.

The first reaction occurs in the nucleus and is catalyzed by the Microprocessor complex. It is composed of the RNase III enzyme Drosha and a cofactor called Dgcr8 in vertebrates, and Pasha in other organisms (Denli et al., 2004; Gregory et al., 2004). The hairpin structures recognized by the Microprocessor complex typically have a 35 bp long stem which is closed by a loop and is flanked by single-stranded segments at both sides. It is long known that Dgcr8 is a RBP and that Drosha endonucleolytically cleaves the hairpin ~22 bp away from the apical loop / 11 bp away from the basal junction. However, over the last decade a debate was ongoing concerning the features which determine the site of Drosha cleavage (Zeng et al., 2005; Han et al., 2006; Ma et al., 2013). A detailed mechanistic insight was achieved only recently after succeeding to express and purify the recombinant Microprocessor complex (Nguyen et al., 2015). These findings were further implemented by the subsequent description of Drosha's crystal structure (Kwon et al., 2016). Taken together, it is now clear that Drosha forms a heterotrimeric complex together with two Dgcr8 proteins. Drosha itself acts as a ruler by binding to the basal junction and positioning its two catalytic domains in such a manner that after cutting a typical pre-miRNA with a two nt overhang at the 3' end is released. A preference for a UG motif spanning the junction between the basal single-stranded region and the double-stranded regions of the hairpin was also observed. Accordingly, the Dgcr8 dimer binds to the apical part and has a strong affinity for a UGU sequence just at the beginning of the loop.

Following processing by Drosha, the resulting pre-miRNA is exported to the cytoplasm by Xpo5, a member of the karyopherin-β family of nucleocytoplasmic transport factors. As already mentioned in section 1.1.7, the ability of Xpo5 to export RNAs from the nucleus was first described independently from its role in the biogenesis of miRNAs (Bohnsack et al., 2002; Brownawell and Macara, 2002; Calado et al., 2002). Only later studies demonstrated that Xpo5 is mainly dedicated to the RanGTP-dependent transfer of pre-miRNAs to the cytoplasm (Yi et al., 2003; Bohnsack et al., 2004; Lund et al., 2004). Structural studies revealed that the Xpo5-RanGTP complex surrounds the stem of pre-miRNAs, whereby both termini of the pre-miRNA, in particular the 3' end, are completely shielded in a tunnel-like structure (Okada et al., 2009). Thus, Xpo5 might not only account for the export of pre-miRNAs but also for their protection from exonucleolytic degradation or trimming (Yi et al., 2003). Indeed, evidences provided in a recent publication confirmed this hypothesis. However, the same study also demonstrated that Xpo5 is not essential for the biogenesis of miRNAs, since they were generated in

Xpo5 knockout cells, even though at lower levels compared to wild type cells (Kim et al., 2016). So far, it is not clear inasmuch alternative maturation pathways might co-exist with the Xpo5-dependent miRNA production or if they serve as a backup mechanism exclusively when the canonical pre-miRNA export machinery is missing.

1.2.2. The Cytoplasmic Part of MiRNA Biogenesis

Following export, pre-miRNAs are subjected to a second endonucleolytic maturation step, which removes the apical loop. This processing event is performed by Dicer (Hutvágner et al., 2001), a multidomain protein, which is also a member of the RNase III family (Lau et al., 2009; Wang et al., 2009). The human genome encodes for a single Dicer protein, which is specialized for production of miRNAs. Also in this case, the enzyme itself acts as a molecular ruler that determines the site of the endonucleolytic cleavage, occurring ~22 nt apart from the open end of double-stranded stem. It has been shown that this exact processing is achieved by positioning the phosphorylated 5' end of the pre-miRNA into a binding pocket located in a RNA-binding domain called PAZ (Park et al., 2011; Tian et al., 2014). The PAZ domain forms one end of the L-shaped Dicer protein (Lau et al., 2012) and it is located in a fixed distance relative to the catalytic center, which consists of two neighboring RNase III domains (Zhang et al., 2004). This structural organization ultimately determines the position where the double-stranded stem is going to be cleaved. Importantly, the PAZ domain also recognizes the 3' end of pre-miRNAs, which have a typical two nt overhang generated by the preceding Drosha processing (Tian et al., 2014). Thus, substrates with a phosphorylated 5' end and with a two nt 3' overhang are most efficiently processed by human Dicer (Park et al., 2011).

Some intriguing aspects concern the N-terminal ATPase/RNA helicase domain, which forms, at the opposite side of the L-shaped Dicer structure, a clamp-like end holding the bound pre-miRNA by interactions with the loop (Lau et al., 2012). Of note, depending on the organism, some specialized Dicer proteins exist that prefer to process long double-stranded RNAs with blunt ends rather than pre-miRNAs. Indeed, the helicase domain was shown to account for this selectivity (Soifer et al., 2008; Welker et al., 2011; Flemr et al., 2013; Taylor et al., 2013; Sinha et al., 2015). Recent cryo-EM structures of the *Drosophila melanogaster* Dicer-2 enzyme shed light onto this aspect and revealed a "threading" mechanism that enables the helicase domain to feed double-stranded RNAs to the catalytic center (Sinha et al., 2018). Nevertheless, it should be mentioned, that the N-

terminus of Dicer also serves as an interface for the interaction with some RBPs, i.e., TRBP or PACT in mammals and Loquacious or R2D2 in flies (Lee et al., 2006; Ye et al., 2007; Daniels et al., 2009; Hartig and Förstemann, 2011). These factors, in turn, were shown to influence the substrate selectivity of Dicer and, among other functions, they also enhance the activity and accuracy of the cleavage reaction (Daniels et al., 2009; Fukunaga et al., 2012; Taylor et al., 2013; Sinha et al., 2015; Wilson et al., 2015; Jakob et al., 2016). Finally, Dicer processing results in a sRNA duplex, which possesses a two nt long overhang at both 3' ends and which is a short-lived intermediate. Only one of the two strands, termed the guide strand, is preferentially assembled into an Ago protein, the direct binding partners of mature miRNAs. The opposite strand, instead, is usually degraded and it is referred to as passenger strand or miRNA*. Depending on the location of the selected strand within the original pre-miRNA sequence, the suffixes -5p or -3p are sometimes used to indicate whether the mature miRNA is derived respectively from the 5' or from the 3' arm of the hairpin.

The selection of the correct strand for Ago-loading follows the so-called asymmetry rule, i.e., the strand with the less stably paired 5' end will become the guide strand (Khvorova et al., 2003; Schwarz et al., 2003). This discrimination process is achieved by the so-called RISC-loading complex, whereby some evidences indicate that Dicer itself might sense the thermodynamic stability of the ends of the sRNA duplex, but, to do so, it requires the interaction to TRBP or PACT (Noland et al., 2011). Importantly, it has been shown for different organisms that the transfer of the sRNA duplex to the Ago proteins is facilitated by the action of the heat shock protein 90 (Hsp90), and of some co-chaperones (Iwasaki et al., 2010, 2015; Johnston et al., 2010). The chaperone machinery might therefore stabilize unloaded Ago molecules in an open conformation, which is prone to accept the sRNA duplex (Iwasaki et al., 2010; Johnston et al., 2010). Nonetheless, the exact molecular mechanism that enables the dissociation of the two strands has not yet been fully understood. In contrast to the aforementioned report by Noland et al. (2011), Ago proteins themselves have been proposed to act as the asymmetry sensor for the sRNA duplex (Suzuki et al., 2015) and the N-terminus of Ago proteins might also directly displace the passenger strand (Kwak and Tomari, 2012).

1.2.3. Ago Proteins, the Key Players of the MiRNA Pathway

The biogenesis steps recapitulated in the previous sections finally give rise to a mature miRNA, which is a single-stranded ribo-oligonucleotide with a characteristic size of ~22 nt, a phosphate at its 5’ terminus and an OH group at its 3’ end. The binding partners of miRNAs are the members of the Ago clade, which, in mammals, comprises four proteins (Ago1-4). They are evolutionarily related to the PIWI protein clade, whereby both clades together form the Argonaute protein family. Although PIWIs bind to a distinct class of sRNAs, termed PIWI-interacting RNAs (piRNAs), they do not have many similarities with the miRNA pathway. The occurrence of the piRNA system, in fact, is restricted mainly to the germline of animals where it protects the genome from the deleterious potential of mobile elements (reviewed in Czech and Hannon, 2016; Huang et al., 2017).

Nevertheless, the members of the Ago protein family share a common structural organization, which is composed of N-terminal, PAZ, MID and PIWI domains. Their respective function has been analyzed in great detail over the past two decades, and several crystal structures of human Ago complexes have nicely contributed to the molecular understanding of miRNA-Ago interactions (Elkayam et al., 2012; Schirle and MacRae, 2012; Schirle et al., 2014). These studies revealed that human Ago2 consists of two lobes comprising the N–PAZ and the MID–PIWI domains, while the central cleft enables positioning of the miRNA along its target mRNA. The 5’ end of the miRNA is tightly anchored in a binding pocket mainly formed by the MID domain, while the 3’ end of the miRNA bends into a dedicated pocket within the PAZ domain. Interestingly, the loading of a miRNA was proposed to confer structural stability to the Ago protein (Elkayam et al., 2012).

Some Ago proteins also possess endonucleolytic cleavage activity, referred to as slicer activity, which is explicitly directed toward the target RNA. In vertebrates, only Ago2 has retained this particular characteristic that is based on the structural similarity between the PIWI domain and the RNase H endonuclease (Liu et al., 2004; Meister et al., 2004; Song et al., 2004). Importantly, a tetrad composed of DEDX, where X is D or H, confers the catalytic activity (Nakanishi et al., 2012), but the mere presence of these essential residues is not sufficient to ensure slicing. Additional elements, located in the N-terminal as well as in the PIWI domains, affect the cleavage ability of human Ago2 (Faehnle et al., 2013; Hauptmann et al., 2013; Nakanishi et al., 2013; Schirle et al., 2014). A central

question within the miRNA field concerns the necessity of maintaining a catalytic competent Ago protein within the genome of vertebrates. Indeed, perfectly complementary target sites, which are a prerequisite for cleavage, are rarely found in mammalian mRNAs (Yekta et al., 2004; Karginov et al., 2010; Shin et al., 2010). Instead, the slicer activity of Ago2 is exploited when full-complementary exogenous small interfering RNAs (siRNAs) are introduced into cells to knock down the expression of a specific gene. In a physiological context, the catalytic activity of Ago2 was proven to be of vital importance for the embryonic development in mouse (Liu et al., 2004). However, this requirement is not related to the slicing of target mRNAs, but rather to the processing of non-canonical miRNAs like, e.g., miR-451 (Liu et al., 2004; Jee et al., 2018; see also section 1.2.5).

In sum, miRNA-mediated gene silencing in mammals is not achieved by Ago2-dependent slicing of the target mRNAs, but the activity of miRISC complexes is executed via a different mechanism (see next section) and all four Ago proteins contribute to an equal extent to this process.

1.2.4. An Interplay of Processes Leads to the Repression of Targeted Transcripts

MiRNAs simply guide Ago proteins to target sites, which are mainly located within the 3’ UTRs of protein-coding transcripts. The region of the miRNA between nt 2-7 is critical for the specific interaction with the target mRNAs and is referred to as the seed sequence (reviewed in Bartel, 2009). MiRNAs, which share a common seed sequence, but differ at the remaining positions, are grouped into miRNA families and are likely to regulate a similar set of transcripts.

Still, the binding of Ago *per se* does not influence the translational output of the targeted mRNA and miRISC complexes need to recruit additional factors for repression (reviewed in Jonas and Izaurralde, 2015). The key players bridging the interaction to such downstream factors are GW182 proteins, named after its representative in *D. melanogaster* (Behm-Ansmant et al., 2006). They are known in vertebrates as trinucleotide repeat-containing 6 (TNRC6) proteins and comprise three paralogs, i.e., TNRC6A-C. Although TNRC6 proteins are largely unstructured, two distinct functional domains were identified: the N-terminal Ago-binding and the C-terminal silencing domains (Till et al., 2007; Eulalio et al., 2009; Lazzaretti et al., 2009). Both regions mediate the contacts to the interaction partners by glycine and tryptophan (GW)-

containing repeats, thus the name GW182 in *D. melanogaster*. The W residues in the Ago-binding domain of TNRC6 can hook into two dedicated pockets on the surface of Ago's PIWI domain (Schirle and MacRae, 2012; Pfaff et al., 2013). Similarly, W residues in the silencing domain of TNRC6 proteins were shown to account for the interaction to other factors (Christie et al., 2013; Chen et al., 2014; Mathys et al., 2014). Resembling a Swiss army knife, miRISCs are equipped with a set of powerful tools, which are grouped together by TNRC6 proteins serving as a scaffold. Among these downstream factors, the most important are two deadenylation complexes: CCR4-NOT and PAN2-PAN3. Deadenylation is also tightly coupled to the decapping of the mRNA 5' end by a complex containing the decapping protein 2 (DCP2). Altogether, these processes finally allow the cytoplasmic 5'→3' exonuclease XRN1 to degrade the targeted transcripts. According to the currently favored model, the miRNA-mediated regulation of gene expression is thus mainly accomplished by the destabilization of the mRNAs (Guo et al., 2010; Eichhorn et al., 2014). In addition, translational repression mechanisms contribute, albeit to a minor extent, to the combination of processes, which ultimately culminate in the inhibition of gene expression (reviewed in Jonas and Izaurralde, 2015).

1.2.5. Many Roads Lead to Ago: Generation of Non-canonical MiRNAs

The biogenesis of miRNAs obeys simple rules and has evolved as a robust system to ensure the production of functional, Ago-loaded sRNAs. Nevertheless, it has been observed recurrently that certain miRNAs are generated by exotic strategies, which do not depend at least on one of the Drosha or Dicer processing steps (reviewed in Daugaard and Hansen, 2017). This is the case, for example, for miRNAs arising from other ncRNA transcripts, as it was demonstrated for a snoRNA-derived miRNA (Ender et al., 2008; Taft et al., 2009) and, apparently, for certain tRNA fragments (see sections 1.1.10.1 and 1.1.10.3). The advent of deep sequencing technologies revealed that the total sRNA population of a cell is characterized by the presence of a multitude of such fragments. Unfortunately, it was tempting to classify as a miRNA any of these processing products just in virtue of their miRNA-like size, while sometimes it was omitted to verify whether they associate with endogenous Ago proteins.

Most commonly, non-canonical miRNAs do not require Drosha processing. Some miRNAs, for instance, are generated from so-called mirtrons. These are short introns with hairpin potential which, after splicing from primary transcripts, are debranched and

exported from the nucleus. The hairpins within such mirton sequences might possess 5' or 3' tails which are trimmed by exonucleases before running through the remaining miRNA biogenesis steps (Berezikov et al., 2007; Okamura et al., 2007; Ruby et al., 2007; Ladewig et al., 2012).

Endogenous siRNAs (endo-siRNAs) are another class of non-canonical miRNAs, which does not require the activity of the Microprocessor complex. In mammals, the expression of endo-siRNAs is mainly restricted to oocytes and to early pre-implantation embryos (Babiarz et al., 2008; Tam et al., 2008; Watanabe et al., 2008). These long, highly-complementary double-stranded RNAs can result, e.g., from bidirectional transcription of a genomic locus or from gene-pseudogene transcript pairs (reviewed in Okamura and Lai, 2008). As already mentioned, endo-siRNAs are not recognized by the Microprocessor complex and also the human Dicer protein cannot easily cope with their unconventional structure. This is mainly due to the strong selectivity conferred by the N-terminal helicase domain (see section 1.2.2.). Interestingly, it has been shown that an oocyte-specific Dicer isoform lacks the helicase domain and can thereby efficiently cleave endo-siRNAs. However, this smart strategy seems to be restricted to rodents and it is not clear how such miRNAs are processed in other mammals (Flemr et al., 2013). In addition, a long debate is ongoing regarding the occurrence in vertebrates of virus-derived siRNAs, which, instead, are widely produced in plants and in many invertebrates as an antiviral immune response (reviewed in Ding and Voinnet, 2007; Cullen et al., 2013).

In contrast to the long, highly complementary endo-siRNAs, endogenous short-hairpin RNAs (shRNA), which were identified in different tissues, are optimal Dicer substrates (Babiarz et al., 2008, 2011). A recent study revealed that this particular pre-miRNA category is more frequent then initially thought. Endogenous shRNAs are transcribed by Pol II and their 5' ends possess a 7-methylguanosine (m^7G) cap, while their 3' ends result from transcriptional termination. Of note, the nuclear export of such shRNAs does not depend on Xpo5. Instead, it utilizes Xpo1 together with the phosphorylated adaptor for RNA export (PHAX), the system which usually shuttles snRNAs to the cytoplasm for their maturation (Xie et al., 2013; Kim et al., 2016).

Interestingly, also some viruses express miRNAs which are processed by the host via non-canonical mechanisms. In the case of the bovine leukemia virus (BLV) miRNA-containing shRNAs are produced by Pol III as individual transcripts which do not require Drosha processing (Kincaid et al., 2012; Rosewick et al., 2013). Follow-up studies further demonstrated that the BLV shRNAs have a triphosphorylated 5' end, which needs to be

converted into a monophosphate to allow for the accumulation of some of these viral miRNAs (Burke et al., 2014, 2016).

Also other viruses have developed strategies to generate Drosha-independent miRNAs. For instance, some viruses encode chimeric transcripts and usurp different cellular endonucleases to liberate the pre-miRNA hairpins. This applies, e.g., to the murine gammaherpesvirus 68 (MHV68), whereby tRNA-like sequence direct RNase Z to release the pre-miRNAs (Bogerd et al., 2010). Similarly, the herpesvirus saimiri (HVS) uses the Integrator complex to separate its pre-miRNAs from other ncRNAs contained in a longer precursor transcript (Cazalla et al., 2011).

As already mentioned in section 1.2.3, the catalytic activity of Ago2 is essential for the development of vertebrates and this is mainly due to the atypical biogenesis mechanism of miR-451 (Cheloufi et al., 2010; Cifuentes et al., 2010). Indeed, the highly complementary stem of pre-miR-451 is too short to be accommodated into Dicer. This, and other conserved characteristics (Yang et al., 2010; Dueck et al., 2012), enable Ago2 to bind and to cleave pre-miR-451 within its 3' hairpin arm. The resulting intermediate is then trimmed by the PARN exonuclease to generate the mature miRNA (Yoda et al., 2013). Interestingly, a recent publication demonstrated that miR-486-5p, although being processed by the canonical biogenesis pathway, strictly requires Ago2 to slice and remove its passenger strand (miR-486-3p) from the miRNA duplex generated by Dicer. If this is impaired, miR-486-3p accumulates and inhibits the function of the complementary miR-486-5p (Jee et al., 2018).

Of note, the strict dependency on Dicer for the biogenesis of miRNAs was questioned by the finding that miRNAs derived from the 5' arm of pre-miRNAs can be generated also in the absence of Dicer, at least to a certain extent. It has been hypothesized that pre-miRNAs are directly loaded into Ago proteins, which thereby protect their 5' ends. At the same time, 3'→5' exonucleases remove part of the hairpin producing miRNAs with a short 3' extension compared to their counterparts matured under physiological conditions (Kim et al., 2016). Finally, a class of Ago-bound fragments that neither depend on Drosha, nor on Dicer was recently described. These so-called agotrons are derived from short intron sequences and are not further processed after debranching. Consequently, agotrons are longer than normal miRNAs (Hansen et al., 2016). They were shown to excerpt miRNA-like functions, however they have been also proposed to modulate the function of Ago proteins, possibly by stabilizing unloaded Ago proteins (Stagsted et al., 2017).

In sum, nature came up with exceptions to any step of the miRNA biogenesis. It is attractive to speculate that these alternative pathways emerged to allow expression of distinct miRNAs independently from regulatory mechanisms, which generally affect the production of classical miRNAs.

2. Aims of the Study

In this PhD project, we aimed to identify and characterize so far unknown non-canonical miRNA biogenesis pathways. To this end, we started studying the effects of the RBP La on cellular miRNAs. In the rest of our analyses, we mainly focussed on the crosstalk between the miRNA pathway and processing of Pol III transcripts, which are the main targets of La.

3. Results

3.1. Generation of a La-specific Antibody

The Lupus antigen La protein plays a central role in the biogenesis of several highly structured RNAs and recent evidences expanded its relevance to sRNA pathways (Liu et al., 2011; Liang et al., 2013). Within this context, we decided to study the function of La in more detail.

In order to investigate La in molecular detail, we aimed to generate a La-specific polyclonal antibody. We expressed and purified full-length recombinant La protein which was used for the immunization of a rabbit (Figure 3.1).

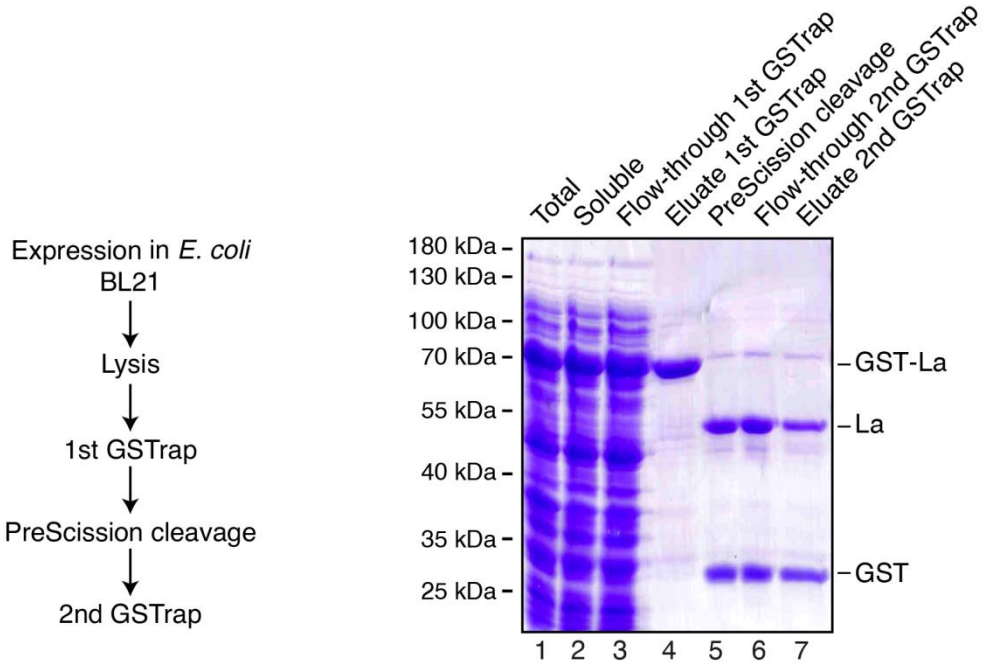

Figure 3.1: Expression of Recombinant La Protein for Antibody Production. Left panel: Schematic overview of the purification strategy. Right panel: Aliquots of the indicated steps (lanes 1-7) were taken during the protein purification and were resolved by SDS-PAGE for Coomassie-staining. The molecular size marker is depicted on the left. Substantial amounts of the cleaved GST-tag were still present in the flow-through of the second GSTrap column. Nevertheless, this fraction was used for the antibody production.

Antibodies were subsequently affinity purified from the animal's serum using recombinant La protein as affinity matrix. Western blot analyses revealed that the purified polyclonal antibody recognized overexpressed FLAG/HA (FH)-tagged, as well as the endogenous La protein (Figure 3.2). The signal appearing at ~50 kDa was proven to be specific as it disappeared upon siRNA-mediated La knockdown. Importantly, Figure 3.2 also indicates that the adopted experimental knockdown conditions ensured an efficient depletion of La.

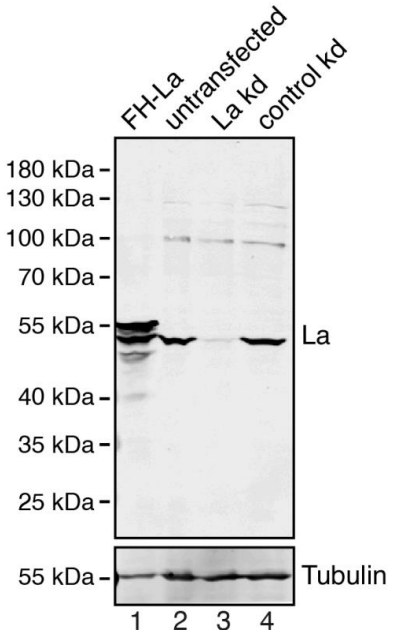

Figure 3.2: The Antibody Specifically Detects La in Total Cell Lysates. FH-La (lane 1), endogenous La (lanes 2-4) from HEK293 or from La knockdown (kd) samples (lane 3) were analyzed by Western blotting. Detection of tubulin served as loading control. Molecular size marker weights are depicted on the left.

3.2. La Affects the Cellular sRNA Population

We next investigated the global impact of La depletion on the sRNA population of the cell. In particular, we hypothesized that the abundance of sRNAs loaded into Ago proteins might be affected by the knockdown of La, since this has been already reported for some miRNAs (Liu et al., 2011). Thus, we decided to profile by deep sequencing the impact of La depletion on total RNA and on the Ago-associated fraction of sRNAs (Figure 3.3).

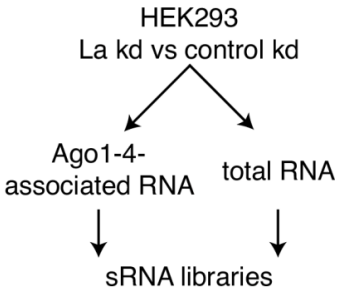

Figure 3.3: Experimental Procedure to Investigate the Relevance of La on sRNA Pathways. HEK293 cells were transfected with either a siRNA against La or a control siRNA. For both conditions, Ago1-4 complexes were isolated by Ago-APP and the co-precipitated RNAs were used to generate sRNA libraries. The sRNAs were also profiled from total RNA which was extracted from the corresponding input samples.

In order to not restrict our view on only one of the four human Ago proteins, we opted for a novel peptide-based method termed ‘‘Ago protein Affinity Purification by Peptides’’ (Ago-APP) (Hauptmann et al., 2015). This strategy allows the simultaneous purification of all Ago proteins. Thereby, a GST-tagged peptide, encompassing the region of TNRC6B interacting with the binding pockets on the surface of all Ago-proteins (Pfaff et al., 2013) is used as bait to precipitate these proteins from cell lysates. Importantly, sRNAs bound to Ago proteins are retained in the isolated complexes and can be further used for library preparation and deep-sequencing approaches. As exemplary shown for Ago2 in Figure 3.4, similar amounts of Ago proteins were isolated upon La and control knockdown treatment of HEK293 cells.

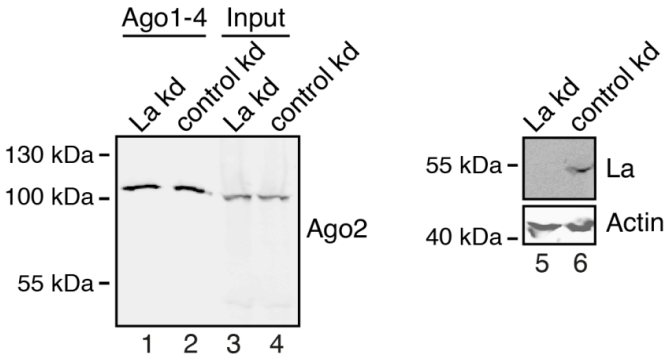

Figure 3.4: Efficient Purification of Ago Complexes and La Depletion. All four Ago proteins were co-purified by Ago-APP following transfection of La or control siRNAs. The Western blot analysis is exemplarily shown for Ago2 in Ago-APP samples (lanes 1-2) and inputs (lanes 3-4). The efficiency of the La knockdown (lanes 5 and 6) was confirmed. Detection of actin served as loading control. The molecular size marker weights are indicated on the left side of the blots.

We next generated sRNA libraries from the Ago-associated RNAs as well as from input samples and mapped the reads to miRNAs and to a custom database comprising known Pol III transcripts. Latter are the canonical La substrates, which are bound and protected immediately after transcription termination. As expected, the great majority of Ago1-4-associated RNAs mapped to known miRNAs. The composition of the input samples instead, was more variable and several sRNAs derived from Pol III transcripts were detected. In general, no prominent difference between La and control knockdown samples became evident from such data analysis (Figure 3.5).

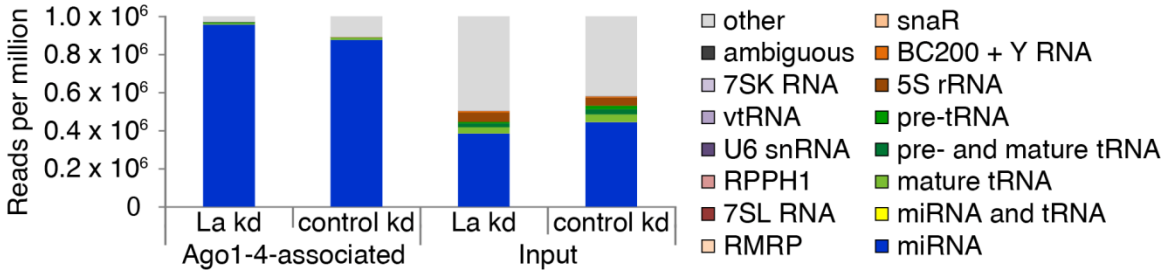

Figure 3.5: Composition of the sRNA Libraries in the Presence or Absence of La. For each indicated library, the sequenced sRNAs counts, given in reads per million, were mapped to known miRNAs and to a custom database of Pol III transcripts. The different categories are indicated on the right. Reads derived from tRNAs are grouped in reads unambiguously derived from pre-tRNA (pre-tRNA), unambiguously derived from mature tRNAs (mature tRNA), and reads which could originate from both (pre- and mature tRNA). A similar distinction was done for miRNAs and tRNAs in case reads mapped to both categories (‘‘miRNA’’ or ‘‘miRNA and tRNA’’). All reads, which mapped to sequences from two or more of the other categories, are referred as ‘‘ambiguous’’. Vault RNA (vtRNA), small NF90-associated RNA (snaR).

However, detailed mapping of the miRNA population revealed that the expression level of single miRNAs was moderately affected by the depletion of La. Consistent with previous reports (Liang et al., 2013), the abundance of let-7 miRNA family members decreased upon La knockdown in the Ago-associated fraction, as well as in the inputs. Few other rather low abundant miRNAs had a similar effect e.g., miR-1255a in the Ago-associated fraction, miR-98-5p and miR-3741-3p in the input samples. Also, a handful of miRNAs, e.g., miR-1290, was positively affected by the knockdown of La (Figure 3.6).

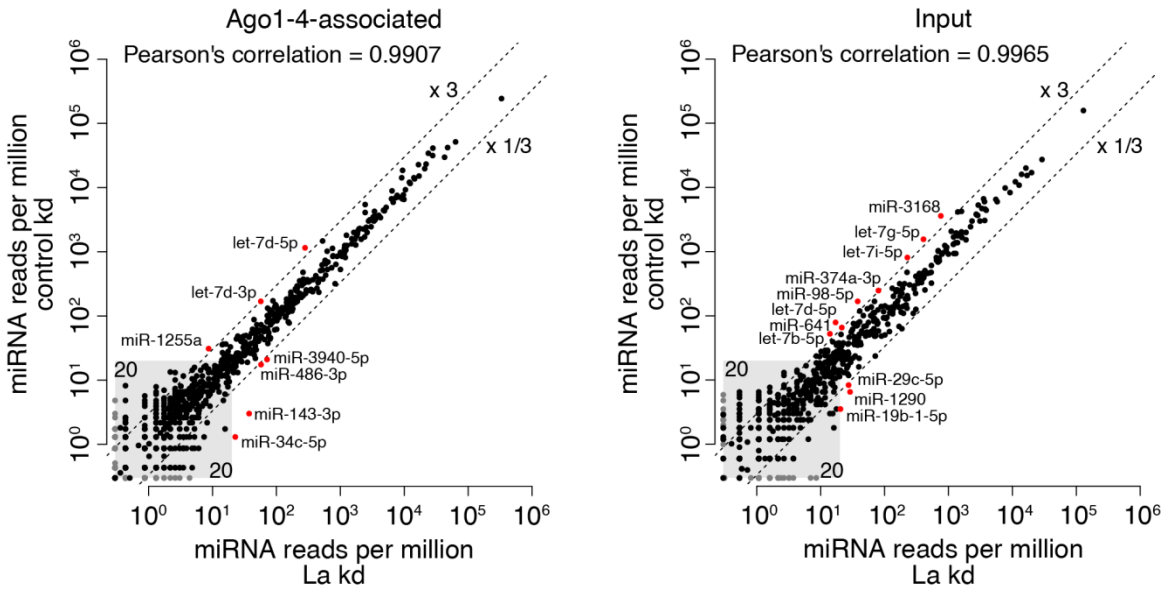

Figure 3.6: La Depletion Affects MiRNA Expression Levels. Scatterplots showing reads per million counts of Ago1-4-associated miRNAs (left) or miRNAs from input samples (right) in La (x axis) versus control (y axis) knockdowns. The dashed lines indicate 3-fold up- or downregulation. The miRNAs exceeding these thresholds are indicated (red). The low abundant miRNAs with 20 or less reads per million in both libraries were not considered (gray box).

The mild miRNA expression changes detected by deep-sequencing could also be validated by Northern blot analyses performed with total RNA (Figure 3.7A). Though, the miRNAs tested in Northern blots appeared to be more moderately affected by the knockdown of La compared to the extent revealed by the deep sequencing analysis (see quantification of the signals in Figure 3.7B compared to Figure 3.6). We conclude from these data that La does not play a major role in the regulation of miRNA biogenesis, since La depletion resulted in small expression changes of only a small subset of miRNAs.

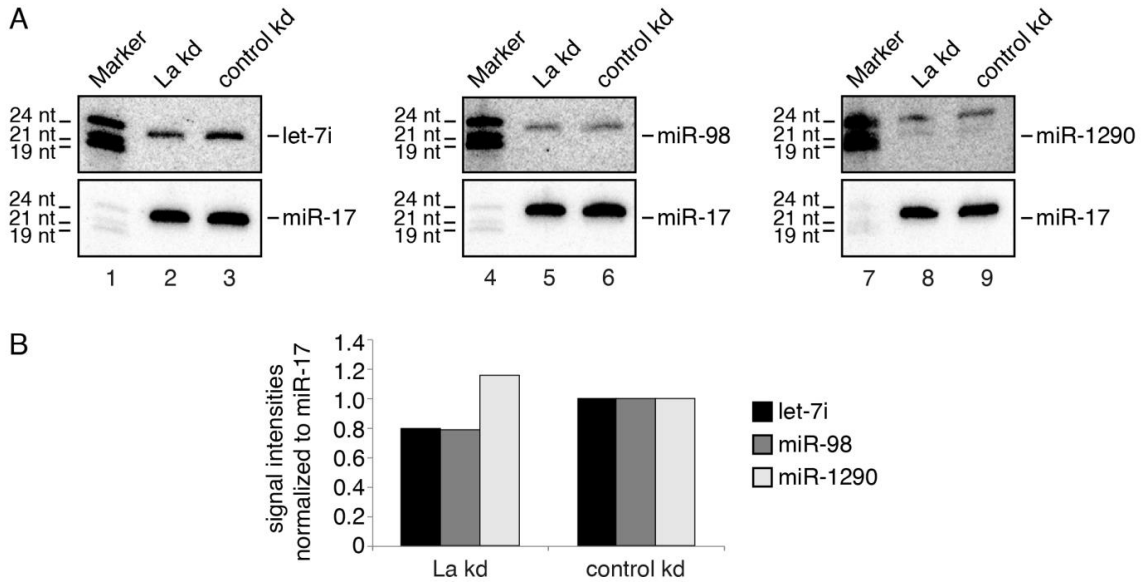

Figure 3.7: Validation of the Effect of La Depletion on MiRNA Expression Levels. (A) HEK293 cells were transfected with a siRNA against La (lanes 2, 5 and 8) or a control siRNA (lanes 3, 6 and 9). Lanes 1, 4 and 7 show a size marker. Total RNAs were analyzed by Northern blotting with probes complementary to let-7i, miR-98, miR-1290 and miR-17. (B) Quantification of the miRNA signal intensities normalized to miR-17 and to the control knockdown.

We next focused on the influence of La depletion on tRNAs, 5S rRNA, U6 snRNA and other known Pol III transcripts. Since tRNAs are processed from longer precursors and La has been shown to govern the tRNA maturation at several steps, we decided to look separately at reads, which are derived unambiguously from pre-tRNAs or unambiguously from mature tRNAs. Those reads that could either be derived from pre-tRNAs or from mature tRNAs were grouped in a distinct category termed ‘‘pre- and mature tRNA’’. This analysis indicated that the greatest effect of La depletion concerned pre-tRNA-derived reads, which were enriched approximately 4-fold in Ago1-4 compared to the control condition. Reads exclusively derived from mature tRNAs were instead twice less frequent upon knockdown of La (Figure 3.8, left panel).

Importantly, we plotted the abundance of each Pol III transcript category and realized that among them, the most abundant Ago1-4-associated fragments were indeed derived from pre-tRNAs as well as from mature tRNAs. Other sRNAs were either affected by La to a lesser extent or they associated poorly with Ago proteins (Figure 3.8, right panel). Therefore, we did not consider them for further investigations.

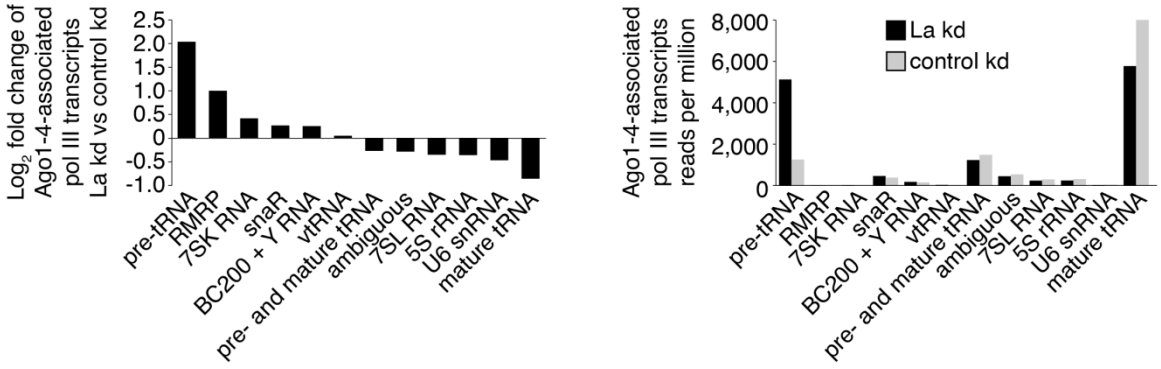

Figure 3.8: La Depletion Affects Ago-loaded sRNAs Originating from tRNAs. Log_2-fold changes of Ago1-4-associated reads from Pol III transcripts detected upon La knockdown or control knockdown (left). The corresponding abundance in reads per million of fragments derived from the indicated transcripts for both conditions is shown (right).

The same analysis was conducted on the libraries obtained from the input samples revealing that the overall abundance of tRNA- and 5S rRNA-derived sRNAs was much greater in the inputs than in Ago1-4. Of note, the knockdown of La led to a reduction of reads unambiguously derived from pre-tRNAs (Figure 3.9). This is the opposite effect compared to what has been observed in Figure 3.8 regarding the Ago1-4-bound pre-tRNA fragments. This might reflect the existence of two distinct groups of pre-tRNA-derived fragments, which are influenced by La in opposite ways (see section 4.2).

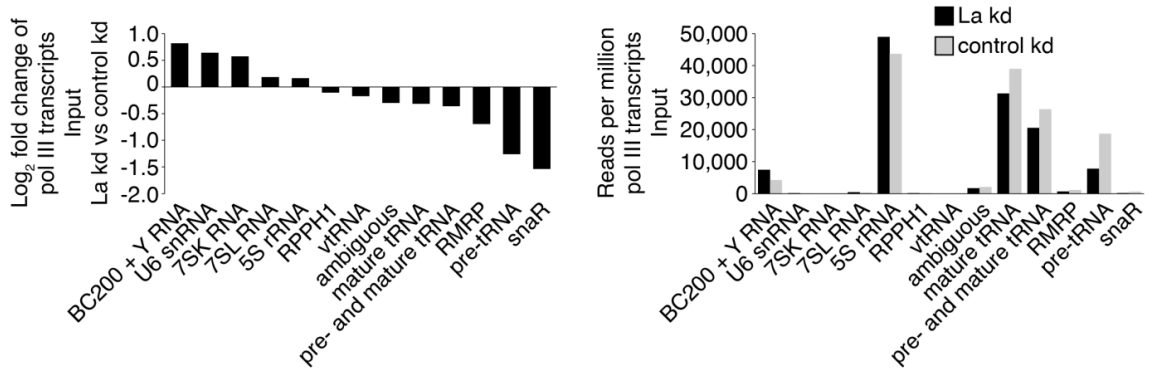

Figure 3.9: **TRNA Fragments Are Less Abundant in the Input Samples upon La Depletion.** The log_2-fold changes of reads derived from the indicated Pol III transcripts detected upon La knockdown or control knockdown (left) and the corresponding abundances in reads per million (right) are shown for the input samples.

3.3. La Regulates the Abundance of Specific Ago-loaded tRNA Fragments

Since the strongest effects observed upon depletion of La concerned sRNAs specifically derived from pre-tRNAs (Figure 3.8 and Figure 3.9), we examined their origin in more detail by determining the tRNA isotype they were processed from. Fragments derived from pre-tRNA-Pro, -Ile, -Ser, -Lys, -Ala and -Leu were enriched more than 3-fold in Ago1-4 upon La knockdown (shown in red in Figure 3.10, left panel). We also observed that this effect was not common to all Ago-bound pre-tRNA fragments. For example, reads mapping to pre-tRNA-Val were among the most abundant, but they were equally present in both conditions. Of note, the knockdown of La did not lead to the reduction of Ago-associated tRNA fragments originating from any isotype. In the input samples, instead, the absence of La resulted in a general decrease of the expression of pre-tRNA fragments, particularly of sRNAs derived from pre-tRNA-Val, -Ser, -Lys and -Asp (shown in red in Figure 3.10, right panel). Only the processing products of pre-tRNA-Pro were enriched upon La knockdown in the Ago1-4 fraction as well as in the input sample (Figure 3.10). In sum, La seems to regulate the abundance of sRNAs derived from a specific subset of pre-tRNA isotypes.

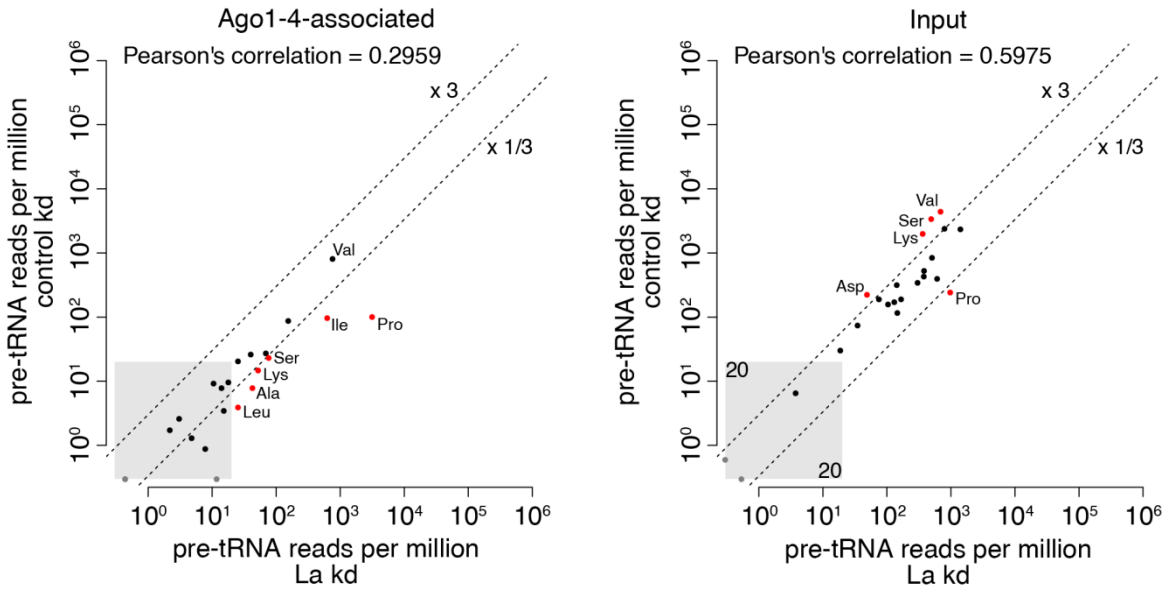

Figure 3.10: Specific Pre-tRNA-Derived Fragments Accumulate in Ago1-4 upon La Depletion. Scatterplots showing reads per million counts in La knockdown or control knockdown samples from Ago1-4-associated (left) or input (right) RNA which are unambiguously mapping to pre-tRNAs. Graphical representation as described in Figure 3.6.

It is well known that different fragments can be processed from the entire tRNA body (Telonis et al., 2015). We asked whether the sequences accumulating in Ago1-4 upon La knockdown originate from all over the pre-tRNA or rather from a specific region. To this end, we performed a coverage analysis for the reads mapping unambiguously to pre-tRNAs or both to pre-tRNAs and mature tRNAs. The lengths of the genomic pre-tRNA sequences differ slightly between each other, mainly due to the different sizes of the variable tRNA arm or due to the presence of introns. Thus, we first mapped the Ago1-4-associated tRNA reads and then we normalized our genomic pre-tRNA database to a common length for the graphical representation depicted in Figure 3.11.

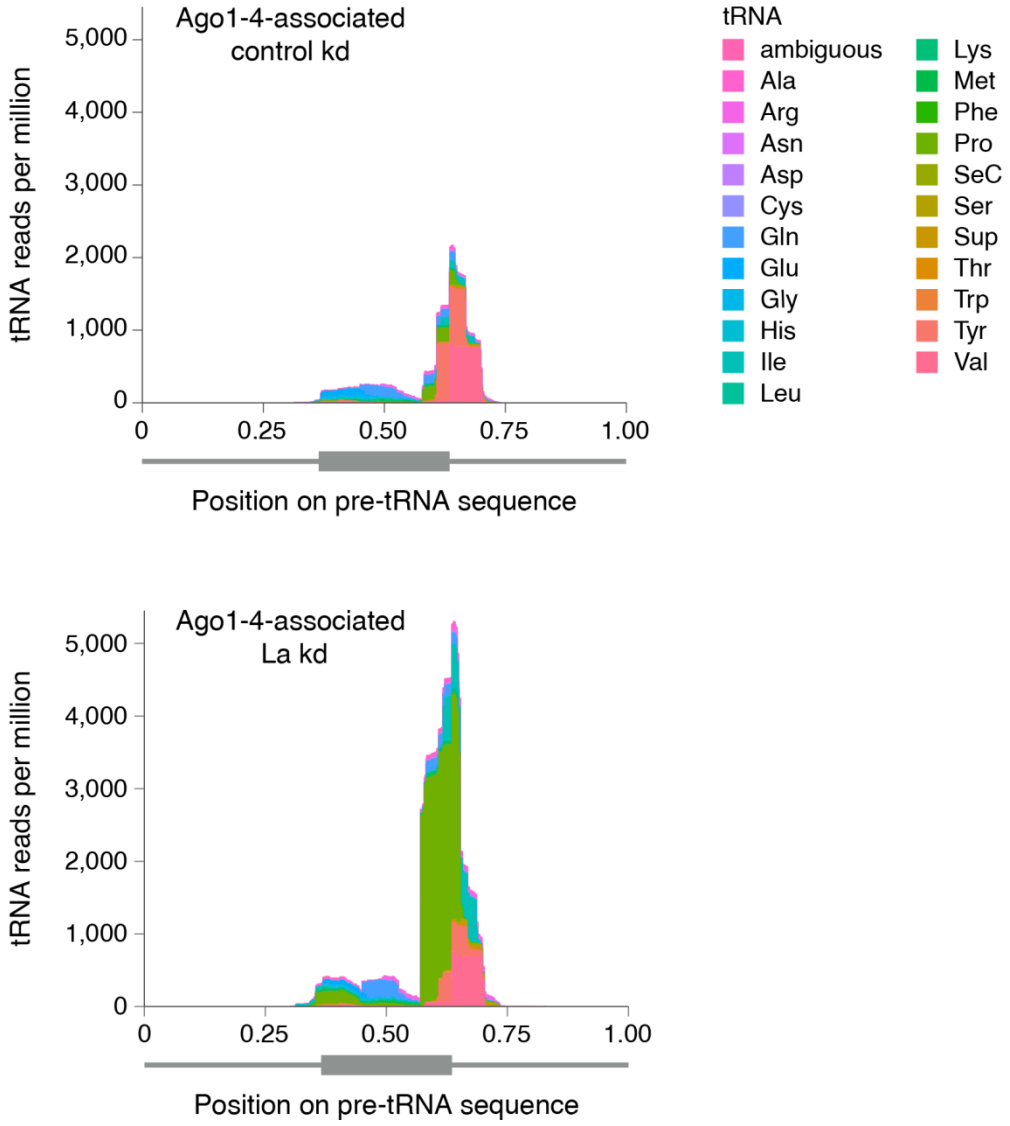

Figure 3.11: 3' Terminal Pre-tRNA Fragments Accumulate in Ago Complexes upon La Depletion. Coverage on pre-tRNA loci by reads detected in Ago1-4 associated RNAs upon control knockdown (upper panel) or La knockdown (lower panel). The sequences mapping unambiguously to pre-tRNAs and sequences, which could originate either from pre-tRNAs or mature tRNAs were used. A schematic representation of the pre-tRNA is shown beneath the graphs. The color code indicates from which tRNA isotype the stacked reads are derived. Reads mapping to two or more different tRNA isotypes are referred as ''ambiguous''.

The coverage analysis indicates that the most abundant tRNA reads span the boundary between the 3’ end of the tRNA and the genomic region further downstream, i.e., they are derived from the 3’ end of pre-tRNAs. Strikingly, Ago-loaded sRNAs from exactly this region strongly accumulate upon knockdown of La, in particular fragments mapping to pre-tRNA-Pro and –Ile (compare upper and lower panel in Figure 3.11).

The pattern emerging from the sequence coverage analysis performed with the input samples differed from the Ago1-4-associating sRNAs inasmuch as 5’ terminal fragments were detected at similar levels like those processed from the 3’ end of pre-tRNAs (compare upper panels in Figure 3.11 and Figure 3.12).

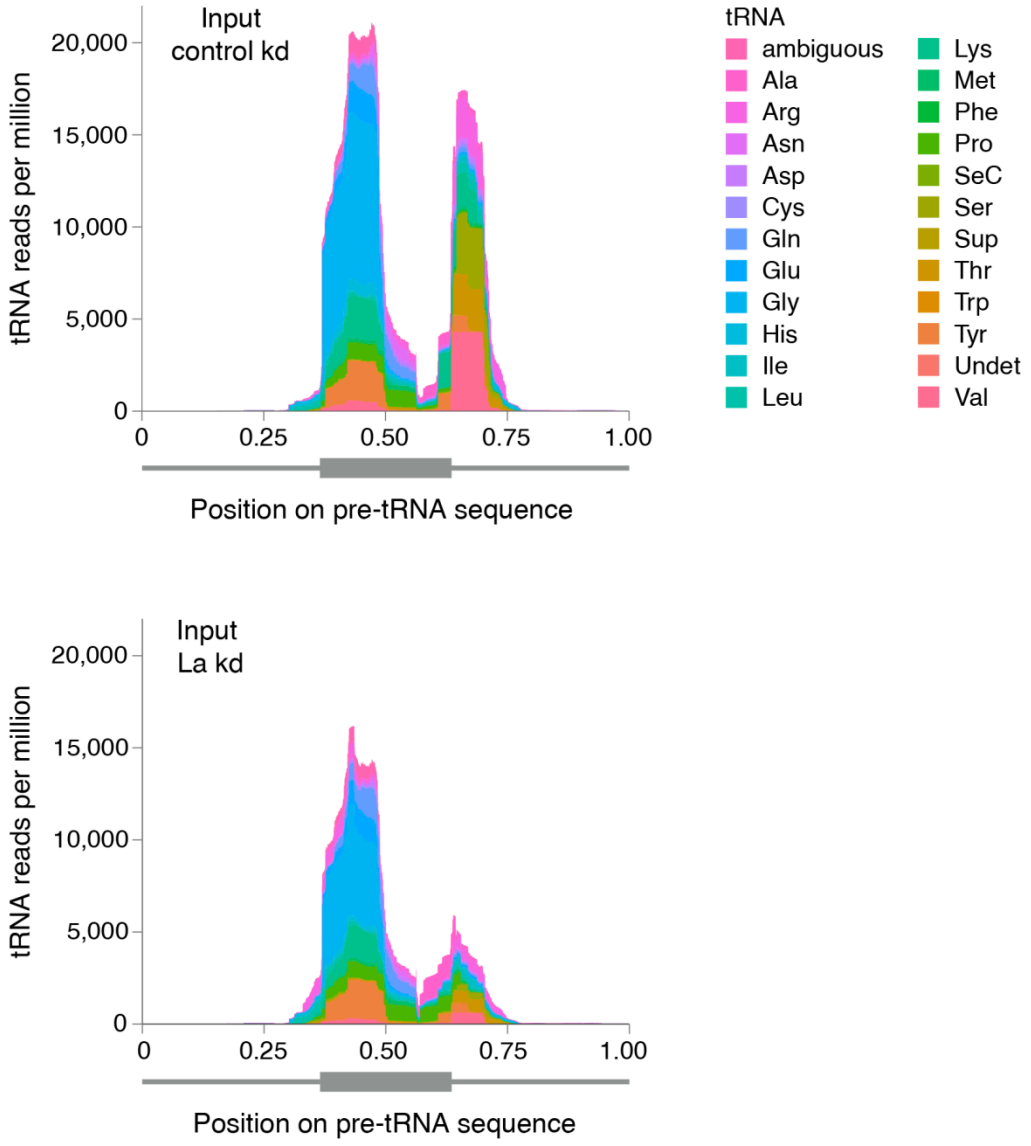

Figure 3.12: La Depletion Causes a Reduction of 3’ Terminal Pre-tRNA Fragments in the Input. Coverage on pre-tRNA loci by reads detected in the total RNA of cells treated with a control siRNA (upper panel) or a siRNA against La (lower panel). The analysis was performed as described in Figure 3.11. Note that some reads were assigned to the category referred to as “undetermined” (Undet) in gtRNAdb 2.0 (Chan and Lowe, 2016). It consists of tRNA pseudogenes for which no clear anticodon sequence could be determined.

Also in this case, the depletion of La mainly affected fragments mapping to the 3' trailer of pre-tRNAs, although, as already noticed, within the input such fragments became less abundant compared to the control (compare upper and lower panel in Figure 3.12).

3.4. La-dependent Pre-tRNA Fragments Have MiRNA Characteristics

TRNA fragments are a heterogeneous and highly abundant class of sRNA (Keam and Hutvagner, 2015; Megel et al., 2015) and their association and function in Ago complexes is a matter of debate. MiRNAs, the canonical interaction partners of Ago proteins, are characterized by a specialized biogenesis pathway, which gives rise to a very definite population of sRNA in the size range of 19-24 nt. This length enables the perfect fitting into the miRNA-binding surface of Ago proteins (Elkayam et al., 2012; Schirle et al., 2014). We therefore analyzed the length distribution of the tRNA-derived reads sequenced in our libraries (Figure 3.13 and Figure 3.14).

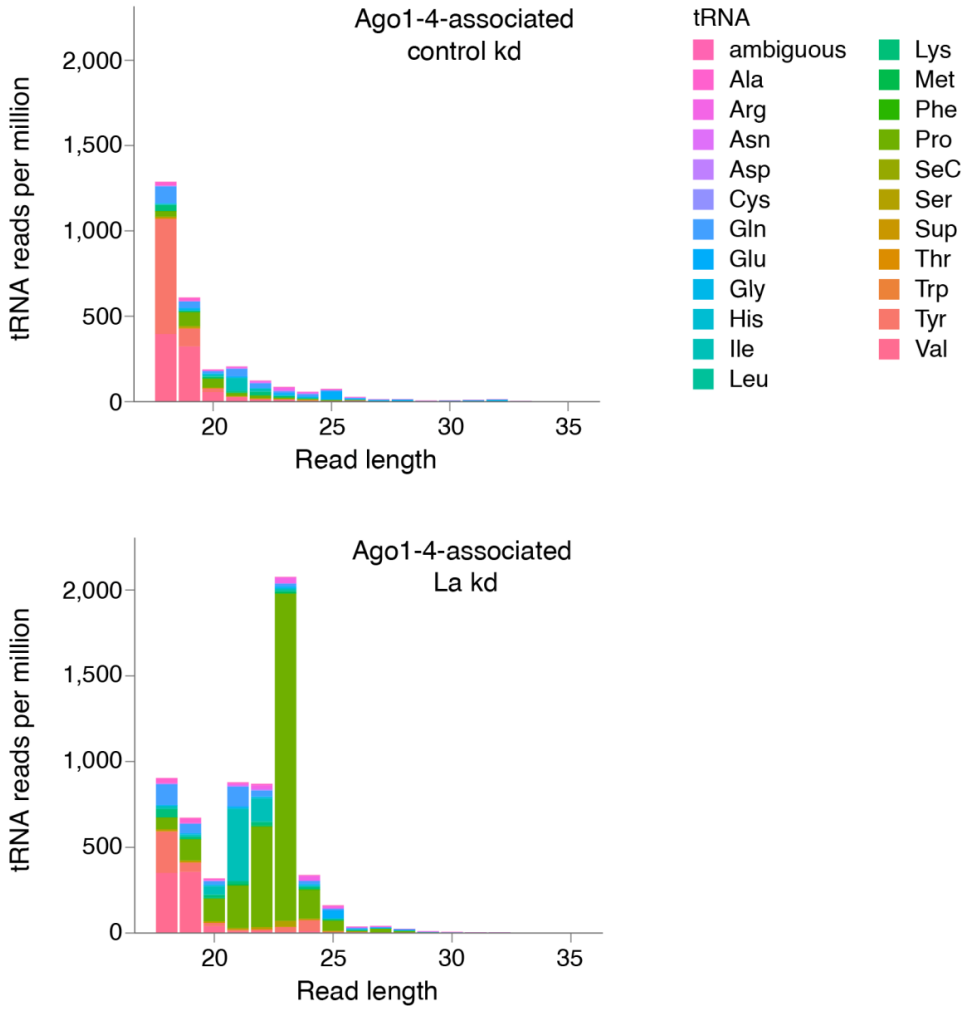

Figure 3.13: TRNA Fragments of MiRNA Size Are Loaded on Ago Proteins upon La Depletion. Length distribution of reads detected in Ago1-4 associated RNAs upon control knockdown (upper panel) or La knockdown (lower panel). The same sequences as in Figure 3.11 were used for the analysis.

Under control conditions (Figure 3.13, upper panel), mainly shorter fragments of about 18-19 nt were found to co-precipitate with Ago proteins. Thus, the majority of Ago1-4-associated tRNA processing products appear to be shorter than functional miRNAs under control knockdown conditions. However, upon depletion of La, a second population of tRNA fragments mainly derived from tRNA-Pro, -Ile and -Gln, appeared in the range of 21-23 nt with a sharp peak at 23 nt (Figure 3.13, lower panel). Importantly, these Ago-associated tRNA processing products have a size similar to miRNAs, suggesting that they might have even more characteristics in common with miRNAs.

A much greater variability in the length distribution of tRNA reads was observed in the input samples although even here, the highest peak appeared at 18 nt and an additional peak at 32 nt (Figure 3.14). Latter consisted mainly of reads derived from the 5' end of tRNAs (Figure 3.12).

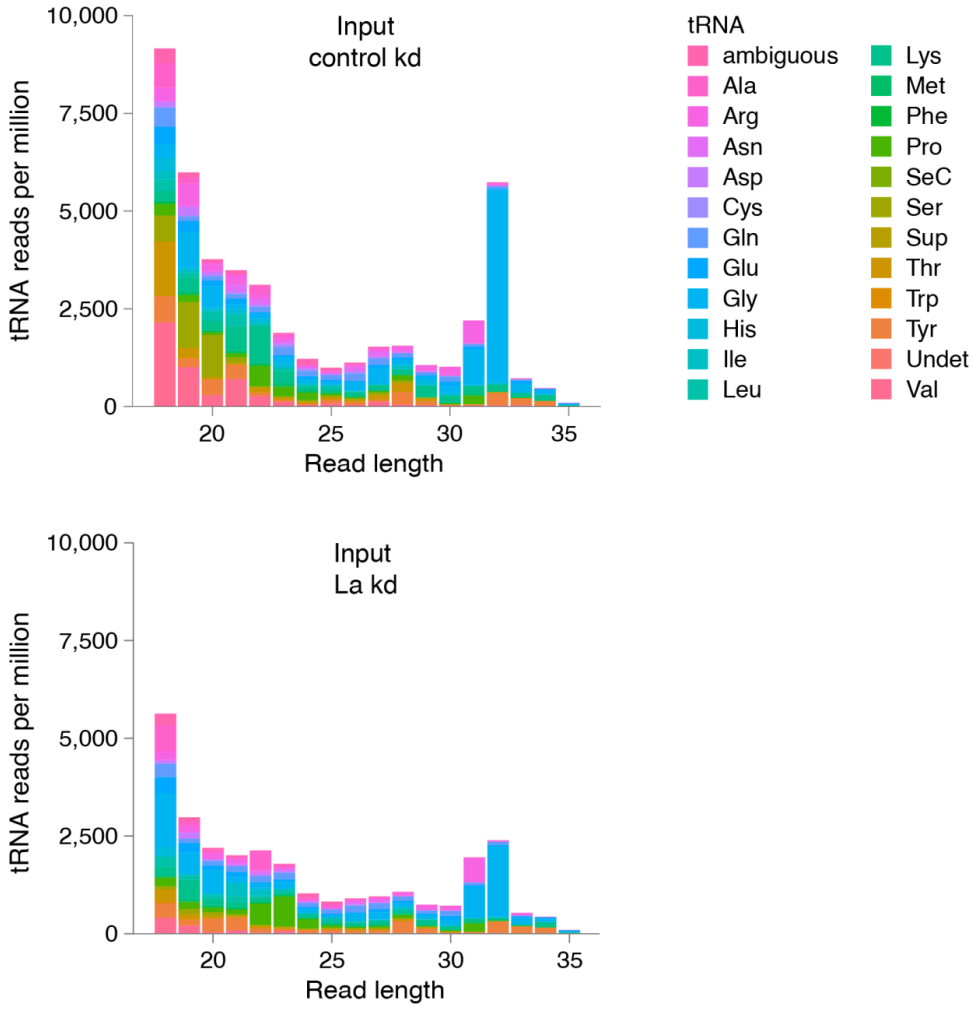

Figure 3.14: The Reduction of TRNA Reads in the Input Is not Restricted to a Particular Fragment Length. Length distribution of reads detected in the input samples upon control knockdown (upper panel) or La knockdown (lower panel). The same sequences as in Figure 3.12 were used for the analysis.

Upon depletion of La, the global decrease in tRNA expression levels applies to the fragments of all sizes and does not seem to be restricted to a specific subpopulation. However, the effect might be more pronounced for the 32 nt long tRNA-Gly processing products.

Altogether, our analyses suggest that La prevents the formation and, by that, the loading of a specific class of pre-tRNA-derived fragments into Ago proteins. These fragments might have the potential to function as miRNAs and we next aimed to characterize them in more detail.

3.5. The Pre-tRNA Pro-CGG-2-1 Generates an Ago-loaded sRNA in the Absence of La

An interesting pre-tRNA that showed a considerably enhanced loading of processing products upon knockdown of La was pre-tRNA-Pro. Since several tRNA-Pro genes exist in human (see section 1.1.2), we investigated whether this effect was driven by a pre-tRNA-Pro originating from one distinct locus. Indeed, most of the reads could be assigned to the Pro-CGG-2-1 pre-tRNA. A coverage analysis of this specific genomic region was then performed using the input libraries (Figure 3.15). For the graphical representation, the sequenced reads were depicted separately depending on whether they mapped unambiguously to the pre-tRNA (black) or to the mature tRNA (light gray) or whether they could be derived either from the pre-tRNA or from the mature tRNA (dark gray).

In the control samples, ~200 reads per million contained the CCA end, which is added post-transcriptionally after maturation. Thus, they originated from the 3’ end of the mature Pro-CGG-2-1 tRNA. In comparison, only few fragments contained the genomically encoded 3’ trailer sequence and mapped to the 3’ end of the pre-tRNA (Figure 3.15, upper panel). Strikingly, the knockdown of La led to a remarkable increase of the pre-tRNA-derived fragments only, in particular of those mapping to the 3’ end and, to a lower extent, also to the 5’ end of the pre-tRNA (compare upper and lower panel in Figure 3.15).

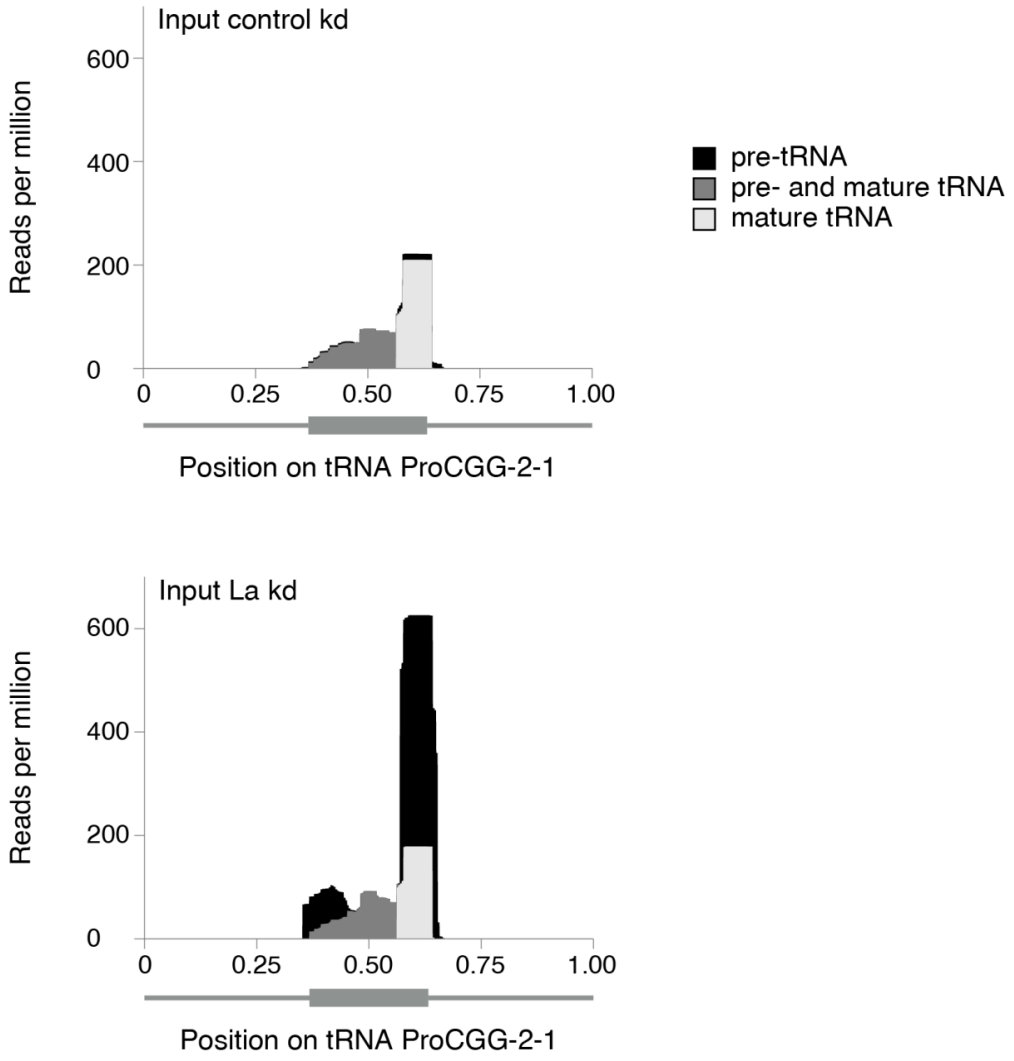

Figure 3.15: The La-dependent Fragment of Pre-tRNA-Pro-CGG-2-1 Overlaps with a sRNA Processed from the Mature tRNA. Coverage of Pro-CGG-2-1 by reads detected in total RNA upon control knockdown (upper panel) or La knockdown (lower panel). See main text for more details.

We next intended to validate the sequencing results by Northern blot assays performed on total RNA from cells treated with different siRNAs against La. In addition, to test for the specificity of the La-dependent effects, we included the knockdown of two La-related proteins (LARPs), LARP1 and LARP4B. The Northern blot probe used was complementary to the 3' terminal fragment of the pre-tRNA-Pro-CGG-2-1. Indeed, a signal was readily detected at the expected size range of the processed sRNA (sRNA-Pro) (Figure 3.16A). Although we confirmed the efficiency of the La knockdowns by qPCR and by Western blotting (Figure 3.16B), no relevant changes between the different treatments were observed regarding the expression of sRNA-Pro (Figure 3.16A). Thus, the sRNA detected in this experiment appears to be produced independently of La. Since the Northern blot probe also strongly recognized the mature tRNA-Pro, we argued that

the sRNA-Pro signal observed in Figure 3.16A might be mainly due to cross-hybridization of the probe to the La-independent fragment derived from the 3' end of the mature tRNA which was sequenced in the input libraries (Figure 3.15).

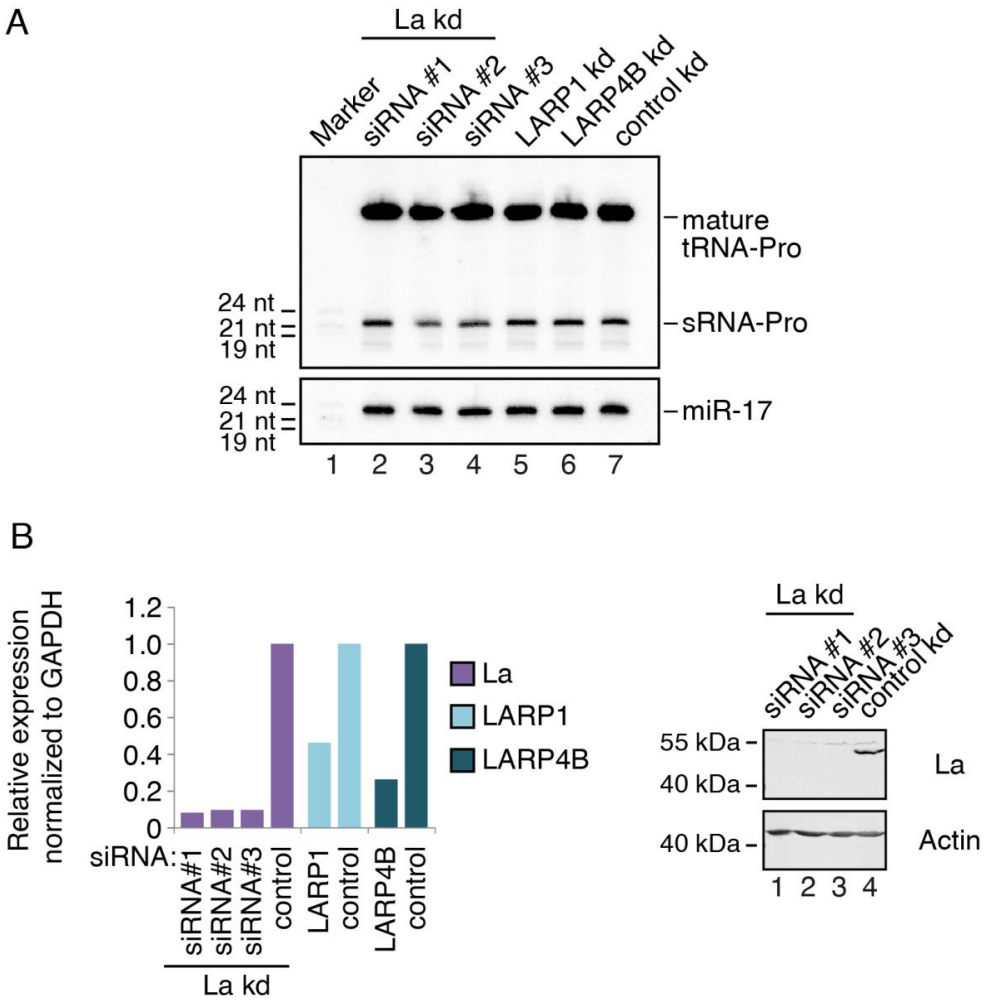

Figure 3.16: Northern Blot of Total RNA Does Not Confirm the Impact of La on sRNA-Pro. (A) HEK293 cells were transfected with three different siRNAs against La (lanes 2-4), LARP1 (lane 5), LARP4B (lane 6), or control siRNA (lane 7). Lane 1 shows a size marker. Total RNAs were analyzed by Northern blotting against the sRNA derived from the 3' end of the Pro-CGG-2-1 pre-tRNA (sRNA-Pro). The membrane was subsequently probed for miR-17 as loading control. (B) Validation of the knockdown efficiencies by qPCR (left panel). Protein levels of La in cells transfected with three different siRNAs against La (lanes 1-3) or with a control siRNA (lane 4) were assayed by Western blotting. Equal loading of the samples was monitored by the detection of actin. The molecular size marker weights are depicted on the left side of the blots (right panel).

In general, we had previously observed that tRNA fragments were highly abundant in the input samples, while a more specific subpopulation of tRNA processing products which is associated with Ago proteins was responsive to the depletion of La. For this reason, we repeated the Northern blot experiment, but this time selectively looking at RNAs co-immunoprecipitating with Ago2. By that, we could avoid the abundant, La-independent

tRNA-Pro fragments which, in total RNA samples, might overshadow the effects occurring to the Ago2-loaded sRNA population. In fact, a specific fragment derived from the pre-tRNA-Pro-CGG-2-1 appeared in Ago2 complexes only upon knockdown of La (Figure 3.17A). The efficient immunoprecipitation of Ago2 from cells transfected with siRNAs against La or with control siRNAs and the successful depletion of La were confirmed by the Western blots shown in Figure 3.17B.

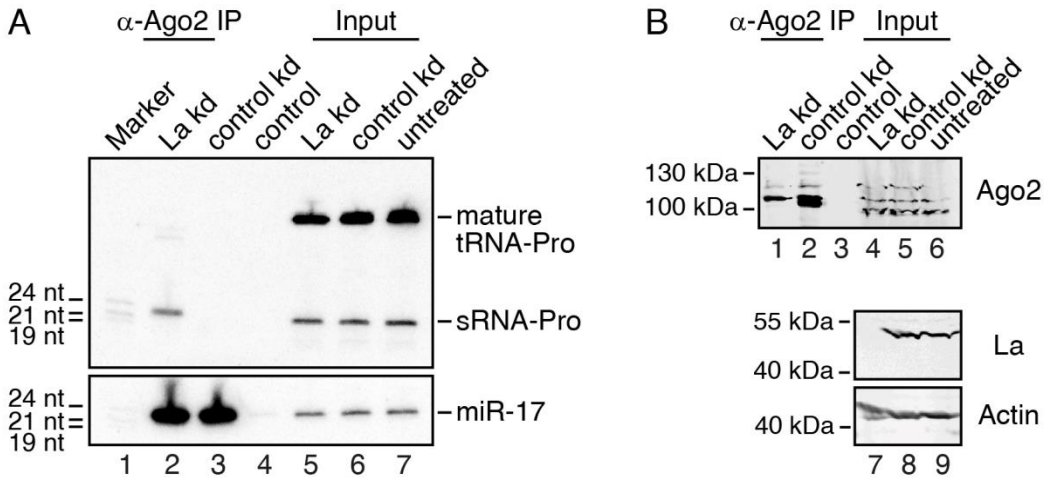

Figure 3.17: A Distinct sRNA-Pro Fragment is Loaded into Ago2 upon La Knockdown. (A) HEK293 cells were transfected with a siRNA against La (lanes 2 and 5) or with a control siRNA (lanes 3 and 6). Ago2 (lanes 2 and 3) was immunoprecipitated and associated RNAs were analyzed by Northern blotting against sRNA-Pro. Lane 4 shows a beads-only control, lanes 5-7 show input samples, and lane 1 shows a size marker. The membrane was subsequently probed for miR-17 as a loading control. The corresponding Western blot controls are shown in (B). Western blot analyses were performed with anti-Ago2 (lanes 1-6), anti-La (lanes 7-9; upper panel) and anti-actin (lanes 7-9; lower panel) antibodies. The molecular size marker weights are depicted on the left side of the blots.

The results so far indicate that La might repress the processing and loading of the pre-tRNA-Pro-derived sRNA into Ago proteins. We next reasoned whether a strong overexpression of the pre-tRNA-Pro-CGG-2-1 would lead to the production and loading of this specific fragment into Ago proteins. Indeed, a strong signal for sRNA-Pro was detected by Northern blot analysis in Ago2 immunoprecipitates upon transfection of a plasmid containing the pre-tRNA-Pro-CGG-2-1 (Figure 3.18A). Importantly, this was sufficient to generate the Ago-bound sRNA-Pro, while no additional knockdown of La was required. Importantly, Western blot analyses confirmed that similar amounts of Ago2 were immunoprecipitated in the experiments shown in Figure 3.17 and Figure 3.18 (compare lanes 1 and 2 in Figure 3.17B with lane 1 in Figure 3.18B). Thus, the strong

signal for sRNA-Pro detected in Ago2 complexes upon overexpression of pre-tRNA-Pro-CGG-2-1 is not due to differences in the amount of immunoprecipitated proteins.

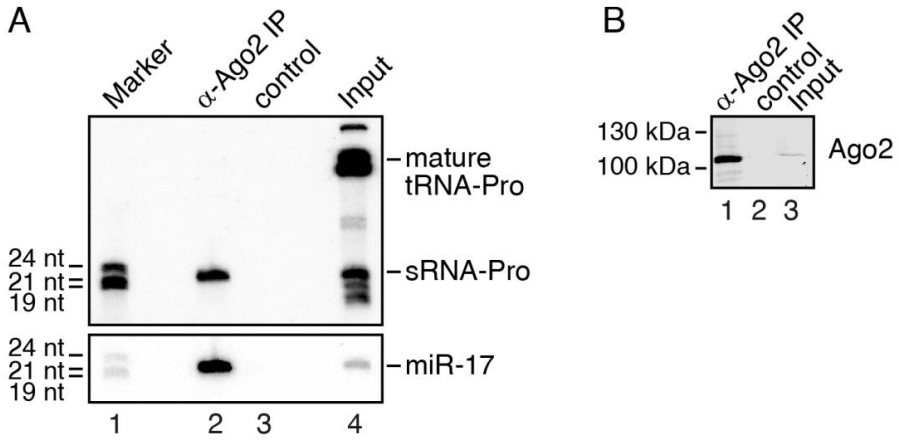

Figure 3.18: The sRNA-Pro Fragment Is Processed and Loaded into Ago2 upon Overexpression of Pre-tRNA-Pro-CGG-2-1. (A) Northern blot experiment with RNA extracted from anti-Ago2 immunoprecipitation (lane 2), beads-only control (lane 3) and input samples of HEK293 cell transfected with an overexpression construct of pre-tRNA-Pro-CGG-2-1. Lane 1 shows a size marker. The membrane was first incubated with a probe complementary to sRNA-Pro (upper panel) and subsequently re-probed for the detection of miR-17 (lower panel). (B) Western blot analysis probing for Ago2 in the corresponding protein samples (lanes 1-3). The molecular size marker weights are shown on the left.

Almost all sRNA loaded into Ago proteins are processed by Dicer from longer precursors containing hairpin structures (Kim et al., 2009). RNA secondary structure predictions performed *in silico* for the pre-tRNA-Pro-CGG-2-1 revealed that it might fold into an alternative hairpin structure possibly resembling a Dicer substrate (Figure 3.19A). Mature tRNAs, instead, adopt the stable cloverleaf secondary structure (Figure 3.19B), which is not likely to be processed by Dicer. For this reason it is more likely that the La-independent sRNA-Pro fragment found in the input samples originates by a different processing mechanism rather than from endonucleolytic cleavage by the miRNA biogenesis machinery.

Figure 3.19: The Secondary Structures of Pre-tRNA-Pro-CGG-2-1 and of the Mature tRNA-Pro-CGG-2-1 Might Strongly Differ. Schematic representations of putative secondary structures of the pre-tRNA-Pro-CGG-2-1 (A) and of the corresponding mature tRNA-Pro (B). Predictions were computed either with the mfold algorithm (see section 5.2.3.8) in case of the pre-tRNA sequence or were adopted from the gtRNAdb 2.0 database (Chan and Lowe, 2015) for the mature tRNA. The region of the pre-tRNA whereof most of the reads are derived upon La knockdown is shown in red, while the fragment processed from the mature tRNA is indicated in blue.

We next aimed to collect experimental evidences for the general ability of Dicer to bind pre-tRNAs and, by that, process them into Ago-bound sRNAs. Since our data indicate that La might interfere with the activity of Dicer, we determined the pre-tRNA population which interacts with Dicer in the presence as well as in the absence of La and compared them with each other (Figure 3.20 and Figure 3.21). For this analysis we performed photo-activatable ribonucleoside-enhanced crosslinking and immunoprecipitation (PAR-CLIP) experiments, a method which has been applied successfully in the recent years to identify the RNA targets of numerous RBPs (Milek et al., 2012). As shown schematically in Figure 3.20A, this method utilizes the incorporation of a nucleoside analogon, usually 4-thiouridine (4SU), into nascent RNA transcripts. The modified nucleoside is photoreactive and can be covalently cross-linked to nearby proteins by irradiation with UV light of 365 nm wavelength. The RBP of interest is then immunoprecipitated together with the cross-linked RNA, which is subsequently applied to a specialized cloning strategy for the generation of deep-sequencing libraries (Hafner et al., 2010).

This method has been already applied for the identification Dicer substrates in different species. We performed the experiment accordingly, using HEK293 cells stably expressing FH-tagged Dicer (Rybak-Wolf et al., 2014). Upon knockdown of La (Figure 3.20B), RNAs crosslinked to FH-Dicer were co-immunoprecipitated and radiolabeled. The complexes were resolved by SDS polyacrylamide gel electrophoresis (PAGE), blotted to a membrane (Figure 3.20C) and the RNA fragments were extracted and finally analyzed by deep-sequencing.

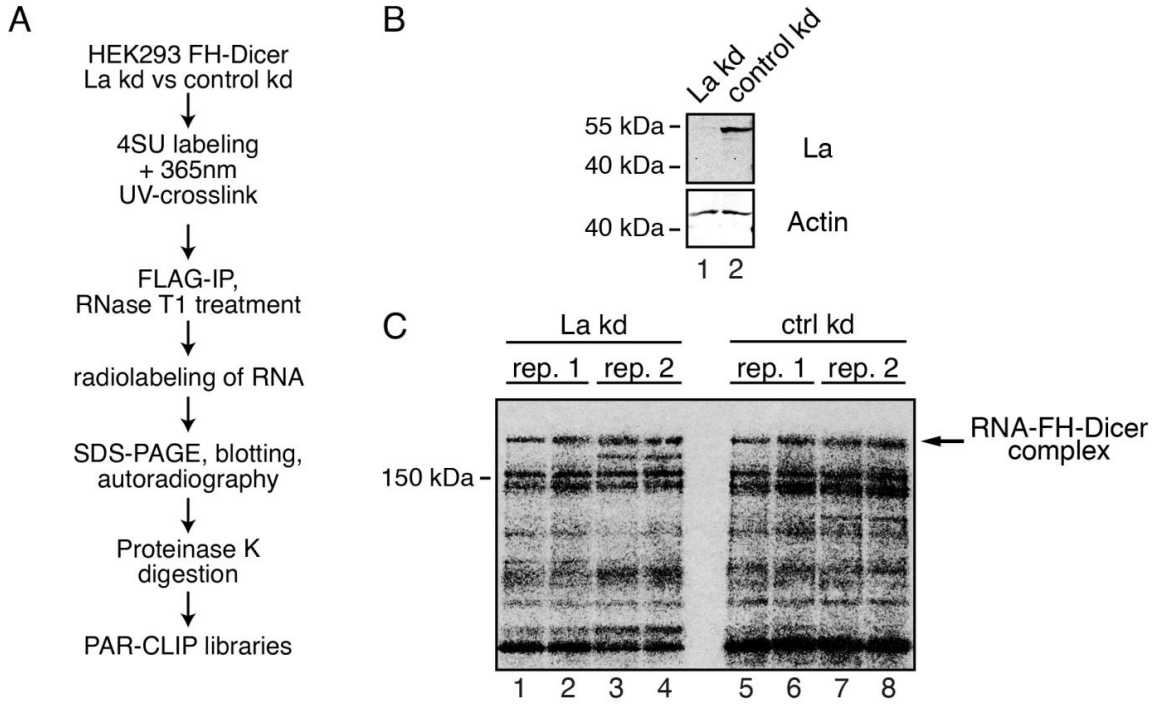

Figure 3.20: PAR-CLIP Experiments with FH-Dicer in La or Control Knockdown Conditions. (A) Schematic representation of the experimental procedure used for PAR-CLIP of FH-Dicer upon La or control knockdown. (B) The efficient depletion of La (lane 1) compared to the control knockdown (lane 2) was assayed by Western blotting. Actin served as loading control. The molecular size marker weights are depicted on the left. (C) Radiolabeled RNA-protein complexes from the FH-Dicer PAR-CLIP experiments performed under La knockdown (lanes 1-4) or control (lanes 5-8) conditions were resolved on a SDS-gel and blotted to a membrane. The signals corresponding to the RNA-FH-Dicer complexes are indicated on the right side of the autoradiogram. This region of the membrane was excised and further processed for the generation of the sRNA libraries.

In agreement with the data of Rybak-Wolf et al. (2014), several reads mapping to tRNA sequences were detected. In general, we found many tRNAs significantly less associated with FH-Dicer upon La depletion (shown in red in the lower part of Figure 3.21). This effect might be due to generally reduced expression levels of these tRNAs. At the same time, sequences mapping to other pre-tRNA transcripts were found significantly enriched

in the FH-Dicer PAR-CLIP libraries generated from La knockdown cells (shown in red in the upper part of the plot).

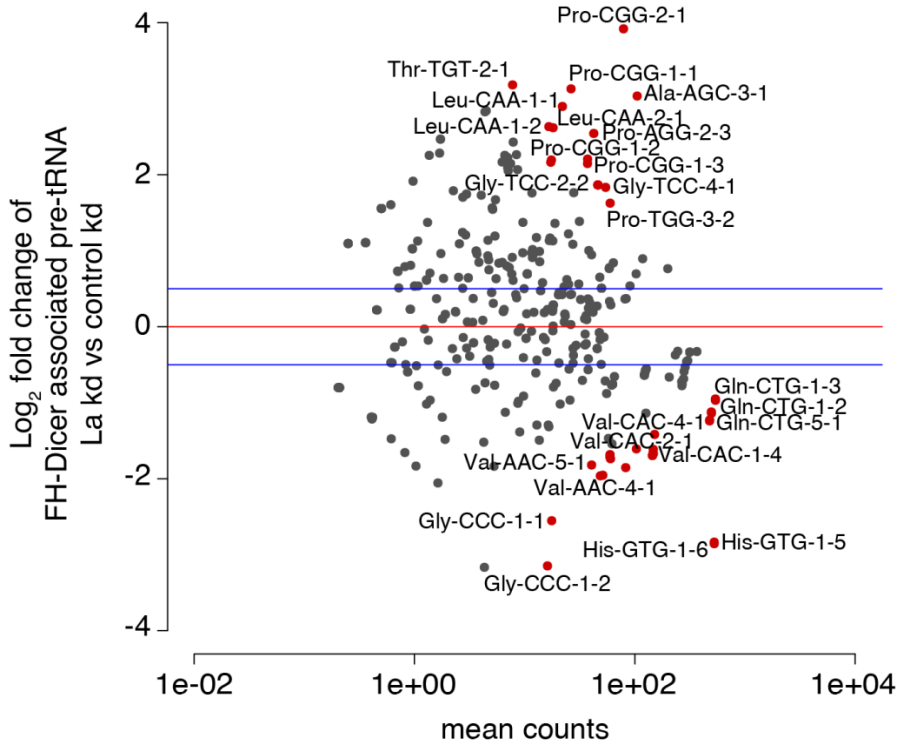

Figure 3.21: The Depletion of La Affects the Pool of tRNA Transcripts Interacting with FH-Dicer. The MA plot shows the differential coverage analysis of reads mapping to pre-tRNA sequences in the FH-Dicer PAR-CLIP libraries. The red dots annotate tRNAs, which associate differentially to FH-Dicer (Benjamini-Hochberg adjusted p value < 0.05).

Most strikingly, the greatest difference between the two conditions was observed for reads originating from Pro-CGG-2-1. This is in agreement with our previous hypothesis, that La prevents the processing of pre-tRNA-Pro-CGG-2-1 by Dicer, which can bind to this particular pre-tRNA either if the La levels are reduced or if the pre-tRNA is highly transcribed, e.g., from an exogenous source.

3.6. A Bona Fide MiRNA is Generated from Pre-tRNA-Ile-TAT-2-3

Another interesting fragment found in the Ago-associated sRNA libraries was derived specifically from the 3' end of pre-tRNA-Ile-TAT-2-3. This sRNA has been already detected before in the total RNA of mouse embryonic stem cells and was annotated as mmu-miR-1983 (Babiarz et al., 2008). The authors of this work proved, by analyzing the RNA content of different knockout cell lines, that the biogenesis of mmu-miR-1983 requires Dicer, but occurs independently of the Microprocessor complex. By that, mmu-miR-1983 differs from the processing of canonical miRNAs. However, neither the association with Ago proteins, nor the functionality of this sRNA has been investigated so far. The occurrence of this specific sRNA in human cells has also not been reported yet and it is not deposited in the most recent human miRNA database (miRBase21; Kozomara and Griffiths-Jones, 2014). The comparison between the genomic sequence of the human tRNA-Ile-TAT-2-3 and the corresponding mouse sequence showed that it is highly conserved between these two species. In particular, the sequence of the detected sRNA-Ile (shown in red) is exactly the same in mouse and in human. The only difference between the two pre-tRNA sequences occurs at one position within the tRNA intron. However, it is not likely that this mismatch could determine overall changes in the secondary structure of the two pre-tRNAs.

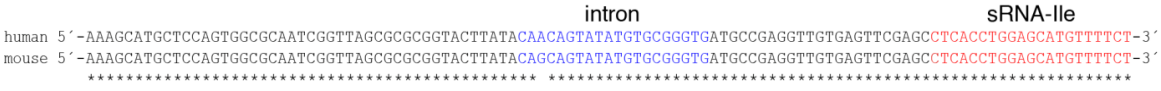

Figure 3.22: Pre-tRNA-Ile-TAT-2-3 Is Conserved between Human and Mouse. Alignment of the human pre-tRNA-Ile-TAT-2-3 and the mouse pre-tRNA-Ile-TAT-2- sequences. The sRNA (annotated in mouse as miR-1983) is shown in red and the tRNA intron in blue. Conserved positions are marked by asterisks.

The tRNA genes listed in the database used for our data analysis (gtRNAdb 2.0; Chan and Lowe, 2015) were predicted by bioinformatic tools. It might be, therefore, that the tRNA-Ile-TAT-2-3 locus is misannotated as a tRNA while its main function is to generate the sRNA-Ile fragment. In order to clarify whether a functional tRNA is indeed processed from Ile-TAT-2-3, we conducted an amino acylation assay. Therefore, the total RNA from HEK293 cells was extracted under acidic conditions which preserve the labile acyl bond between tRNAs and the loaded amino acids. An aliquot was then incubated at alkaline pH to deacylate the tRNAs. The size difference between acylated and deacylated tRNAs can be determined by running the samples on an acidic denaturing polyacrylamide

gel followed by Northern blotting. As shown in Figure 3.23, we carried out the assay with untreated (lanes 5 and 6) or mock treated (lanes 3 and 4) samples as well as with RNA from cells overexpressing pre-tRNA-Ile-TAT-2-3 from a plasmid (lanes 1 and 2). This permitted us to exclude misinterpretation of the results due to a possible cross-hybridization of the Northern blot probe with other endogenous tRNA-Ile of different genomic origin. For all conditions, the acylated tRNAs migrated slower than in the deacylated samples, suggesting that endogenous as well as overexpressed tRNA-Ile-TAT-2-3 are processed to functional tRNAs, which are competent for protein translation. This finding was corroborated further by the occurrence of tRNA-Ile in polyribosomal fractions (data not shown). Surprisingly, we noticed in the aminoacylation assay that a band corresponding to the charged tRNA was still visible upon alkaline treatment, while this was not the case for the control tRNA-Lys.

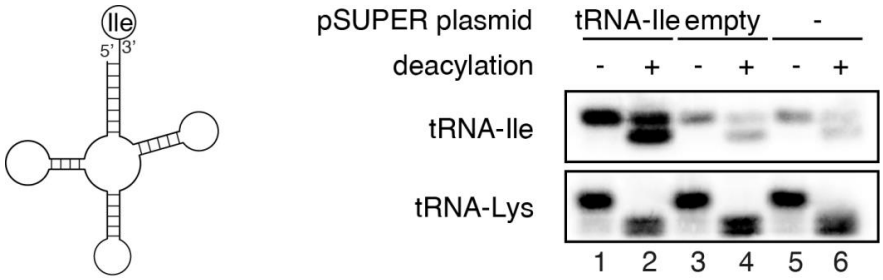

Figure 3.23: Pre-tRNA-Ile-TAT-2-3 Generates a Functional tRNA. A schematic representation of the mature tRNA-Ile-TAT-2-3 secondary structure is depicted on the left side. On the right, amino-acylation assays performed with total RNA isolated from HEK293 cells. The samples in lanes 1, 3 and 5 were kept under acidic conditions preserving the aminoacylation state, while the samples in lanes 2, 4 and 6 were alkali-treated to deacylate the tRNAs. Probes either for the mature tRNA-Ile-TAT-2-3 or for tRNA-Lys, as positive control, were used for Northern blotting.

We next aimed to characterize in more details the sRNA-Ile fragment, which is generated from pre-tRNA-Ile-TAT-2-3. Similar to classical miRNAs, Northern blot analysis revealed that sRNA-Ile is differentially expressed across several human cell lines, at low levels e.g., in DLD-1 cells and at high levels in SK-N-MC cells (Figure 3.24). Interestingly, the Northern blot probe detected also the mature tRNA-Ile, which was present at similar levels in all samples, and the pre-tRNA-Ile, which, instead, was differentially expressed across the cell lines. In addition, a fragment migrating between the mature tRNA and the sRNA fragment was particularly prominent in DLD-1 cells and might correspond to the 3' splicing intermediate of the tRNA-Ile-TAT-2-3.

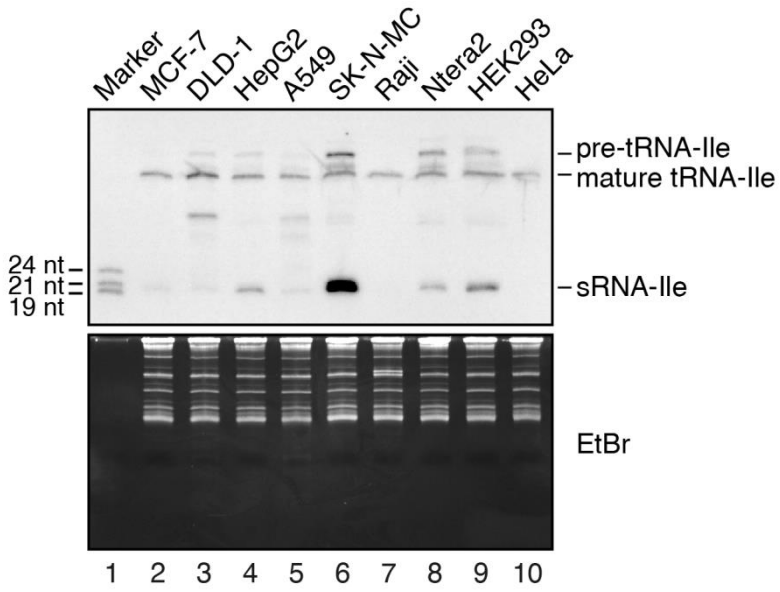

Figure 3.24: The sRNA-Ile Is Differentially Expressed across Human Cell Lines. Northern blot experiments were performed with total RNA extracted from the indicated cell lines (lanes 2-10). A size marker was loaded on lane 1. The lower panel shows the ethidium bromide (EtBr) staining of the gel before blotting and served as a control for RNA quality and for equal loading of the samples.

In order to execute their biological function, miRNAs are required to be expressed at sufficiently high levels. To clarify whether this is the case for sRNA-Ile as well, we determined its absolute expression in HEK293 (Figure 3.25A) and SK-N-MC (Figure 3.25B) cells by quantitative Northern blotting using serial dilutions of a synthetic oligonucleotide as a reference. The results of this experiment allowed us to calculate a value of ~250 copies per cell in HEK293 and ~750 copies per cell in SK-N-MC (Figure 3.25C), which is comparable to the amount of a medium abundant miRNA (Bissels et al., 2009).

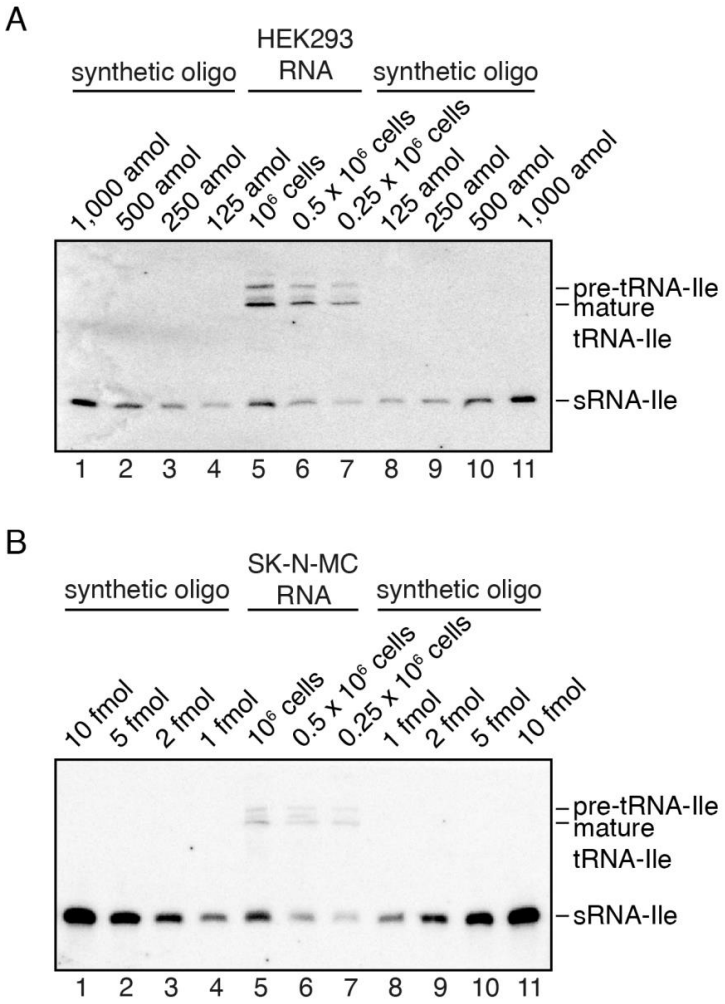

C

cell line	copies/cell
HEK293	254±45
SK-N-MC	762±153

Figure 3.25: The sRNA-Ile Is Expressed at Similar Levels Compared to Canonical MiRNAs. Quantitative Northern blots were performed by loading serial dilutions of defined amounts of the synthetic sRNA-Ile (lanes 1-4 and 8-11) and the total RNA extracted from the indicated amount of HEK293 (A) or SK-N-MC (B) cells (lanes 5-7). (C) The signal intensities of the synthetic ribooligonucleotide were used to generate standard curves, allowing for the absolute quantification of the miR-1983 copy numbers per cell. The average and the standard deviation were determined for lanes 5-7 of the respective blot and are indicated in the table.

The results so far indicate that sRNA-Ile shares some characteristic features with miRNAs and we further aimed to clarify whether it is also processed similarly. Pre-tRNA-Ile-TAT-2-3 is unusual since its 5' and 3' extensions are complementary, which is rarely found in other pre-tRNAs. By that, pre-tRNA-Ile-TAT-2-3 can fold into an alternative secondary structure with an extended double-stranded stem (Figure 3.26). This folding differs from the typical cloverleaf structure, which is acquired already by pre-tRNA transcripts. Of note, beside the interaction of the leader and trailer sequences with each other, also additional unconventional base pairings are necessary to permit this alternative folding. These concern the interactions between nucleotides normally forming the D- and T-arms of the mature tRNA, as well as interactions between the intron and

nucleotides located within the D- and the anticodon-arms. Importantly, within this alternative structure, sRNA-Ile (shown in red) is entirely embedded in the double-stranded terminal stem and might therefore be processed by Dicer.

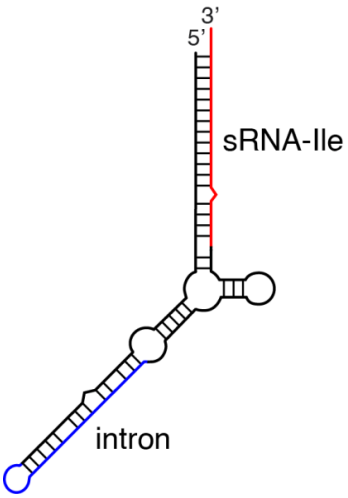

Figure 3.26: Pre-tRNA-Ile-TAT-2-3 Can Fold into a Structure with an Extended Terminal Stem. The schematic representation is based on *in silico* predictions computed with the mfold algorithm The portion corresponding to the processed sRNA-Ile is shown in red and the intron in blue.

To experimentally test this hypothesis, we first performed cleavage assays with *in vitro* transcribed pre-tRNA-Ile-TAT-2-3 and immunoprecipitated FH-Dicer. Indeed, a sRNA was produced upon incubation of the pre-tRNA with FH-Dicer but not in a control reaction (Figure 3.27).

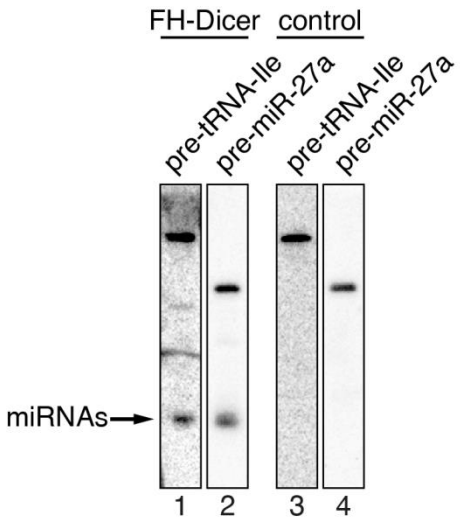

Figure 3.27: FH-Dicer Processes Pre-tRNA-Ile-TAT-2-3 to sRNA-Ile *in vitro*. Anti-FLAG immunoprecipitations were performed from HEK293 cells transfected with FH-Dicer (lanes 1 and 2) or from non-transfected cells (lanes 3 and 4). Beads were incubated with *in vitro* transcribed pre-tRNA-Ile-TAT-2-3 (lanes 1 and 3) or pre-miR-27a (lanes 2 and 4). After cleavage reaction, the RNA was extracted from the samples and was used for Northern blotting with probes against sRNA-Ile (lanes 1 and 3) or miR-27a (lanes 2 and 4). The processing products of miRNA size are highlighted by an arrow on the left.

We next investigated the Dicer-dependency of sRNA-Ile *in vivo* and performed Northern blot assays with total RNA isolated from wild type (Dcr +/+) as well as Dicer-deficient (Dcr -/-) mouse embryonic fibroblasts (MEFs). The sRNA-Ile was detected in Dcr +/+ MEFs, but not in cells lacking functional Dicer (Figure 3.28, upper panel). Thus, Dicer seems to be required for the biogenesis of the sRNA-Ile fragment.

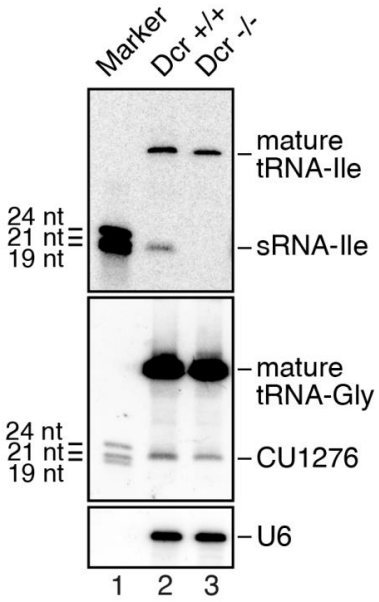

Figure 3.28: The sRNA-Ile Fragment Is Absent in Dcr -/- Cells. Northern blot analysis performed with total RNA extracted from Dcr +/+ MEFs (lane 2) or Dcr -/- MEFs (lane 3). A size marker was loaded on lane 1. The membrane was first probed for sRNA-Ile and, subsequently, for the CU1276 fragment (see main text). Detection of the U6 snRNA served as loading control.

This finding was further strengthened by the reduction of sRNA-Ile levels upon knockdown of Dicer which we conducted with two different siRNAs (Figure 3.29A and C). To analyze the involvement of further components of the miRNA biogenesis machinery, we knocked down Xpo5 as well. Also in this case, the abundance of sRNA-Ile was severely affected (Figure 3.29B and C). Of note, we subsequently probed the membranes for a sRNA which is derived from a mature tRNA-Gly. This sRNA was suggested in a previous study to have several miRNA characteristics and was termed CU1276 (Maute et al., 2013). Differing from what we observed for sRNA-Ile, the expression of CU1276 did not change across the different samples tested (Figure 3.28 and Figure 3.29).

In summary, we conclude from our results that pre-tRNA-Ile-TAT-2-3 can be either processed to a functional tRNA or to a sRNA, which has several characteristics in common with miRNAs.

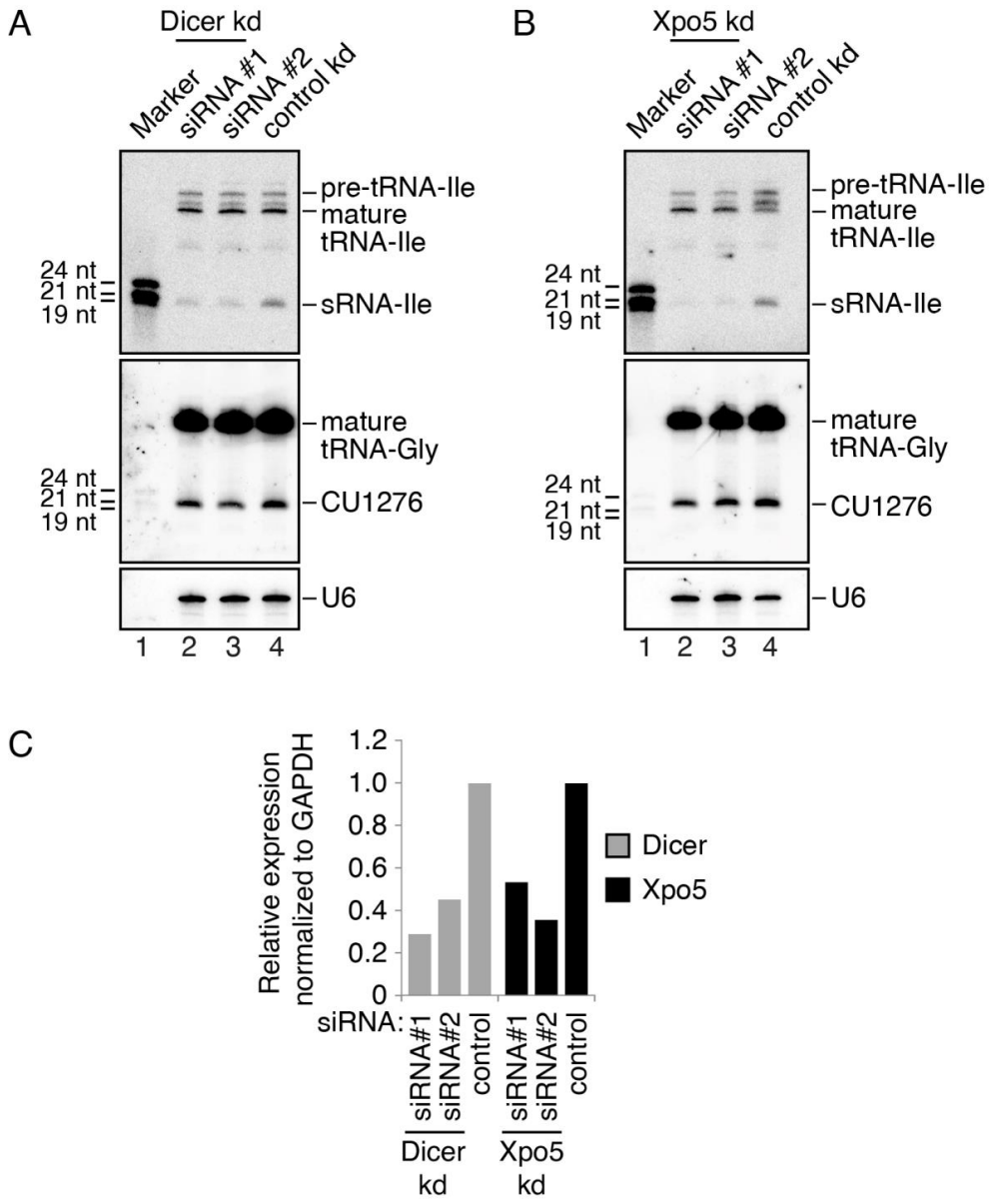

Figure 3.29: The Biogenesis of sRNA-Ile Depends on the MiRNA Processing Machinery. HEK293 cells were transfected with two different siRNAs against Dicer (A) or against Xpo5 (B). After three days the total RNA was extracted and used for Northern blot assays. Samples of the corresponding knock-downs were loaded on lanes 2 and 3, a control knockdown on lane 4. A size marker is shown in lane 1. Probing of the membrane occurred as described in Figure 2.28. (C) The efficiencies of the knockdowns performed in (A) and (B) were validated by qPCR.

3.7. The sRNA-Ile Is Loaded into Functional Silencing Complexes

The evidences collected so far linked the occurrence of sRNA-Ile to several components of the miRNA biogenesis pathway. We intended to clarify whether sRNA-Ile is indeed a functional miRNA and consequently associates with the effectors of gene silencing. For this, we performed Northern blot analyses (Figure 3.30A) with RNA co-purified with immunoprecipitated endogenous Ago1, Ago2 and Ago3 (corresponding Western blot

controls shown in Figure 3.30B). In agreement with our previous deep sequencing results (Figure 3.10), we found sRNA-Ile associating with Ago proteins, while neither the pre-tRNA, nor the mature tRNA-Ile were bound (Figure 3.30A).

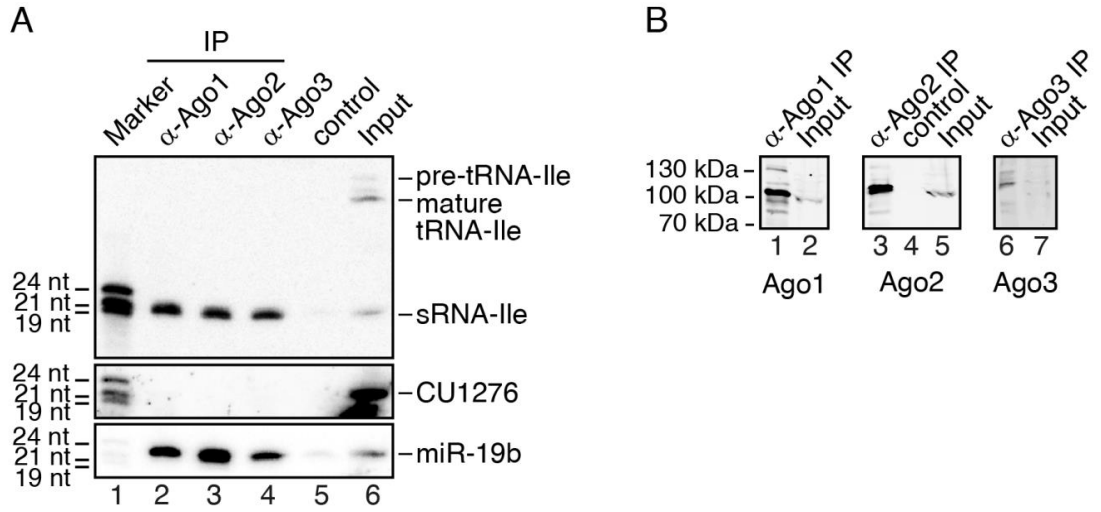

Figure 3.30: The sRNA-Ile Is Loaded into Ago Proteins. (A) Endogenous Ago1, Ago2 and Ago3 (lanes 2-4) were immunoprecipitated from HEK293 cells. Co-precipitated RNAs were assayed by Northern blotting for the indicated RNAs. Lane 5 shows a beads-only control, lane 6 shows an input sample, and lane 1 shows a size marker. (B) Western blots were performed with aliquots from the indicated samples and were probed for human Ago1 (lanes 1 and 2), Ago2 (lanes 3-5), and Ago3 (lanes 6 and 7). The molecular size marker weights are depicted on the left.

To further corroborate the interaction of sRNA-Ile with functional gene silencing complexes, we immunoprecipitated TNRC6 proteins and repeated the Northern blot assay (Figure 3.31A). TNRC6 proteins are key proteins within the miRNA-dependent repression pathway and they directly interact with Ago proteins, which can be co-purified in anti-TNRC6 immunoprecipitates (Figure 3.31B). They act as scaffolds recruiting several downstream factors, which are responsible for the post-transcriptional inhibition of mRNAs targeted by miRNA-Ago complexes (reviewed in Jonas and Izaurralde, 2015, see also section 1.2.4). Importantly, we were able to enrich sRNA-Ile with anti-TNRC6 antibodies (Figure 3.31A). This finding suggests that sRNA-Ile interacts with Ago proteins and that together they participate to the repression of gene expression via the classical miRNA pathway. In contrast, the tRNA-Gly fragment CU1276 was neither co-precipitated with the Ago nor with the TNRC6 proteins (Figure 3.30A and Figure 3.31A), further confirming our hypothesis that it might rather have miRNA-independent functions, at least in the cell lines tested here.

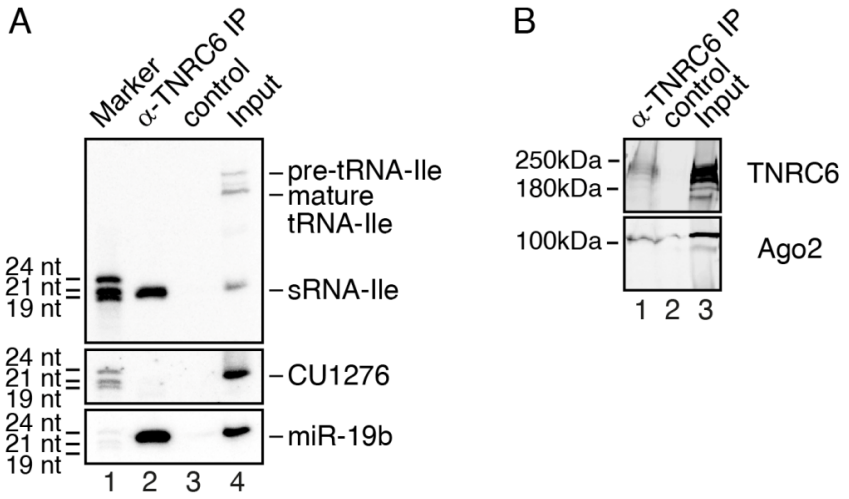

Figure 3.31: The sRNA-Ile Associates with TNRC6 Complexes. (A) RNAs extracted from pan-TNRC6 immunoprecipitation (lane 2), beads-only control (lane 3), and input samples (lane 4) were used for Northern blotting with the same probes as in Figure 2.30. Lane 1 shows a size marker. (B) Western blot control for the immunoprecipitation of pan-TNRC6 (lane 1), control (lane 2), and the input (lane 3). TNRC6 proteins and co-precipitated Ago2 are detected in the TNRC6 immunoprecipitation (lane 1). The molecular size marker weights are depicted on the left.

MiRNAs inhibit gene expression by binding to complementary sequences on target mRNAs, mainly located within their 3' UTR (Bartel, 2009). In order to identify the mRNAs regulated by sRNA-Ile, we applied a bioinformatic tool (TargetScan 5.2, Friedman et al., 2008) and predicted potential target transcripts. We chose to validate three genes out of this candidate list, namely RIMS2, which is involved in the regulation of synaptic membrane exocytosis, and BACH1 and BACH2, two transcription factors involved in the metabolism of heme and oxidative stress response pathways. We cloned their 3' UTR sequences into reporter plasmids downstream of the firefly luciferase gene. Additionally, an artificial target construct containing two full-complementary sRNA-Ile binding sites was generated as a positive control. We then transfected the reporters in HEK293 cells either together with a mimic RNA or together with plasmids expressing sRNA-Ile from a short hairpin (sh)RNA or from the complete pre-tRNA-Ile-TAT-2-3 context (Figure 3.32). As expected, the firefly activity of the artificial target construct was strongly reduced upon overexpression of sRNA-Ile, independently of the system used. The effect was completely abrogated if the assay was performed with an artificial reporter containing mutated sRNA-Ile target sites (Figure 3.32). Importantly, the overexpression of sRNA-Ile consistently led to a reduced expression of the reporter constructs containing the 3' UTRs of RIMS2, BACH1 or BACH2. Also in this case, the sRNA-Ile-mediated repression was abolished if the putative target sites within the RIMS2, BACH1 or BACH2 3' UTRs were mutated (Figure 3.32).

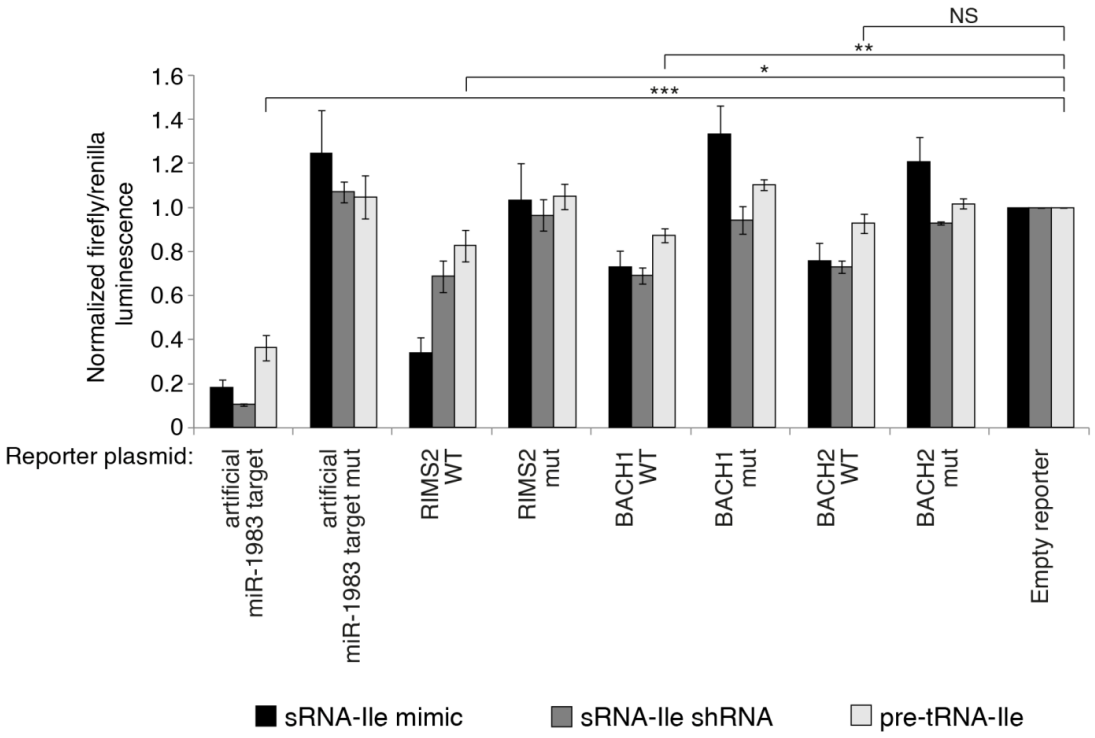

Figure 3.32: The sRNA-Ile Functions as a *Bona Fide* miRNA Repressing Translation. Two fully complemen-tary target sequences for sRNA-Ile (artificial miR-1983 target) or 3'-UTRs from predicted sRNA-Ile targets were fused to the firefly luciferase gene. Constructs with the mutated seed sequences of the artificial or the predicted target sites were generated as well. The reporter plasmids were tested in dual luciferase assays by co-transfecting the indicated RNAs (see main text). Firefly/renilla luminescence ratios were normalized to corresponding ratios of the empty reporter plasmid and to the corresponding control co-transfections. These were a control siRNA, the empty shRNA expression plasmid, or a plasmid overexpressing a different pre-tRNA-Ile, which does not generate the sRNA-Ile fragment. The quantifications from three biological replicates are shown. The error bars represent ±SD and significance was assessed by two-sided Student's t test (*$p < 0.05$, **$p < 0.01$, ***$p < 0.001$, and NS = not significant).

It should be noted that the inhibition of gene expression achieved by the pre-tRNA-Ile-TAT-2-3 construct was always milder compared to the mimic RNA or the shRNA and did not reach statistical significance in the case of the BACH2 reporter (Figure 3.32). This is likely due to the fact that sRNA-Ile was produced less efficiently from the pre-tRNA-Ile-TAT-2-3 plasmid in comparison to the two other constructs (Figure 3.33).

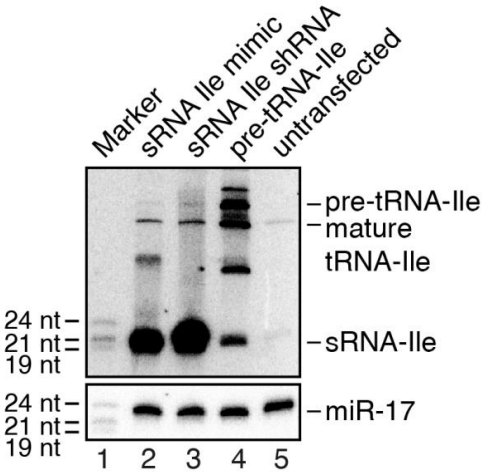

Figure 3.33: The Overexpression of sRNA-Ile from the Pre-tRNA Is Weaker Compared to the Other Constructs. Northern blot for sRNA-Ile generated from the different constructs applying the same conditions as in Figure 3.32 (lanes 2-4). The total RNA extracted from non-transfected cells (lane 5) was used for comparison. Lane 1 shows a size marker. Equal loading of the sample was assayed by detection of miR-17.

Nevertheless, the results of the luciferase reporter assay indicate that sRNA-Ile is capable of inhibiting target gene expression (Figure 3.32). For this reason and congruent with our previous findings we claim that sRNA-Ile is indeed a *bona fide* miRNA and we therefore refer to it as hsa-miR-1983.

3.8. La is the Main Regulator for the Transition of Pre-tRNA-Ile-TAT-2-3 to miR-1983

We identified miR-1983 in our initial screening for sRNAs, which are loaded into Ago proteins in a La-dependent manner. The experiments conducted so far indicate that two different and functionally active products can arise from the tRNA-Ile-TAT-2-3 precursor, either miR-1983 or the mature tRNA-Ile. In some of the cell lines tested, both of them exist in parallel and we set out to identify which factors determine the fate of pre-tRNA-Ile-TAT-2-3.

The expression levels of miR-1983 were analyzed by Northern blotting (Figure 3.34A)

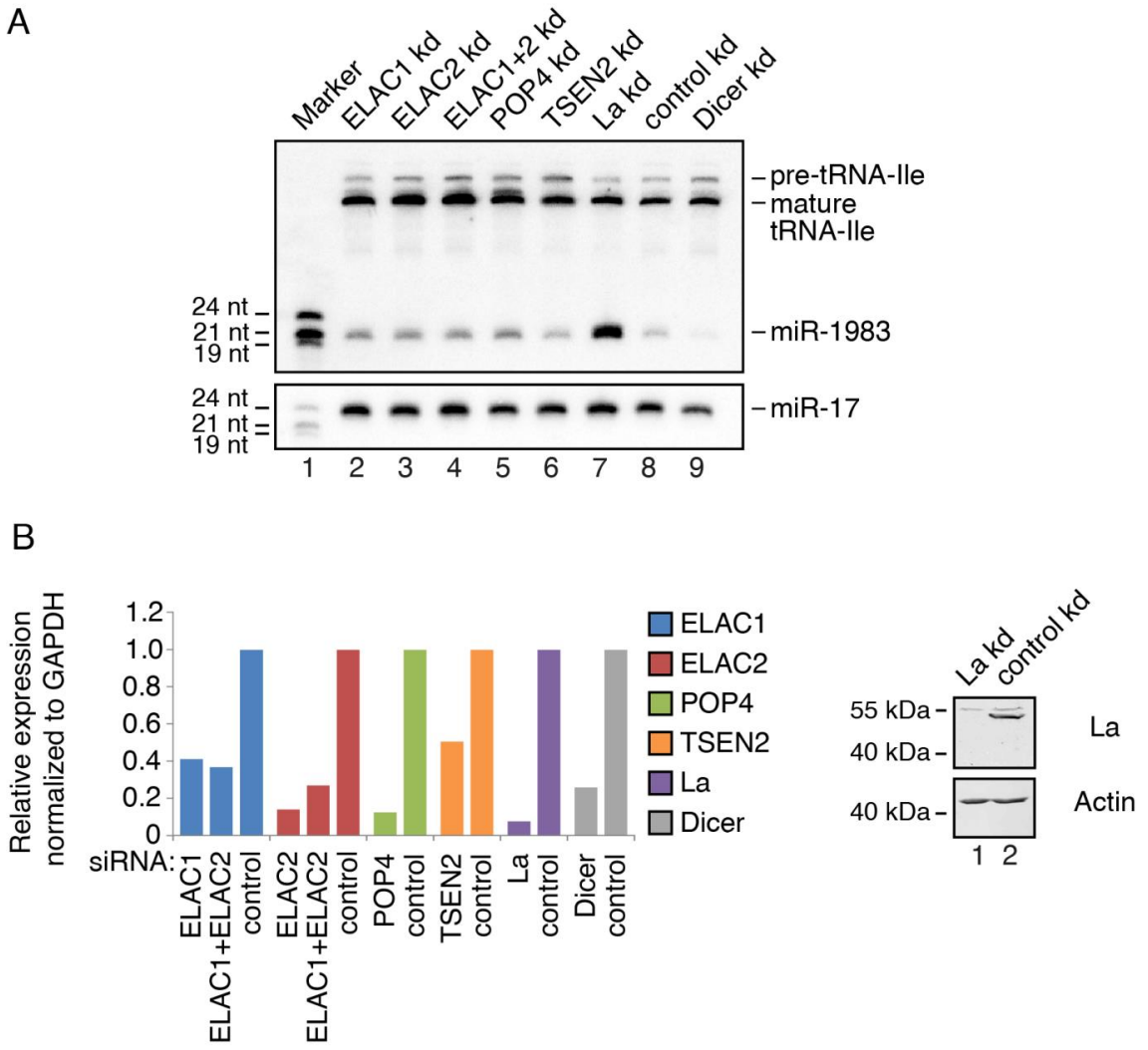

Figure 3.34: Effect of the tRNA Processing Machinery on MiR-1983 Expression. (A) HEK293 cells were transfected with siRNAs against two different forms of RNase Z (lanes 2-4), the POP4 subunit of RNase P (lane 5), a catalytic subunit (TSEN2) of the tRNA-splicing complex (lane 6), the La protein (lane 7), or Dicer (lane 9).Control siRNA transfection is shown in lane 8. The expression levels of miR-1983 were analyzed by Northern blotting, detection of miR-17 served as loading control. Lane 1 shows a size marker. (B) Validation of knockdown efficiencies by qPCR for the samples used in (A) (left). Protein levels of La in cells transfected with a siRNA against La (lane 1) or with a control siRNA (lane 2) were assayed by Western blotting (right). Equal loading of the samples was assayed by detection of actin. The molecular size marker weights are shown on the left.

upon siRNA-mediated depletion of different proteins involved in the tRNA processing pathway (Figure 3.34B). The result presented in Figure 3.34A shows that neither the knockdown of 3' end processing enzymes (ELAC1/2) nor of components of the 5' end processing complex (POP4) or of the tRNA splicing complex (TSEN2) had a relevant influence on the abundance of miR-1983. Instead, depletion of La severely increased miR-1983 levels. This effect was proven to be specific as it was reproduced by using three different siRNAs against La, while the knockdown of LARP1 or LARP4B had no effect (Figure 3.35A). Furthermore, the increase of miR-1983 upon La knockdown were reproducible independently of the cell line used as it occurred in SK-N-MC cells as well (Figure 3.35B).

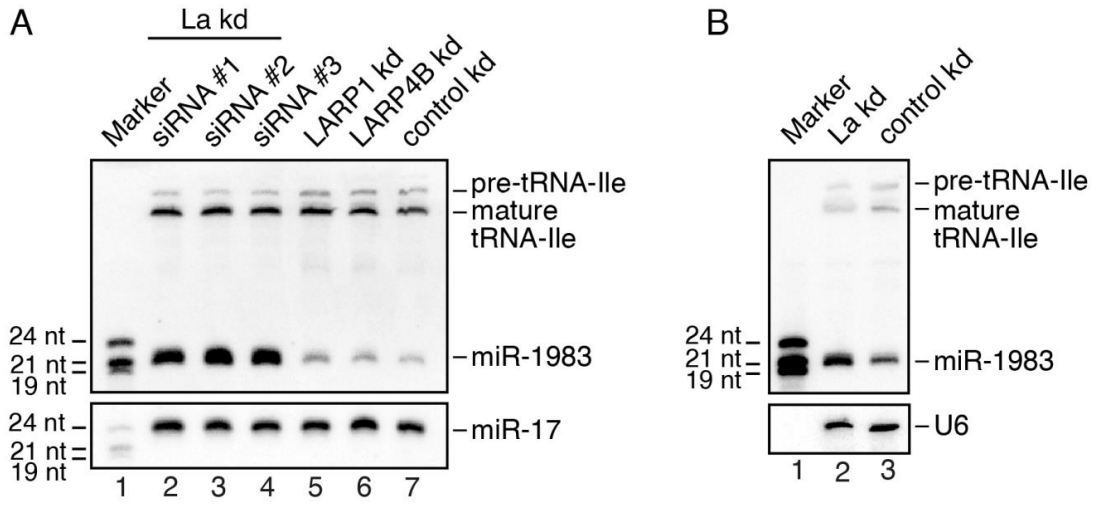

Figure 3.35: La Determines the Expression Levels of miR-1983. (A) HEK293 cells were transfected with three different siRNAs against La (lanes 2-4), a siRNA against LARP1 (lane 5), LARP4B (lane 6), or a control siRNA (lane 7). The expression levels of miR-1983 were analyzed by Northern blotting and detection of miR-17 served as loading control. Lane 1 shows a size marker. (B) Northern blot experiment performed with total RNA extracted from SK-N-MC cells following La knockdown (lane 2) or control knockdown (lane 3). A size marker was loaded on lane 1. The membrane was assayed for the U6 snRNA which served as loading control.

In addition, we performed anti-Ago2 immunoprecipitations from La-depleted or control cells and confirmed by Northern blotting that the levels of miR-1983 were increased in the Ago-bound sRNA fraction as well (Figure 3.36A). The efficient immunoprecipitation of Ago2 from cells transfected with siRNAs against La or with control siRNAs and the successful depletion of La were confirmed by the Western blots shown in Figure 3.36B. Due to all this findings, we hypothesize that La is a key factor controlling the processing of miR-1983 from pre-tRNA-Ile-TAT-2-3.

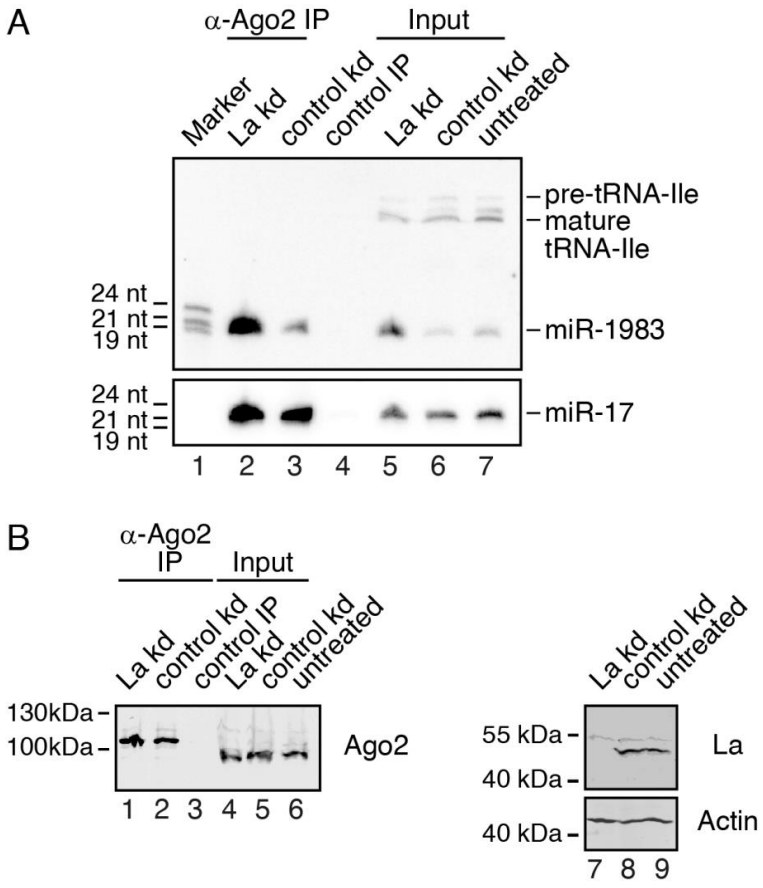

Figure 3.36: Increased MiR-1983 Levels upon La Depletion Correlate with Increased Binding to Ago2. (A) La knockdown (lanes 2 and 5) and control knockdown (lanes 3 and 6) were performed in HEK293 cells. Ago2 (lanes 2 and 3) was immunoprecipitated and miR-1983 levels were assayed by Northern blotting. Lane 4 shows beads-only control and lanes 5-7 show input samples. A size marker was loaded on lane 1. The signals for miR-17 are shown in the lower panel. (B) Western blot controls for the experiment shown in (A). Samples were assayed for the presence of Ago2 (lanes 1-6, left panel). The efficient depletion of La (lane 7) compared to the control samples (lanes 8 and 9) is shown on the right. The molecular size marker weights are indicated on the left side of the blots.

We therefore speculated whether differences in La protein levels might account for the varying expression of miR-1983 across several cell lines, as we noted previously (Figure 3.24). However, Western blot analyses revealed that La was almost equally expressed between the different samples (Figure 3.37 upper panel), indicating that other factors are responsible for the different miR-1983 steady-state levels. Some studies have shown in the past that the differential expression of components of the miRNA biogenesis machinery drive changes in the miRNA profile of different cell types (Kumar et al., 2009; Melo et al., 2010; Ma et al., 2011; Ott et al., 2016). We thus analyzed by Western blotting the levels of Dicer and Xpo5 in the cell lines we previously used (Figure 3.37, central and lower panels). Indeed, a correlation between Xpo5 and/or Dicer and mir-1983 expression might hold true. Xpo5, for example, is more abundant in SK-N-MC, Ntera2 and HEK293 cells compared to other cell lines, which is similar to the expression pattern of miR-1983 (compare Figure 3.37 lower panels with Figure 3.24).

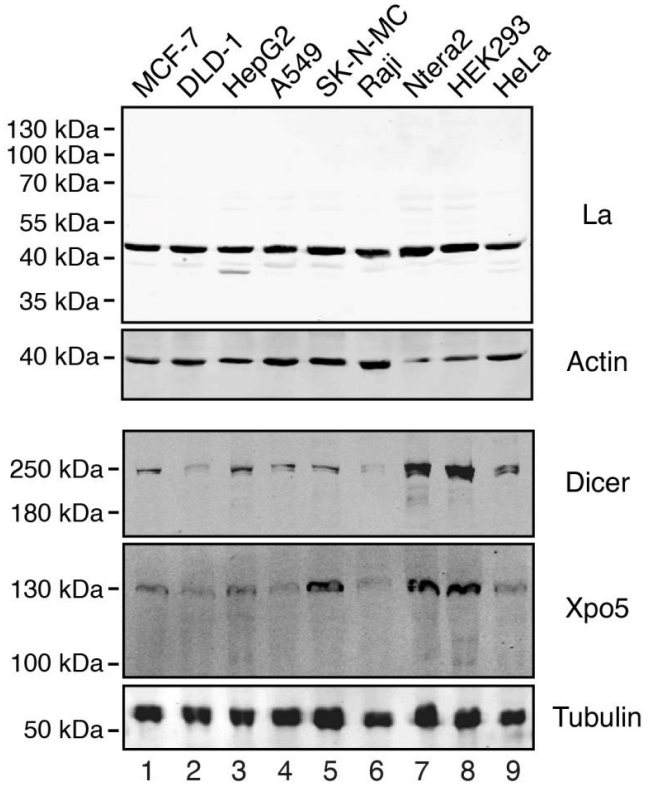

Figure 3.37: La Is Expressed at Similar Levels across Different Cell Lines. Western blotting for La, Dicer, and Xpo5 with the same cell lines used for Northern blotting of sRNA-Ile in Figure 3.24 (lanes 1–9). Detection of actin and tubulin served as controls. The molecular size marker weights are depicted on the left.

3.9. Full-length La Protein is Required for the Interaction with Pre-tRNA-Ile-TAT-2-3

The hallmark of all LARPs is the so-called La module, which consists of a defined winged-helix fold, denoted La motif (LAM), and a RNA recognition motif (RRM). In addition, genuine La proteins usually contain a second RRM in their C-terminal part (reviewed in Maraia et al., 2017). However, the La module on its own is responsible for binding to the 3' terminal U-stretch of Pol III (Alfano et al., 2004; Teplova et al., 2006). Additional interactions between other regions of La and pre-tRNAs have been shown to occur (Jacks et al., 2003; Bayfield and Maraia, 2009; Kucera et al., 2011). Some evidences exist, which indicate that La also binds to Pol II transcripts independently of terminal U-stretches (Holcik and Korneluk, 2000; Trotta et al., 2003; Martino et al., 2012; Liang et al., 2013). For this reason we aimed to investigate in more detail the nature of the interaction of La to pre-tRNA-Ile-TAT-2-3. First, we confirmed the binding of endogenous La to pre-tRNA-Ile by anti-La immunoprecipitations and subsequent Northern blotting of the co-purified RNAs. A signal corresponding to the size of full-length pre-tRNA-Ile-TAT-2-3 was detected specifically in the anti-La and not in the control immunoprecipitation. Furthermore, additional signals of smaller RNA species were present and probably correspond to some processing intermediates, i.e., 5' end processed pre-tRNA and 3' splicing intermediate. As expected, the mature tRNA-Ile was detected at high levels in the input but did not associate with La (Figure 3.38).

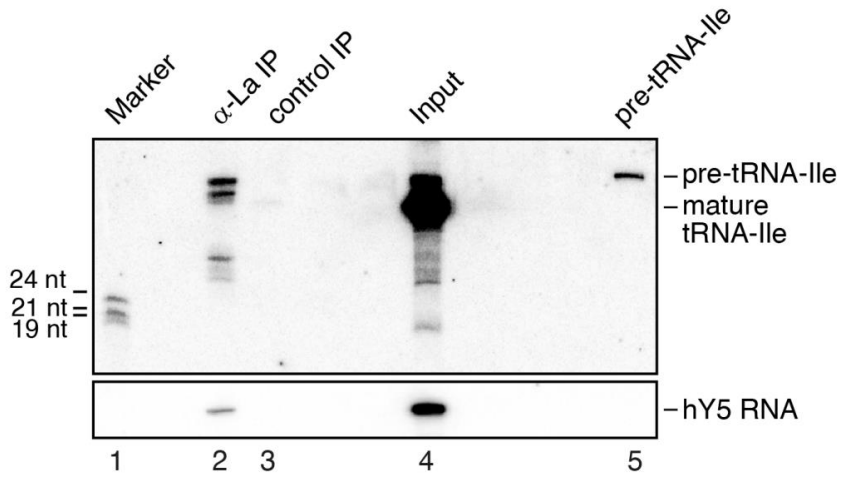

Figure 3.38: Pre-tRNA-Ile-TAT-2-3 Associates with Endogenous La. Immunoprecipitation of La was performed from SK-N-MC lysate (lane 2) and co-immunoprecipitated RNAs were analyzed by Northern blotting. Lane 3 shows a control immunoprecipitation with pre-immune serum, lane 4 is the input sample, and lanes 1 and 5 are size markers. The signals were detected with the *in vitro* transcribed, 5' end-labeled, antisense pre-tRNA-Ile. Hybridization of the membrane with a probe for the Pol III transcribed Y5 RNA served as positive control.

We then generated several mutant versions of FH-tagged La and dissected the structural requirements accounting for the binding of La to pre-tRNA-Ile-TAT-2-3. To this end, we performed Northern blot analyses (Figure 3.39A) with RNA co-precipitated with the overexpressed and anti-FLAG immunoprecipitated constructs (Figure 3.39B).

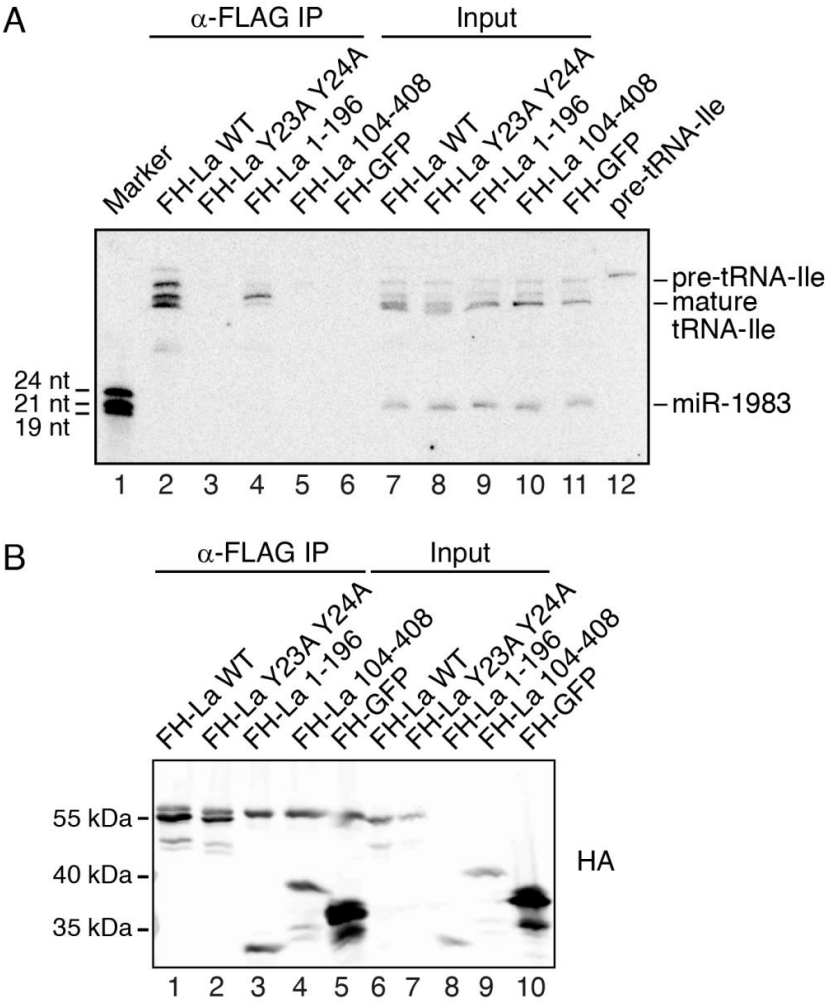

Figure 3.39: The Binding of La to Pre-tRNA-Ile-TAT-2-3 Requires All RNA Binding Domains. (A) HEK293 cells were transfected with constructs expressing either wild type (WT) FH-tagged La (lanes 2 and 7) or variants of FH-La (lanes 3-5 and lanes 8-10; see main text for details). FH-GFP was used as a control (lanes 6 and 11). The overexpressed proteins were immunoprecipitated with anti-FLAG beads (lanes 2-6) and the interacting RNAs were extracted for Northern blotting with a probe complementary to miR-1983. Lanes 7–11 show inputs, lane 1 shows a marker for sRNAs, and *in vitro* transcribed pre-tRNA-Ile served as size marker in lane 12. (B) Aliquot samples from the experiment shown in (A) were analyzed by Western blotting using an anti-HA antibody. The molecular size marker weights are depicted on the left.

Similar to the experiment performed with endogenous La (Figure 3.38), the full-length pre-tRNA-Ile-TAT, as well as some processing intermediates, were co-precipitated with wild type FH-La. However, an additional distinct band was also detected, and probably corresponds to the mature tRNA-Ile (Figure 3.39A, lane 2). Since La does not interact with mature tRNAs, this finding is likely to be an overexpression artifact.

Instead, all other FH-La constructs tested did not associate with full-length pre-tRNA-Ile-TAT-2-3. Confirming the importance of the La module for the interaction to Pol III transcripts, no signals were detected in case critical residues were mutated (La Y23A/Y24A) or in case the La motif was removed (La 104-408). Interestingly, the presence of the intact La module in the La 1-196 variant was not sufficient to maintain the binding to the full-length pre-tRNA-Ile, but only to a smaller processing intermediate. As expected, the mature miR-1983 was neither found within endogenous nor within overexpressed La complexes. Altogether, these results indicate that both, the La module as well as the C-terminal RRM2 of La, are required for efficient binding of full-length pre-tRNA-Ile-TAT-2-3.

To further corroborate this finding, we performed rescue experiments comparing the effects of the different FH-La truncations on the expression levels of miR-1983 in the absence of the endogenous protein (Figure 3.40). For this purpose, we used a siRNA directed against the 3' UTR of La which, however, did not target the overexpressed constructs and performed Northern blot analyses. A representative blot, out of three biological replicates, is shown in Figure 3.40A. We quantified the signal intensities for miR-1983 and normalized them, in the corresponding samples, to the expression of miR-17, which does not react to La depletion (Figure 3.40B). In comparison to the FH-GFP samples, we consistently observed that the miR-1983 levels increased to a lesser extent when full-length FH-La was transfected, reaching statistical significance (Figure 3.40B). In agreement with the results of the immunoprecipitation experiment (Figure 3.39A), the two La truncations were unable to rescue the effect of the La knockdown (Figure 3.40A and B). We confirmed by Western blotting, that the observed effects were not due to unequal expression of the different constructs (Figure 3.40C).

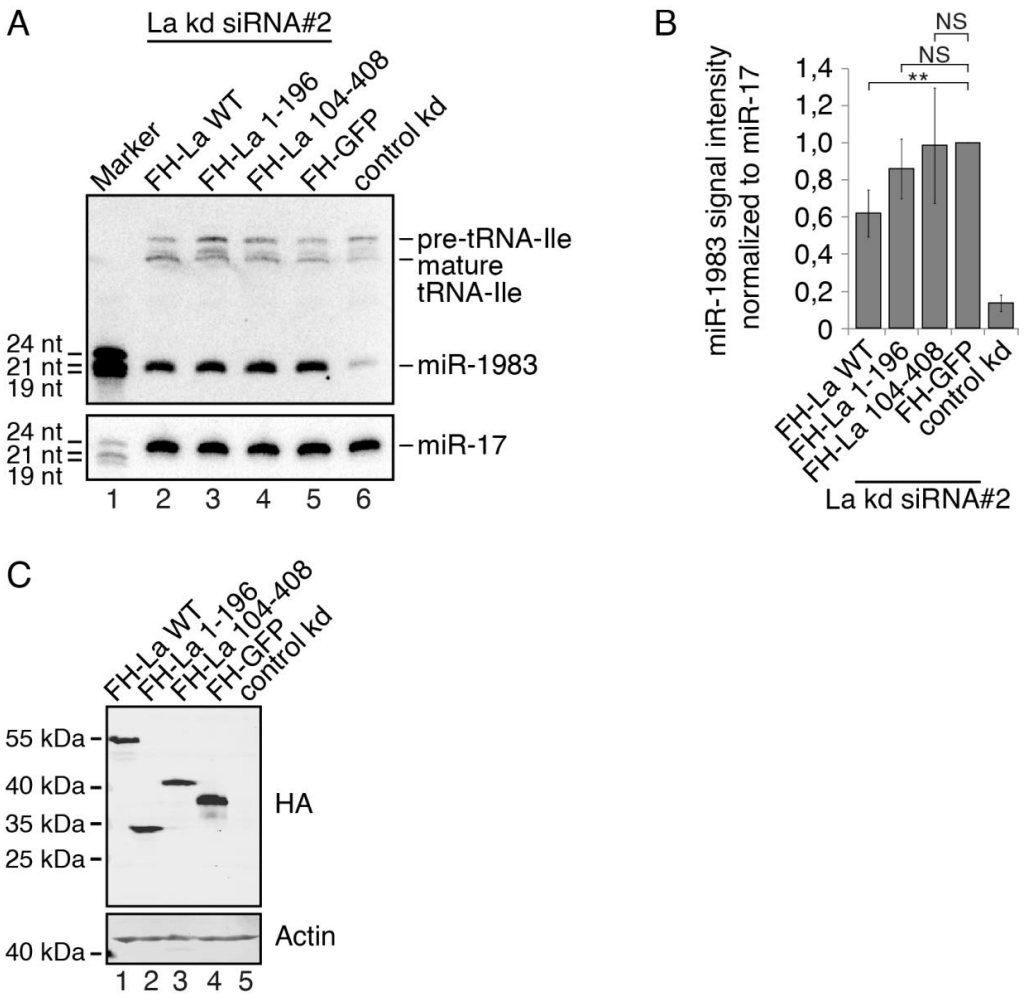

Figure 3.40: The Increased Levels of Mir-1983 Are Partially Rescued by Full-length FH-La. (A) The indicated overexpression constructs were transfected into HEK293 cells. The following day, cells were transfected with a siRNA specific for the endogenous La mRNA (lanes 2-5). Cells were harvested three days post knockdown transfections and the levels of miR-1983 were assayed by Northern blotting. Cells transfected with a control siRNA served as reference (lane 6). Lane 1 shows a size marker. (B) The signals for miR-1983 shown in (A) were quantified and normalized to the corresponding miR-17 signals. The experiment was performed in three biological replicates. The error bars represent ±SD and significance was assessed by two-sided Student's t test (**$p < 0.01$, and NS = not significant). (C) Western blot analysis with an anti-HA antibody confirmed the correct overexpression of the proteins (lanes 1-4). No FH-tagged protein was overexpressed for the control in lane 5. Detection of actin served as a loading control. The molecular size marker weights are shown on the left.

3.10. The Double-stranded Stem of Pre-tRNA-Ile-TAT-2-3 Reduces its Affinity to La

A peculiarity of pre-tRNA-Ile-TAT-2-3 is the complementarity of the 5' and 3' overhangs which can form a RNA double-strand and thereby contribute to the folding into a Dicer substrate. Owing to the fact that La primarily binds to transcripts ending on a single-stranded U-stretch, we reasoned that this interaction might be hindered by the double-stranded termini of pre-tRNA-Ile-TAT-2-3. We aimed to prove this hypothesis by performing electromobility shift assays (EMSAs) with recombinant GST-tagged La protein versions (Figure 3.41) and several *in vitro* transcribed pre-tRNAs.

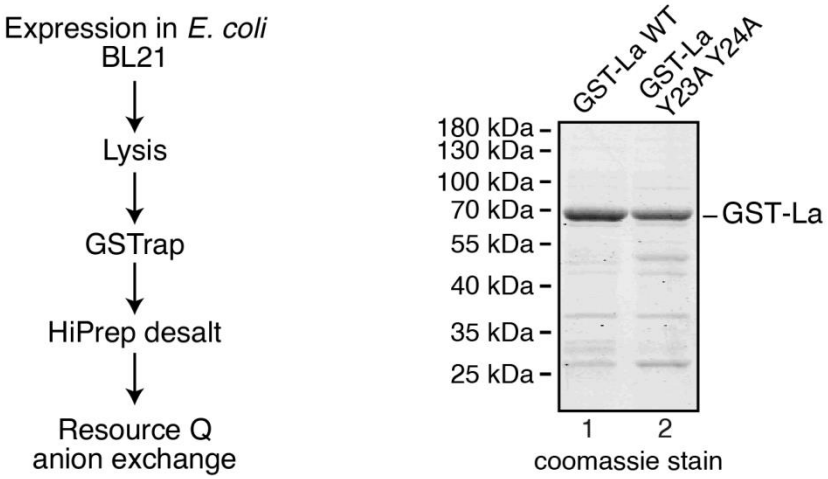

Figure 3.41: Recombinant Protein Expression of GST-tagged La Constructs. Left panel: Schematic overview of the purification strategy. Right panel: Coomassie-stained SDS gel of recombinant GST-tagged La WT (lane 1) or Y23A Y24A mutant. The molecular size marker is indicated on the left.

First of all, we tested our assay conditions with an optimal La-substrate consisting of a 5' processed pre-tRNA intermediate which terminates on the canonical U-stretch. For this initial EMSA experiment we used WT GST-La protein and a mutated version wherein two tyrosine residues involved in RNA binding were mutated to alanine (Y23A Y24A). As expected, we observed a strong binding of the WT protein to the RNA substrate, while the interaction was severely impaired in the La mutant (Figure 3.42).

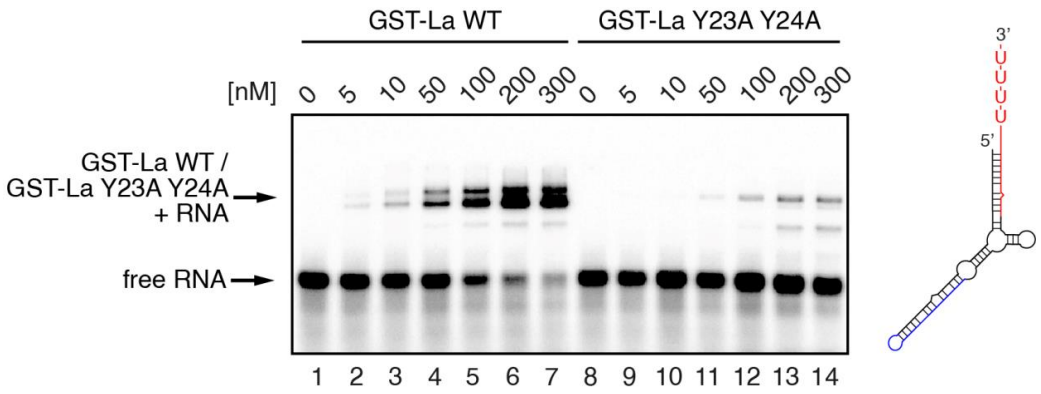

Figure 3.42: GST-La Efficiently Binds Pre-tRNA Substrates with Single-Stranded 3' Trailer. EMSA performed with increasing amounts of recombinant GST-La WT (lanes 1-7) or GST-La Y23A Y24A mutant (lanes 8-14) which were incubated with an optimal substrate for La binding, having the 5'end of the mature tRNA and the 3' trailer of the precursor terminating on –UUUU-3'. Schematic representation of the substrate is represented on the right.

Next, we compared the affinity of GST-La to the pre-tRNA-Ile-TAT-2-3 producing miR-1983 and a pre-tRNA of different genomic origin. We opted for an isodecoder tRNA, Ile-TAT-2-2, which generates a mature tRNA consisting of exactly the same sequence as Ile-TAT-2-3. However, the two pre-tRNAs differ in the composition of their leader, trailer and intron sequences. Interestingly, the result of the EMSA shown in Figure 3.43 indicates that GST-La binds to pre-tRNA-Ile-TAT-2-3 weaker than to the other substrate.

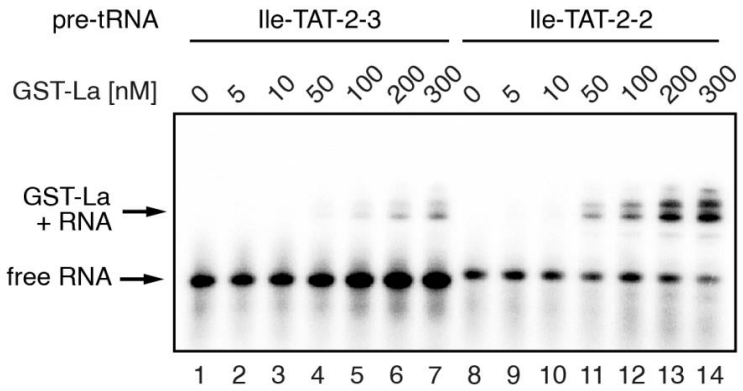

Figure 3.43: GST-La Binds Weaker to Pre-tRNA-Ile-TAT-2-3 Compared to Another Pre-tRNA-Ile. Two different ^{32}P-labeled pre-tRNA-Ile-TAT transcripts were incubated with increasing amounts of recombinant GST-La. In lanes 1–7, the precursor for Ile-TAT-2-3 was used, wherefrom a functional tRNA or miR-1983 is generated, and in lanes 8–14, pre-tRNA-Ile-TAT-2-2 was used, which is a tRNA-only precursor.

Of note, the sequence of pre-tRNA-Ile-TAT-2-3, which we have used in our experiments terminates on 5'-UUUUCU-3' which is at the same time the 3' end of the mature mir-1983. Although this is an uncommon terminus for a Pol III transcript, the occurrence of non-canonical termination sites in humans has been already reported in the past (Gunnery

et al., 1999; Orioli et al., 2011). Nevertheless, structural studies indicate that the occurrence of a cytidine at the penultimate position of the RNA might be incompatible with an efficient binding to La (Teplova et al., 2006). In order to exclude that the reduced affinity to pre-tRNA-Ile-TAT-2-3 is due to this particular sequence composition, we generated an artificial version of the control pre-tRNA-Ile-TAT-2-2 which has exactly the same 5'-UUUUCU-3' terminus as pre-tRNA-Ile-TAT-2-3. Also in this case, we observed a weaker binding of GST-La to pre-tRNA-Ile-TAT-2-3 compared to the 3'-CU ending pre-tRNA-Ile-TAT-2-2 construct (Figure 3.44). We therefore speculate that the reduced affinity of GST-La to the transcript generating miR-1983 is not due to the sequence variations but is mainly influenced by its particular secondary structure which could reduce the accessibility of the 3' end.

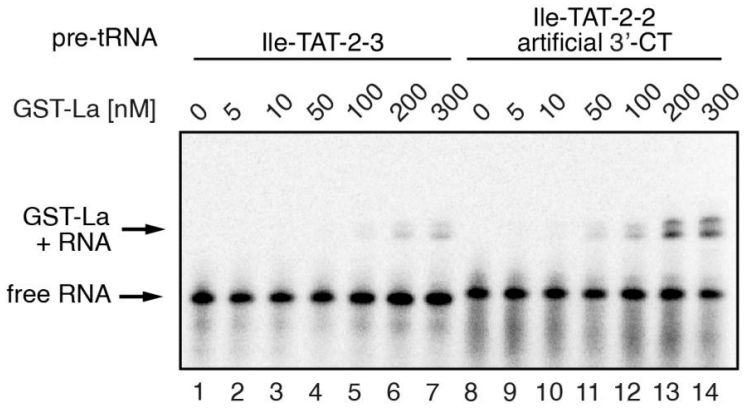

Figure 3.44: The Terminal 3' Sequence of Pre-tRNA-Ile-TAT-2-3 Does not Account for the Decreased Affinity to La. The EMSA shows ^{32}P-labeled pre-tRNA-Ile-TAT-2-3 (lanes 1-7) and an artificial variant of pre-tRNA-Ile-TAT-2-2 terminating on -UUUUCU-3' (lanes 8-14), exactly like pre-tRNA-Ile-TAT-2-3, incubated with increasing amounts of recombinant GST-La.

To further corroborate this assumption, we performed an additional EMSA using either the full-length pre-tRNA-Ile-TAT-2-3 transcript or a substrate lacking the 5' leader sequence. This transcript would correspond to a processing intermediate following the cleavage by the RNase P complex. Supporting our hypothesis, the affinity to GST-La strongly increased when the complementary 5' extension was removed leaving a single-stranded 3' overhang which can be easily bound by La (Figure 3.45).

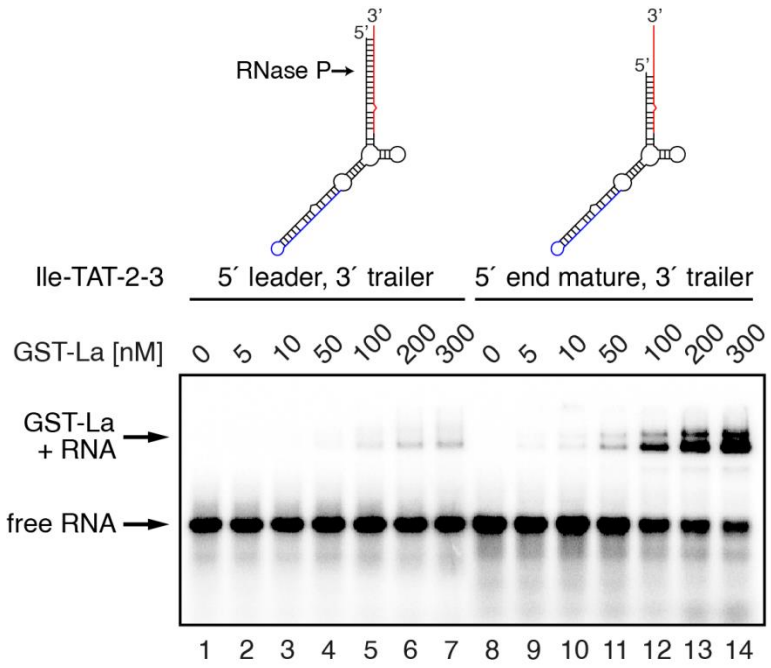

Figure 3.45: La Binding to Pre-tRNA-Ile-TAT-2-3 Is Compromised by the High Complementarity of the 5' Leader and 3' Trailer Sequences. Increasing amounts of recombinant GST-La WT were incubated either with ^{32}P-labeled full-length pre-tRNA-Ile-TAT-2-3 (lanes 1–7) or with a substrate having the 5' end of the mature tRNA and the 3' trailer of the precursor (lanes 8–14). Schematic representations of the substrates are shown on top.

3.11. Viral Pol III Transcripts Sequester La and Influence the Cellular Landscape of sRNAs

Our investigations suggest that La constantly supervises the channeling of pre-tRNA transcripts into the correct tRNA maturation pathway or, at least, determines the equilibrium between two different processing events as shown for the tRNA-Ile-TAT-2-3/miR-1983 chimera. We wondered whether the functionality of La might be perturbed under certain physiological conditions leading to similar effects, which we observed in our La knockdown experiments. Our attention was caught by viral ncRNAs, which are transcribed from the viral genome by Pol III. Several examples of such transcripts have been identified (reviewed in Tycowski et al., 2015); among them, the most prominent are two virus-associated (VA) RNAs encoded by adenoviruses (Reich et al., 1966; Söderlund et al., 1976) and the Epstein-Barr virus (EBV)-encoded RNA 1 (EBER1) and EBER2 (Rosa et al., 1981). Importantly, VA RNAs as well as EBER1/2 associate stably with La and are highly expressed in infected cells (Lerner et al., 1981). Their abundance has in fact been estimated to range between 2.5×10^5 and 10^8 copies per cell (reviewed by Mathews and Shenk, 1991; Tycowski et al., 2015). We hypothesized that the induction of

such abundant Pol III transcripts would demand a great portion of the available La pool. Consequently, under viral infection, less pre-tRNAs might be bound by La and thus the production of more tRNA fragments like miR-1983 could be favored.

To test this assumption, we generated a plasmid, which allowed the expression of both EBERs from their endogenous promoters. We transfected EBV negative HEK293 cells and achieved similar expression levels of EBER1/2 compared to EBV positive cell lines (Figure 3.46), ruling out unspecific effects due to strong overexpression. Of note, the probes used for the detection of the two EBER transcripts also revealed the occurrence of smaller fragments, which have been recently described (Lung et al., 2009, 2013).

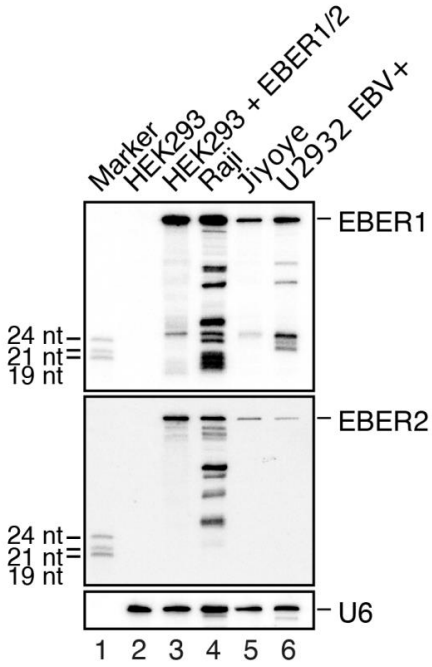

Figure 3.46: Expression of EBER1/2 across Different Cell Lines. HEK293 cells were transfected with a plasmid expressing the viral RNAs from their endogenous promoters (lane 3). For comparison, total RNA was extracted from untransfected HEK293 cells (lane 2) or from EBV positive cell lines (lanes 4–6). The expression levels of EBER1/2 were detected by Northern blot analysis. A radioactive size marker was loaded on lane 1. The signals for the U6 snRNA were detected as loading control.

Next, we aimed to confirm the interaction of the viral transcripts with La. We therefore performed immunoprecipitations from the EBV positive Raji cells (Figure 3.47A) as well as from HEK293 cells transfected with the EBER1/2 plasmid or from mock transfected cells (Figure 3.47B). In both conditions, EBER1/2 were co-precipitated with La as revealed by subsequent Northern blot analyses. Interestingly, some of the smaller EBER fragments were also bound by La. In particular, a fragment of ca. 25 nt derived from the 5’ end of EBER1 was strongly enriched in the anti-La immunoprecipitation samples (Figure 3.47A and B upper panels).

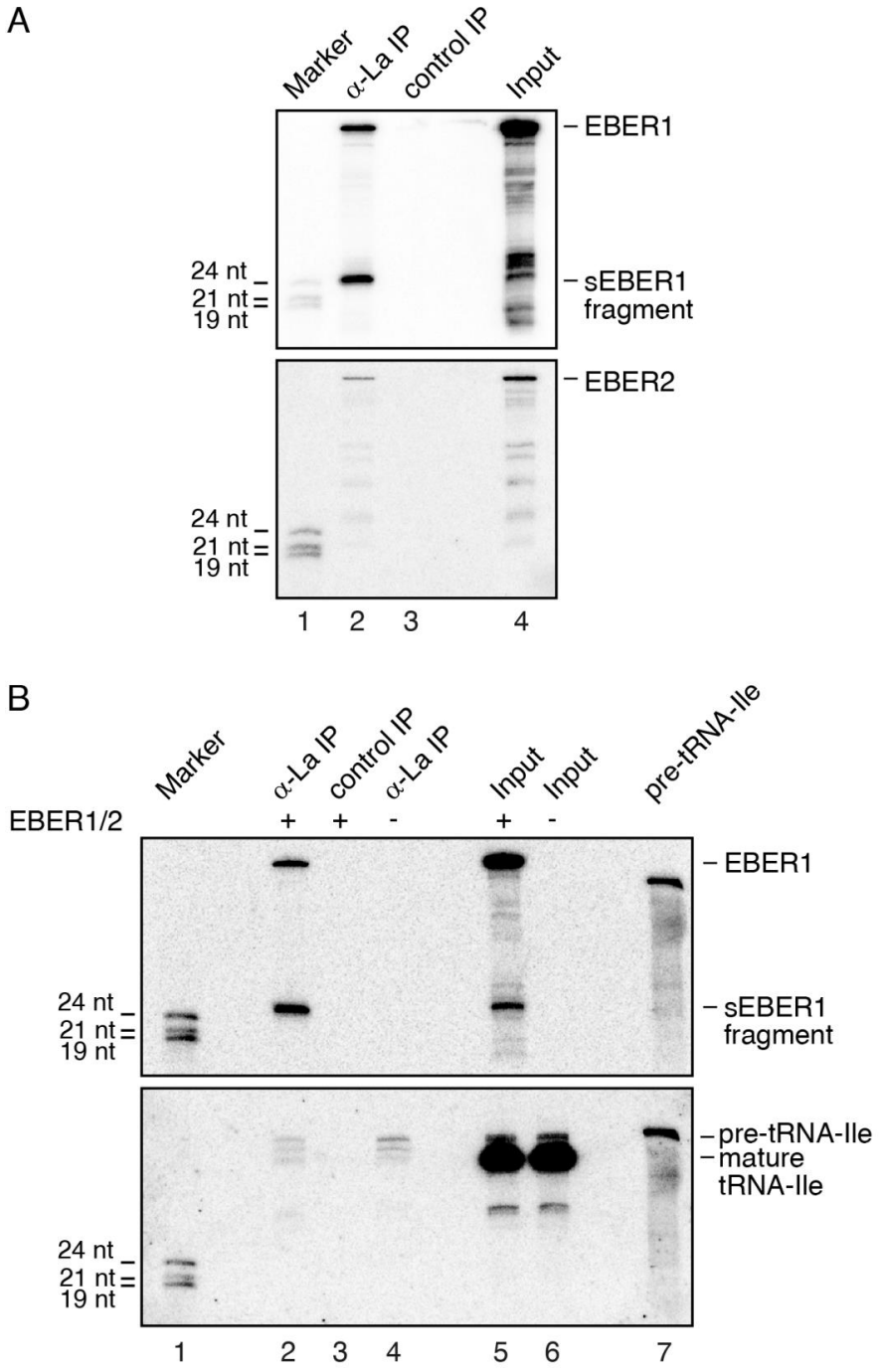

Figure 3.47: Endogenous La Interacts with Full-length EBER1/2 and with Short EBER (sEBER) Fragments. (A) Endogenous La was immunoprecipitated from Raji cell lysate (lane 2) and co-immunoprecipitated RNAs were analyzed by Northern blotting for EBER1/2. Lane 3 shows a control immunoprecipitation with pre-immune serum, lane 4 is the input sample and lane 1 is a size marker. (B) Anti-La immunoprecipitations were performed with the lysate of HEK293 cells transfected with an EBER1/2 over-expression construct (lane 2) or with the lysate of mock transfected cells (lane 4). The immunoprecipitation from EBER1/2 transfected cells with pre-immune serum served as control (lane 3). Co-immunoprecipitated RNAs and total RNA extracted from input samples (lanes 5 and 6) were analyzed by Northern blotting. Lanes 1 and 7 are size markers. Signals were detected with a probe complementary to the 5' end of the EBER1 RNA (upper panel) and with the *in vitro* transcribed, 5'end-labeled, antisense pre-tRNA-Ile-2-3 (lower panel).

Importantly, when we assayed for pre-tRNA-Ile-TAT-2-3 co-immunoprecipitating with La with or without overexpression of EBERs, we observed a reduced interaction to the pre-tRNA in the presence of the viral Pol III transcripts (Figure 3.47B, lower panel, compare lanes 2 and 4). This indication is in agreement with our hypothesis that viral ncRNAs might sequester La, precluding its efficient binding to cellular transcripts.

Finally, we analyzed the effect of EBER1/2 overexpression on the pre-tRNA-derived sRNA population and focused our investigations on the La-dependent sRNA-Pro and miR-1983. We have shown previously that sRNA-Pro is generated exclusively upon La knockdown. However, this effect was overshadowed in Northern blot assays by the existence of a distinct fragment of similar size and sequence which, instead, is derived from the mature tRNA-Pro. To overcome this cross-hybridization problem, we achieved a reliable detection of sRNA-Pro by assaying RNA co-precipitated by anti-Ago2 immunoprecipitations (Figure 3.17A). We adopted the same strategy and probed anti-Ago2 immuoprecipitated samples for the occurrence of sRNA-Pro upon EBER1/2 over-expression or upon transfection of an empty plasmid (Figure 3.48).

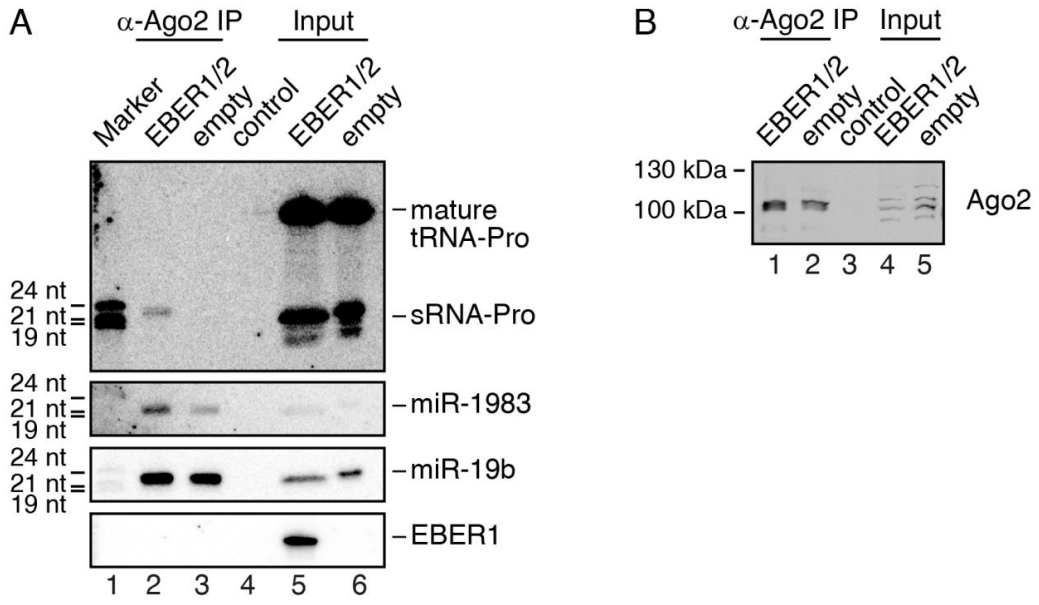

Figure 3.48: Pre-tRNA Fragments Accumulate in Ago2 upon Overexpression of EBER1/2. (A) HEK293 cells were transfected with am EBER1/2 overexpression construct (lanes 2 and 5) or with an empty plasmid (lanes 3 and 6). Ago2 (lanes 2 and 3) was immunoprecipitated and associated RNAs were analyzed as indicated by Northern blotting. Lane 4 shows a beads-only control, lanes 5-7 show input samples, and lane 1 shows a size marker. (B) A Western blot assay with protein aliquots of the same samples used in (A) (lanes 1-5) was performed as a control for the immunoprecipitations. The molecular size marker weights are depicted on the left.

Indeed, a faint signal appeared specifically if the EBV ncRNAs were expressed (Figure 3.48A, upper panel, compare lanes 2 and 3). The same membrane was probed afterwards

for miR-1983, which was apparently more abundant in Ago2 complexes isolated from EBER1/2 transfected cells, while the effect was less pronounced for miR-19b, which served as a control (Figure 3.48A, lower panels). Western blot analysis confirmed that euqual amounts of Ago protein complexes were immunoprecipitated in the presence or absence of EBER1/2 overexpression (Figure 3.48B).

To gain a deeper insight into this phenomenon, we followed by Northern blotting the effects, over several days, of EBER1/2 overexpression on the total levels of the functional miR-1983 (Figure 3.49A). The levels of EBER1/2 increased until day two and then steadily decreased. Similarly, the abundance of miR-1983 increased and decreased in correlation with the viral RNAs. We performed the experiments in triplicates and quantified the range of miR-1983 expression changes by normalizing the Northern blot signals of miR-1983 to the levels of miR-17, which was detected at almost equal levels over the different time points (Figure 3.49B). The strongest effect was observed at day three, when miR-1983 was approximately two times more abundant than in the untransfected sample (Figure 3.49B). In summary, our data suggest that EBER1/2, which are highly expressed during EBV infection, can sequester La and, by that, they can influence the cellular sRNA landscape of the cell mimicking the outcome of La depletion.

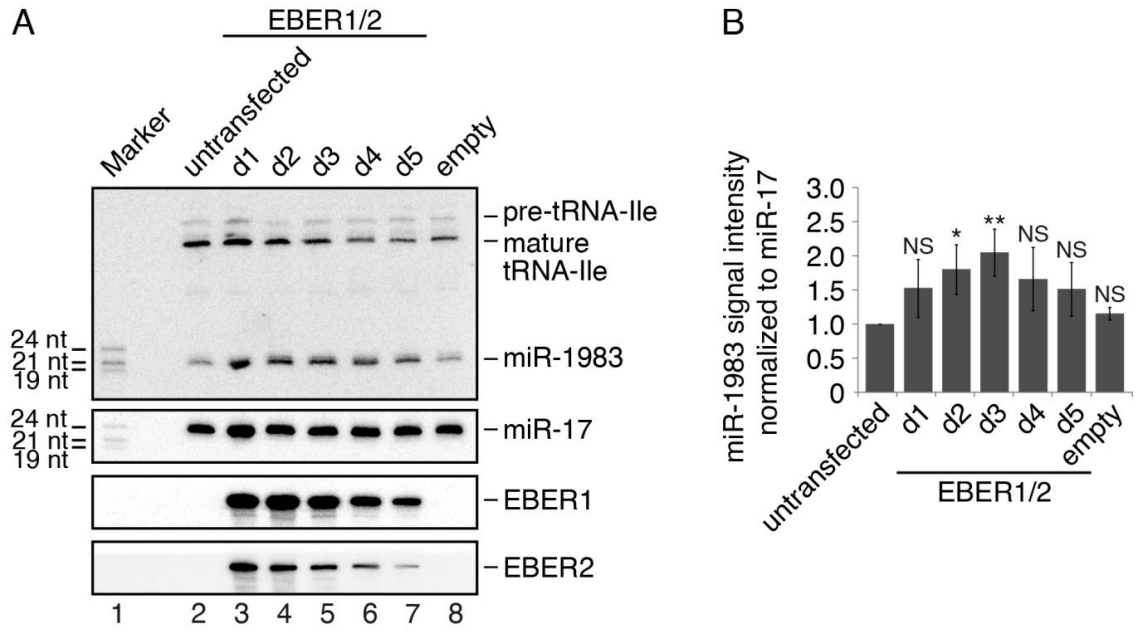

Figure 3.49: Time Course of the Effect of the EBV-encoded EBER1/2 RNAs on the MiR-1983 Expression Levels. (A) EBER1/2 were overexpressed in HEK293 cells for 5 days and total RNA was extracted every 24 hr (lanes 3–7) and was subjected to Northern blot analysis. Lane 2 shows total RNA from non-transfected cells and lane 8 from cells transfected with an empty plasmid. A size marker was loaded on lane 1. The membrane was probed for miR-1983, miR-17, EBER1, and EBER2 expression. (B) The signal intensities of the experiment shown in (A) were quantified and the values for miR-1983 were normalized to the corresponding miR-17 signals. The quantifications are based on three biological replicates. The error bars represent ±SD. Significance was assessed by two-sided Student's t test (*$p < 0.05$, **$p < 0.01$, and NS = not significant).

4. Discussion

4.1. Crosstalk Between La and the MiRNA Machinery

Beyond any doubts, the main function of La is to immediately bind and, thereby, protect nascent Pol III transcripts, which terminate with the typical U stretch (Fairley et al., 2005). Nevertheless, La has long been implicated in other cellular processes as well, e.g., by binding and promoting translation of cellular mRNAs, either by IRES-dependent (Holcik and Korneluk, 2000; Kim et al., 2001; Sommer et al., 2011; Petz et al., 2012) or by IRES-independent mechanisms (Trotta et al., 2003; Heise et al., 2016). More recently, La has also stepped into the miRNA field as it was reported to interact with Ago2 (Liu et al., 2011; Zheng et al., 2017). Biochemical evidences suggest that La might act as a factor promoting multiple-turnover reactions of RISC during RNA interference (RNAi) in flies. This specific mechanism only occurs if either exogenous or endogenous siRNAs are fully complementary to a target transcript and thereby direct catalytically active Ago proteins to cleave the target. In this context, La might facilitate the release of the nicked target RNA, liberating the Ago-containing silencing complex for another round of catalysis (Liu et al., 2011). Although endogenous RNAi does not occur commonly in mammalian cells, it is widely applied by other organisms like, e.g., *D. melanogaster*. Further studies are required to elucidate the relevance of La for RNAi processes in more detail and to clarify whether La is also involved in miRNA-directed gene silencing reactions.

An additional crosstalk between La and the miRNA pathway caught our attention as it was shown that this protein might affect the biogenesis of miRNAs (Liang et al., 2013). The expression of miRNAs is tightly regulated at the transcriptional as well at the post-transcriptional level. In particular, several examples of RBPs binding to sequence elements within miRNA precursors have been described so far. These RBPs are able to modulate the biogenesis rate of specific miRNAs (reviewed in Ha and Kim, 2014) and, by that, they can have a tremendous impact on the cellular homeostasis (reviewed in Lin and Gregory, 2015). The work by Liang et al. (2013) indicates that La is able to bind *in vitro* and *in vivo* to the stem-loop structure of miRNA precursors, apparently without any

sequence specificity. The authors further propose that La binding protects a broad number of different pre-miRNAs from degradation by ZC3H12A (also known as MCPIP1), an RNA endonuclease, which was shown to cleave within the loop of pre-miRNAs antagonizing Dicer processing (Suzuki et al., 2011; Roy et al., 2013). As a consequence, depletion of La in HeLa cells triggers the reduction of several miRNAs' expression levels as determined by a TaqMan qPCR array (Liang et al., 2013).

In our study, we performed a similar experiment in HEK293 cells and profiled the impact of La knockdown on the miRNA population by deep sequencing. Indeed, we confirmed the negative consequence of La depletion on certain miRNAs, in particular our data are in agreement with the observations by Liang et al. (2013) concerning let-7 miRNA family members, miR-98 and miR-374a (Figure 3.6). However, validation of selected candidates by Northern blot analyses resulted in less pronounced effects (Figure 3.7). This might be an inherent problem of comparing miRNA expression levels by deep sequencing, as this method is susceptible to different kinds of technical biases (Raabe et al., 2014).

Furthermore, thanks to our experimental setup, we were able to distinguish between La-dependent sRNA changes in the total RNA population and the effect of La knockdown specifically on Ago-loaded sRNAs. Of note, the overlap between miRNAs reaching a 3-fold deregulation threshold in both subsets was low and only members of the let-7 miRNA family were consistently reduced in the Ago-loaded fraction as well as in the input sample. This might either be due to relatively stringent threshold settings or, alternatively, the turnover of certain miRNAs might differ between both populations and might thus react with different kinetics to La depletion. In sum, although expression levels of some miRNAs diminished, the global impact of La knockdown on miRNA levels was rather moderate (see high correlation rates between La and control experiments in Figure 3.6). This finding argues against a general influence of La on miRNA biogenesis as proposed by Liang et al. (2013), who observed reduced levels of ~60% of the tested miRNAs. Furthermore, upon La depletion we detected increased levels of some miRNAs in the Ago-associated pool, as well as in the input sample. Hence, our data suggest that La has a positive or negative influence only on a restricted number of miRNAs, which is in line with another recently published study (Zheng et al., 2017). The fact that La is able to promote or to inhibit the processing of certain miRNAs presumably reflects a more sophisticated regulatory mechanism. Although it remains still an open question how this is exactly achieved, Zheng et al. (2017) propose a different model than Liang et al. (2013) to explain the role of La in miRNA biogenesis. The authors of the

former study noted that La specifically associates in a RNA-dependent manner to DGCR8, a component of the Microprocessor complex responsible for the first step of miRNA maturation. Interestingly, no interaction was detected between La and Drosha, the catalytic component of the Microprocessor complex. Zheng et al. (2017) speculate that La promotes DGCR8 binding to specific miRNA precursors possibly by inducing conformational changes of the pri-miRNA.

4.2. Processing Products of tRNAs are Abundant and Affected by La Depletion

It is known since many years, that different Pol III transcripts can give rise to sRNA fragments, originating for example from tRNAs, 5S rRNA, Y RNAs and vault RNAs (Speer et al., 1979; Persson et al., 2009; Meiri et al., 2010; Chen and Heard, 2013). Some of them have been also detected in association with Ago proteins (Cole et al., 2009; Burroughs et al., 2011; Maute et al., 2013; Pekarsky et al., 2016). Indeed, by our Ago-APP approach we did not only co-precipitate miRNAs (Figure 3.5), but to a minor extent also several sRNAs derived from different Pol III transcripts, e.g., 5S rRNA, 7SL RNA and snaRs, an evolutionarily recent ncRNA class, which has not been extensively characterized so far (Parrott and Mathews, 2007). Of note, among Pol III transcripts, tRNAs were the major source of Ago-associated reads. We also determined that most of these tRFs were unambiguously derived from mature tRNAs, i.e., the reads either covered the exon-exon junction of intron-containing tRNAs (see section 1.1.6) or they terminated on the CCA sequence, which is post-transcriptionally added to the 3’ end of mature tRNAs (see section 1.1.5) (Figure 3.8). Intriguingly, these tRFs resulted to be rather short and, at least with the experimental and computational strategy we applied, they peaked at a length of 18 nt (Figure 3.13). This observation is largely consistent with previous reports (Kumar et al., 2014; Telonis et al., 2015) and clearly differs from the size of miRNAs, which usually ranges between 19 and 23 nt. Although some short tRFs are reliably detected in the libraries of Ago1-4-associated sRNA, they were not enriched from the input to a comparable level as miRNAs (Figure 3.5). Taken together, we rather speculate that the 18 nt tRFs might be side-products of RNA pathways unrelated to the miRNA metabolism. A small subset of these tRFs might transiently interact with Ago proteins without affecting its function and might therefore be tolerated without any side-effects. An intriguing scenario, for example, could be that 18 nt tRFs act as a buffer system for Ago proteins which are not loaded with a miRNA. Such tRFs might be

beneficial for storing Ago proteins in a folded conformation and protecting them from proteolytic degradation. As soon as a miRNA becomes available, it might easily displace the short tRF due to its correct size, which is likely to result in a stronger affinity to Ago proteins. However, we do not have any experimental evidence supporting this hypothesis, which is so far a mere speculation.

We next wondered whether the occurrence of Pol III-derived sRNAs is influenced by La-depletion. Interestingly, most of these fragments, which were especially abundant in the total RNA sequencings, did not react dramatically to the knockdown of La, e.g., in the case of reads mapping to the 5S rRNA sequence (Figure 3.9). This might indicate that La is neither strictly required for the generation nor for the stabilization of such fragments or of the full-length transcripts they originate from. Other proteins with a redundant function might for example compensate the lack of La, or, alternative maturation pathways might circumvent the La-dependency (Yoo and Wolin, 1997).

Strikingly, the greatest effect we observed upon La depletion concerned read counts mapping to tRNA genes (Figure 3.9). This might reflect the fact, that, among all Pol III transcripts, tRNAs most strongly require the interaction with La for their correct processing as pinpointed in a nice review by Maraia and Arimbasseri (2017). The decreased abundance of tRNA-reads in the input sample could therefore partially be due to a general reduction of pre-tRNAs and/or mature tRNAs which are the source of the sRNAs we detect. Nevertheless, the coverage analysis performed with tRNA reads of the inputs (Figure 3.12) further highlights that the most substantial drop concerned fragments which are apparently 3’ trailers of pre-tRNAs, also called 3’ U-tRFs (see section 1.1.10.1). Again, the disappearance of such sRNAs could be caused by a backup mechanism for tRNA maturation observed in yeast lacking the orthologous La protein. In this situation, the 3’ end of pre-tRNAs are immediately processed by exonucleolytic cleavage (Yoo and Wolin, 1997; Copela et al., 2008; see as well section 1.1.4.3). Consequently, 3’ trailer fragments would not be generated at all from freshly transcribed tRNAs. However, the depletion of La might account on a second way for the reduced 3’ U-tRF levels. This alternative explanation is based on the evidence that removal of the 3’ trailer by RNase Z might occur while La is still bound to the pre-tRNA. Although the interaction of La to the resected 3’ trailers was shown to be weaker than to full-length pre-tRNAs (Bayfield and Maraia, 2009), we noticed that some 3’ U-tRFs are highly enriched in anti-La immunoprecipitations (data not shown). Thus, La might in particular stick to long 3’ trailer fragments which, therefore, would be protected and stabilized by this interaction.

Vice versa, La-interacting 3' U-tRFs would be rapidly degraded under knockdown conditions accounting for the phenomenon which emerged from our analyses.

4.3. La is a Gatekeeper Preventing Mis-channeling of tRNA Fragments into the Human MiRNA Pathway

In contrast to the decrease observed in the input, La depletion resulted in a 4-fold accumulation of Ago-associated fragments, which unambiguously originate from pre-tRNAs (Figure 3.8 and Figure 3.10). When analyzing their position within the tRNA transcripts, we noticed that the enriched sRNAs covered the tRNA body at its 3' terminal region and protruded into the 3' trailer (Figure 3.11). Importantly, these Ago1-4-associated tRNA reads clearly differed from the simple trailer fragments, which were more abundant in the input samples (Figure 3.12). At the same time, the length of the accumulating Ago-loaded tRFs ranged between 21-23 nt with a prominent peak at 23 nt. The accurate processing of these fragments in terms of size and location within the tRNA sequence, corroborate the specificity of this observations. This is further supported by the fact that the abundance of these fragments increases upon La knockdown within Ago1-4 complexes while simultaneously decreasing in the input. We therefore hypothesized that La might prevent certain pre-tRNAs to be erroneously processed by the miRNA biogenesis machinery into Ago-loaded tRFs. Indeed, validation experiments performed with two different candidates (Figure 3.17 and Figure 3.36), confirmed that specific tRFs accumulate in Ago1-4 complexes upon knockdown of La. Furthermore, when performing Dicer PAR-CLIP experiments, we observed some tRNAs to be much stronger associated with Dicer in the absence of La (Figure 3.21). Among them, reads originating from tRNA-Pro, -Ala and –Leu were detected, which are tRNA isotypes generating Ago-loaded and La-dependent fragments (Figure 3.10). Of note, several tRNAs were also less frequently found in the Dicer PAR-CLIP libraries upon La knockdown (Figure 3.21). Again, this might be a secondary effect, since La is required for the stabilization of pre-tRNAs. This is along the same line with the observation that the abundance of pre-tRNA fragments generally decreased upon knockdown of La in the profiling of input samples (Figure 3.9). We finally also confirmed by independent *in vitro* and *in vivo* assays that Dicer and Xpo5 are required for the generation of Ago-loaded tRFs in the absence of La (Figure 3.27Figure 3.-Figure 3.29). Nevertheless, some interesting issues emerging from our analyses still require to be addressed in more detail:

1) Surprisingly, a clear bias for the enrichment of fragments originating from the 3’ end of pre-tRNAs became evident in the coverage analysis of Ago1-4-associated sRNA (Figure 3.11). Such a strict selectivity is interesting, since the actual knowledge regarding the mechanism of miRNA strand-selection is probably not sufficient to explain this phenomenon. For canonical miRNAs, Dicer processing from hairpin structures results in intermediate RNA-duplex products. The decision which of the two strands is finally giving rise to the mature miRNA obeys the so-called asymmetry rule, i.e., the strand with the thermodynamic less stable interactions at its 5’ end is handed over to an Ago protein (Khvorova et al., 2003; Schwarz et al., 2003; see as well section 1.2.2). Our data indicate that Dicer is also responsible for the generation of certain tRFs in a La-dependent manner. Nevertheless, why do only the processing products from the 3’ end of pre-tRNAs accumulate in the Ago1-4 complexes, while their 5’ counterparts are selectively depleted? A possible explanation for this finding is the chemical composition of the 5’ end of pre-tRNAs. As all primary Pol III transcripts, pre-tRNAs possess a triphosphate at their 5’ termini. Although Dicer has been shown to bind the 5’ monophosphate of pre-miRNAs (Park et al., 2011), it has not been experimentally addressed within the indicated reference, whether a 5’ triphosphate would be incompatible with Dicer processing. Indeed substrates with even more exotic 5’ ends, i.e., 7-methylguanosine (m^7G)-capped miRNA precursors, have been shown to be efficiently cleaved by Dicer. However, only the opposite strand, which does not possess the m^7G cap at its 5’ end, is loaded into Ago proteins (Xie et al., 2013). Thus, it is likely that Ago proteins cannot accommodate sRNAs with 5’ ends other than monophosphates. In such cases, Ago itself acts as a filter for strand-selection. Consistently, the 5’ triphosphorylated ends of some viral miRNAs were shown to be first converted by DUSP11 into 5’ monophosphates before they get loaded into Ago proteins (Burke et al., 2014, 2016). In this regard, our data seem to argue that DUSP11 is not able to dephosphorylate pre-tRNA substrates, otherwise we would expect 5’ terminal pre-tRNA fragments to accumulate in Ago complexes equally well as their 3’ terminal counterparts.

2) Another interesting aspect concerns the fact that the La-dependent accumulation of tRFs in Ago1-4 was restricted to only a subset of tRNA isotypes (Figure 3.10). A possible explanation for this selectivity is that individual tRNA transcripts might depend to a varying degree on the function of La. For instance, several studies have emphasized the particular requirement of La for the correct folding of defective pre-tRNAs, e.g., in the

absence of selected tRNA modifications or impaired base pairings (Calvo et al., 1999; Chakshusmathi et al., 2003; Copela et al., 2006; Huang et al., 2006). In addition, certain tRNAs might be more efficiently processed by alternative maturation pathways (Copela et al., 2008; Maraia and Lamichhane, 2011) and owing to that they would not be sensitive to La depletion. The heterogeneity of pre-tRNA 3' ends might also contribute to this phenomenon since the length of the 3' terminal U-stretch was shown to influence their interaction with La in yeast and human (Huang et al., 2005; Gogakos et al., 2017). Furthermore, our biochemical data suggest that the ability of certain pre-tRNAs to form alternative structures (Figure 3.19 and Figure 3.26) might reduce their affinity towards La (Figure 3.45). These substrates would in turn be more susceptible to mis-channeling into tRNA-unrelated pathways, e.g., by allowing processing by Dicer and loading of tRFs into Ago proteins (Figure 4.1).

It would be interesting to see whether this gatekeeping function is shared by other proteins with RNA chaperone activity and whether other pathways might concur with each other for the same RNA substrates.

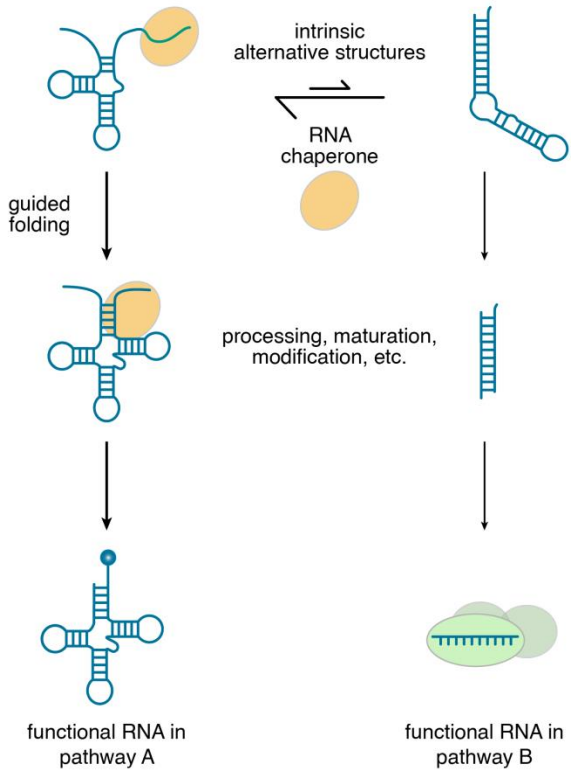

Figure 4.1: RNA Chaperones Can Contribute to the Channeling of their Substrates into the Correct Pathway. General model based on our observations concerning the function of La. It ensures that transcripts having an intrinsic potential to fold into alternative structures are channeled into the tRNA maturation pathway (represented on the left) and not into the miRNA pathway (represented on the right). RNA chaperones other than La might assist RNAs to adopt the correct structure and ensure that the RNA fulfill its actual function without being hampered by the machinery of competing pathways.

4.4. Hidden Pitfalls in the Analysis of tRFs

In general, sRNAs are classified into distinct groups due to the presence of well-defined sequence elements or structural characteristics that determine the biogenesis and function of, e.g., miRNAs, snoRNAs, snRNAs and tRNAs. Unfortunately, the common denominator of short tRF is merely the fact that they originate from tRNA transcripts. Apart from that, tRFs are generated by various enzymes and the molecular mode of action described for some tRFs is a potpourri of different mechanisms (see section 1.1.10). In addition, profiling of tRFs goes along with a series of technical issues which concerns for instance the sequence similarity between tRNA isodecoders, the occurrence of tRNA-derived repetitive elements or lookalikes and the negative influence of tRNA modification on sequencing-based detection methods (Telonis et al., 2014, 2015; Cozen et al., 2015; Zheng et al., 2015). In our study we come across an additional problem, namely the co-existence of different tRFs having a similar sequence (Figure 3.15). Our data indicate that one of these tRFs, sRNA-Pro, is processed by Dicer from pre-tRNA-Pro-CGG-2-1 in a La-dependent manner (Figure 3.15 and Figure 3.21). This fragment originates from a region of the pre-tRNA, which partially overlaps the sequence of a 3' CCA-tRF. However, we assume that latter sRNA is processed via a Dicer-independent mechanism from the mature tRNA-Pro-CGG. This example depicts the caution which is required to entangle the many functional aspects of tRFs. In this particular case we were able to distinguish between the two related fragments only by isolating the Ago-associated tRFs from the multitude of tRFs, which otherwise overshadowed the effect we were interested in (Figure 3.16 and Figure 3.17). Indeed, the misinterpretation of tRNA fragments as potential miRNAs is another pitfall to be aware of when referring to the partially contradictory literature (Haussecker et al., 2010; Schopman et al., 2010; Thomson et al., 2014). This seems to be also the case for a 3' CCA-tRF termed CU1276 which has been described to excerpt a miRNA function (Maute et al., 2013). In the cell lines we tested, CU1276 neither appeared to be processed by the miRNA biogenesis machinery (Figure 3.28Figure 3. and Figure 3.29) nor to associate with miRNA-repression complexes (Figure 3.30 and Figure 3.31). Although we cannot exclude that CU1276 might acquire all these characteristics in other cell types, we rather think that its relevance for proliferation and for the DNA damage response, as shown in B cells by Maute et al. (2013), might occur via miRNA-unrelated pathways.

4.5. Pre-tRNA-Ile-2-3 Escapes La Binding by an Alternative Folding

The key point of our work is the discovery that the well-known function of La for tRNA biology is not only beneficial for the production of mature tRNAs but also ensures that pre-tRNAs are not erroneously fed into the miRNA biogenesis pathway. This mechanism appears to work quite well in HEK293 cells, since the amount of Ago-associated tRFs with miRNA-like characteristics is relatively low (Figure 3.11). Nevertheless, we noticed that pre-tRNA-Ile-TAT-2-3 escapes La regulation even in untreated samples and gives rise to an Ago-loaded sRNA. *In silico* predictions suggest that the high degree of complementarity between the 5' leader and the 3' trailer sequences contributes to the formation of an alternative secondary structure, which finally renders pre-tRNA-Ile-TAT-2-3 an optimal prey for miRNA biogenesis factors (Figure 3.26). In detail, we performed EMSAs comparing the interaction of La to pre-tRNA-Ile-TAT-2-3 and pre-tRNA-Ile-TAT-2-2, which are very similar in their overall sequence composition but the latter transcript does not generate an Ago-loaded tRF. Importantly, La did not bind to pre-tRNA-Ile-TAT-2-3 equally well as to pre-tRNA-Ile-TAT-2-2 (Figure 3.43 and Figure 3.44). We speculate that this reduced affinity is due to the fact that the 5' and 3' ends of pre-tRNA-Ile-TAT-2-3 form a stem structure, wherein the La interaction motif, i.e., the 3' terminal U-stretch, is buried into a stable double-stranded environment. However, as soon as the 3' end is presented in a single-stranded context, high affinity binding is restored (Figure 3.45). Although the interaction of La with the full-length pre-tRNA-Ile-TAT-2-3 appears to be weaker compared to other substrates, it is still sufficient to ensure binding of La to pre-tRNA-Ile-TAT-2-3 *in vivo,* as confirmed by endogenous immunoprecipitation experiments (Figure 3.38). Since multiple regions of the La protein contribute to contact the RNA substrates (Alfano et al., 2004; Huang et al., 2006; Teplova et al., 2006; Bayfield and Maraia, 2009; Kucera et al., 2011), we tested different La truncations for their ability to precipitate endogenous pre-tRNA-Ile-TAT-2-3. Our data indicate that both, the functional La module together with the C-terminal region of La, are required for an efficient interaction with pre-tRNA-Ile-TAT-2-3. Interestingly, also the constructs containing the complete La module (1-196) did not precipitate the full-length pre-tRNA-Ile-TAT-2-3 but a RNA, which is likely to be a 5' end-matured, 3' trailer containing processing intermediate (Figure 3.39). This was rather surprising, since the La module alone was shown to be sufficient for high affinity binding to substrates containing a 3' terminal U-stretch (Ohndorf et al., 2001) . It would be interesting to compare the ability

of the La 1-196 truncation to precipitate pre-tRNAs other than pre-tRNA-Ile-TAT-2-3. The aforementioned structural peculiarity of pre-tRNA-Ile-TAT-2-3, i.e., the stable stem formed by the 5' and 3' ends, might be responsible for an increased requirement of La's C-terminal region to support efficient binding. Of note, when we tried to rescue the effect of La knockdown on the increased production of miR-1983, we also observed that La 1-196 did not behave as the full-length construct (Figure 3.40).

4.6. The Chimeric Pre-tRNA-Ile-TAT-2-3 Generates Either a Functional tRNA or MiR-1983

In our study, we collected evidences suggesting that miR-1983 is indeed a genuine miRNA, which is processed from pre-tRNA-Ile-TAT-2-3 owing to its ability to escape, at least in part, from La binding. We showed that miR-1983 is broadly detected across different cell lines (Figure 3.24) at expression levels comparable to a medium-abundant miRNA (Figure 3.25) and is clearly co-precipitating with Ago and TNRC6 protein complexes (Figure 3.30 and Figure 3.31). We further corroborated the functionality of this particular tRF by luciferase reporter assays and, importantly, we observed repression of the identified targets not only via artificial miR-1983 overexpression constructs but also by transfecting pre-tRNA-Ile-TAT-2-3 as a source for the production of miR-1983 (Figure 3.32). Our data, together with the profiling study of Babiarz et al. (2008), demonstrate that miR-1983 is conserved between mouse and human (Figure 3.22) and is a non-canonical miRNA inasmuch it is processed in a Drosha-independent but Xpo5- and Dicer-dependent manner (Figure 3.27 - Figure 3.29).

Importantly, pre-tRNA-Ile-TAT-2-3 can also generate a functional tRNA-Ile (Figure 3.23) and La is the main switch dictating whether this pre-tRNA undergoes processing to a tRNA or to a miRNA (Figure 3.34). The model presented in Figure 4.2 summarizes all these findings.

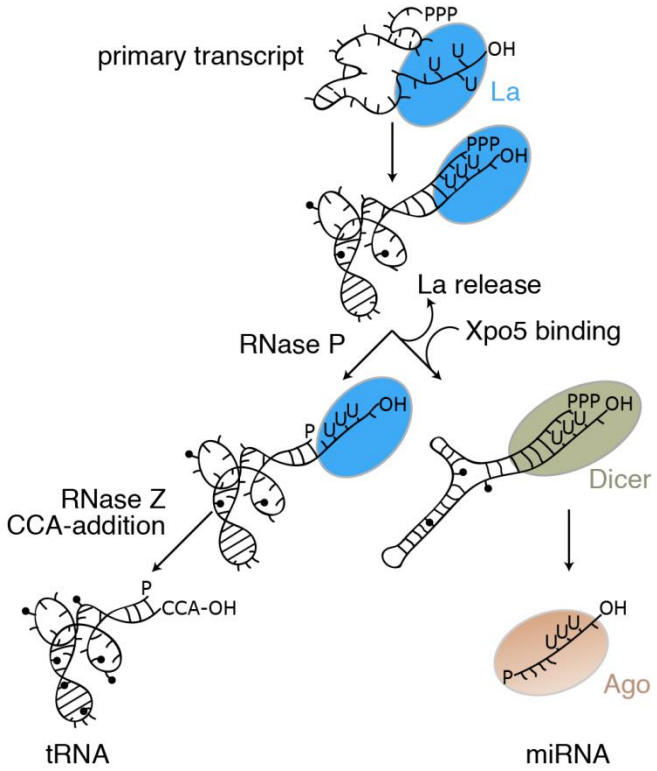

Figure 4.2: Model for the Regulatory Role of the La Protein in Safeguarding the Fate of Pre-tRNAs. La (blue) ensures that pre-tRNAs are processed to mature tRNAs (left). However, pre-tRNAs with complementary 5' and 3' ends can escape this control and are recognized by Xpo5 and Dicer (oliv). This finally results in the production pre-tRNA-derived miRNAs which are bound by Ago proteins (light brown) (right).

Why did pre-tRNA-Ile-TAT-2-3 evolve to a chimeric transcript maintaining both functions? Answering this question leaves room for several speculations:

1) As shown in Figure 1.5, the human genome encodes four other tRNA-Ile-TAT isodecoders, and the corresponding AUA codon is the less frequently used for Ile. It might therefore be that losing a tRNA-Ile-TAT gene in favor of a miRNA gene would be deleterious for the efficient translation of mRNAs enriched for AUA codons. Thus, it would be interesting to find out whether tRNA-Ile-TAT-2-3 crucially contributes to the synthesis of such Ile-containing proteins. A possible strategy could be to generate stable tRNA-Ile-TAT-2-3 knockout cell lines and, if viable, determine the translational efficiency of AUA codons in comparison to wild type cells by mRNA sequencing and ribosomal profiling experiments (Ingolia et al., 2011). However, these time and cost expensive experiments would have gone beyond the scope of this study.

2) An alternative interpretation of the chimeric nature of pre-tRNA-Ile-TAT-2-3 could be that it represents a snapshot on live evolution for the birth of a new miRNA and catches

the moment inbetween the transition from a tRNA to a miRNA gene. In this view, those pre-tRNAs, which give rise to Ago-loaded sRNAs only by the artificial depletion of La, might be a step further back on this evolutionary process. In order to escape from the tight regulation by La also under physiological conditions, such pre-tRNAs might still be awaiting to gain few other mutations making their secondary structure more appetizing for the miRNA biogenesis machinery.

3) In recent years it became more and more evident that the tRNA pool of a cell varies between different cell types and conditions (Dittmar et al., 2006; Gingold et al., 2014; Goodarzi et al., 2016). However, almost nothing is known concerning the molecular mechanisms accounting for the modulation of tRNA levels (see section 1.1.3.2). An intriguing scenario could be that the miRNA biogenesis pathway is intentionally hijacked to regulate the expression levels of a subset of pre-tRNAs. As we have shown, some pre-tRNAs can adopt alternative folding, which allow for processing into a tRNA or a miRNA-like sRNA. In our model, we have shown that these two biogenesis pathways compete with each other for the same transcripts (Figure 4.1) and by perturbing the abundance of La the equilibrium is altered into a specific direction. Since a multitude of mechanisms exist, which can regulate the expression level of a protein, it might be convenient to fine-tune the levels of such tRNAs simply by modulating the abundance of La or Xpo5. Although La appeared to be expressed at similar levels among the cell lines we have tested (Figure 3.37), its abundance is altered in cancer (Trotta et al., 2003; Sommer et al., 2011). The same holds true also for Xpo5 (Melo et al., 2010; Ott et al., 2016). Interestingly, in our experiments the expression of miR-1983 seemed to correlate with the protein levels of Xpo5 and Dicer (compare Figure 3.24 to Figure 3.37). In addition, when we performed knockdown experiments targeting Xpo5 we sometimes observed a correlation between the decrease of miR-1983 levels and the accumulation of mature tRNA-Ile (Figure 3.29). However, we did not extensively focus on this aspect. In particular, a more reliable experimental set up should be applied for the quantification of the tRNA-Ile levels. Ideally, the analysis could be expanded to the global impact of Xpo5 depletion on tRNA levels, which is nowadays less problematic thanks to the development of more adequate sequencing techniques (Cozen et al., 2015; Zheng et al., 2015; Gogakos et al., 2017). Nevertheless, our observations confirm, at least in part, the model we propose regarding the potential modulation of tRNA levels via the interplay of La and the miRNA biogenesis machinery.

4.7. Making a Fool of La?

We have widely emphasized that apparently just one specific pre-tRNA has acquired the ability to partially escape from La binding, while other pre-tRNAs are mis-channeled into the miRNA pathways only in the absence of La. However, this tight control over the fate of such pre-tRNAs can be easily perturbed. It should be mentioned that, despite its extraordinary abundance of approximately 2×10^7 molecules per cell (Gottlieb and Steitz, 1989), the protein levels of La might not be sufficient to cope with the sustained Pol III transcriptional output (Huang et al., 2005). In this study we collected some hints confirming that La cannot efficiently satisfy such a great demand.

First of all, we noticed that the generation of the Ago-loaded sRNA-Pro can be achieved also without La knockdown by simply forcing an increased production of pre-tRNA-Pro-CGG-2-1 (Figure 3.18). We thus speculate that the cell is not equipped with an adequate amount of La to ensure the processing of all overexpressed transcripts to mature tRNAs and, consequently, a fraction of pre-tRNA transcripts get channeled into the miRNA pathway.

Similarly, when we attempted to rescue the effect of La knockdown on the increased production of miR-1983, we only obtained a moderate success (Figure 3.40). Although additional factors might contribute to this observation, it should be noted that the overexpression of La did not exceed by much the endogenous levels (Figure 3.2), which might account for the partial rescue shown in Figure 3.40.

The aforementioned findings are derived from rather artificial experimental setups, so we wondered whether more physiological conditions could impact the efficiency of the surveillance by La over the fate of pre-tRNAs. We realized that several viruses rely on the action of La to fulfill own purposes. For example, binding of La to viral mRNAs is required for their efficient translation. This has been reported in the case of poliovirus (Meerovitch et al., 1989, 1993), human immunodeficiency virus (Svitkin et al., 1994) and hepatitis C virus (Ali and Siddiqui, 1997; Costa-Mattioli et al., 2004). Upon infection by poliovirus, La was also shown to re-localize from the nucleus to the cytoplasm, which might have a deep impact on the processes governed by La in the nucleus (Meerovitch et al., 1993). An even more striking fact is the recurrent interaction between viral ncRNAs and La (reviewed in Tycowski et al., 2015). This is the case for the adenoviral VAI/II as well as the EBV-encoded EBER1/2 RNAs, which are transcribed by Pol III and accumulate in the host at extremely high levels (between 2.5×10^5 and 10^8 copies per

cell) (reviewed by Mathews and Shenk, 1991; Tycowski et al., 2015). Differing from all the other cellular transcripts, La stays stably associated to these ncRNAs. Furthermore, we also demonstrated that shorter EBER fragments, which also terminate on U-stretches (data not shown), are as well highly enriched in anti-La immunoprecipitations (Figure 3.47A). Therefore, in EBV-infected cells, a great portion of endogenous La might be sequestered either by the full-length EBER1/2 or by the smaller EBER1/2 fragments. Owing to that, we assayed whether these interactions might consequently interfere with the tasks La fulfills under normal conditions. In our experiments, we overexpressed EBER1/2 in EBV-negative cells and monitored, as a functional readout, the production of Ago-loaded, pre-tRNA-derived sRNAs. Indeed, our data indicate that the interaction of La to pre-tRNA-Ile-TAT-2-3 is reduced in the presence of the EBERs (Figure 3.47B), while, at the same time, miR-1983 and sRNA-Pro accumulate in Ago2 complexes (Figure 3.48). These effects mimic exactly the same phenotype as seen upon knockdown of La, suggesting that the highly transcribed viral RNAs can perturb the fragile equilibrium which is usually safeguarded by La.

Since the evolution of a host and of its pathogens is always an arms race, the question arises whether the consequences of the EBER1/2-La interaction are beneficial for the host or for the virus. The former one might for instance use the interplay between the tRNA and the miRNA machineries as a sensor to quickly detect and react to viral infections. These could be achieved for example if the Ago-loaded pre-tRNA fragments would target some viral transcripts. However, this possibility needs to be addressed in future investigations. Another alternative scenario could be that the virus abuses the Ago-loaded pre-tRNA fragments to repress genes that are involved in the antiviral response or that could be otherwise harmful for the virus. In fact, the importance of EBERs for EBV infections is not yet fully understood. Several studies indicate that they play multiple roles for the viral life cycle and that EBER1/2 might also contribute to the oncogenic potential of EBV infections, which have been associated with different kinds of lymphomas and carcinomas (Kitagawa et al., 2000; Nanbo et al., 2002; Iwakiri et al., 2005; Lee et al., 2015). At the same time, however, EBERs can be recognized by the innate immunity system of the host and, by that, they trigger antiviral responses (Samanta et al., 2006; Ablasser et al., 2009; Iwakiri et al., 2009). Interestingly, also La was shown both, to promote antiviral responses (Liu et al., 2011; Mahony et al., 2017), and, in other contexts, to protect viral transcripts from being recognized by cellular detection systems (Domitrovich et al., 2005; Bitko et al., 2008).

Another intriguing finding suggesting that the EBER-mediated production of pre-tRNA fragments could be beneficial for the virus is that we identified BACH1 and BACH2 among the mRNAs, which are possibly targeted by miR-1983 (Figure 3.32). They are related transcription factors belonging to the basic region–leucine zipper family (Oyake et al., 1996) and, among other functions, both are involved in the regulation of the adaptive and innate immune systems, e.g. by contributing to the differentiation of B cells (Muto et al., 2004; Roychoudhuri et al., 2013; Swaminathan et al., 2013; Tsukumo et al., 2013; Itoh-Nakadai et al., 2014). Importantly, B cells are also the primary targets of EBV infections (reviewed in Küppers, 2003; Hatton et al., 2014). An appealing scenario could therefore be that sequestration of La by the EBER RNAs increases the production of miR-1983, which in turn leads to the repression of BACH1/2. EBV is a member of the γ-herpesvirus subfamily, which also comprises the Kaposi's sarcoma-associated herpesvirus (KSHV). Intriguingly, KSHV was shown to express viral miRNAs targeting BACH1 (Gottwein et al., 2007). Thus, it appears that reducing the expression of this transcription factor is a common mechanism exploited during infection by γ-herpesviruses. However, KSHV and EBV appear to have evolved different strategies to achieve the same purpose.

Still, the implications of EBERs hindering La from its physiological functions are likely to be more far-reaching than the simple regulation of BACH1 by miR-1983 and should be addressed in future. An interesting aspect, for example, might be to determine whether EBV-infection leads to an alteration of the cellular tRNA pool by the La-EBERs interaction. This might in turn contribute to the remodeling of the cellular proteome, which has been observed at different stages of the EBV infection (Ersing et al., 2017).

5. Material and Methods

5.1. Material

5.1.1. Consumables and Chemicals

Consumables and other plasticware products were ordered from Greiner Bio-One International GmbH (Kremsmünster, Austria), GE Healthcare (Buckinghamshire, UK), Sarstedt AG & Co. KG (Nümbrecht, Germany) and TPP Techno Plastic Products AG (Trasadingen, Switzerland). Glassware was obtained from Schott AG (Mainz, Germany), VWR International GmbH (Darmstadt, Germany) and Wheaton Industries Inc. (Millville, USA).

If not stated otherwise, all chemicals were purchased at the highest degree of purity from AppliChem GmbH (Darmstadt, Germany), Carl Roth GmbH + Co. KG (Karlsruhe, Germany), Merck KGaA (Darmstadt, Germany), SERVA Electrophoresis GmbH (Heidelberg, Germany) and Sigma-Aldrich Co. (St. Louis, USA).

The source of specific enzymes is indicated in the respective method sections. Common enzymes and reagents, as well as commercial DNA ladders or protein molecular weight markers, were purchased from Thermo Fisher Scientific Inc. (Waltham, USA) and New England Biolabs Inc. (Ipswich, USA).

Custom DNA oligonucleotides were synthesized by metabion international AG (Planegg, Germany), while short RNA oligonucleotides were obtained from biomers.net GmbH (Ulm, Germany).

5.1.2. Kits and Ready-made Solutions

The kits and the ready-made solutions used in this study are listed in Table 5.1 together with their corresponding manufacturer and application.

Table 5.1: Kits and Ready-made Solutions.

Name	Manufacturer	Application
First Strand cDNA Synthesis Kit	Thermo Fisher Scientific Inc.	cDNA synthesis for qPCR
Lipofectamine™ 2000	Thermo Fisher Scientific Inc.	Transfection of plasmid DNA
Lipofectamine™ RNAiMAX	Thermo Fisher Scientific Inc.	Transfection of siRNA
NucleoBond®-Xtra-Midi	MACHEREY-NAGEL GmbH & Co. KG (Düren, Germany)	Large scale plasmid purification
NucleoSpin®-Extract	MACHEREY-NAGEL GmbH & Co. KG	DNA purification from agarose gel slices, PCR reactions or other enzymatic reactions
NucleoSpin®-Plasmid	MACHEREY-NAGEL GmbH & Co. KG	Small scale plasmid purification
Passive Lysis 5X Buffer	Promega Corporation (Fitchburg, USA)	Cell lysis for luciferase assays
pGEM®-T Easy Vector System	Promega Corporation	Subcloning of DNA sequences
Phusion™ High-Fidelity DNA Polymerase	Thermo Fisher Scientific Inc.	PCR amplification
Roti®-Phenol/Chloroform/Isoamyl alcohol (25:24:1), pH 4.5-5	Carl Roth GmbH + Co. KG	Extraction of total RNA from immunoprecipitated samples
Roti®-Quant (5X)	Carl Roth GmbH + Co. KG	Protein quantitation according to Bradford
SequaGel® UreaGel™ System	National Diagnostics Inc., (Atlanta, USA)	Denaturing PAGE
SsoFast™ EvaGreen® Supermix	Bio-Rad Laboratories Inc. (Hercules, USA)	qPCR
SuperScript™ III First Strand Synthesis Super Mix	Thermo Fisher Scientific Inc.	cDNA synthesis for small RNA cloning
TRIzol Reagent	Thermo Fisher Scientific Inc.	Extraction of total RNA

5.1.3. Materials for Small-scale Purifications and Chromatography Columns

Small-scale purifications of proteins or nucleic acids were performed with the materials indicated in Table 5.2.

Table 5.2: Materials for Small-scale Purifications.

Material	Manufacturer	Specification
ANTI-FLAG® M2 Affinity Agarose Gel	Sigma-Aldrich Co.	Immunoprecipitation
CNBr-activated Sepharose™ 4 Fast Flow	GE Healthcare	Purification of antibodies
Glutathione Sepharose™ 4 Fast Flow	GE Healthcare	Ago-APP
illustra™ MicroSpin™ G-25 Columns	GE Healthcare	Purification of radiolabeled oligonucleotides
Protein A Sepharose™ 4 Fast Flow	GE Healthcare	Immunoprecipitation
Protein G Sepharose™ 4 Fast Flow	GE Healthcare	Immunoprecipitation

The chromatography columns listed in Table 5.3 were used in combination with the ÄKTApurifier™ system (GE Healthcare) for large scale protein purification.

Table 5.3: Chromatography Columns.

Column	Material	Manufacturer	Specification
GSTrap™ FF	Glutathione Sepharose™ 4 Fast Flow	GE Healthcare	Affinity chromatography
Hiprep™ 26/10 Desalting	Sephadex™ G-25	GE Healthcare	Size exclusion chromatography
RESOURCE™ Q	SOURCE™ 15Q	GE Healthcare	Anion exchange chromatography

5.1.4. Laboratory Equipment

The instruments which were used in the course of this study are listed in Table 5.4.

Table 5.4: Instruments.

Instrument	Manufacturer
Agilent 2100 Bioanalyzer	Agilent Technologies Inc. (Santa Clara, USA)
ÄKTApurifier™ system	GE Healthcare
Biological safety cabinet HeraSafe™ KS	Thermo Fisher Scientific Inc.
Centrifuge 5417 R	Eppendorf AG (Hamburg, Germany)
Centrifuge Avanti J-20 XP	Beckman Coulter (Brea, USA)
Centrifuge Heraeus™ Biofuge™ pico	Thermo Fisher Scientific Inc.

Centrifuge Heraeus™ Megafuge™ 40	Thermo Fisher Scientific Inc.
CO_2 Incubator HeraCell™ 240i	Thermo Fisher Scientific Inc.
Gel imaging system Quantum ST4	Vilber Lourmat (Collégien, France)
Hybridization oven Shake 'n' stack™	Thermo Fisher Scientific Inc.
Incubator shaker Innova 44	New Brunswick Scientific Co., Inc. (Enfield, USA)
Microplate Reader Mithras LB 940	BERTHOLD TECHNOLOGIES GmbH & Co. KG (Bad Wildbad, Germany)
Odyssey Infrared Imaging System	LI-COR Bioscience, Lincoln, USA
Personal Molecular Imager™	Bio-Rad Laboratories Inc.
Power supply EV233	Consort bvba (Turnhout, Belgium)
Power supply PowerPac HC	Bio-Rad Laboratories Inc.
Real time PCR detection system MyiQ™	Bio-Rad Laboratories Inc.
Screen Eraser-K	Bio-Rad Laboratories Inc.
Semi-dry transfer cell Trans-Blot® SD	Bio-Rad Laboratories Inc.
Sequencing platform MiSeq™	Illumina Inc. (San Diego, USA)
Spectrophotometer Nanodrop® ND-1000	Thermo Fisher Scientific Inc.
Spectrophotometer Ultraspec 3300 pro	Amersham Biosciences AB (Uppsala, Sweden)
Thermal cycler 2720	Applied Biosystems Inc. (Foster City, USA)
Thermal cycler peqSTAR	Peqlab Biotechnologie GmbH (Erlangen, Germany)
Thermomixer® comfort	Eppendorf AG (Hamburg, Germany)
Ultrasonics sonifier 450	BRANSON Ultrasonics Corporation (Danbury, USA)

5.1.5. Buffers and Solutions

The composition of common buffers and solutions is given in Table 5.5.

Table 5.5: Composition of Common Buffers and Solutions

Buffer/Solution	Composition
Denhardt's solution (50X)	1% BSA; 1% Polyvinylpyrrolidon K30; 1% Ficoll® 400
Sodium phosphate buffer (1M)	Titration of NaH_2PO_4 (1M) and Na_2HPO_4 (1M) solutions until desired pH is reached.
Potassium phosphate buffer (1M)	Titration of KH_2PO_4 (1M) and K_2HPO_4 (1M) solutions until desired pH is reached.
PBS (1X)	10 mM Na_2HPO_4; 1.8 mM KH_2PO_4; 137 mM NaCl; 2.7 mM KCl; pH 7.5
SDS-gel running buffer (1X)	25 mM Tris; 0.2 M glycine; 0.1% (w/v) SDS; pH 7.5
SSC (20X)	3 M NaCl; 0.3 M trisodium citrate; pH 7.0
TB (0.5X)	45 mM Tris; 45 mM boric acid; pH 8.0
TBE (1X)	89 mM Tris; 89 mM boric acid; 2 mM EDTA; pH 8.3
TBS-T (1X)	10 mM Tris; 150 mM NaCl; 0.1% (v/v) Tween® 20; pH 8.0

The composition of the buffers and solutions used for specific applications is indicated in the respective method section.

5.1.6. RNA and DNA Oligonucleotides

5.1.6.1. Oligonucleotides Used for Preparation of Deep-sequencing Libraries

The RNA/DNA adapters and DNA primers shown in Table 5.6 were used for the preparation of deep-sequencing libraries, which were compatible with the Illumina-sequencing sytem.

Table 5.6: Oligonucleotides Used for Preparation of Small RNA and PAR-CLIP Libraries.

Name	Sequence 5'→3'
3' adenylated DNA adapter	App-TGGAATTCTCGGGTGCCAAGG-(C7-amino)
5' RNA adapter	GUUCAGAGUUCUACAGUCCGACGAUC
RT primer	GCCTTGGCACCCGAGAATTCCA
5' PCR primer	AATGATACGGCGACCACCGAGATCTACACGTTCAGA GTTCTACAGTCCGA
3' PCR index primer	CAAGCAGAAGACGGCATACGAGAT- 6 nt index -GTGAC TGGAGTTCCTTGGCACCCGAGAATTCCA
3' PAR-CLIP DNA adapter	Phos-NNNNTGGAATTCTCGGGTGCCAAGG-Inv(dT)
5' PAR-CLIP RNA adapter	GUUCAGAGUUCUACAGUCCGACGAUCNNNN

5.1.6.2. RNA Oligonucleotides

The oligoribonucleotide pairs listed in Table 5.7 were used as siRNAs for knockdown experiments.

Table 5.7: RNA Oligonucleotides Used as siRNAs. The corresponding target transcript is indicated with the NCBI official gene symbol. The position targeted by each siRNA within the respective transcripts is indicated in the last column. CDS = coding sequence.

Name	Sequence 5'→3'	Target Transcript (official symbol)	Target Position
control-S	r(UUGUCUUGCAUUCGACUAAU)dT	Control sequence	-
control-AS	r(UUAGUCGAAUGCAAGACAAU)dT		
Dicer-S siRNA#1	r(GGUAAGAGAACUACAGAAAUU)	DICER1	CDS
Dicer-AS siRNA#1	r(UUUCUGUAGUUCUCUUACCAU)		
Dicer-S siRNA#2	r(GGUUGAUACUGGUGAGACUGU)	DICER1	CDS
Dicer-AS siRNA#2	r(AGUCUCACCAGUAUCAACCGU)		

ELAC1-S ELAC1-AS	r(UGGACAAAGCAAAGGAGCAU)dT r(UGCUCCUUUGCUUUGUCCAU)dT	DICER1	CDS
ELAC2-S ELAC2-AS	r(GUGAAUGCCUCCUCAAGUAC)dT r(UACUUGAGGAGGCAUUCACC)dT	ELAC2	CDS
La-S siRNA #1 La-AS siRNA#1	r(AGAUUGGAUGCUUGCUGAA)dTdT r(UUCAGCAAGCAUCCAAUCU)dTdT	SSB	CDS
La-S siRNA#2 La-AS siRNA#2	r(CCAUUAAAUUGCCUUUGUA)dTdT r(UACAAAGGCAAUUUAAUGG)dTdT	SSB	3’ UTR
La-S siRNA#3 La-AS siRNA#3	r(GGACAAGUUUCUAAAGGAA)dTdT r(UUCCUUUAGAAACUUGUCC)dTdT	SSB	CDS
Pop4-S Pop4-AS	r(CACAGAUGAUUCAGGCCAAG)dT r(UUGGCCUGAAUCAUCUGUGG)dT	POP4	CDS
TSEN2-S TSEN2-AS	r(CUGGGAUGUUUAAGUAUUU)dTdT r(AAAUACUUAAACAUCCCAG)dTdT	TSEN2	CDS
Xpo5-S siRNA#1 Xpo5-AS siRNA#1	r(CCGUGAUCCUUUGCUAUUAU)dT r(UAAUAGCAAAGGAUCACGGU)dT	XPO5	CDS
Xpo5-S siRNA#2 Xpo5-AS siRNA#2	r(GCGUCAGAAGGUGUUCCUAU)dT r(UAGGAACACCUUCUGACGCU)dT	XPO5	CDS

The oligoribonucleotide pairs listed in Table 5.8 were used as a control or as miRNA mimic in dual luciferase assays. MiR-1983-mimic-S corresponds to the mature sequence of miR-1983. Note that miR-1983-mimic-AS is not fully complementary to miR-1983-mimic-S. The annealing of the two oligoribonucleotides results in thermodynamically less stable interactions at the 5’ end of miR-1983-mimic-S. This artificial design was created to ensure loading of the correct strand of the miR-1983-mimic into Ago proteins (see section 1.2.2).

Table 5.8: RNA Oligonucleotides Used as miRNA Mimic or Control in Luciferase Assays.

Name	**Sequence 5’→3’**
control-S control-AS	r(UUGUCUUGCAUUCGACUAAU)dT r(UUAGUCGAAUGCAAGACAAU)dT
miR-1983-mimic-S miR-1983-mimic-AS	r(CUCACCUGGAGCAUGUUUUCU) r(AAAACAUGCUCCAGGUAAACC)

The following synthetic, 5’ phosphorylated, ribooligonucleotide was used for the determination of miR-1983 copy numbers per cell:

5’-Phos-CUCACCUGGAGCAUGUUUUCU-3’

5.1.6.3. DNA Oligonucleotides

The oligonucleotides listed in Table 5.9 were used as probes for Northern blot assays.

Table 5.9: DNA Oligonucleotides Used for Northern Blot Assays.

Name	Sequence 5'→3'
CU1276	TGGTGCATTGGCCGGGAATCGA
EBER1	TCTAGGGCAGCGTAGGTCCT
EBER2	AACAGCGGACAAGCCGAATAC
let-7i	AACAGCACAAACTACTACCTCA
miR-17	CTACCTGCACTGTAAGCACTTTG
miR-19b	TCAGTTTTGCATGGATTTGCACA
miR-27a	GCGGAACTTAGCCACTGTGAA
miR-98	AACAATACAACTTACTACCTCA
miR-1290	TCCCTGATCCAAAAATCCA
miR-1983/sRNA-Ile	AGAAAACATGCTCCAGGTGAG
sRNA-Pro	GAAGTGGGCTCGTCCGGGATTT
tRNA-Ile	GCTCGAACTCACAACCTCGGCAT
tRNA-Lys	CTGATGCTCTACCGACTGAGCTATCCGGGC
U6	GAATTTGCGTGTCATCCTTGCGCAGGGGCCATGCTAA
Y5	AATAACCCACAACACTCGGACCAACT

Expression levels of mRNAs were determined by qPCR analyses using the primer pairs indicated in Table 5.10.

Table 5.10: Primers Used for qPCR Analyses.

Name	Sequence 5'→3'	Target Transcript (official symbol)
Dicer-F	GAAGACCAGGTTCCACGAAA	DICER1
Dicer-R	GGCTGATCAGGTCTGGGATA	
ELAC1-F	GGCTCTTTGACTGTGGGGAGGG	ELAC1
ELAC1-R	AGAGGAGCCCAGGAAGGCCAA	
ELAC2-F	GAGGGGTCAGGGACTCTTCCCT	ELAC2
ELAC2-R	CGATGGCAGCTGTCCCAACTGG	
GAPDH-F	AATGGAAATCCCATCACCATCT	GAPDH
GAPDH-R	CGCCCCACTTGATTTTGG	
La-F	CGGAACCTTAAAGATAGCCGCA	SSB
La-R	CCCGTGGCAAATTGAAGTCG	

LARP1-F LARP1-R	GTGATGGATTCCCGTGAGCA ACTTGGGCAATGACTGAGGG	LARP1
LARP4B-F LARP4B-R	CGAGACAGGAGGAAATGAGTCT CATGTCACTAGCAAGGTTCTCC	LARP4B
POP4-F POP4-R	CAGGCAAAGGAGGGAGCTGCG TGGCTTGAGCCCACTGCACAG	POP4
TSEN2-F TSEN2-R	GGAGGCTGCCCCAAATGAG AAAAAGGCCTCTTCTAGGCTGA	TSEN2
Xpo5-F Xpo5-R	TTCTTGACAATTTGCTTGCG GCATATCCAGAGCCTTGGTG	XPO5

PCR amplification of DNA fragments as templates for *in vitro* transcription reactions was performed with the oligonucleotides indicated in Table 5.11.

Table 5.11: Primers for PCR amplification of Templates for *In Vitro* Transcriptions. The T7 promoter sequence is highlighted in blue.

Name	**Sequence 5'→3'**
tRNA-AS-F	AAAGCATGCTCCAGTGGCG
tRNA-Ile29-ivt-R	AAAACAATGCTCCAGGTGAGGC
tRNA-Ile29-ivt-CT-R	AGAAAACAATGCTCCAGGTGAGGC
tRNA-Ile29-T7-F	TAATACGACTCACTATAGGGAAACTGGGTGCTCCAGTGGC
tRNA-mat-T7-F	TAATACGACTCACTATAGGGGCTCCAGTGGCGCAATCG
tRNA-short-AS-T7-R	TAATACGACTCACTATAGGGGAAGAAAACATGCTCCAGGTGAGG
tRNA-short-end-R	AGAAAACATGCTCCAGGTGAG
tRNA-short-R-TTTT	AAAACATGCTCCAGGTGAGGC
tRNA-T7-F	TAATACGACTCACTATAGGGAAAGCATGCTCCAGTGGCG

The following complementary oligonucleotides were annealed and directly used for ligations or *in vitro* transcriptions (Table 5.12).

Table 5.12: Complementary DNA Oligonucleotides Used for Different Applications upon Annealing. Overhangs resulting upon annealing which were used for ligation purposes are shown in red. The T7 promoter sequence is highlighted in blue.

Name	**Sequence 5'→3'**
miR-1983-sense	GATCTCCAGAAAACATGCTCCAGGTGAGTTCAAGAGACTCACCTGGAGCATGTTTTCTA
miR-1983-antisense	AGCTTAGAAAACATGCTCCAGGTGAGTCTCTTGAACTCACCTGGAGCATGTTTTCTGGA

miR1983-multiple-1S	CTAGTATCGCCACCTTGTTTAAGCCAGA
miR1983-multiple-1AS	ATGTTTTCTGGCTTAAACAAGGTGGCGATA
miR1983-multiple-2S	AAACATGCTCCAGGTGAGATCGCCAGA
miR1983-multiple-2AS	ATGTTTTCTGGCGATCTCACCTGGAGC
miR1983-multiple-3S	AAACATGCTCCAGGTGAGATTAGACCTACGCACTCCAGGAGCT
miR1983-multiple-3AS	CCTGGAGTGCGTAGGTCTAATCTCACCTGGAGC
miR1983-mul-mut-2S	AAACATGCTCCGGATCCGATCGCCAGA
miR1983-mul-mut-2AS	ATGTTTTCTGGCGATCGGATCCGGAGC
miR1983-mul-mut-3S	AAACATGCTCCGGATCCGATTAGACCTACGCACTCCAGGAGCT
miR1983-mul-mut-3AS	CCTGGAGTGCGTAGGTCTAATCGGATCCGGAGC
pre-miR-27a-T7-S	TAATACGACTCACTATAGGGAGGGCTTAGCTGCTTGTGAGCA GGGTCCACACCAAGTCGTGTTCACAGTGGCTAAGTTCCGC
pre-miR-27a-T7-AS	GCGGAACTTAGCCACTGTGAACACGACTTGGTGTGGACCCT GCTCACAAGCAGCTAAGCCCTCCCTATAGTGAGTCGTATTA

PCR amplification of DNA fragments for cloning purposes was performed with the oligonucleotides indicated in Table 5.13.

Table 5.13: PCR Primers Used for Cloning Purposes. Restriction sequences used for cloning are shown in red. The sequence corresponding to the Tobacco Etch Virus (TEV) cleavage site is highlighted in blue.

Name	**Sequence 5'→3'**
30-ProGCC-BglII-F	CAGAGATCTCTAAGTGGCTCGTTGGTCTAGGGG
30-ProGCC-HindIII-R	CTGAAGCTTAAATGAAGTGGGCTCGTCCGGG
BACH1-UTR-SacI-R	CATGAGCTCGTATGCCATCTTCTACCATTATGGC
BACH1-UTR-SpeI-F	CATACTAGTACTTGCATTCACTTCCTTCAAACC
BACH2-UTR-F3	GGTCAACTTTGCCACTTGCACTG
BACH2-UTR-R4	GGGACTTGAGAAAGCTTTGCAGGCAG
EBER1-100-EcoRI-F	CAGGAATTCGGCAACCCCCGCCTACAC
EBER2-HindIII-R	CTGAAGCTTAAAAAAACAGCGGACAAGCCG
Fw-La-NotI	CGCTGCGGCCGCATGGCTGAAAATGGTGAT
hLa-104-408-NotI-F	CGCTGCGGCCGCTATAAAAATGATGTAAAAAACAGATCT
hLa-tr-196-EcoRI-R	CGCTGAATTCCTATCTTTCTTCATTTTTTTTGGCAAAG
Ile29-BglII-F	CAGAGATCTAAACTGGGTGCTCCAGTGG
Ile29-HindIII-R	CTGAAGCTTAAAACAATGCTCCAGGTGAGGC
La-BamHI-F	ATAGGATCCATGGCTGAAAATGGTGATAATG
La-NotI-R	TACGCGGCCGCCTACTGGTCTCCAGCAC
La-TEV-BamHI-F	ATAGGATCCGAAAACCTGTATTTTCAGGGAATGGCTGAAAA TGGTGAT
Rev-La-EcoRI	CGCTGAATTCCTACTGGTCTCCAGCACCAT
RIMS2-UTR-F2	CAGCTGTAAAAAAATTGTTGTCACAGC
RIMS2-UTR-R2	GATTATGTGACTGCATCTTAGTATCAGG

tRNA-BglII-F	CAGAGATCTAAAGCATGCTCCAGTGGCG
tRNA-short-HindIII-R	CTGAAGCTTGGAAGAAAACATGCTCC

Mutagenesis PCRs were performed with the oligonucleotides indicated in Table 5.14.

Table 5.14: Primers Used for Mutagenesis PCRs. The mutations introduced in comparison to the templates used are highlighted in green.

Name	Sequence 5'→3'
BACH1-UTR-mut-F	CGGTGAATTCTCGGATCCACTTTTTTCAGTTATAAAAC
BACH1-UTR-mut-R	GTTTTATAACTGAAAAAAGTGGATCCGAGAATTCACCG
BACH2-mut-F	CTAATTAAAAAGCACTCGGATCCTAATTATGTAGGAAAAAC
BACH2-mut-F2	CAGGCTTTGGACGGATCCGTGATTTGCTGTATGTG
BACH2-mut-R	GTTTTTCCTACATAATTAGGATCCGAGTGCTTTTTAATTAG
BACH2-mut-R2	CACATACAGCAAATCACGGATCCGTCCAAAGCCTG
hLa-Y23A-Y24A-F	CTGTCATCAAATTGAGGCCGCCTTTGGCGACTTCAATTTG
hLa-Y23A-Y24A-R	CAAATTGAAGTCGCCAAAGGCGGCCTCAATTTGATGACAG
RIMS2-mut-F	CTAAAGAAGGCCCTCGGATCCAAGAGCAGAGCTGTG
RIMS2-mut-F2	GAAGCGGTGTTACGGATCCGGAGTGTAATCC
RIMS2-mut-F3	CTAGGAAGCATCGGATCCAAAGCAGGAGAC
RIMS2-mut-R	CACAGCTCTGCTCTTGGATCCGAGGGCCTTCTTTAG
RIMS2-mut-R2	GGATTACACTCCGGATCCGTAACACCGCTTC
RIMS2-mut-R3	GTCTCCTGCTTTGGATCCGATGCTTCCTAG
tRNA-IleTAT-human-F	GCGGTACTTATACAACAGTATATGTGCGGGTG
tRNA-IleTAT-human-R	CACCCGCACATATACTGTTGTATAAGTACCGC

Sequencing reactions were performed with the primers listed in Table 5.15. The last column indicates for which plasmid backbones the primers were used.

Table 5.15: Sequencing Primers.

Name	Sequence 5'→3'	Sequenced Plasmids
M13-F	TGTAAAACGACGGCCAGT	pSUPER, pMIR-RNL-TK, pGEM®-T Easy, pMA-T
M13-R	CAGGAAACAGCTATGACCATG	pSUPER, pGEM®-T Easy
pGEX-F	GGGCTGGCAAGCCACGTTTGGTG	pGEX-4T-1, pGEX-6P-1
pGEX-R	GGAGCTGCATGTGTCAGAG	pGEX-4T-1, pGEX-6P-1
pMIR-Seq-F	TCATAAAGGCCAAGAAGGG	pMIR-RNL-TK
VP5-F	CGAAATTAATACGACTCACTATAG	VP5
VP5-R	CCCAACAGCTGGCCCTCGCAGA	VP5

5.1.7. Plasmids

An overview of the empty vectors and of the available plasmids which were used during the course of this study is given in Table 5.16.

Table 5.16: Empty Vectors and Available Plasmids.

Name	Source and Comments
pGEX-4T-1	GE Healthcare, contains GST-tag.
pGEX-6P-1	GE Healthcare; contains GST-tag and cleavage site for PreScission protease between the GST and the multiple cloning site.
pMIR-RNL-TK	pMIR-REPORT™ from Ambion Inc. (Austin, USA), modified according to Höck et al. (2007).
pSUPER	OligoEngine Inc. (Seattle, USA), modified according to Zhu et al. (2009).
VP5	pIRESneo from Clontech Laboratories Inc. (Mountain View, USA), modified according to Meister et al. (2004).
VP5 + Dicer	Meister et al. (2005)
VP5 + GFP	Meister et al. (2004)
VP5 + La WT	Contains the open reading frame (ORF) of La, which was PCR-amplified from human cDNA using the Fw-La-NotI and Rev-La-EcoRI primers; cloned by Dr. Julia Stöhr, Meister group (University of Regensburg, Germany).

The plasmid pMA-T containg the mouse pre-tRNA-Ile-TAT-2-1 sequence was synthetized by Geneart AG (Regensburg, Germany).

All other plasmids generated during the course of this work are listed in Table 5.17 with a brief description of the respective cloning strategy.

Table 5.17: Generated Plasmids.

Name	Cloning Strategy
pGEX-4T-1 + La WT	PCR amplification from VP5 + La WT with the primers La-TEV-BamHI-F and La-NotI-R; cloning via BamHI and NotI.
pGEX-4T-1 + La F44A	PCR amplification from VP5 + La Y23A Y24A with the primers La-TEV-BamHI-F and La-NotI-R; cloning via BamHI and NotI.
pGEX-6P-1 + La WT	PCR amplification from VP5 + La WT with the primers La-BamHI-F and La-NotI-R
pMIR-RNL-TK + artificial miR-1983 target	Constructed using miR1983-multiple-1S/AS, -2S/AS and -3S/AS oligo-nucleotides according to the manufacturer's protocol using the restriction enzymes BglII and HindIII.

pMIR-RNL-TK + artificial miR-1983 target mutated	Constructed using miR1983-multiple-1S/AS, miR1983-mul-mut-2S/AS and -3S/AS oligonucleotides according to the manufacturer's protocol using the restriction enzymes BglII and HindIII.
pMIR-RNL-TK + BACH1 mutated	Subcloning into pGEM®-T Easy and mutagenesis PCR with the primers BACH1-UTR-mut-F/R; cloning into pMIR-RNL-TK similar to the corresponding WT construct.
pMIR-RNL-TK + BACH1 WT	PCR amplification from HEK293 genomic DNA with BACH1-UTR-SpeI-F and BACH1-UTR-SacI-R; cloning via SpeI and SacI.
pMIR-RNL-TK + BACH2 mutated	Subcloning into pGEM®-T Easy and mutagenesis PCR with the primers BACH2-mut-F/R, and -F2/R2; cloning into pMIR-RNL-TK similar to the corresponding WT construct.
pMIR-RNL-TK + BACH2 WT	PCR amplification from HEK293 genomic DNA with the primers BACH2-UTR-F3/R4; blunt ligation into pMIR-RNL-TK linearized by PmeI restriction digest.
pMIR-RNL-TK + RIMS2 mutated	Subcloning into pGEM®-T Easy and mutagenesis PCR with the primers RIMS2-mut-F/R, -F2/R2, and F3/R3; cloning into pMIR-RNL-TK similar to the corresponding WT construct.
pMIR-RNL-TK + RIMS2 WT	PCR amplification from HEK293 genomic DNA with the primers RIMS2-UTR-F2/R2; blunt ligation into pMIR-RNL-TK linearized by PmeI restriction digest.
pSUPER + EBER1/2	PCR amplification from DNA extracted from EBV-positive Raji cells with the EBER1-100-EcoRI-F and EBER2-HindIII-R primers; PCR product contained both EBER RNAs, as well as additional 100 nts at the 5' end. Cloning via EcoRI and HindIII resulted in the removal of the H1 promoter of the vector. Therefore, expression is achieved from the endogenous EBER RNAs' promoter.
pSUPER + pre-tRNA-Ile-TAT-2-2	PCR amplification from human genomic DNA with the primers Ile29-BglII-F and Ile29-HindIII-R; cloning via BglII and HindIII.
pSUPER + pre-tRNA-Ile-TAT-2-3	Mutagenesis PCR of pMA-T + pre-tRNA-Ile-TAT-2-1 with the primers tRNA-IleTAT-human-F/R; PCR-amplification from a positive clone with tRNA-BglII-F and tRNA-short-HindIII-R; cloning via BglII and HindIII.
pSUPER + sRNA Ile shRNA	Constructed using miR-1983-sense/antisense oligonucleotides according to the manufacturer's protocol using the restriction enzymes BglII and HindIII.
VP5 + La 104-408	PCR amplification from VP5 + La WT with the primers hLa-104-408-NotI-F and Rev-La-EcoRI primers; cloning via EcoRI and NotI.
VP5 + La 1-196	PCR amplification from VP5 + La WT with the primers Fw-La-NotI and hLa-tr-196-EcoRI-R; cloning via EcoRI and NotI.
VP5 + La Y23A Y24A	Subcloning of the La ORF from VP5 + La WT into pGEM®-T Easy and mutagenesis PCR with the primers hLa-Y23A-Y24A-F/R; cloning into VP5 via EcoRI and NotI.

5.1.8. Antibodies

On overview of the antibodies used and of their respective applications is given in Table 5.18.

Table 5.18: Antibodies Used and Their Application. ID = identification, mAB = monoclonal antibody, pAB = polyclonal antibody, WB = Western blot, IP = immunoprecipitation.

Antigen	Origin	Clonality (ID)	Purity	Application	Source
HA.11	mouse	mAB (16B12)	purified	WB (1:1,000)	Covance Inc. (Princeton, USA)
α-Tubulin	mouse	mAB (DM1A)	purified	WB (1:10,000)	Sigma-Aldrich Co.
β-Actin	mouse	mAB (AC15)	purified	WB (1:10,000)	Abcam plc (Cambridge, UK)
Ago1	rat	mAB (4B8)	hybridoma supernatant	IP (undiluted) WB (1:5)	Beitzinger et al. (2007)
Ago2	rat	mAB (11A9)	hybridoma supernatant	IP (undiluted) WB (1:5)	Rüdel et al. (2008)
Ago3	rat	mAB (5A3)	hybridoma supernatant	IP (undiluted) WB (1:5)	Dueck et al. (2012)
pan-TNRC6	rat	mAB (7A9)	hybridoma supernatant	IP (undiluted) WB (1:5)	Schraivogel et al. (2015)
Dicer	rabbit	pAB (A301-936A)	purified	WB (1:1,000)	Bethyl Laboratories Inc. (Montgomery, USA)
La	rabbit	pAB (SY6175)	serum purified	IP (1:50) WB (1:1,000)	This study

Western blot signals were detected, according to the manufacturer's instructions, with the secondary antibodies IRDye 800CW and IRDye 680RD (LI-COR Bioscience).

5.1.9. Bacterial Strains and Cell Lines

5.1.9.1. Bacterial Strains

Following *E. coli* strain was used for molecular cloning:

XL1-Blue	endA1 gyrA96(nalR) thi-1 recA1 relA1 lac glnV44 F'[::Tn10 proAB^{+} lacI^{q} Δ(lacZ)M15] hsdR17(rK- mK+)

Following *E. coli* strain was used for protein expression:

BL21 [DE3]	F- ompT hsdSB (rB-, mB-) gal dcm (DE3)

5.1.9.2. Mammalian Cell Lines and Growth Media

Dulbecco's modified Eagle's medium (DMEM) and RPMI-1640 medium were obtained from Sigma-Aldrich Co.. An overview of the mammalian cell lines used is given in Table 5.19.

Table 5.19: Mammalian Cell Lines.

Cell line	Origin / Description	Growth Medium
A549	Human lung carcinoma	DMEM
DLD-1	Human colorectal adenocarcinoma	RPMI-1640
Flp-In 293 T-REx + FH-Dicer	Human embryonic kidney; stable, inducible expression of FH-Dicer (Rybak-Wolf et al., 2014)	DMEM
HEK293	Human embryonic kidney	DMEM
HeLa	Human cervix adenocarcinoma	DMEM
HepG2	Human hepatocellular carcinoma	DMEM
MCF-7	Human breast adenocarcinoma	DMEM
MEF Dcr -/-	Mouse embryonic fibroblast with Dicer deletion (Glasmacher et al., 2010)	DMEM
MEF Dcr +/+	Mouse embryonic fibroblast; wildtype but Dicer alleles floxed (Glasmacher et al., 2010)	DMEM
Ntera2	Human testicular embryonic carcinoma	DMEM
Raji	Human B lymphocyte, derived from Burkitt's lymphoma, EBV positive	RPMI-1640
SK-N-MC	Human brain neuroepithelioma	DMEM

Lysates of the B lymphocyte cell lines Jiyoye and U2932 EBV+ were kindly provided by the group of Prof. Dr. Friedrich A. Grässer (Saarland University Medical School, Homburg/Saar, Germany). The generation of the latter cell line has been described in Imig et al. (2011).

5.2. Methods

5.2.1. Molecular Biological Methods

5.2.1.1. Determination of Nucleic Acid Concentration

The concentration and purity of DNAs and RNAs were determined by measuring the absorbance of 1-2 µl of the samples with the Nanodrop® ND-1000 spectrophotometer (Thermo Fisher Scientific Inc.).

5.2.1.2. Polymerase Chain Reaction (PCR)

Amplification of DNA fragments was performed with the Phusion™ High-Fidelity (HF) DNA Polymerase (Thermo Fisher Scientific Inc.) according to the manufacturer's instruction and with the primers listed in Table 5.11 and Table 5.13. The standard PCR reaction mixture consisted of the following components:

Template	250 ng	genomic DNA or
	10 ng	plasmid DNA or
	1µl	cDNA
Phusion™ HF Buffer (5X)	10 µl	
dNTPs (10 mM each)	1 µl	
Forward Primer (10 µM)	1.25 µl	
Reverse Primer (10 µM)	1.25 µl	
Phusion™ HF Polymerase	0.5 µl	
H_2O	*ad* 50 µl	

PCRs were performed with the following cycling conditions, whereby the annealing temperature was determined for each primer pair with the Tm calculator tool (Thermo Fisher Scientific Inc.):

Initial denaturation	98°C	60 s	for genomic DNA or
	98°C	30 s	for plasmid DNA or cDNA
Denaturation	98°C	30 s	} 30-35 cycles
Annealing	X°C	30 s	
Extension	72°C	30 s/kb	
Final extension	72°C	5 min	

5.2.1.3. Agarose Gel Electrophoresis

DNA fragments were resolved on 0.5-2% (w/v) agarose gels by electrophoresis in 1X TBE buffer. The gels contained 0.1 µg/ml EtBr for the visualization of the DNA under UV light. If required, bands of the correct size were excised from the gel and the DNA was extracted with the NucleoSpin®-Extract kit (MACHEREY-NAGEL GmbH & Co. KG) according to the manufacturer's instruction.

5.2.2. Molecular Cloning

5.2.2.1. Restriction Digest of DNA and Dephosphorylation of Linearized Vectors

Restriction digest of purified PCR products (ca. 100 ng) or plasmid DNA (ca. 5 µg) was performed for >1h at 37°C with the FastDigest™ restriction enzyme system (Thermo Fisher Scientific Inc.) in a reaction volume of 20-30 µl. Digested PCR fragments were directly purified with the NucleoSpin®-Extract kit (MACHEREY-NAGEL GmbH & Co. KG), while digested plasmids were first purified by agarose gel electrophoresis before being extracted from the gel.

The 5' ends of the linearized plasmid DNA were dephosphorylated with the FastAP thermosensitive alkaline phosphatase (Thermo Fisher Scientific Inc.) according to the manufacturer's instruction. This treatment reduces the probability of re-ligation of empty plasmids during the following cloning step (5.2.2.3).

5.2.2.2. Annealing and Phosphorylation of DNA Fragments

The generation of the plasmids pMIR-RNL-TK + artificial miR-1983 target, pMIR-RNL-TK + artificial miR-1983 target mutated and pSUPER + sRNA Ile shRNA synthethic occurred without any PCR amplification procedure. Instead, complementary, synthethic DNA oligonucleotides (Table 5.12) were designed in such a way, that the annealed sense and antisense oligonucleotide pairs had overhangs compatible with the digested plasmid DNA. For annealing, the respective oligonucleotide pairs were diluted in water to a concentration of 5 µM. The mixture heated for 5 min at 95°C and was then immediately transferred to 37°C for 30-60 min.

To allow ligation into the target vectors, the annealed oligonucleotides required to be phosphorylated at their 5' ends. This was achieved with the T4 polynucleotide kinase (PNK) (Thermo Fisher Scientific Inc.) according to the manufacturer's instruction. Briefly, 20 pmol of the annealed oligonucleotides were incubated in 20 µl reaction volume with 1 mM ATP and 1 U/µl T4 PNK in 1X PNK buffer A (Thermo Fisher Scientific Inc.). The reaction was carried out for 20 min at 37°C and the enzyme was heat-inactivated for 10 min at 75°C. No purification of the reaction was performed prior ligation.

Purified PCR products, which were directly used for blunt-end ligations, were 5' phosphorylated. In this case, the maximal possible volume of DNA was applied (ca. 500 ng).

5.2.2.3. DNA Insert Ligation into Vectors

DNA fragments were ligated into linearized, dephosphorylated vectors (5.2.2.1) using the T4 DNA ligase (Thermo Fisher Scientific Inc.).

The following reaction conditions were applied in case of sticky-end ligations:

Linearized vector DNA	50-150 ng
Insert DNA (molar ratio over vector)	3:1
T4 DNA ligase buffer (10X)	2 µl
T4 DNA ligase	5 U
H_2O	*ad* 20 µl

The ligation mixture was incubated at least for 30 min at 16°C followed by 30 min at room temperature. Alternatively, the samples were incubated for several hours at 16°C.

For blunt-end ligations, the reaction conditions were modified as follows:

Linearized vector DNA	50-150 ng
Insert DNA (molar ratio over vector)	5:1
T4 DNA ligase buffer (10X)	2 µl
50% PEG 4000 solution	2 µl
T4 DNA ligase	5 U
H_2O	*ad* 20 µl

The ligation mixture was incubated for several hours at 4°C.

5.2.2.4. Transformation and Cultivation of *E. coli*

Chemically competent *E. coli* XL1-Blue cells were transformed by the heat-shock method. To this end, 50 µl of cell suspension was thawed on ice and mixed with 10 µl of the ligation reaction (5.2.2.3). After 20 min on ice, the cells were incubated for 1 min at 42°C, followed by additional 5 min on ice. Depending on the antibiotic resistance encoded on the plasmid for the selection of transformed clones, a recovery phase was performed by adding 800 µl of LB medium (without antibiotics) to the transformation reaction. Cells were incubated for 30 min at 37°C and shaking. The bacteria were then centrifuged at 5,000 rcf for 1 min and resuspended in 50 µl of LB medium. In case of selection with ampicillin (Amp), the recovery phase was omitted. The bacteria were finally plated on LB-Agar plates containing an appropriate selection antibiotic and the plates were incubated overnight at 37°C.
The following day, single clones were inoculated into 5 ml LB medium and were incubated shaking overnight at 37°C.

LB medium: 1% (w/v) tryptone; 1% (w/v) NaCl; 0.5% (w/v) yeast extract

LB-Agar plates were composed of LB-medium containing 1.5% (w/v) agar.
The following antibiotics were added to the LB medium depending on the backbone of the plasmid used for transformation:

100 µg/ml Amp: pGEX-4T-1, pGEX-6P-1, pMA-T pMIR-RNL-TK and VP5
50 µg/ml Kanamycin: pSUPER

5.2.2.5. Extraction of Plasmid DNA from *E. coli* and Test Digest

A pre-screening of the inoculated clones was performed, in most of the cases, by a test digest of the plasmid DNA which was extracted by an alkaline treatment of the bacterial pellet obtained from 2 ml of an overnight culture (5.2.2.4). To this end, cells were resuspended in 40 µl Easy Prep buffer and heated for 1 min at 95°C. Following 1 min incubation on ice, the lysates were cleared by 15 min centrifugation at maximal speed. Test digestions were performed by incubating 5 µl of the lysate in a reaction mixture containing 5.8 µl H_2O, 1.2 µl 10X FastDigest™ buffer green (Thermo Fisher Scientific Inc.) and 0.1 µl of the desired Fast-Digest restriction enzyme(s).

Easy Prep buffer: 10 mM Tris (pH 8.0); 1 mM EDTA; 15% (w/v) saccharose; 2 mg/ml lysozyme; 0.2 mg/ml RNase A; 0.1 mg/ml BSA

The plasmid DNA of positive clones was extracted from the remaining overnight cultures with the NucleoSpin®-Plasmid kit (MACHEREY-NAGEL GmbH & Co. KG) according to the manufacturer's instructions. The plasmid DNA of all newly generated plasmids was submitted to sequencing (5.2.2.7).
If required, larger amounts of plasmid DNA were recovered from 150-200 ml overnight cultures with the NucleoBond®-Xtra-Midi kit (MACHEREY-NAGEL GmbH & Co. KG).

5.2.2.6. Mutagenesis PCR

Mutations of target constructs were generated by subcloning the sequence of interest into the pGEM®-T Easy vector (Promega Corporation), mutagenesis PCR and re-insertion of the mutated constructs into the target vectors. A brief overview of the mutagenesis strategy is given in Table 5.17 for the respective plasmids.
In more detail, the sequence of interest was amplified from the original plasmids with the Phusion™ High-Fidelity (HF) DNA Polymerase (Thermo Fisher Scientific Inc.), which generates blunt-ended amplification products. However, subcloning into the pGEM®-T Easy vector requires 3' A-overhangs, which were added by the following tailing reaction with:

Gel-purified PCR product	6.7 µl
Taq Buffer with $(NH_4)_2SO_4$ (10X)	1 µl
$MgCl_2$ (25 mM)	0.8 µl
dATP (2 mM)	2 µl
Taq DNA Polymerase (recombinant) (5U/µl) (Thermo Fisher Scientific Inc.)	0.5 µl

The mixture was incubated at 72°C for 30 min and directly purified with the NucleoSpin®-Extract kit (MACHEREY-NAGEL GmbH & Co. KG). Subcloning was performed with the pGEM®-T Easy Vector Sytsem (Promega Corporation), according to the manufacturer's instructions. Following transformation of *E. coli* (5.2.2.4), the cell suspension was plated on LB_{Amp} plates supplemented with 40 µl of X-Gal solution (50 mg/ml dissolved in DMF) and 2 µl of IPTG (1M). This procedure allowed for the selection of recombinants by blue/white screening. The plasmid DNA of a positive clone

was used for mutagenesis PCR with the primers indicated in Table 5.14. The PCR amplification conditions differed from the method described in 5.2.1.2 inasmuch as 50 ng plasmid DNA and half of the amount of primers were used and only 25 amplification cycles were performed. The PCR reaction was purified with the NucleoSpin®-Extract kit (MACHEREY-NAGEL GmbH & Co. KG) and a restriction digest with the Dpn I enzyme allowed for the selective degradation of the template plasmid DNA. Following heat-inactivation of the enzyme for 5 min at 80°C *E. coli* cells were transformed with the reaction mixture (5.2.2.4). Positive clones were then screened by sequencing. Correctly mutated fragments were re-inserted into the destination vector either by PCR amplification, or, directly via restriction digest of the pGEM plasmids with the indicated enzymes.

5.2.2.7. Sequencing of Plasmid DNA

Sequencing of plasmid DNA was performed by GATC Biotech AG (Konstanz, Germany) or Macrogen Inc. Europe (Amsterdam, Netherlands). The sample submission was prepared according to the company's guideline. The sequencing primers used are listed Table 5.15.

5.2.3. RNA-based Methods

5.2.3.1. Isolation of RNA

RNA was extracted with the TRIzol Reagent (Thermo Fisher Scientific Inc.) which was directly applied to cells previously washed with ice cold PBS. Total RNA from Jiyoye and U2932 EBV-positive cells was isolated from lysates.

5.2.3.2. CDNA Synthesis and Quantitative Real-time PCR (qPCR)

CDNA synthesis was carried out using 1 µg of total RNA and random hexamer primers with the First Strand cDNA Synthesis Kit (Thermo Fisher Scientific Inc.), according to the manufacturer's instructions. The cDNA was diluted 1:10 and 2 µl per sample were mixed with 10 pmol each of forward and reverse primer and 10 µL of SsoFast™ EvaGreen® Supermix (Bio-Rad Laboratories Inc.) in a total volume of 20 µL. Measurements were performed on a MyiQ Analyzer (Bio-Rad Laboratories Inc.).

Relative gene expression levels were determined by the $\Delta\Delta C_T$ method. The values were normalized to the expression of the housekeeping gene GAPDH.

5.2.3.3. Denaturing Polyacrylamide Gel Electrophoresis (PAGE)

RNA samples were resolve by PAGE on polyacrylamide (acrylamide/bis-acrylamide 19:1) urea gels (National Diagnostics Inc.), which were prepared according to the manufacturer's instructions. Electrophoresis was performed in 1X TBE and gels were pre-run for approximately 20 min until they were hand-warm. Samples were mixed with equal amounts of 2X RNA loading dye and were heated at 95°C for 2-3 min before being loaded into the freshly rinsed wells.

RNA loading dye (2X): 0.025% (w/v) bromophenol blue; 0.025% (w/v) xylene cyanol; dissolved in deionized formamide

5.2.3.4. *In vitro* Transcription

In vitro transcriptions were performed from PCR amplified DNA templates or from annealed synthetic oligonucleotides containing the T7 promoter sequence. The sequences of the primers for the PCR amplification of the templates are listed in Table 5.11. For the *in vitro* transcription of pre-tRNA-Ile-TAT-2-3 substrates, PCR amplifications were performed from the pSUPER + pre-tRNA-Ile-TAT-2-3 plasmid using the following primer combinations: tRNA-T7-F and - tRNA-short-end-R for the full-length pre-tRNA, tRNA-mat-T7-F and tRNA-short-end-R for the tRNA-Ile intermediate with 5' mature end and 3' trailer, and tRNA-mat-T7-F and tRNA-short-R-TTTT for the tRNA-Ile intermediate with 5' mature end and 3' trailer terminating on –UUUU-3'. The antisense pre-tRNA-Ile transcript used as Northern blot probe was generated from a PCR product amplified using the primers tRNA-AS-F and 5'- tRNA-short-AS-T7-R. For the *in vitro* transcription of pre-tRNA-Ile-TAT-2-2, PCR amplifications from the pSUPER + pre-tRNA-Ile-TAT-2-2 plasmid were performed using the following primer combinations: tRNA-Ile29-T7-F and tRNA-Ile29-ivt-R for the wildtype pre-tRNA and tRNA-Ile29-T7-F and tRNA-Ile29-ivt-CT for the artificial pre-tRNA terminating on –CU-3'. Pre-miR-27a was *in vitro* transcribed after annealing the oligonucleotide pair pre-miR-27a-T7-S/pre-miR-27a- AS (Table 5.12).

In vitro transcription reactions were carried out using 0.1 mg/ml self-made T7 RNA polymerase in 30 mM Tris (pH 8.0), 25 mM $MgCl_2$, 10 mM each NTP, 2 mM spermidine, 1 mM dithiothreitol (DTT), 0.01% Triton™ X-100 and 2 U/ml thermostable inorganic pyrophosphatase (England Biolabs Inc.) for 4 h at 37°C. *In vitro* transcribed RNAs were purified by PAGE on a 6% polyacrylamide urea gel (see 5.2.3.3) and precipitated. The RNAs were then dissolved in water.

5.2.3.5. ^{32}P-Labeling of Nucleic Acids

DNA oligonucleotides, which were used as Northern blot probes (see 5.2.3.6), were labeled by incubating 20 pmol of the oligonucleotides with 20 µCi of γ-^{32}P-ATP (HARTMANN ANALYTIC GmbH, Braunschweig, Germany) and 0.5 U/µl T4 PNK in 1X PNK buffer A (Thermo Fisher Scientific Inc.) in a total volume of 20 µl. Following 30-60 min incubation at 37°C, the reaction was stopped by adding 30 µl of a 30 mM EDTA solution (pH 8.0). Unincorporated nucleotides were separated on a G-25 column (GE Healthcare) according to the manufacturer's instructions. A custom RNA ladder, consisting of equimolar amounts of synthetic oligoribonucleotides with a length of 19, 21 and 24 nt, was labeled accordingly.

In vitro transcribed RNAs were dephosphorylated prior ^{32}P-labeling by incubating 30 pmol RNA with 0.1 U/mL FastAP thermosensitive alkaline phosphatase (Thermo Fisher Scientific Inc.) in 1X PNK buffer A supplemented with 2 U/µl RiboLock RNase Inhibitor (Thermo Fisher Scientific Inc.). The reaction was carried out for 30 min at 37°C and the enzyme was heat-inactivated for 20 min at 75°C. The ^{32}P-labeling reaction was performed as described above. In case the RNA was intended to be used for EMSAs, the T4 PNK was heat-inactivated for 10 min at 75°C without adding EDTA and subsequently purified with a G-25 column (GE Healthcare).

5.2.3.6. Northern Blot and Determination of Copy Number per Cell

Northern blots were carried out with 5–15 µg of total RNA or RNA isolated from immunoprecipitations. RNAs were separated by denaturing PAGE (see 5.2.3.3). Synthetic ribooligonucleotides with a length of 19, 21 and 24 nt or the *in vitro* transcribed pre-tRNA-Ile (see 5.2.3.4) were labeled with γ-^{32}P-ATP prior to loading and served as size

markers. For the determination of copy number per cell, a dilution series of a synthetic 5' phosphorylated ribooligonucleotide corresponding to the mature miR-1983 sequence (see 5.1.6.1) was loaded in the given amounts.

Samples were mixed with equal amounts of 2X RNA loading dye and the RNA was resolved by PAGE on 12% polyacrylamide urea gels (see 5.2.3.3). After electrophoresis, the RNA was stained with EtBr to ensure equal loading of the lanes and to determine the RNA quality. The RNA was then blotted for 30 min at 20 V onto an Amersham™ Hybond™-N membrane (GE Healthcare) and crosslinked to the membrane for 1 h at 50°C using a crosslinking solution with 1-ethyl-3-(3-dimethylamino-propyl)carbodiimide (EDC) (Pall and Hamilton, 2008). The membrane was incubated overnight at 50°C in hybridization solution with a ^{32}P-labeled oligonucleotide antisense to the small RNA. The membrane was washed twice with wash buffer I, once with wash buffer II and wrapped in saran. For Northern blotting with RNA probes, hybridization and washings were performed at 65°C. Signals were detected by exposure to a storage phosphor screen and scanning with the Personal Molecular Imager™ (Bio-Rad Laboratories Inc.). Before re-probing a membrane, the hybridized oligonucleotide was removed by incubating the membrane twice with a boiling 0.1% SDS solution for at least 10 min. If indicated, signal intensities were quantified from three biological replicates using Quantity One Software (version 4.6.9, Bio-Rad Laboratories Inc.). Error bars display ± standard deviations of the normalized signals.

EDC-crosslinking solution:	188 mg EDC; 61.25 µl 1-methylimidazol; 75 µl HCl (1M); *ad* 6 ml H_2O
Hybridization solution:	5X SSC, 7% SDS, 20 mM sodium phosphate buffer pH 7.2, 1X Denhardt's solution
Wash I solution:	5X SSC; 1% SDS
Wash II solution:	1X SSC; 1% SDS

5.2.3.7. Aminoacylation Assay

Aminoacylation assays were carried out according to (Zaborske et al., 2009) with some modifications. In short, total RNA was extracted with TRIzol (Thermo Fisher Scientific Inc.) performing all steps on ice. Precipitated RNA was dissolved in 10 mM sodium acetate (pH 5.0) for 15 min at 37°C, whereby aminoacylation of tRNAs was preserved. An aliquot of the RNA was then subjected to deacylation by incubation under alkaline

conditions, 200 mM Tris (pH 9.5), for 1 h at 37°C. Acylated and deacylated RNAs were mixed 1:1 with 2X acidic sample loading buffer. Samples were resolved on a 6.5% polyacrylamide urea gel containing 100 mM sodium acetate (pH 5.0) and no TBE. Electrophoresis was carried out overnight at 4°C and 100 V in 100 mM sodium acetate (pH 5.0). All further steps were performed similarly as described in section 5.2.3.6 for Northern blot assays.

Acidic sample RNA loading buffer (2X):
90% deionized formamide; 100 mM sodium acetate (pH 5.0); 0.05% (w/v) bromophenol blue; 0.05% (w/v) xylene cyanol

5.2.3.8. *In silico* RNA Methods

RNA secondary structures were predicted with the mfold web server for nucleic acid folding and hybridization prediction (Zuker, 2003) and possible structures were depicted schematically. The secondary structures of mature tRNAs were drawn according to the predictions deposited in gtRNAdb 2.0 (Chan and Lowe, 2015).

Potential mRNA targets of miR-1983 were predicted by TargetScan Human custom (release 5.2) using the seed sequence of miR-1983 (nts 2-8: UCACCUG) as a query (Friedman et al., 2008).

5.2.4. Biochemical Methods

5.2.4.1. Determination of Protein Concentration

The total protein concentration of cell lysates was determined by diluting 2 µl of the sample in 1 ml of Roti®-Quant solution (Carl Roth GmbH + Co. KG), which allows the quantitation of proteins based on the Bradford method (Bradford, 1976).
The concentration of recombinant proteins was determined with the Nanodrop® ND-1000 spectrophotometer (Thermo Fisher Scientific Inc.) at a wavelength of 280 nm. The values were corrected for a factor determined *in silico* for each protein sequece with the ExPASy ProtParam tool. This factor is based on the calculation of the respective extinction coefficient.

5.2.4.2. SDS- PAGE

Proteins were resolved on 6% (for TNRC6 Western blots) or 10% polyacrylamide gels. Either 50-100 µg total protein from cell lysates or 1/5 aliquots of immunoprecipitaed samples were mixed with Laemmli buffer and incubated at 95°C for 5 min prior loading. Gels were run in SDS-gel running buffer in self-made chambers at a constant voltage (180-200 V) until the bromophenol blue running front reached the bottom of the gel.

Laemmli buffer (4X):	250 mM Tris (pH 6.8); 40% (w/v) glycerol; 8% (w/v) SDS; 20% (v/v) β-mercaptoethanol; 0.025% (w/v) bromophenol blue
Stacking gel:	5% (w/v) acrylamide/bis-acrylamide (37.5:1); 125 mM Tris (pH 6.8) 0.1% (w/v) SDS; 0.15% (v/v) TEMED; 0.05% (w/v) APS
Separating gel:	6-10% (w/v) acrylamide/bis-acrylamide (37.5:1); 380 mM Tris (pH 8.8) 0.1% (w/v) SDS; 0.1% (v/v) TEMED; 0.05% (w/v) APS
SDS-gel running buffer:	25 mM Tris; 0.2 M glycine; 0.1% (w/v) SDS; pH 7.5

5.2.4.3. Coomassie staining

SDS-gels were transferred to a container with Coomassie staining solution, briefly heated in a microwave avoiding boiling, and incubated on a shaker for 30-60 min. The solution was replaced with Coomassie destaining solution, briefly heated and incubated on a shaker for 30-60 min. This procedure was repeated for a second time until the background staining achieved the desired intensity.

Coomassie staining solution:	30% (v/v) ethanol; 10% (v/v) acetic acid; 0.25% (w/v) Coomassie® Brilliant Blue R-250
Coomassie destaining solution:	30% (v/v) ethanol; 10% (v/v) acetic acid

5.2.4.4. Western Blot

Following SDS-PAGE, proteins were transferred by electro-blotting onto a nitrocellulose membrane (Amersham™ Protran™ Premium 0.45 NC, GE Healthcare). Before blotting the gel, the membrane and six Whatman® 3MM blotting papers (GE Healthcare) of the same size of the gel were soaked into transfer buffer. The gel lying on the membrane was enclosed between the blotting papers and assembled in the semid-dry Trans-Blot® SD (Bio-Rad Laboratories Inc.) cell. The transfer was carried out at constant current of 2 mA

per square centimeter of the assembled transfer sandwich.The transfer duration was determined based on the molecular weight of the protein of interest (i.e., 1 min per kDa).

Transfer buffer:	25 mM Tris (pH 8.6); 192 mM glycine; 20% (v/v) methanol
Antibody solution:	5% (w/v) mik; 0.02% (w/v) sodium azide; dissolved in TBS-T

5.2.4.5. Immunoprecipitation, Ago-APP and Isolation of Co-precipitated RNAs

Immunoprecipitations were performed as described in Dueck et al. (2012). In brief, antibodies against the protein of interest were incubated overnight under rotation at 4°C with 40 µl Protein A (for antibodies raised in rabbits) or Protein G (for antibodies raised in rats) Sepharose™ 4 Fast Flow (GE Healthcare) bead slurry. Purified antibodies or sera were diluted as indicated in Table 5.18 in 1 ml PBS. For antibodies produced from monoclonal hybridoma cell lines, 1 ml of the respective cell culture supernatant was used without dilution. Immunoprecipitations of FH-tagged proteins were performed with 30 µl ANTI-FLAG® M2 Affinity Agarose Gel (Sigma-Aldrich Co.).

For each immunoprecipitation reaction, one to three cell culture dishes (150 mm diameter) or ~10^7 Raji cells were lysed on ice in 1.5 ml IP lysis buffer. Lysates were cleared by 30 min full-speed centrifugation at 4°C. Small aliquots were taken, which served as input samples for subsequent Western blot (25 µl) and Northern blot analyses (75 µl). The remaining 1.4 ml lysate was transferred to a fresh tube containining the antibody-coupled beads. In a control reaction, the lysate was incubated with beads only. The mixtures were incubated under constant rotation for 2-3 h at 4°C. In case of immuno-precipitation experiments performed in parallel with samples originating from cells treated differently, the total protein concentration of the lysates was first determined as described in 5.2.4.1. The volumes taken for the input samples were adjusted accordingly, and the different immunoprecipitations were performed from equal amounts of starting material.

Following the incubation at 4°C, the beads were transferred to a fresh reaction tube and they were washed four to five times with ice-cold IP wash buffer, and once with ice-cold PBS. The beads were resuspended in 100 µl PBS and a 20 µl aliquot was taken for Western blot analysis. The remaining beads were collected and they were mixed with 200 µl proteinase K buffer containing 0.2 mg/ml proteinase K (Thermo Fisher Scientific Inc.). Proteins were digested for 30 min at 50°C and the co-precipitated RNA was

extracted with 200 µl Roti®-phenol/chloroform/isoamyl alcohol solution (Carl Roth GmbH + Co. KG). The samples were mixed vigourosly and centrifuged for 10 min at 4°C and 17,000 rcf. The aqueous phase was transferred to a fresh reaction tube and the RNA was precipitated overnight at -20°C by adding 600 µl 100% ethanol and 1 µl glycogen as carrier. The following day, the RNA was collected by full-speed centrifugation at 4°C for at least 30 min, and the pellet was washed once with 80% (v/v) ethanol (pre-cooled at -20°C). The air-dried RNA pellet was finally dissolved in 15 µl H_2O by incubation at 65°C for 5 min and was later analyzed by Northern blotting (5.2.3.6). The RNA was extracted from the input samples using TRIzol Reagent (Thermo Fisher Scientific Inc.) according to the manufacturer's instructions.

For Ago-APPs, 100 mg of the GST-tagged TNRC6B 599-683 peptide (Hauptmann et al., 2015) were coupled to 40 µl Glutathione Sepharose™ 4 Fast Flow (GE Healthcare) beads. Lysate preparation, precipitation of RNA-protein complexes, and RNA extraction from the precipitated samples were carried out as described above for immunoprecipitations.

IP lysis buffer:	25 mM Tris (pH 7.5); 150 mM KCl; 2 mM EDTA; 1 mM NaF; 0.5% (v/v) NP-40 alternative; 1 mM DTT; 0.5 mM AEBSF
IP wash buffer:	50 mM Tris (pH 7.5); 350 mM KCl; 1 mM $MgCl_2$; 0.5% (v/v) NP-40 alternative
Proteinase K buffer:	200 mM Tris (pH 7.5); 300 mM NaCl; 25 mM EDTA; 2% (w/v) SDS

5.2.4.6. Small RNA Cloning and Data Analysis

Ago-associated RNA isolated either by immunoprecipitation or by Ago-APP was ligated to an adenylated 3' DNA adapter using a self-made truncated T4 RNA ligase 2. The ligation of the 5' RNA was performed with T4 RNA ligase 1 (New England Biolabs Inc.). 3 µg of total RNA were used for small RNA cloning from the input samples.

The resulting ligation products were reverse-transcribed using the RT primer the SuperScript™ III First Strand Synthesis Super Mix SuperScript III First Strand Synthesis Super Mix (Thermo Fisher Scientific Inc.), followed by PCR amplification with the primers 5' PCR primer and 3' PCR index primer, wherein index sequences and other Illumina-specific sequences were added. The sequences of the adapters and primers used are indicated in Table 5.6.

The samples were run in 1X TBE buffer on 6% polyacrylamide urea gels (see 5.2.3.3) under non-denaturing conditions. The DNA was stained by incubating the gels for 10 min

in a 1X TBE solution containing 50 µg/ml EtBr. The bands corresponding to PCR amplification products containing miRNA-sized inserts were cut out and eluted overnight in 300 mM NaCl and 2 mM EDTA. The supernatants containing the libraries were collected using Costar® Spin-X® filter tubes (Corning Inc., Corning, USA), precipitated with ethanol overnight at -20 °C, pelleted and dissolved in water.
The quality of the libraries was assessed on an Agilent 2100 Bioanalyzer (Agilent Technologies Inc.) and the libraries were quantified by qPCR measurements. After library pooling, the deep sequencing run was performed on a MiSeq™ platform (Illumina Inc.). The raw data for these experiments can be accessed at the Gene Expression Omnibus (GEO) data repository (Edgar, 2002) under the number GSE76676.

For data analysis, 3' adapters were trimmed using cutadapt, all reads <18 nts and >35 nts, as well as untrimmed reads, were discarded. Reads were collapsed, annotated using custom scripts to the indicated datatypes allowing one mismatch and no insertions/deletions. All reads which mapped to sequences from two or more datatypes (see below) were counted as a separate group. Data were processed similarly for subgroups within the given datatype (e.g. miRNA families, tRNA isotype, etc.). Within subgroups, annotations were counted to single records. The count of reads mapping to ambiguous annotations were split on affected annotations. Reads per million were calculated on valid reads. Plots were drawn with R (library ggplot2). The following databases were used: pre-tRNA: gtRNAdb 2.0 (Chan and Lowe, 2015), sequences were extended by 100 nt genomic sequence at the 5' end and at the 3' end; mature tRNA: sequences from gtRNAdb were processed by removing introns at the indicated splice positions and CCA was added at the 3'end of the sequences; miRNAs: miRBase21 (Kozomara and Griffiths-Jones, 2014) miRNA sequences; sequences for 5S rRNA, U6 snRNA, 7SL RNA, 7SK RNA, Y RNA and BC200 were obtained from the Repeat Masker USCS hg19.rmsk Table browser, status 2015-11; Sequences for snaR, vtRNA and RMRP were obtained from UCSC refGene (hg19).

5.2.4.7. PAR-CLIP Experiments and Data Analysis

PAR-CLIP experiments were performed together with Dr. Yasuhiro Murakawa in the group of Prof. Dr. Markus Landthaler at the Max-Delbrück Center for Molecular Medicine (Berlin, Germany). Stable, inducible FH-Dicer HEK293 cells (Rybak-Wolf et

al., 2014) were transfected with siRNAs against La or control siRNAs and were harvested after 4 days. Induction of protein expression with 1 µg/ml doxycycline and labeling with 100 µM 4SU was performed 9-12 h before crosslinking. Cells were treated additionally with 100 µM 4SU (Sigma-Aldrich Co.) 4 h before crosslinking. All subsequent steps were performed as described in (Rybak-Wolf et al., 2014). For generation of small RNA libraries the 3' PAR-CLIP DNA adapter and the 5' PAR-CLIP RNA adapter (Table 5.6) were used. Libraries were sequenced on a HighSeq™2000 platform (Illumina Inc.) at the Max-Delbrück Center for Molecular Medicine (Berlin, Germany). The raw data can be accessed at GEO data repository (Edgar, 2002) under the number GSE77897.

Data analysis of PAR-CLIP experiments was performed by Dr. Filippos Klironomos in the group of Prof. Dr. Nikolaus Rajewsky at the Max-Delbrück Center for Molecular Medicine (Berlin, Germany). The 5' end as well as 3' end adapters were trimmed from sequenced reads using flexbar (v2.5) (Dodt et al., 2012). Reads were then collapsed so that PCR amplification biases could be eliminated. Consequently, the random 4mers at the 5' and 3' ends of the collapsed reads were trimmed and the resulting reads were mapped against the hg19 genome using bwa mem (v0.7.12-r1039) (Li and Durbin, 2010). A custom script identified aligned reads with at least one RNA T:C. The overlaps with annotated tRNAs of reads with at least one RNA T:C transition, were counted using the GenomicAlignment Bioconductor package (Lawrence et al., 2013). Differential expression of tRNAs based on those counts was done using the DESeq2 Bioconductor package (Love et al., 2014).

5.2.4.8. Dicer Cleavage Assay

HEK293 cells were transfected with plasmids for FH-Dicer overexpression and anti-FLAG immunoprecipitations were performed. After washing, beads were resuspended in Dicer cleavage buffer and ~50 fmol *in vitro* transcribed RNA was added. Samples were incubated for 30-60 min at 37°C under constant agitation. Subsequently, proteins were digested with proteinase K and the RNA was extracted as described in 5.2.4.5.

Dicer cleavage buffer: PBS supplemented with 7.5 mM $MgCl_2$, 5 mM ATP;
1 U/µl RiboLock RNase Inhibitor (Thermo Fisher Scientific Inc.)

5.2.4.9. Expression and Purification of Recombinant Proteins

Expression of proteins was performed in the *E. coli* strain BL21 [DE3]. All purification steps were performed at 4°C.

Recombinant La protein used for the generation of anti-La antibodies was expressed from the pGEX-6P-1 + La WT plasmid. Cells were grown at 37°C to an OD_{600} of 0.6 and protein expression was induced by the addition of 1 mM IPTG. Cells were grown overnight at 18 °C under constant agitation. The lysis occurred in 1X PBS supplemented with 1M NaCl, 1 mg/ml lysozyme, 1 mM AEBSF, 1 mM DTT and 5 U/ml Benzonase® nuclease (Merck KGaA). Following washing with lysis buffer, bound proteins were eluted with 20 mM glutathione dissolved in PBS (pH 7.5). The pGEX-6P-1 + La WT plasmid contains a cleavage site for the PreScission protease between the GST-tag and the La protein. Thus, self-made, GST-tagged PreScission protease and 1 mM DTT were added to the eluate, while dialyzing overnight against PBS. The following day, the mixture was used for a second affinity purification on a GSTrap™ FF column (GE Healthcare) to get rid of the cleaved tag and of the GST-tagged protease. The flowthrough was pooled and concentrated by ultrafiltration with Vivaspin® 20 centrifugal concentrators (Sartorius AG, Göttingen, Germany). Glycerol was added to 5% and the samples were flash-frozen in liquid nitrogen and stored at -80°C.

Recombinant GST-tagged La protein variants used for EMSA assays were expressed from pGEX-4T-1 plasmids. Pelleted cells were resuspended in lysis buffer supplemented with 1 mg/ml lysozyme, 1 mM AEBSF, 1 mM DTT and 5 U/ml Benzonase® nuclease (Merck KGaA). Sonication occurred subsequently. The supernatant obtained after centrifugation (48,000 rcf for 40 min at 4°C) was filtered and loaded on a 5 ml GSTrap™ FF column (GE Healthcare) equilibrated with lysis buffer. The column was washed with 7 column volumes (cv) of wash buffer and bound proteins were eluted with elution buffer. GST fusion protein containing fractions were pooled and applied to a Hiprep™ 26/10 Desalting column (GE Healthcare), exchanging the buffer to buffer A. After desalting, anionic exchange chromatography was performed on a 6 ml RESOURCE™ Q column (GE Healthcare), eluting in a linear gradient over 20 cv from 0% to 50% buffer B. Fractions containing GST fusion proteins were pooled, glycerol was added to a final concentration of 5% and samples were flash-frozen in liquid nitrogen and stored at -80°C.

Lysis buffer:	50 mM Tris (pH 7.5); 1 M NaCl; 10 mM $MgCl_2$
Elution buffer:	50 mM Tris (pH 7.5); 1 M NaCl; 10 mM $MgCl_2$; 20 mM gluthathione
Wash buffer:	50 mM Tris (pH 7.5); 300 mM NaCl; 10 mM $MgCl_2$; 1 mM DTT
Buffer A:	20 mM Tris (pH 7.5); 50 mM NaCl; 1 mM DTT
Buffer B:	20 mM Tris (pH 7.5); 2 M NaCl; 1 mM DTT

5.2.4.10. Generation and Purification of Polyclonal Antibodies

The polyclonal anti-La antibody was generated by the company Eurogentec SA (Seraing, Belgium) with a protocol consisting of four immunizations with 100 µg recombinant La protein each.

Antibodies were affinity purified from 10 ml rabbit serum. All steps were performed at 4°C if not stated otherwise. First of all, 20 mg recombinant La protein were dialyzed overnight against coupling buffer. The following day, 300 mg CNBr-activated Sepharose™ 4 Fast Flow (GE Healthcare) beads were swollen for 30 min in 1 M HCl and were then transferred to a gravity flow Poly-Prep® column (Bio-Rad Laboratories Inc.). The beads were washed with 15 ml 1 mM HCl before equilibration of the column with coupling buffer. Recombinant La protein was added in 6.5 ml coupling buffer, the column was sealed and incubated overnight under constant rotation. The coupled matrix was washed with 6.5 ml coupling buffer and the sealed column was incubated with 6.5 ml of 1 M ethanolamine (pH 8.0) solution under constant rotation for 2 h at room temperature. By that, any unreacted site of the matrix was blocked. The column was then washed eigth times alternating wash buffer 1 and wash buffer 2 (2.5 ml each) and an additional time with 10 ml PBS. The serum of a rabbit immunized with recombinant La protein was added and the sealed column was incubated overnight under constant rotation. The following day, the matrix was washed with 10 ml PBS and the antibodies were eluted with 10 ml 100 mM glycine (pH 2.3). Approximately 1 ml fractions were collected in separate reactions tubes containing 100 µl Tris (pH 8.8), for neutralization, and, 65 µl 100% glycerol to preserve the antibodies during flash-freezing in liquid nitrogen. The purified anti-La antibody used in this study was derived from the most concentrated, first fraction.

Coupling buffer:	0.1 M $NaHCO_3$ (pH 8.3); 0.5 M NaCl
Wash buffer 1:	0.1 M sodium acetate (pH 3-4); 0.5 M NaCl
Wash buffer 2:	0.1 M Tris (pH 8-9); 0.5 M NaCl

5.2.4.11. EMSA

EMSAs were performed according to Bayfield and Maraia (2009) with some modifications. In short, 500 pmol ^{32}P-labeled RNA were incubated in EMSA buffer with various amounts of recombinant GST-La proteins at 37°C for 30 min and were then cooled on ice for 20 min. Complexes were resolved on 8% native polyacrylamide gels. Electrophoresis was carried out overnight at 4°C and 50 V in 0.5X TB buffer. Gels were dried and signals were detected using the Personal Molecular Imager™ System (Bio-Rad Laboratories Inc.).

EMSA buffer:	20 mM Tris (pH 8.0); 100 mM KCl; 1 mM $MgCl_2$; 5 mM β-mercaptoethanol; 5% (v/v) glycerol; 30 mg/ml heparin
Native gel:	0.5X TB with 8% (w/v) acrylamide/bis-acrylamide (37.5:1); 5% (v/v) glycerol; 0.1% (v/v) TEMED; 0.05% (w/v) APS

5.2.5. Cell Culture Methods

Cells were grown in a humidified incubator at 37°C (atmosphere 95 % air, 5 % CO_2). All media were supplemented with 10% fetal bovine serum (Thermo Fisher Scientific Inc.), 100 U/ml penicillin (Sigma-Aldrich Co.), and 100 mg/ml streptomycin (Sigma-Aldrich Co.). An overview of the cell lines and of the respective media used for their cultivation is given in section 5.1.9.2.

5.2.5.1. Transfection of Mammalian Cells

The siRNA pairs indicated in Table 5.7 were annealed by heating a 20 µM stock solution for 5 min at 95°C and immediately transferring the mixture to 37°C for 30 min. For knockdown experiments, cells were reverse transfected with Lipofectamine™ RNAiMax (Thermo Fisher Scientific Inc.) according to the manufacturer's instructions using 40 nM siRNA. Cells were expanded after 2 days and harvested at day 4 post-transfection.
If not stated otherwise, transfections were performed in 6-well format using 3.5 µg plasmid DNA and Lipofectamine™ 2000 (Thermo Fisher Scientific Inc.) according to the manufacturer's instructions.

For immunoprecipitations of overexpressed proteins, HEK293 cells were plated and transfected 3-4 h later with the calcium phosphate method. For each cell culture dish cell culture dish with a diameter of 150 mm, 10 µg of plasmid DNA were mixed with 1 ml 250 mM $CaCl_2$ solution which was then added dropwise to 1 ml 2X HEPES buffered saline. Following a short incubation time at room temperature, the mixture containing calcium phosphate-DNA precipitates was added dropwise to the cell culture dishes. Cells were harvested for experiments after 48 h or 72 h.

2X HEPES buffered saline: 54.6 mM HEPES; 274 mM NaCl; 1.5 mM Na_2HPO_4; (pH 7.1)

5.2.5.2. Dual Luciferase Assay

HEK293 cells were reverse transfected in 48-well plates with pMIR-RL-TK constructs (50 ng/well) and pSUPER constructs (200 ng/well) or miRNA mimic (40 nM/well) using Lipofectamine™ 2000 (Thermo Fisher Scientific Inc.) according to the manufacturer's instructions. Two days after transfection, cells were lysed in 100 µl 1X passive lysis buffer (Promega Corporation) and 15 µl were assayed for firefly activities on a microplate reader Mithras LB 940 (BERTHOLD TECHNOLOGIES GmbH & Co. KG).
All samples were assayed in four replicates. Firefly/renilla luminescence ratios for individual samples were normalized to corresponding ratios of the empty pMIR-RL-TK plasmid and control pSUPER construct/control miRNA mimic transfected samples. Experiments were performed in three biological replicates and the mean values and standard deviations of the normalized firefly/renilla luminescence ratios were calculated from all biological replicates. Error bars display ± standard deviations.

Firefly luciferase buffer:	20 mM tricine (pH 8.0); 5.3 mM $MgSO_4$; 0.1 mM EDTA; 530 µM ATP; 470 µM D-luciferin; 270 µM coenzyme A
Renilla luciferase buffer:	220 mM potassium phosphate buffer (pH 5.0); 1.1 M NaCl; 2.2 mM EDTA; 1.3 mM sodium azide; 0.44 mg/ml BSA Freshly supplemented with 1.43 µM coelenterazine (from 1000X stock solution dissolved in methanol)

ATP, D-luciferin, coenzyme A and coelenterazine were purchased from PJK GmbH (Kleinblittersdorf, Germany).

6. Contributions

PAR-CLIP experiments were performed together with Dr. Yasuhiro Murakawa in the group of Prof. Dr. Markus Landthaler at the Max-Delbrück Center for Molecular Medicine (Berlin, Germany).

Data analysis of PAR-CLIP experiments was performed by Dr. Filippos Klironomos in the group of Prof. Dr. Nikolaus Rajewsky at the Max-Delbrück Center for Molecular Medicine (Berlin, Germany).

Data analysis of small RNA sequencing data was performed together with Gerhard Lehmann who also created several custom scripts.

Norbert Eichner contributed to the sequencing of small RNA libraires by performing the adenylation of the 3' DNA adapter, the BioAnalyzer and qPCR analyses and by performing the sequencing run on the MiSeq™ platform.

Protein purifications were performed with the support of Dr. Leonhard Jakob.

Prof. Dr. Friedrich A. Grässer (Saarland University Medical School, Homburg/Saar, Germany) kindly provided lysates of the B lymphocyte cell lines Jiyoye and U2932 EBV and contributed to the project with discussions.

The deep-sequencing data presented in this thesis have been deposited in NCBI's GEO data repository (Edgar, 2002) and can be accessed as the SuperSeries GSE77898.

7. Data Publication

Parts of this thesis have been published in the following articles:

Hasler, D., Lehmann, G., Murakawa, Y., Klironomos, F., Jakob, L., Grässer, F.A., Rajewsky, N., Landthaler, M., Meister, G., 2016. The Lupus Autoantigen La Prevents Mis-channeling of tRNA Fragments into the Human MicroRNA Pathway. Mol. Cell 63, 110–124. doi:10.1016/j.molcel.2016.05.026

Hasler, D., Meister, G., 2016. From tRNA to miRNA: RNA-folding contributes to correct entry into noncoding RNA pathways. FEBS Lett. 590, 2354–2363. doi:10.1002/1873-3468.12294

Alles, J., Hasler, D., Kazmi, S., Tesson, M., Hamilton, A., Schlegel, L., Marx, S., Eichner, N., Reinhardt, R., Meister, G., Wilson, J., Grässer, F., 2015. Epstein-Barr Virus EBER Transcripts Affect miRNA-Mediated Regulation of Specific Targets and Are Processed to Small RNA Species. Non-Coding RNA 1, 170–191. doi:10.3390/ncrna1030170

Parts of this thesis have been presented at the following conferences:

4th Biennial Meeting of the LARP Society, Stockton (England)
Title of the presentation: The Lupus Autoantigen La Prevents Mis-channeling of tRNA Fragments into the Human MicroRNA Pathway

RNA 2016, Annual Meeting of the RNA Society, Kyoto (Japan)
Title of the presentation: The Lupus Autoantigen La Prevents Mis-channeling of tRNA Fragments into the Human MicroRNA Pathway

Furthermore, I contributed to the following articles:

Grassmann, F., Schoenberger, P.G.A., Brandl, C., Schick, T., Hasler, D., Meister, G., Fleckenstein, M., Lindner, M., Helbig, H., Fauser, S., Weber, B.H.F., 2014. A Circulating MicroRNA Profile Is Associated with Late-Stage Neovascular Age-Related Macular Degeneration. PLoS One 9, e107461. doi:10.1371/journal.pone.0107461

Hasler, D., Meister, G., 2012. An Argonaute Protein Directs Nuclear Xrn2 Function. Mol. Cell 48, 485–486. doi:10.1016/j.molcel.2012.11.015

8. Abbreviations

A

A	Adenine
AARS	Alanyl-tRNA synthetase
ADP	Adenosine diphosphate
AEBSF	4-(2-aminoethyl)benzenesulfonyl fluoride
Ago	Argonaute
Ago-APP	Ago protein Affinity Purification by Peptides
AIMP1-3	Aminoacyl tRNA synthetase complex-interacting multifunctional protein 1-3
Ala	Alanine
amol	Attomole
AMP	Adenosine monohosphate
Amp	Ampicillin
ANG	Angiogenin
APOER2	Apolipoprotein E receptor 2
APS	Ammonium persulfate
Arg	Arginine
ARS	Aminoacyl-tRNA Synthetase
Asn	Asparagine
Asp	Aspartic acid
ASW	Ashwin
ATP	Adenosine triphosphate
A549	Human lung carcinoma cell line

B

BACH 1/2	BTB Domain And CNC Homolog 1/2
BDP	TFIIIB component B" homolog
BLV	Bovine leukemia virus
bp	Base pair
BRF1/2	TFIIB-related factor 1/2
BSA	Bovine serum albumin

C

C	Cysteine (in protein sequences) / Cytosine (in RNA sequences)
Cbp1	Cytochrome b mRNA processing 1
CCR4-NOT	Carbon catabolite repressor 4-negative on TATA
cDNA	Complementary DNA
CDS	Coding sequence
ChIP	Chromatin immunoprecipitation
CLP1	Cleavage/polyadenylation factor Ia subunit
CPSF-73	Cleavage and polyadenylation specificity factor 73

C-terminus	Carboxyl-terminus
Ctrl	Control
Cys	Cysteine
C7-amino	C7-amino linker ($C_7H_{16}NO_4P$)

D

dATP	Deoxyadenosine triphosphate
DCP2	Decapping protein 2
Dcr	Dicer
DDX1	DEAD-Box Helicase 1
DEAD	Asp-Glu-Ala-Asp
DEDX	Asp-Glu-Asp-Asp/His
Dgcr8	DiGeorge syndrome critical region 8
DLD-1	Human colorectal adenocarcinoma cell line
D. melanogaster	*Drosophila melanogaster*
DMEM	Dulbecco's modified Eagle's medium
DMF	Dimethylformamide
DNA	Desoxyribonucleic acid
DNMT2	DNA methyltransferase 2
dNTP	Deoxynucleoside triphosphate
DSE	Distal sequence element
dT	Deoxythymidine
DTT	Dithiothreitol
DUSP11	Dual specificity phosphatase 11

E

EBER1/2	Epstein-Barr virus encoded RNA 1/2
EBV	Epstein-Barr virus
E. coli	*Escherichia coli*
EDTA	Ethylenediaminetetraacetic acid
eEF1A	Eukaryotic translation elongation factor 1
EF-Tu	Elongation factor thermo unstable
eIF4F	Eukaryotic translation initiation factor 4F
eIF4G	Eukaryotic translation initiation factor 4G
ELAC1/2	ElaC Ribonuclease Z 1/2
EM	Electron microscopy
EMSA	Electromobility shift assay
Endo-siRNA	Endogenous small interfering RNA
EPRS	Glutamyl-prolyl-tRNA synthetase
EtBr	Ethidium bromide

F

FAM98B	Family with sequence similarity 98 member B
fmol	Femtomole
FH	FLAG/HA

G

g	Gram
G	Guanine
GAPDH	Glycerinaldehyd-3-phosphat-dehydrogenase
GEO	Gene Expression Omnibus
Gln	Glutamine
Glu	Glutamic acid
Gly	Glycine
GMP	Guanosine monophosphate
GST	Glutathione-S-transferase
GTP	Guanosine triphosphate
GtRNAdb	Genomic tRNA Database

H

h	hour
HA	Human influenza hemagglutinin
HAC1	Homologous to Atf/Creb1
HEK293	Human embryonic kidney 293
HeLa	Henrietta Lacks
HEPES	4-(2-hydroxyethyl)-1-piperazineethanesulfonic acid
HepG2	Human hepatocellular carcinoma cell line
His	Histidine
Hsp	Heat shock protein
HVS	Herpesvirus saimiri

I

ID	Identification
IE	Intermediate element
Ile	Isoleucine
Inv(dT)	5’-3’ reverse deoxythymidine
IP	Immunoprecipitation
IPTG	Isopropyl β-D-1-thiogalactopyranoside
IRES	Internal ribosomal entry site
i-tRF	Internal tRNA-derived fragment

K

kb	Kilo base pair
kd	Knockdown
kDa	Kilodalton
KSHV	Kaposi’s sarcoma-associated herpesvirus

L

LAM	La motif
LARP	La-related protein
LB	Luria Broth
Let-7	Lethal-7
Leu	Leucine
Lhp1	La homologous protein 1

Los1	Loss of suppression 1
LTR	Long terminal repeat
Lys	Lysine

M

M	Molar
mA	Milliampere
mAB	Monoclonal antibody
MCF-7	Michigan Cancer Foundation - 7 cell line
MEF	Mouse embryonic fibroblast
Met	Methionine
Mex67	Messenger RNA export factor of 67 kDa
mg	Milligramm
µg	Microgramm
MHV68	Murine gammaherpesvirus 68
MID domain	Middle domain
min	Minute
miRBase	MiRNA database
MiRISC	MiRNA-induced silencing complex
MiR-X	MicroRNA-X
MiRNA	MicroRNA
MiRNA*	MicroRNA star
ml	Milliliter
µl	Microliter
mM	Millimolar
µM	Micromolar
Mtr2	Mrna transport 2
mt-tRNA	Mitochondrial tRNA
MuERV-L	Murine endogenous retrovirus-like
Mut	Mutant
m^7G	7-methylguanosine

N

N	Any nucleotide (in Figures and Tables)
ncRNA	Non-coding RNA
nm	Nanometer
N-terminus	Amino-terminus
NS	Not significant
NSun2	NOP2/Sun RNA Methyltransferase Family Member 2
nt	Nucleotide
Ntera2	Human testicular embryonic carcinoma cell line
NXF1	Nuclear export factor 1
NXT1	Nuclear transport factor 2 like export factor 1

O

OCT1	Octapeptidyl aminopeptidase
OD_{600}	Optical density at 600 nm wavelength
OH	Hydroxyl
ORF	Open reading frame

P

pAB	Polyclonal antibody
PACT	Protein activator of interferon induced protein kinase EIF2AK
PAGE	Polyacrylamide gel electrophoresis
PAN2-PAN3	Poly(A)-binding protein-dependent poly(A) ribonuclease 2-3
PAR-CLIP	Photo-activatable ribonucleoside-enhanced crosslinking and Immunoprecipitation
PAZ	PIWI–ARGONAUTE–ZWILLE
PBS	Phosphate buffered saline
PCR	Polymerase chain reaction
PHAX	Phosphorylated adaptor for RNA export
Phe	Phenylalanine
Phos	Phosphate
piRNAs	PIWI-interacting RNAs
PIWI	P-element induced wimpy testis
pmol	picomole
Pol III	RNA Polymerase III
POP4	POP4 homolog, ribonuclease P/MRP
Pre-miRNA	Precursor miRNA
Pre-tRNA	Precursor tRNA
Pri-miRNA	Primary miRNA
Pro	Proline
PSE	Proximal sequence element

Q

qPCR	Quantitative polymerase chain reaction

R

Raji	Human B lymphocyte cell line
RBP	RNA-binding protein
rcf	Relative centrifugal force
Rep	Replicate
RIMS2	Regulating synaptic membrane exocytosis protein 2
RNA	Ribonucleic acid
RNAi	RNA interference
RNase	Ribonuclease
RNP	Ribonucleoprotein
Rny1	Ribonuclease T2
RPPH1	Ribonuclease P RNA component H1
RPS	Ribosomal protein S
RRM	RNA recognition motif
rRNA	Ribosomal RNA
RSV	Respiratory syncytial virus
RTCB	RNA 2’,3’-cyclic phosphate and 5’-OH Ligase
RTD	Rapid tRNA decay
RTRAF	RNA transcription, translation and transport factor (also known as CGI-99)

S

s	second
S. cerevisiae	*Saccharomyces cerevisiae*
SD	Standard deviation
SDS	Sodium dodecyl sulfate
sEBER	Short Epstein-Barr virus encoded RNA
SeC	Selenocysteine
Sen	Splicing endonuclease
Ser	Serine
SHOTRNA	Sex hormone-dependent tRNA-derived RNA
shRNA	Short hairpin RNA
siRNA	Small interfering RNA
SK-N-MC	Human brain neuroepithelioma cell line
$SNAP_c$	Small nuclear RNA-activating protein complex
snaR	Small NF90-associated RNA
snoRNA	Small nucleolar RNA
snRNA	Small nuclear RNA
S. pombe	*Schizosaccharomyces pombe*
sRNA	Small RNA
sRNA-Ile	tRNA-Ile derived small RNA
sRNA-Pro	tRNA-Pro derived small RNA
SSB	Sjögren's syndrome antigen B
SSC	Saline sodium citrate
STAF	Selenocysteine tRNA gene transcription-activating factor
Sup	Suppressor
4SU	4-thiouridine

T

T	Thymine
Taq	*Thermus aquaticus*
TB	Tris-borate
TBE	Tris-borate-EDTA
TBP	TATA box-binding protein
TBS-T	Tris-buffered saline with Tween® 20
TEMED	Tetramethylethylenediamine
TEV	Tobacco etch virus
TFIIB	Transcription factor IIB
TFIIIA	Transcription factor IIIA
TFIIIB	Transcription factor IIIB
TFIIIC	Transcription factor IIIC
Thr	Threonine
tiRNA	TRNA-derived stress-induced small RNA
TNRC6	Trinucleotide repeat-containing 6
Tpt1	TRNA 2'-phosphotransferase 1
TRAMP	Trf4/Air2/Mtr4 polyadenylation
TRBP	Trans-activation responsive RNA-binding protein (also known as TARBP2)
TRDMT1	TRNA aspartic acid methyltransferase 1
tRF	TRNA-derived fragment
Tris	Tris(hydroxymethyl)aminomethane

Trf4	Also known as poly(A) RNA polymerase D7 (PAPD7)
Trl1	TRNA ligase 1
Trp	Tryptophan
tRNA	Transfer RNA
TSEN	TRNA splicing endonuclease
TUTase	Terminal RNA uridylyltransferases
Tyr	Tyrosine

U

U	Unit
U	Uracil
Undet	undetermined
UTR	Untranslated region
UV	Ultraviolet

V

V	Volt
Val	Valine
VA RNA	Virus-associated RNA

W

WB	Western blot
Wt	Wildtype

X

XBP1	X-box binding protein 1
X-Gal	5-bromo-4-chloro-3-indolyl-β-D-galactopyranoside
Xpo1/5	Exportin-1/-5
Xpo-t	Exportin for tRNA
Xrn1/2	5’-3’ exoribonuclease 1/2

Y

YBX1	Y-box binding protein 1
YBX1-tRF	Y-box binding protein 1 interacting tRNA fragment
Ψ	Pseudouridine

Z

ZBTB8O	Zinc finger and BTB domain containing 8 opposite strand

%	Per cent
% v/v	Per cent volume/volume (ml/100 ml)
% w/v	Per cent weight/volume (g/100 ml)

°C	Degree Celsius

9. List of Figures

10. List of Tables

11. References

Abascal-Palacios, G., Ramsay, E.P., Beuron, F., Morris, E., Vannini, A., 2018. Structural basis of RNA polymerase III transcription initiation. Nature 553, 301–306. doi:10.1038/nature25441

Ablasser, A., Bauernfeind, F., Hartmann, G., Latz, E., Fitzgerald, K.A., Hornung, V., 2009. RIG-I-dependent sensing of poly(dA:dT) through the induction of an RNA polymerase III–transcribed RNA intermediate. Nat. Immunol. 10, 1065–1072. doi:10.1038/ni.1779

Akawi, N.A., Ben-Salem, S., Hertecant, J., John, A., Pramathan, T., Kizhakkedath, P., Ali, B.R., Al-Gazali, L., 2016. A homozygous splicing mutation in ELAC2 suggests phenotypic variability including intellectual disability with minimal cardiac involvement. Orphanet J. Rare Dis. 11, 139. doi:10.1186/s13023-016-0526-8

Alexandrov, A., Chernyakov, I., Gu, W., Hiley, S.L., Hughes, T.R., Grayhack, E.J., Phizicky, E.M., 2006. Rapid tRNA Decay Can Result from Lack of Nonessential Modifications. Mol. Cell 21, 87–96. doi:10.1016/j.molcel.2005.10.036

Alfano, C., Sanfelice, D., Babon, J., Kelly, G., Jacks, A., Curry, S., Conte, M.R., 2004. Structural analysis of cooperative RNA binding by the La motif and central RRM domain of human La protein. Nat. Struct. Mol. Biol. 11, 323–9. doi:10.1038/nsmb747

Ali, N., Siddiqui, A., 1997. The La antigen binds 5' noncoding region of the hepatitis C virus RNA in the context of the initiator AUG codon and stimulates internal ribosome entry site-mediated translation. Proc. Natl. Acad. Sci. 94, 2249–54.

Allison, D.S., Hall, B.D., 1985. Effects of alterations in the 3' flanking sequence on in vivo and in vitro expression of the yeast SUP4-o tRNATyr gene. EMBO J. 4, 2657–64.

Andersen, G.R., Pedersen, L., Valente, L., Chatterjee, I., Kinzy, T.G., Kjeldgaard, M., Nyborg, J., 2000. Structural Basis for Nucleotide Exchange and Competition with tRNA in the Yeast Elongation Factor Complex eEF1A:eEF1Bα. Mol. Cell 6, 1261–1266. doi:10.1016/S1097-2765(00)00122-2

Anderson, J., Phan, L., Cuesta, R., Carlson, B.A., Pak, M., Asano, K., Björk, G.R., Tamame, M., Hinnebusch, A.G., 1998. The essential Gcd10p-Gcd14p nuclear complex is required for 1-methyladenosine modification and maturation of initiator methionyl-tRNA. Genes Dev. 12, 3650–62.

Aravind, L., Koonin, E. V, 1999. DNA polymerase beta-like nucleotidyltransferase superfamily: identification of three new families, classification and evolutionary history. Nucleic Acids Res. 27, 1609–18.

Arimbasseri, A.G., Kassavetis, G.A., Maraia, R.J., 2014. Comment on "Mechanism of eukaryotic RNA polymerase III transcription termination." Science (80-.). 345,

524–524. doi:10.1126/science.1253783

Arimbasseri, A.G., Maraia, R.J., 2015. Mechanism of Transcription Termination by RNA Polymerase III Utilizes a Non-template Strand Sequence-Specific Signal Element. Mol. Cell 58, 1124–1132. doi:10.1016/j.molcel.2015.04.002

Arimbasseri, A.G., Maraia, R.J., 2013. Distinguishing core and holoenzyme mechanisms of transcription termination by RNA polymerase III. Mol. Cell. Biol. 33, 1571–81. doi:10.1128/MCB.01733-12

Arimbasseri, A.G., Rijal, K., Maraia, R.J., 2013. Transcription termination by the eukaryotic RNA polymerase III. Biochim. Biophys. Acta - Gene Regul. Mech. 1829, 318–330. doi:10.1016/j.bbagrm.2012.10.006

Arts, G.J., Fornerod, M., Mattaj, I.W., 1998a. Identification of a nuclear export receptor for tRNA. Curr. Biol. 8, 305–14.

Arts, G.J., Kuersten, S., Romby, P., Ehresmann, B., Mattaj, I.W., 1998b. The role of exportin-t in selective nuclear export of mature tRNAs. EMBO J. 17, 7430–41. doi:10.1093/emboj/17.24.7430

Babiarz, J.E., Hsu, R., Melton, C., Thomas, M., Ullian, E.M., Blelloch, R., 2011. A role for noncanonical microRNAs in the mammalian brain revealed by phenotypic differences in Dgcr8 versus Dicer1 knockouts and small RNA sequencing. RNA 17, 1489–501. doi:10.1261/rna.2442211

Babiarz, J.E., Ruby, J.G., Wang, Y., Bartel, D.P., Blelloch, R., 2008. Mouse ES cells express endogenous shRNAs, siRNAs, and other Microprocessor-independent, Dicer-dependent small RNAs. Genes Dev. 22, 2773–2785. doi:10.1101/gad.1705308

Baldi, M.I., Mattoccia, E., Bufardeci, E., Fabbri, S., Tocchini-Valentini, G.P., 1992. Participation of the intron in the reaction catalyzed by the Xenopus tRNA splicing endonuclease. Science 255, 1404–8.

Baldwin, A.N., Berg, P., 1966. Transfer Ribonucleic Acid-induced Hydrolysis of Valyladenylate Bound to Isoleucyl Ribonucleic Acid Synthetase. J. Biol. Chem. 241, 839–845.

Balzi, E., Choder, M., Chen, W.N., Varshavsky, A., Goffeau, A., 1990. Cloning and functional analysis of the arginyl-tRNA-protein transferase gene ATE1 of Saccharomyces cerevisiae. J. Biol. Chem. 265, 7464–7471.

Bandyopadhyay, A.K., Deutscher, M.P., 1971. Complex of aminoacyl-transfer RNA synthetases. J. Mol. Biol. 60, 113–22.

Bartel, D.P., 2009. MicroRNAs: target recognition and regulatory functions. Cell 136, 215–33. doi:10.1016/j.cell.2009.01.002

Bartel, D.P., 2004. MicroRNAs: genomics, biogenesis, mechanism, and function. Cell 116, 281–97.

Bayfield, M. a, Maraia, R.J., 2009. Precursor-product discrimination by La protein during tRNA metabolism. Nat. Struct. Mol. Biol. 16, 430–7. doi:10.1038/nsmb.1573

Behm-Ansmant, I., Rehwinkel, J., Doerks, T., Stark, A., Bork, P., Izaurralde, E., 2006. mRNA degradation by miRNAs and GW182 requires both CCR4:NOT deadenylase and DCP1:DCP2 decapping complexes. Genes Dev. 20, 1885–98. doi:10.1101/gad.1424106

Beitzinger, M., Peters, L., Zhu, J.Y., Kremmer, E., Meister, G., 2007. Identification of Human microRNA Targets From Isolated Argonaute Protein Complexes. RNA Biol. 4, 76–84. doi:10.4161/rna.4.2.4640

Belfort, M., Weiner, A., 1997. Another bridge between kingdoms: tRNA splicing in archaea and eukaryotes. Cell 89, 1003–6. doi:10.1016/S0092-8674(00)80287-1

Belisova, A., Semrad, K., Mayer, O., Kocian, G., Waigmann, E., Schroeder, R., Steiner, G., 2005. RNA chaperone activity of protein components of human Ro RNPs. RNA 11, 1084–1094. doi:10.1261/rna.7263905

Berezikov, E., Chung, W.-J., Willis, J., Cuppen, E., Lai, E.C., 2007. Mammalian Mirtron Genes. Mol. Cell 28, 328–336. doi:10.1016/j.molcel.2007.09.028

Betat, H., Mörl, M., 2015. The CCA-adding enzyme: A central scrutinizer in tRNA quality control. BioEssays 37, 975–982. doi:10.1002/bies.201500043

Bevilacqua, E., Wang, X., Majumder, M., Gaccioli, F., Yuan, C.L., Wang, C., Zhu, X., Jordan, L.E., Scheuner, D., Kaufman, R.J., Koromilas, A.E., Snider, M.D., Holcik, M., Hatzoglou, M., 2010. eIF2α Phosphorylation Tips the Balance to Apoptosis during Osmotic Stress. J. Biol. Chem. 285, 17098–17111. doi:10.1074/jbc.M110.109439

Bissels, U., Wild, S., Tomiuk, S., Holste, A., Hafner, M., Tuschl, T., Bosio, A., 2009. Absolute quantification of microRNAs by using a universal reference. RNA 15, 2375–2384. doi:10.1261/rna.1754109

Bitko, V., Musiyenko, A., Bayfield, M.A., Maraia, R.J., Barik, S., 2008. Cellular La Protein Shields Nonsegmented Negative-Strand RNA Viral Leader RNA from RIG-I and Enhances Virus Growth by Diverse Mechanisms. J. Virol. 82, 7977–7987. doi:10.1128/JVI.02762-07

Björk, G.R., Huang, B., Persson, O.P., Byström, A.S., 2007. A conserved modified wobble nucleoside (mcm5s2U) in lysyl-tRNA is required for viability in yeast. RNA 13, 1245–55. doi:10.1261/rna.558707

Björk, G.R., Jacobsson, K., Nilsson, K., Johansson, M.J., Byström, A.S., Persson, O.P., 2001. A primordial tRNA modification required for the evolution of life? EMBO J. 20, 231–9. doi:10.1093/emboj/20.1.231

Blanco, S., Dietmann, S., Flores, J. V, Hussain, S., Kutter, C., Humphreys, P., Lukk, M., Lombard, P., Treps, L., Popis, M., Kellner, S., Hölter, S.M., Garrett, L., Wurst, W., Becker, L., Klopstock, T., Fuchs, H., Gailus-Durner, V., Hrabě de Angelis, M., Káradóttir, R.T., Helm, M., Ule, J., Gleeson, J.G., Odom, D.T., Frye, M., 2014. Aberrant methylation of tRNAs links cellular stress to neuro-developmental disorders. EMBO J. 33, 1–20. doi:10.15252/embj.201489282

Bogenhagen, D.F., Brown, D.D., 1981. Nucleotide sequences in Xenopus 5S DNA required for transcription termination. Cell 24, 261–70.

Bogerd, H.P., Karnowski, H.W., Cai, X., Shin, J., Pohlers, M., Cullen, B.R., 2010. A mammalian herpesvirus uses noncanonical expression and processing mechanisms to generate viral MicroRNAs. Mol. Cell 37, 135–42. doi:10.1016/j.molcel.2009.12.016

Bohnsack, M.T., Czaplinski, K., Gorlich, D., 2004. Exportin 5 is a RanGTP-dependent dsRNA-binding protein that mediates nuclear export of pre-miRNAs. RNA 10, 185–91. doi:14730017

Bohnsack, M.T., Regener, K., Schwappach, B., Saffrich, R., Paraskeva, E., Hartmann, E., Görlich, D., 2002. Exp5 exports eEF1A via tRNA from nuclei and synergizes with other transport pathways to confine translation to the cytoplasm. EMBO J. 21, 6205–6215. doi:10.1093/emboj/cdf613

Bradford, M.M., 1976. A rapid and sensitive method for the quantitation of microgram quantities of protein utilizing the principle of protein-dye binding. Anal. Biochem. 72, 248–254. doi:10.1016/0003-2697(76)90527-3

Brownawell, A.M., Macara, I.G., 2002. Exportin-5, a novel karyopherin, mediates nuclear export of double-stranded RNA binding proteins. J. Cell Biol. 156, 53–64. doi:10.1083/jcb.200110082

Brzezniak, L.K., Bijata, M., Szczesny, R.J., Stepien, P.P., 2011. Involvement of human ELAC2 gene product in 3' end processing of mitochondrial tRNAs. RNA Biol. 8, 616–626. doi:10.4161/rna.8.4.15393

Burke, J.M., Bass, C.R., Kincaid, R.P., Sullivan, C.S., 2014. Identification of triphosphatase activity in the biogenesis of retroviral microRNAs and RNAP III-generated shRNAs. Nucleic Acids Res. 42, 13949–13962. doi:10.1093/nar/gku1247

Burke, J.M., Kincaid, R.P., Nottingham, R.M., Lambowitz, A.M., Sullivan, C.S., 2016. DUSP11 activity on triphosphorylated transcripts promotes Argonaute association with noncanonical viral microRNAs and regulates steady-state levels of cellular noncoding RNAs. Genes Dev. 30, 2076–2092. doi:10.1101/gad.282616.116

Burroughs, A.M., Ando, Y., de Hoon, M.L.J.L., Tomaru, Y., Suzuki, H., Hayashizaki, Y., Daub, C.O., 2011. Deep-sequencing of human Argonaute-associated small RNAs provides insight into miRNA sorting and reveals Argonaute association with RNA fragments of diverse origin. RNA Biol. 8, 158–177. doi:10.4161/rna.8.1.14300

Cabarcas, S., Schramm, L., 2011. RNA polymerase III transcription in cancer: the BRF2 connection. Mol. Cancer 10, 47. doi:10.1186/1476-4598-10-47

Calado, A., Treichel, N., Müller, E.-C.C., Otto, A., Kutay, U., 2002. Exportin-5-mediated nuclear export of eukaryotic elongation factor 1A and tRNA. EMBO J. 21, 6216–24. doi:10.1093/emboj/cdf620

Calvo, O., Cuesta, R., Anderson, J., Gutiérrez, N., García-Barrio, M.T., Hinnebusch, A.G., Tamame, M., 1999. GCD14p, a Repressor of GCN4 Translation, Cooperates with Gcd10p and Lhp1p in the Maturation of Initiator Methionyl-tRNA in Saccharomyces cerevisiae. Mol. Cell. Biol. 19, 4167–4181. doi:10.1128/MCB.19.6.4167

Canella, D., Praz, V., Reina, J.H., Cousin, P., Hernandez, N., 2010. Defining the RNA polymerase III transcriptome: Genome-wide localization of the RNA polymerase III transcription machinery in human cells. Genome Res. 20, 710–21. doi:10.1101/gr.101337.109

Cazalla, D., Xie, M., Steitz, J. a, 2011. A primate herpesvirus uses the integrator complex to generate viral microRNAs. Mol. Cell 43, 982–92. doi:10.1016/j.molcel.2011.07.025

Cerini, C., Kerjan, P., Astier, M., Gratecos, D., Mirande, M., Sémériva, M., 1991. A component of the multisynthetase complex is a multifunctional aminoacyl-tRNA synthetase. EMBO J. 10, 4267–77.

Chakravarty, A.K., Smith, P., Jalan, R., Shuman, S., 2014. Structure, Mechanism, and Specificity of a Eukaryal tRNA Restriction Enzyme Involved in Self-Nonself Discrimination. Cell Rep. 7, 339–347. doi:10.1016/j.celrep.2014.03.034

Chakshusmathi, G., Kim, S. Do, Rubinson, D.A., Wolin, S.L., 2003. A La protein requirement for efficient pre-tRNA folding. EMBO J. 22, 6562–72. doi:10.1093/emboj/cdg625

Chamberlain, J.R., Lee, Y., Lane, W.S., Engelke, D.R., 1998. Purification and characterization of the nuclear RNase P holoenzyme complex reveals extensive subunit overlap with RNase MRP. Genes Dev. 12, 1678–90. doi:10.1101/gad.12.11.1678

Chan, C.T.Y., Dyavaiah, M., DeMott, M.S., Taghizadeh, K., Dedon, P.C., Begley, T.J., 2010. A Quantitative Systems Approach Reveals Dynamic Control of tRNA Modifications during Cellular Stress. PLoS Genet. 6, e1001247. doi:10.1371/journal.pgen.1001247

Chan, P.P., Lowe, T.M., 2015. GtRNAdb 2.0: an expanded database of transfer RNA genes identified in complete and draft genomes. Nucleic Acids Res. 44, D184-189. doi:10.1093/nar/gkv1309

Cheloufi, S., Dos Santos, C.O., Chong, M.M.W., Hannon, G.J., 2010. A dicer-independent miRNA biogenesis pathway that requires Ago catalysis. Nature 465, 584–589. doi:10.1038/nature09092

Chen, C.-J., Heard, E., 2013. Small RNAs derived from structural non-coding RNAs. Methods 63, 76–84. doi:10.1016/j.ymeth.2013.05.001

Chen, J.Y., Joyce, P.B., Wolfe, C.L., Steffen, M.C., Martin, N.C., 1992. Cytoplasmic and mitochondrial tRNA nucleotidyltransferase activities are derived from the same gene in the yeast Saccharomyces cerevisiae. J. Biol. Chem. 267, 14879–83.

Chen, Q., Yan, M., Cao, Z., Li, X., Zhang, Y., Shi, J., Feng, G. -h., Peng, H., Zhang, X., Zhang, Y., Qian, J., Duan, E., Zhai, Q., Zhou, Q., 2016. Sperm tsRNAs contribute to intergenerational inheritance of an acquired metabolic disorder. Science (80-.). 351, 397–400. doi:10.1126/science.aad7977

Chen, Y., Boland, A., Kuzuoğlu-Öztürk, D., Bawankar, P., Loh, B., Chang, C.-T., Weichenrieder, O., Izaurralde, E., 2014. A DDX6-CNOT1 Complex and W-Binding Pockets in CNOT9 Reveal Direct Links between miRNA Target Recognition and Silencing. Mol. Cell 54, 737–750. doi:10.1016/j.molcel.2014.03.034

Chernyakov, I., Whipple, J.M., Kotelawala, L., Grayhack, E.J., Phizicky, E.M., 2008. Degradation of several hypomodified mature tRNA species in Saccharomyces cerevisiae is mediated by Met22 and the 5’-3’ exonucleases Rat1 and Xrn1. Genes Dev. 22, 1369–1380. doi:10.1101/gad.1654308

Christie, M., Boland, A., Huntzinger, E., Weichenrieder, O., Izaurralde, E., 2013. Structure of the PAN3 Pseudokinase Reveals the Basis for Interactions with the PAN2 Deadenylase and the GW182 Proteins. Mol. Cell 51, 360–373. doi:10.1016/j.molcel.2013.07.011

Chu, S., Zengel, J.M., Lindahl, L., 1997. A novel protein shared by RNase MRP and RNase P. RNA 3, 382–91.

Cifuentes, D., Xue, H., Taylor, D.W., Patnode, H., Mishima, Y., Cheloufi, S., Ma, E.,

Mane, S., Hannon, G.J., Lawson, N.D., Wolfe, S.A., Giraldez, A.J., 2010. A novel miRNA processing pathway independent of Dicer requires Argonaute2 catalytic activity. Science 328, 1694–8. doi:10.1126/science.1190809

Cirakoglu, B., Mirande, M., Waller, J.P., 1985. A model for the structural organization of aminoacyl-tRNA synthetases in mammalian cells. FEBS Lett. 183, 185–90.

Cole, C., Sobala, A., Lu, C., Thatcher, S.R., Bowman, A., Brown, J.W.S., Green, P.J., Barton, G.J., Hutvagner, G., 2009. Filtering of deep sequencing data reveals the existence of abundant Dicer-dependent small RNAs derived from tRNAs. RNA 15, 2147–60. doi:10.1261/rna.1738409

Cook, A.G., Fukuhara, N., Jinek, M., Conti, E., 2009. Structures of the tRNA export factor in the nuclear and cytosolic states. Nature 461, 60–5. doi:10.1038/nature08394

Copela, L.A., Chakshusmathi, G., Sherrer, R.L., Wolin, S.L., 2006. The La protein functions redundantly with tRNA modification enzymes to ensure tRNA structural stability. RNA 12, 644–54. doi:10.1261/rna.2307206

Copela, L.A., Fernandez, C.F., Sherrer, R.L., Wolin, S.L., 2008. Competition between the Rex1 exonuclease and the La protein affects both Trf4p-mediated RNA quality control and pre-tRNA maturation. RNA 14, 1214–1227. doi:10.1261/rna.1050408

Costa-Mattioli, M., Svitkin, Y., Sonenberg, N., 2004. La Autoantigen Is Necessary for Optimal Function of the Poliovirus and Hepatitis C Virus Internal Ribosome Entry Site In Vivo and In Vitro. Mol. Cell. Biol. 24, 6861–6870. doi:10.1128/MCB.24.15.6861-6870.2004

Couvillion, M.T., Bounova, G., Purdom, E., Speed, T.P., Collins, K., 2012. A Tetrahymena Piwi Bound to Mature tRNA 3′ Fragments Activates the Exonuclease Xrn2 for RNA Processing in the Nucleus. Mol. Cell 48, 509–520. doi:10.1016/j.molcel.2012.09.010

Cozen, A.E., Quartley, E., Holmes, A.D., Hrabeta-Robinson, E., Phizicky, E.M., Lowe, T.M., 2015. ARM-seq: AlkB-facilitated RNA methylation sequencing reveals a complex landscape of modified tRNA fragments. Nat. Methods 12, 879–884. doi:10.1038/nmeth.3508

Cozzarelli, N.R., Gerrard, S.P., Schlissel, M., Brown, D.D., Bogenhagen, D.F., 1983. Purified RNA polymerase III accurately and efficiently terminates transcription of 5S RNA genes. Cell 34, 829–35.

Cullen, B.R., Cherry, S., TenOever, B.R., 2013. Is RNA Interference a Physiologically Relevant Innate Antiviral Immune Response in Mammals? Cell Host Microbe 14, 374–378. doi:10.1016/j.chom.2013.09.011

Culver, G.M., McCraith, S.M., Zillmann, M., Kierzek, R., Michaud, N., LaReau, R.D., Turner, D.H., Phizicky, E.M., 1993. An NAD derivative produced during transfer RNA splicing: ADP-ribose 1“-2” cyclic phosphate. Science 261, 206–8.

Czech, A., Wende, S., Mörl, M., Pan, T., Ignatova, Z., 2013. Reversible and Rapid Transfer-RNA Deactivation as a Mechanism of Translational Repression in Stress. PLoS Genet. 9, e1003767. doi:10.1371/journal.pgen.1003767

Czech, B., Hannon, G.J., 2016. One Loop to Rule Them All: The Ping-Pong Cycle and piRNA-Guided Silencing. Trends Biochem. Sci. 41, 324–337. doi:10.1016/j.tibs.2015.12.008

Daniels, C.J., Gupta, R., Doolittle, W.F., 1985. Transcription and excision of a large intron in the tRNATrp gene of an archaebacterium, Halobacterium volcanii. J. Biol. Chem. 260, 3132–4.

Daniels, S.M., Melendez-Peña, C.E., Scarborough, R.J., Daher, A., Christensen, H.S., El Far, M., Purcell, D.F., Lainé, S., Gatignol, A., 2009. Characterization of the TRBP domain required for Dicer interaction and function in RNA interference. BMC Mol. Biol. 10, 38. doi:10.1186/1471-2199-10-38

Daugaard, I., Hansen, T.B., 2017. Biogenesis and Function of Ago-Associated RNAs. Trends Genet. 33, 208–219. doi:10.1016/j.tig.2017.01.003

de la Sierra-Gallay, I.L., Mathy, N., Pellegrini, O., Condon, C., 2006. Structure of the ubiquitous 3' processing enzyme RNase Z bound to transfer RNA. Nat. Struct. Mol. Biol. 13, 376–7. doi:10.1038/nsmb1066

de la Sierra-Gallay, I.L., Pellegrini, O., Condon, C., 2005. Structural basis for substrate binding, cleavage and allostery in the tRNA maturase RNase Z. Nature 433, 657–661. doi:10.1038/nature03284

Deng, J., Ptashkin, R.N., Chen, Y., Cheng, Z., Liu, G., Phan, T., Deng, X., Zhou, J., Lee, I., Lee, Y.S., Bao, X., 2015. Respiratory Syncytial Virus Utilizes a tRNA Fragment to Suppress Antiviral Responses Through a Novel Targeting Mechanism. Mol. Ther. 23, 1622–1629. doi:10.1038/mt.2015.124

Denli, A.M., Tops, B.B.J., Plasterk, R.H.A., Ketting, R.F., Hannon, G.J., 2004. Processing of primary microRNAs by the Microprocessor complex. Nature 432, 231–235. doi:10.1038/nature03049

Deutscher, M.P., 1972. Reactions at the 3' terminus of transfer ribonucleic acid. II. Purification and physical and chemical properties of rabbit liver transfer ribonucleic acid nucleotidyltransferase. J. Biol. Chem. 247, 450–8.

Dewe, J.M., Whipple, J.M., Chernyakov, I., Jaramillo, L.N., Phizicky, E.M., 2012. The yeast rapid tRNA decay pathway competes with elongation factor 1A for substrate tRNAs and acts on tRNAs lacking one or more of several modifications. RNA 18, 1886–1896. doi:10.1261/rna.033654.112

Dhahbi, J.M., Spindler, S.R., Atamna, H., Yamakawa, A., Boffelli, D., Mote, P., Martin, D.I., 2013. 5′ tRNA halves are present as abundant complexes in serum, concentrated in blood cells, and modulated by aging and calorie restriction. BMC Genomics 14, 298. doi:10.1186/1471-2164-14-298

Dhungel, N., Hopper, A.K., 2012. Beyond tRNA cleavage: novel essential function for yeast tRNA splicing endonuclease unrelated to tRNA processing. Genes Dev. 26, 503–14. doi:10.1101/gad.183004.111

Di Nicola Negri, E., Fabbri, S., Bufardeci, E., Baldi, M.I., Gandini Attardi, D., Mattoccia, E., Tocchini-Valentini, G.P., 1997. The eucaryal tRNA splicing endonuclease recognizes a tripartite set of RNA elements. Cell 89, 859–66.

Dichtl, B., Tollervey, D., 1997. Pop3p is essential for the activity of the RNase MRP and RNase P ribonucleoproteins in vivo. EMBO J. 16, 417–29.

Ding, S.-W., Voinnet, O., 2007. Antiviral Immunity Directed by Small RNAs. Cell 130, 413–426. doi:10.1016/j.cell.2007.07.039

Diodato, D., Ghezzi, D., Tiranti, V., 2014. The Mitochondrial Aminoacyl tRNA

Synthetases: Genes and Syndromes. Int. J. Cell Biol. 2014, 787956. doi:10.1155/2014/787956

Dittmar, K. a, Goodenbour, J.M., Pan, T., 2006. Tissue-specific differences in human transfer RNA expression. PLoS Genet. 2, e221. doi:10.1371/journal.pgen.0020221

Dodt, M., Roehr, J., Ahmed, R., Dieterich, C., 2012. FLEXBAR—Flexible Barcode and Adapter Processing for Next-Generation Sequencing Platforms. Biology (Basel). 1, 895–905. doi:10.3390/biology1030895

Domitrovich, A.M., Diebel, K.W., Ali, N., Sarker, S., Siddiqui, A., 2005. Role of La autoantigen and polypyrimidine tract-binding protein in HCV replication. Virology 335, 72–86. doi:10.1016/j.virol.2005.02.009

Dubrovsky, E.B., Dubrovskaya, V.A., Levinger, L., Schiffer, S., Marchfelder, A., 2004. Drosophila RNase Z processes mitochondrial and nuclear pre-tRNA 3' ends in vivo. Nucleic Acids Res. 32, 255–62. doi:10.1093/nar/gkh182

Dueck, A., Ziegler, C., Eichner, A., Berezikov, E., Meister, G., 2012. microRNAs associated with the different human Argonaute proteins. Nucleic Acids Res. 40, 9850–9862. doi:10.1093/nar/gks705

Dupasquier, M., Kim, S., Halkidis, K., Gamper, H., Hou, Y.-M., 2008. tRNA integrity is a prerequisite for rapid CCA addition: implication for quality control. J. Mol. Biol. 379, 579–88. doi:10.1016/j.jmb.2008.04.005

Dutta, T., Malhotra, A., Deutscher, M.P., 2013. How a CCA sequence protects mature tRNAs and tRNA precursors from action of the processing enzyme RNase BN/RNase Z. J. Biol. Chem. 288, 30636–44. doi:10.1074/jbc.M113.514570

Edgar, R., 2002. Gene Expression Omnibus: NCBI gene expression and hybridization array data repository. Nucleic Acids Res. 30, 207–210. doi:10.1093/nar/30.1.207

Eichhorn, S.W., Guo, H., McGeary, S.E., Rodriguez-Mias, R.A., Shin, C., Baek, D., Hsu, S.-H., Ghoshal, K., Villén, J., Bartel, D.P., 2014. mRNA Destabilization Is the Dominant Effect of Mammalian MicroRNAs by the Time Substantial Repression Ensues. Mol. Cell 56, 104–115. doi:10.1016/j.molcel.2014.08.028

El Yacoubi, B., Bailly, M., de Crécy-Lagard, V., 2012. Biosynthesis and Function of Posttranscriptional Modifications of Transfer RNAs. Annu. Rev. Genet. 46, 69–95. doi:10.1146/annurev-genet-110711-155641

El Yacoubi, B., Lyons, B., Cruz, Y., Reddy, R., Nordin, B., Agnelli, F., Williamson, J.R., Schimmel, P., Swairjo, M.A., de Crécy-Lagard, V., 2009. The universal YrdC/Sua5 family is required for the formation of threonylcarbamoyladenosine in tRNA. Nucleic Acids Res. 37, 2894–909. doi:10.1093/nar/gkp152

Elkayam, E., Kuhn, C.-D., Tocilj, A., Haase, A.D., Greene, E.M., Hannon, G.J., Joshua-Tor, L., 2012. The Structure of Human Argonaute-2 in Complex with miR-20a. Cell 150, 100–110. doi:10.1016/j.cell.2012.05.017

Emara, M.M., Ivanov, P., Hickman, T., Dawra, N., Tisdale, S., Kedersha, N., Hu, G.-F., Anderson, P., 2010. Angiogenin-induced tRNA-derived Stress-induced RNAs Promote Stress-induced Stress Granule Assembly. J. Biol. Chem. 285, 10959–10968. doi:10.1074/jbc.M109.077560

Emilsson, V., Näslund, A.K., Kurlad, C.G., 1992. Thiolation of transfer RNA in Escherichia coli varies with growth rate. Nucleic Acids Res. 20, 4499–4505.

doi:10.1093/nar/20.17.4499

Ender, C., Krek, A., Friedländer, M.R., Beitzinger, M., Weinmann, L., Chen, W., Pfeffer, S., Rajewsky, N., Meister, G., 2008. A human snoRNA with microRNA-like functions. Mol. Cell 32, 519–28. doi:10.1016/j.molcel.2008.10.017

Ersing, I., Nobre, L., Wang, L.W., Soday, L., Ma, Y., Paulo, J.A., Narita, Y., Ashbaugh, C.W., Jiang, C., Grayson, N.E., Kieff, E., Gygi, S.P., Weekes, M.P., Gewurz, B.E., 2017. A Temporal Proteomic Map of Epstein-Barr Virus Lytic Replication in B Cells. Cell Rep. 19, 1479–1493. doi:10.1016/j.celrep.2017.04.062

Esakova, O., Krasilnikov, A.S., 2010. Of proteins and RNA: the RNase P/MRP family. RNA 16, 1725–47. doi:10.1261/rna.2214510

Esakova, O., Perederina, A., Quan, C., Schmitt, M.E., Krasilnikov, A.S., 2008. Footprinting analysis demonstrates extensive similarity between eukaryotic RNase P and RNase MRP holoenzymes. RNA 14, 1558–67. doi:10.1261/rna.1106408

Eulalio, A., Tritschler, F., Izaurralde, E., 2009. The GW182 protein family in animal cells: New insights into domains required for miRNA-mediated gene silencing. RNA 15, 1433–1442. doi:10.1261/rna.1703809

Faehnle, C.R., Elkayam, E., Haase, A.D., Hannon, G.J., Joshua-Tor, L., 2013. The Making of a Slicer: Activation of Human Argonaute-1. Cell Rep. 3, 1901–1909. doi:10.1016/j.celrep.2013.05.033

Fairley, J.A., Kantidakis, T., Kenneth, N.S., Intine, R. V, Maraia, R.J., White, R.J., 2005. Human La is found at RNA polymerase III-transcribed genes in vivo. Proc. Natl. Acad. Sci. U. S. A. 102, 18350–5. doi:10.1073/pnas.0506415102

Fan, H., Goodier, J.L., Chamberlain, J.R., Engelke, D.R., Maraia, R.J., 1998. 5’ processing of tRNA precursors can Be modulated by the human La antigen phosphoprotein. Mol. Cell. Biol. 18, 3201–11.

Fernández-Tornero, C., Böttcher, B., Riva, M., Carles, C., Steuerwald, U., Ruigrok, R.W.H., Sentenac, A., Müller, C.W., Schoehn, G., 2007. Insights into Transcription Initiation and Termination from the Electron Microscopy Structure of Yeast RNA Polymerase III. Mol. Cell 25, 813–823. doi:10.1016/j.molcel.2007.02.016

Fett, J.W., Strydom, D.J., Lobb, R.R., Alderman, E.M., Bethune, J.L., Riordan, J.F., Vallee, B.L., 1985. Isolation and characterization of angiogenin, an angiogenic protein from human carcinoma cells. Biochemistry 24, 5480–6.

Filipowicz, W., Konarska, M., Gross, H.J., Shatkin, A.J., 1983. RNA 3’-terminal phosphate cyclase activity and RNA ligation in HeLa cell extract. Nucleic Acids Res. 11, 1405–18.

Filipowicz, W., Shatkin, A.J., 1983. Origin of splice junction phosphate in tRNAs processed by HeLa cell extract. Cell 32, 547–57.

Finnegan, E.F., Pasquinelli, A.E., 2013. MicroRNA biogenesis: regulating the regulators. Crit. Rev. Biochem. Mol. Biol. 48, 51–68. doi:10.3109/10409238.2012.738643

Flemr, M., Malik, R., Franke, V., Nejepinska, J., Sedlacek, R., Vlahovicek, K., Svoboda, P., 2013. A Retrotransposon-Driven Dicer Isoform Directs Endogenous Small Interfering RNA Production in Mouse Oocytes. Cell 155, 807–816. doi:10.1016/j.cell.2013.10.001

Fornerod, M., Ohno, M., Yoshida, M., Mattaj, I.W., 1997. CRM1 is an export receptor for leucine-rich nuclear export signals. Cell 90, 1051–60.

Frenkel-Morgenstern, M., Danon, T., Christian, T., Igarashi, T., Cohen, L., Hou, Y.-M., Jensen, L.J., 2012. Genes adopt non-optimal codon usage to generate cell cycle-dependent oscillations in protein levels. Mol. Syst. Biol. 8, 572. doi:10.1038/msb.2012.3

Friedman, R.C., Farh, K.K.-H., Burge, C.B., Bartel, D.P., 2008. Most mammalian mRNAs are conserved targets of microRNAs. Genome Res. 19, 92–105. doi:10.1101/gr.082701.108

Fu, H., Feng, J., Liu, Q., Sun, F., Tie, Y., Zhu, J., Xing, R., Sun, Z., Zheng, X., 2009. Stress induces tRNA cleavage by angiogenin in mammalian cells. FEBS Lett. 583, 437–42. doi:10.1016/j.febslet.2008.12.043

Fukunaga, R., Han, B.W., Hung, J.-H., Xu, J., Weng, Z., Zamore, P.D., 2012. Dicer partner proteins tune the length of mature miRNAs in flies and mammals. Cell 151, 533–46. doi:10.1016/j.cell.2012.09.027

Gebetsberger, J., Polacek, N., 2013. Slicing tRNAs to boost functional ncRNA diversity. RNA Biol. 10, 1798–1806. doi:10.4161/rna.27177

Giegé, R., 2008. Toward a more complete view of tRNA biology. Nat. Struct. Mol. Biol. 15, 1007–14. doi:10.1038/nsmb.1498

Giegé, R., Jühling, F., Pütz, J., Stadler, P., Sauter, C., Florentz, C., 2012. Structure of transfer RNAs: similarity and variability. Wiley Interdiscip. Rev. RNA 3, 37–61. doi:10.1002/wrna.103

Gingold, H., Tehler, D., Christoffersen, N.R., Nielsen, M.M., Asmar, F., Kooistra, S.M., Christophersen, N.S., Christensen, L.L., Borre, M., Sørensen, K.D., Andersen, L.D., Andersen, C.L., Hulleman, E., Wurdinger, T., Ralfkiær, E., Helin, K., Grønbæk, K., Ørntoft, T., Waszak, S.M., Dahan, O., Pedersen, J.S., Lund, A.H., Pilpel, Y., 2014. A Dual Program for Translation Regulation in Cellular Proliferation and Differentiation. Cell 158, 1281–1292. doi:10.1016/j.cell.2014.08.011

Giuliodori, S., Percudani, R., Braglia, P., Ferrari, R., Guffanti, E., Ottonello, S., Dieci, G., 2003. A composite upstream sequence motif potentiates tRNA gene transcription in yeast. J. Mol. Biol. 333, 1–20. doi:10.1016/j.jmb.2003.08.016

Glasmacher, E., Hoefig, K.P., Vogel, K.U., Rath, N., Du, L., Wolf, C., Kremmer, E., Wang, X., Heissmeyer, V., 2010. Roquin binds inducible costimulator mRNA and effectors of mRNA decay to induce microRNA-independent post-transcriptional repression. Nat. Immunol. 11, 725–733. doi:10.1038/ni.1902

Gogakos, T., Brown, M., Garzia, A., Meyer, C., Hafner, M., Tuschl, T., 2017. Characterizing Expression and Processing of Precursor and Mature Human tRNAs by Hydro-tRNAseq and PAR-CLIP. Cell Rep. 20, 1463–1475. doi:10.1016/j.celrep.2017.07.029

Goodarzi, H., Liu, X., Nguyen, H.C.B., Zhang, S., Fish, L., Tavazoie, S.F., 2015. Endogenous tRNA-Derived Fragments Suppress Breast Cancer Progression via YBX1 Displacement. Cell 161, 790–802. doi:10.1016/j.cell.2015.02.053

Goodarzi, H., Nguyen, H.C.B., Zhang, S., Dill, B.D., Molina, H., Tavazoie, S.F., 2016. Modulated Expression of Specific tRNAs Drives Gene Expression and Cancer

Progression. Cell 165, 1416–1427. doi:10.1016/j.cell.2016.05.046

Gottlieb, E., Steitz, J.A., 1989. The RNA binding protein La influences both the accuracy and the efficiency of RNA polymerase III transcription in vitro. EMBO J. 8, 841–50.

Gottwein, E., Mukherjee, N., Sachse, C., Frenzel, C., Majoros, W.H., Chi, J.-T.A., Braich, R., Manoharan, M., Soutschek, J., Ohler, U., Cullen, B.R., 2007. A viral microRNA functions as an orthologue of cellular miR-155. Nature 450, 1096–1099. doi:10.1038/nature05992

Gouge, J., Satia, K., Guthertz, N., Widya, M., Thompson, A.J., Cousin, P., Dergai, O., Hernandez, N., Vannini, A., 2015. Redox Signaling by the RNA Polymerase III TFIIB-Related Factor Brf2. Cell 163, 1375–1387. doi:10.1016/j.cell.2015.11.005

Greer, C.L., Peebles, C.L., Gegenheimer, P., Abelson, J., 1983. Mechanism of action of a yeast RNA ligase in tRNA splicing. Cell 32, 537–46.

Gregory, R.I., Yan, K., Amuthan, G., Chendrimada, T., Doratotaj, B., Cooch, N., Shiekhattar, R., 2004. The Microprocessor complex mediates the genesis of microRNAs. Nature 432, 235–40. doi:10.1038/nature03120

Griffin, B.E., Jarman, M., Reese, C.B., Sulston, J.E., Trentham, D.R., 1966. Some Observations Relating to Acyl Mobility in Aminoacyl Soluble Ribonucleic Acids. Biochemistry 5, 3638–3649. doi:10.1021/bi00875a037

Grosshans, H., Hurt, E., Simos, G., 2000. An aminoacylation-dependent nuclear tRNA export pathway in yeast. Genes Dev. 14, 830–40. doi:10.1101/gad.14.7.830

Gudipati, R.K., Xu, Z., Lebreton, A., Séraphin, B., Steinmetz, L.M., Jacquier, A., Libri, D., 2012. Extensive Degradation of RNA Precursors by the Exosome in Wild-Type Cells. Mol. Cell 48, 409–421. doi:10.1016/j.molcel.2012.08.018

Guerrier-Takada, C., Gardiner, K., Marsh, T., Pace, N., Altman, S., 1983. The RNA moiety of ribonuclease P is the catalytic subunit of the enzyme. Cell 35, 849–57.

Gunnery, S., Ma, Y., Mathews, M.B., 1999. Termination sequence requirements vary among genes transcribed by RNA polymerase III. J. Mol. Biol. 286, 745–57. doi:10.1006/jmbi.1998.2518

Guo, H., Ingolia, N.T., Weissman, J.S., Bartel, D.P., 2010. Mammalian microRNAs predominantly act to decrease target mRNA levels. Nature 466, 835–840. doi:10.1038/nature09267

Guo, Y., Bosompem, A., Mohan, S., Erdogan, B., Ye, F., Vickers, K.C., Sheng, Q., Zhao, S., Li, C.-I., Su, P.-F., Jagasia, M., Strickland, S.A., Griffiths, E.A., Kim, A.S., 2015. Transfer RNA detection by small RNA deep sequencing and disease association with myelodysplastic syndromes. BMC Genomics 16, 1–11. doi:10.1186/s12864-015-1929-y

Guy, M.P., Young, D.L., Payea, M.J., Zhang, X., Kon, Y., Dean, K.M., Grayhack, E.J., Mathews, D.H., Fields, S., Phizicky, E.M., 2014. Identification of the determinants of tRNA function and susceptibility to rapid tRNA decay by high-throughput in vivo analysis. Genes Dev. 28, 1721–1732. doi:10.1101/gad.245936.114

Guzman, N., Agarwal, K., Asthagiri, D., Saji, M., Ringel, M.D., Paulaitis, M.E., 2015. Breast Cancer-Specific miR Signature Unique to Extracellular Vesicles includes “microRNA-like” tRNA Fragments. Mol. Cancer Res. 1–29. doi:10.1158/1541-7786.MCR-14-0533

Ha, M., Kim, V.N., 2014. Regulation of microRNA biogenesis. Nat. Rev. Mol. Cell Biol. 15, 509–524. doi:10.1038/nrm3838

Haack, T.B., Kopajtich, R., Freisinger, P., Wieland, T., Rorbach, J., Nicholls, T.J., Baruffini, E., Walther, A., Danhauser, K., Zimmermann, F.A., Husain, R.A., Schum, J., Mundy, H., Ferrero, I., Strom, T.M., Meitinger, T., Taylor, R.W., Minczuk, M., Mayr, J.A., Prokisch, H., 2013. ELAC2 Mutations Cause a Mitochondrial RNA Processing Defect Associated with Hypertrophic Cardiomyopathy. Am. J. Hum. Genet. 93, 211–223. doi:10.1016/j.ajhg.2013.06.006

Hafner, M., Landthaler, M., Burger, L., Khorshid, M., Hausser, J., Berninger, P., Rothballer, A., Ascano, M., Jungkamp, A.-C., Munschauer, M., Ulrich, A., Wardle, G.S., Dewell, S., Zavolan, M., Tuschl, T., 2010. Transcriptome-wide identification of RNA-binding protein and microRNA target sites by PAR-CLIP. Cell 141, 129–41. doi:10.1016/j.cell.2010.03.009

Han, J., Lee, Y., Yeom, K.-H., Nam, J.-W., Heo, I., Rhee, J.-K., Sohn, S.Y., Cho, Y., Zhang, B.-T., Kim, V.N., 2006. Molecular basis for the recognition of primary microRNAs by the Drosha-DGCR8 complex. Cell 125, 887–901. doi:10.1016/j.cell.2006.03.043

Hanada, T., Weitzer, S., Mair, B., Bernreuther, C., Wainger, B.J., Ichida, J., Hanada, R., Orthofer, M., Cronin, S.J., Komnenovic, V., Minis, A., Sato, F., Mimata, H., Yoshimura, A., Tamir, I., Rainer, J., Kofler, R., Yaron, A., Eggan, K.C., Woolf, C.J., Glatzel, M., Herbst, R., Martinez, J., Penninger, J.M., 2013. CLP1 links tRNA metabolism to progressive motor-neuron loss. Nature 495, 474–80. doi:10.1038/nature11923

Hansen, T.B., Venø, M.T., Jensen, T.I., Schaefer, A., Damgaard, C.K., Kjems, J., 2016. Argonaute-associated short introns are a novel class of gene regulators. Nat. Commun. 7, 11538. doi:10.1038/ncomms11538

Hartig, J. V, Förstemann, K., 2011. Loqs-PD and R2D2 define independent pathways for RISC generation in Drosophila. Nucleic Acids Res. 39, 3836–3851. doi:10.1093/nar/gkq1324

Hatton, O.L., Harris-Arnold, A., Schaffert, S., Krams, S.M., Martinez, O.M., 2014. The interplay between Epstein–Barr virus and B lymphocytes: implications for infection, immunity, and disease. Immunol. Res. 58, 268–276. doi:10.1007/s12026-014-8496-1

Hauptmann, J., Dueck, A., Harlander, S., Pfaff, J., Merkl, R., Meister, G., 2013. Turning catalytically inactive human Argonaute proteins into active slicer enzymes. Nat. Struct. Mol. Biol. 20, 814–7. doi:10.1038/nsmb.2577

Hauptmann, J., Schraivogel, D., Bruckmann, A., Manickavel, S., Jakob, L., Eichner, N., Pfaff, J., Urban, M., Sprunck, S., Hafner, M., Tuschl, T., Deutzmann, R., Meister, G., 2015. Biochemical isolation of Argonaute protein complexes by Ago-APP. Proc. Natl. Acad. Sci. 201506116. doi:10.1073/pnas.1506116112

Haussecker, D., Huang, Y., Lau, A., Parameswaran, P., Fire, A.Z., Kay, M. a, 2010. Human tRNA-derived small RNAs in the global regulation of RNA silencing. RNA 16, 673–95. doi:10.1261/rna.2000810

Hecht, L.I., Zamecnik, P.C., Stephenson, M.L., Scott, J.F., 1958. Nucleoside triphosphates as precursors of ribonucleic acid end groups in a mammalian system. J. Biol. Chem. 233, 954–63.

Heise, T., Kota, V., Brock, A., Morris, A.B., Rodriguez, R.M., Zierk, A.W., Howe, P.H., Sommer, G., 2016. The La protein counteracts cisplatin-induced cell death by stimulating protein synthesis of anti-apoptotic factor Bcl2. Oncotarget 7. doi:10.18632/oncotarget.8819

Helm, M., Giegé, R., Florentz, C., 1999. A Watson-Crick base-pair-disrupting methyl group (m1A9) is sufficient for cloverleaf folding of human mitochondrial tRNALys. Biochemistry 38, 13338–46.

Ho, C.K., Rauhut, R., Vijayraghavan, U., Abelson, J., 1990. Accumulation of pre-tRNA splicing "2/3" intermediates in a Saccharomyces cerevisiae mutant. EMBO J. 9, 1245–52.

Hoagland, M.B., Stephenson, M.L., Scott, J.F., Hecht, L.I., Zamecnik, P.C., 1958. A soluble ribonucleic acid intermediate in protein synthesis. J. Biol. Chem. 231, 241–57.

Höck, J., Weinmann, L., Ender, C., Rüdel, S., Kremmer, E., Raabe, M., Urlaub, H., Meister, G., 2007. Proteomic and functional analysis of Argonaute-containing mRNA–protein complexes in human cells. EMBO Rep. 8, 1052–1060. doi:10.1038/sj.embor.7401088

Hoffmann, N.A., Jakobi, A.J., Moreno-Morcillo, M., Glatt, S., Kosinski, J., Hagen, W.J.H., Sachse, C., Müller, C.W., 2015. Molecular structures of unbound and transcribing RNA polymerase III. Nature 528, 231–6. doi:10.1038/nature16143

Holcik, M., Korneluk, R.G., 2000. Functional characterization of the X-linked inhibitor of apoptosis (XIAP) internal ribosome entry site element: role of La autoantigen in XIAP translation. Mol. Cell. Biol. 20, 4648–57. doi:10.1128/MCB.20.13.4648-4657.2000

Holzmann, J., Frank, P., Löffler, E., Bennett, K.L., Gerner, C., Rossmanith, W., 2008. RNase P without RNA: Identification and Functional Reconstitution of the Human Mitochondrial tRNA Processing Enzyme. Cell 135, 462–474. doi:10.1016/j.cell.2008.09.013

Honda, S., Loher, P., Shigematsu, M., Palazzo, J.P., Suzuki, R., Imoto, I., Rigoutsos, I., Kirino, Y., 2015. Sex hormone-dependent tRNA halves enhance cell proliferation in breast and prostate cancers. Proc. Natl. Acad. Sci. 112, E3816–E3825. doi:10.1073/pnas.1510077112

Hopper, A.K., 2013. Transfer RNA post-transcriptional processing, turnover, and subcellular dynamics in the yeast Saccharomyces cerevisiae. Genetics 194, 43–67. doi:10.1534/genetics.112.147470

Hopper, A.K., Huang, H.-Y., 2015. Quality Control Pathways for Nucleus-Encoded Eukaryotic tRNA Biosynthesis and Subcellular Trafficking. Mol. Cell. Biol. 35, 2052–8. doi:10.1128/MCB.00131-15

Hopper, A.K., Pai, D. a, Engelke, D.R., 2010. Cellular dynamics of tRNAs and their genes. FEBS Lett. 584, 310–7. doi:10.1016/j.febslet.2009.11.053

Hopper, A.K., Schultz, L.D., Shapiro, R.A., 1980. Processing of intervening sequences: a new yeast mutant which fails to excise intervening sequences from precursor tRNAs. Cell 19, 741–51.

Hori, H., 2014. Methylated nucleosides in tRNA and tRNA methyltransferases. Front.

Genet. 5, 144. doi:10.3389/fgene.2014.00144

Houseley, J., Tollervey, D., 2009. The many pathways of RNA degradation. Cell 136, 763–76. doi:10.1016/j.cell.2009.01.019

Huang, D., Wang, W., Gough, S., Kannangara, C., 1984. delta-Aminolevulinic acid-synthesizing enzymes need an RNA moiety for activity. Science (80-.). 225, 1482–1484. doi:10.1126/science.6206568

Huang, H.-Y., Hopper, A.K., 2015. In vivo biochemical analyses reveal distinct roles of β-importins and eEF1A in tRNA subcellular traffic. Genes Dev. 29, 772–83. doi:10.1101/gad.258293.115

Huang, X., Fejes Tóth, K., Aravin, A.A., 2017. piRNA Biogenesis in Drosophila melanogaster. Trends Genet. 33, 882–894. doi:10.1016/j.tig.2017.09.002

Huang, Y., Bayfield, M.A., Intine, R. V., Maraia, R.J., 2006. Separate RNA-binding surfaces on the multifunctional La protein mediate distinguishable activities in tRNA maturation. Nat. Struct. Mol. Biol. 13, 611–618. doi:10.1038/nsmb1110

Huang, Y., Intine, R. V, Mozlin, A., Hasson, S., Maraia, R.J., 2005. Mutations in the RNA polymerase III subunit Rpc11p that decrease RNA 3' cleavage activity increase 3'-terminal oligo(U) length and La-dependent tRNA processing. Mol. Cell. Biol. 25, 621–36. doi:10.1128/MCB.25.2.621-636.2005

Hurt, D.J., Wang, S.S., Lin, Y.H., Hopper, A.K., 1987. Cloning and characterization of LOS1, a Saccharomyces cerevisiae gene that affects tRNA splicing. Mol. Cell. Biol. 7, 1208–16.

Hutvágner, G., McLachlan, J., Pasquinelli, A.E., Bálint, E., Tuschl, T., Zamore, P.D., 2001. A cellular function for the RNA-interference enzyme Dicer in the maturation of the let-7 small temporal RNA. Science (80-.). 293, 834–8. doi:10.1126/science.1062961

Ibba, M., Soll, D., 2000. Aminoacyl-tRNA synthesis. Annu. Rev. Biochem. 69, 617–50. doi:10.1146/annurev.biochem.69.1.617

Imig, J., Motsch, N., Zhu, J.Y., Barth, S., Okoniewski, M., Reineke, T., Tinguely, M., Faggioni, A., Trivedi, P., Meister, G., Renner, C., Grässer, F.A., 2011. microRNA profiling in Epstein–Barr virus-associated B-cell lymphoma. Nucleic Acids Res. 39, 1880–1893. doi:10.1093/nar/gkq1043

Ingolia, N.T., Lareau, L.F., Weissman, J.S., 2011. Ribosome Profiling of Mouse Embryonic Stem Cells Reveals the Complexity and Dynamics of Mammalian Proteomes. Cell 147, 789–802. doi:10.1016/j.cell.2011.10.002

Intine, R.V.A., Sakulich, A.L., Koduru, S.B., Huang, Y., Pierstorff, E., Goodier, J.L., Phan, L., Maraia, R.J., 2000. Control of Transfer RNA Maturation by Phosphorylation of the Human La Antigen on Serine 366. Mol. Cell 6, 339–348. doi:10.1016/S1097-2765(00)00034-4

Intine, R. V, Tenenbaum, S.A., Sakulich, A.L., Keene, J.D., Maraia, R.J., 2003. Differential phosphorylation and subcellular localization of La RNPs associated with precursor tRNAs and translation-related mRNAs. Mol. Cell 12, 1301–7.

Irvin, J.D., Hardesty, B., 1972. Binding of aminoacyl transfer ribonucleic acid synthetases to ribosomes from rabbit reticulocytes. Biochemistry 11, 1915–20.

Ishii, R., Minagawa, A., Takaku, H., Takagi, M., Nashimoto, M., Yokoyama, S., 2005. Crystal Structure of the tRNA 3′ Processing Endoribonuclease tRNase Z from Thermotoga maritima. J. Biol. Chem. 280, 14138–14144. doi:10.1074/jbc.M500355200

Itoh-Nakadai, A., Hikota, R., Muto, A., Kometani, K., Watanabe-Matsui, M., Sato, Y., Kobayashi, M., Nakamura, A., Miura, Y., Yano, Y., Tashiro, S., Sun, J., Ikawa, T., Ochiai, K., Kurosaki, T., Igarashi, K., 2014. The transcription repressors Bach2 and Bach1 promote B cell development by repressing the myeloid program. Nat. Immunol. 15, 1171–1180. doi:10.1038/ni.3024

Ivanov, P., Emara, M.M., Villen, J., Gygi, S.P., Anderson, P., 2011. Angiogenin-Induced tRNA Fragments Inhibit Translation Initiation. Mol. Cell 43, 613–623. doi:10.1016/j.molcel.2011.06.022

Ivanov, P., O'Day, E., Emara, M.M., Wagner, G., Lieberman, J., Anderson, P., O'Day, E., Emara, M.M., Wagner, G., Lieberman, J., Anderson, P., 2014. G-quadruplex structures contribute to the neuroprotective effects of angiogenin-induced tRNA fragments. Proc. Natl. Acad. Sci. 111, 18201–18206. doi:10.1073/pnas.1407361111

Iwakiri, D., Sheen, T.-S., Chen, J.-Y., Huang, D.P., Takada, K., 2005. Epstein–Barr virus-encoded small RNA induces insulin-like growth factor 1 and supports growth of nasopharyngeal carcinoma-derived cell lines. Oncogene 24, 1767–1773. doi:10.1038/sj.onc.1208357

Iwakiri, D., Zhou, L., Samanta, M., Matsumoto, M., Ebihara, T., Seya, T., Imai, S., Fujieda, M., Kawa, K., Takada, K., 2009. Epstein-Barr virus (EBV)-encoded small RNA is released from EBV-infected cells and activates signaling from Toll-like receptor 3. J. Exp. Med. 206, 2091–9. doi:10.1084/jem.20081761

Iwasaki, S., Kobayashi, M., Yoda, M., Sakaguchi, Y., Katsuma, S., Suzuki, T., Tomari, Y., 2010. Hsc70/Hsp90 chaperone machinery mediates ATP-dependent RISC loading of small RNA duplexes. Mol. Cell 39, 292–9. doi:10.1016/j.molcel.2010.05.015

Iwasaki, S., Sasaki, H.M., Sakaguchi, Y., Suzuki, T., Tadakuma, H., Tomari, Y., 2015. Defining fundamental steps in the assembly of the Drosophila RNAi enzyme complex. Nature 521, 533–536. doi:10.1038/nature14254

Izaurralde, E., Kutay, U., von Kobbe, C., Mattaj, I.W., Görlich, D., 1997. The asymmetric distribution of the constituents of the Ran system is essential for transport into and out of the nucleus. EMBO J. 16, 6535–47. doi:10.1093/emboj/16.21.6535

Jacks, A., Babon, J., Kelly, G., Manolaridis, I., Cary, P.D., Curry, S., Conte, M.R., 2003. Structure of the C-Terminal Domain of Human La Protein Reveals a Novel RNA Recognition Motif Coupled to a Helical Nuclear Retention Element. Structure 11, 833–843. doi:10.1016/S0969-2126(03)00121-7

Jahn, D., Verkamp, E., So¨ll, D., 1992. Glutamyl-transfer RNA: a precursor of heme and chlorophyll biosynthesis. Trends Biochem. Sci. 17, 215–218. doi:10.1016/0968-0004(92)90380-R

Jakob, L., Treiber, T., Treiber, N., Gust, A., Kramm, K., Hansen, K., Stotz, M., Wankerl, L., Herzog, F., Hannus, S., Grohmann, D., Meister, G., 2016. Structural and functional insights into the fly microRNA biogenesis factor Loquacious. RNA 22, 383–396. doi:10.1261/rna.055426.115

Jakubowski, H., 2012. Quality control in tRNA charging. Wiley Interdiscip. Rev. RNA 3, 295–310. doi:10.1002/wrna.122

Jarrous, N., Wolenski, J.S., Wesolowski, D., Lee, C., Altman, S., 1999. Localization in the nucleolus and coiled bodies of protein subunits of the ribonucleoprotein ribonuclease P. J. Cell Biol. 146, 559–72.

Jee, D., Yang, J.-S., Park, S.-M., Farmer, D.T., Wen, J., Chou, T., Chow, A., McManus, M.T., Kharas, M.G., Lai, E.C., 2018. Dual Strategies for Argonaute2-Mediated Biogenesis of Erythroid miRNAs Underlie Conserved Requirements for Slicing in Mammals. Mol. Cell 69, 265–278.e6. doi:10.1016/j.molcel.2017.12.027

Jöchl, C., Rederstorff, M., Hertel, J., Stadler, P.F., Hofacker, I.L., Schrettl, M., Haas, H., Hüttenhofer, A., 2008. Small ncRNA transcriptome analysis from Aspergillus fumigatus suggests a novel mechanism for regulation of protein synthesis. Nucleic Acids Res. 36, 2677–2689. doi:10.1093/nar/gkn123

Johansson, M.J.O., Esberg, A., Huang, B., Björk, G.R., Byström, A.S., 2008. Eukaryotic wobble uridine modifications promote a functionally redundant decoding system. Mol. Cell. Biol. 28, 3301–12. doi:10.1128/MCB.01542-07

Johnston, M., Geoffroy, M.-C., Sobala, A., Hay, R., Hutvagner, G., 2010. HSP90 protein stabilizes unloaded argonaute complexes and microscopic P-bodies in human cells. Mol. Biol. Cell 21, 1462–9. doi:10.1091/mbc.E09-10-0885

Jonas, S., Izaurralde, E., 2015. Towards a molecular understanding of microRNA-mediated gene silencing. Nat. Rev. Genet. 16, 421–433. doi:10.1038/nrg3965

Jurkin, J., Henkel, T., Nielsen, A.F., Minnich, M., Popow, J., Kaufmann, T., Heindl, K., Hoffmann, T., Busslinger, M., Martinez, J., 2014. The mammalian tRNA ligase complex mediates splicing of XBP1 mRNA and controls antibody secretion in plasma cells. EMBO J. 33, 2922–36. doi:10.15252/embj.201490332

Kadaba, S., Krueger, A., Trice, T., Krecic, A.M., Hinnebusch, A.G., Anderson, J., 2004. Nuclear surveillance and degradation of hypomodified initiator tRNAMet in S. cerevisiae. Genes Dev. 18, 1227–40. doi:10.1101/gad.1183804

Kaji, H., 1968. Further studies on the soluble amino acid incorporating system from rat liver. Biochemistry 7, 3844–50.

Kaminska, M., Havrylenko, S., Decottignies, P., Le Maréchal, P., Negrutskii, B., Mirande, M., 2009. Dynamic Organization of Aminoacyl-tRNA Synthetase Complexes in the Cytoplasm of Human Cells. J. Biol. Chem. 284, 13746–54. doi:10.1074/jbc.M900480200

Kanerva, P.A., Mäenpää, P.H., 1981. Codon-specific serine transfer ribonucleic acid degradation in avian liver during vitellogenin induction. Acta Chem. Scand. B. 35, 379–85.

Karaca, E., Weitzer, S., Pehlivan, D., Shiraishi, H., Gogakos, T., Hanada, T., Jhangiani, S.N., Wiszniewski, W., Withers, M., Campbell, I.M., Erdin, S., Isikay, S., Franco, L.M., Gonzaga-Jauregui, C., Gambin, T., Gelowani, V., Hunter, J.V., Yesil, G., Koparir, E., Yilmaz, S., Brown, M., Briskin, D., Hafner, M., Morozov, P., Farazi, T.A., Bernreuther, C., Glatzel, M., Trattnig, S., Friske, J., Kronnerwetter, C., Bainbridge, M.N., Gezdirici, A., Seven, M., Muzny, D.M., Boerwinkle, E., Ozen, M., Clausen, T., Tuschl, T., Yuksel, A., Hess, A., Gibbs, R.A., Martinez, J., Penninger, J.M., Lupski, J.R., 2014. Human CLP1 Mutations Alter tRNA

Biogenesis, Affecting Both Peripheral and Central Nervous System Function. Cell 157, 636–650. doi:10.1016/j.cell.2014.02.058

Karginov, F. V, Cheloufi, S., Chong, M.M.W., Stark, A., Smith, A.D., Hannon, G.J., 2010. Diverse endonucleolytic cleavage sites in the mammalian transcriptome depend upon microRNAs, Drosha, and additional nucleases. Mol. Cell 38, 781–8. doi:10.1016/j.molcel.2010.06.001

Keam, S., Hutvagner, G., 2015. tRNA-Derived Fragments (tRFs): Emerging New Roles for an Ancient RNA in the Regulation of Gene Expression. Life 5, 1638–1651. doi:10.3390/life5041638

Keam, S.P., Sobala, A., ten Have, S., Hutvagner, G., 2017. tRNA-Derived RNA Fragments Associate with Human Multisynthetase Complex (MSC) and Modulate Ribosomal Protein Translation. J. Proteome Res. 16, 413–420. doi:10.1021/acs.jproteome.6b00267

Keam, S.P., Young, P.E., McCorkindale, A.L., Dang, T.H.Y., Clancy, J.L., Humphreys, D.T., Preiss, T., Hutvagner, G., Martin, D.I.K., Cropley, J.E., Suter, C.M., 2014. The human Piwi protein Hiwi2 associates with tRNA-derived piRNAs in somatic cells. Nucleic Acids Res. 42, 8984–95. doi:10.1093/nar/gku620

Kerjan, P., Cerini, C., Sémériva, M., Mirande, M., 1994. The multienzyme complex containing nine aminoacyl-tRNA synthetases is ubiquitous from Drosophila to mammals. Biochim. Biophys. Acta 1199, 293–7.

Khvorova, A., Reynolds, A., Jayasena, S.D., 2003. Functional siRNAs and miRNAs Exhibit Strand Bias. Cell 115, 209–216. doi:10.1016/S0092-8674(03)00801-8

Kikovska, E., Svärd, S.G., Kirsebom, L.A., 2007. Eukaryotic RNase P RNA mediates cleavage in the absence of protein. Proc. Natl. Acad. Sci. U. S. A. 104, 2062–7. doi:10.1073/pnas.0607326104

Kim, H.K., Fuchs, G., Wang, S., Wei, W., Zhang, Y., Park, H., Roy-Chaudhuri, B., Li, P., Xu, J., Chu, K., Zhang, F., Chua, M.-S., So, S., Zhang, Q.C., Sarnow, P., Kay, M.A., 2017. A transfer-RNA-derived small RNA regulates ribosome biogenesis. Nature. doi:10.1038/nature25005

Kim, M.J., Park, B.-J., Kang, Y.-S., Kim, H.J., Park, J.-H., Kang, J.W., Lee, S.W., Han, J.M., Lee, H.-W., Kim, S., 2003. Downregulation of FUSE-binding protein and c-myc by tRNA synthetase cofactor p38 is required for lung cell differentiation. Nat. Genet. 34, 330–6. doi:10.1038/ng1182

Kim, S.H., Quigley, G.J., Suddath, F.L., McPherson, A., Sneden, D., Kim, J.J., Weinzierl, J., Rich, A., 1973. Three-dimensional structure of yeast phenylalanine transfer RNA: folding of the polynucleotide chain. Science 179, 285–8.

Kim, V.N., 2005. MicroRNA biogenesis: coordinated cropping and dicing. Nat. Rev. Mol. Cell Biol. 6, 376–385. doi:10.1038/nrm1644

Kim, V.N., Han, J., Siomi, M.C., 2009. Biogenesis of small RNAs in animals. Nat. Rev. Mol. Cell Biol. 10, 126–139. doi:10.1038/nrm2632

Kim, Y.-K., Kim, B., Kim, V.N., 2016. Re-evaluation of the roles of DROSHA , Exportin 5 , and DICER in microRNA biogenesis. Proc. Natl. Acad. Sci. 113, E1881–E1889. doi:10.1073/pnas.1602532113

Kim, Y.K., Back, S.H., Rho, J., Lee, S.H., Jang, S.K., 2001. La autoantigen enhances

translation of BiP mRNA. Nucleic Acids Res. 29, 5009–16.

Kincaid, R.P., Burke, J.M., Sullivan, C.S., 2012. RNA virus microRNA that mimics a B-cell oncomiR. Proc. Natl. Acad. Sci. 109, 3077–3082. doi:10.1073/pnas.1116107109

Kirchner, S., Ignatova, Z., 2014. Emerging roles of tRNA in adaptive translation, signalling dynamics and disease. Nat. Rev. Genet. doi:10.1038/nrg3861

Kirino, Y., Yasukawa, T., Ohta, S., Akira, S., Ishihara, K., Watanabe, K., Suzuki, T., 2004. Codon-specific translational defect caused by a wobble modification deficiency in mutant tRNA from a human mitochondrial disease. Proc. Natl. Acad. Sci. U. S. A. 101, 15070–5. doi:10.1073/pnas.0405173101

Kitagawa, N., Goto, M., Kurozumi, K., Maruo, S., Fukayama, M., Naoe, T., Yasukawa, M., Hino, K., Suzuki, T., Todo, S., Takada, K., 2000. Epstein-Barr virus-encoded poly(A)(-) RNA supports Burkitt's lymphoma growth through interleukin-10 induction. EMBO J. 19, 6742–50. doi:10.1093/emboj/19.24.6742

Klassen, R., Paluszynski, J.P., Wemhoff, S., Pfeiffer, A., Fricke, J., Meinhardt, F., 2008. The primary target of the killer toxin from Pichia acaciae is tRNA Gln. Mol. Microbiol. 69, 681–697. doi:10.1111/j.1365-2958.2008.06319.x

Knies, U.E., Behrensdorf, H.A., Mitchell, C.A., Deutsch, U., Risau, W., Drexler, H.C.A., Clauss, M., 1998. Regulation of endothelial monocyte-activating polypeptide II release by apoptosis. Proc. Natl. Acad. Sci. 95, 12322–12327. doi:10.1073/pnas.95.21.12322

Kosmaczewski, S.G., Edwards, T.J., Han, S.M., Eckwahl, M.J., Meyer, B.I., Peach, S., Hesselberth, J.R., Wolin, S.L., Hammarlund, M., 2014. The RtcB RNA ligase is an essential component of the metazoan unfolded protein response. EMBO Rep. 15, 1278–85. doi:10.15252/embr.201439531

Kostelecky, B., Pohl, E., Vogel, A., Schilling, O., Meyer-Klaucke, W., 2006. The Crystal Structure of the Zinc Phosphodiesterase from Escherichia coli Provides Insight into Function and Cooperativity of tRNase Z-Family Proteins. J. Bacteriol. 188, 1607–1614. doi:10.1128/JB.188.4.1607-1614.2006

Kozomara, A., Griffiths-Jones, S., 2014. miRBase: annotating high confidence microRNAs using deep sequencing data. Nucleic Acids Res. 42, D68–D73. doi:10.1093/nar/gkt1181

Kramer, E.B., Hopper, A.K., 2013. Retrograde transfer RNA nuclear import provides a new level of tRNA quality control in Saccharomyces cerevisiae. Proc. Natl. Acad. Sci. 110, 21042–21047. doi:10.1073/pnas.1316579110

Kucera, N.J., Hodsdon, M.E., Wolin, S.L., 2011. An intrinsically disordered C terminus allows the La protein to assist the biogenesis of diverse noncoding RNA precursors. Proc. Natl. Acad. Sci. U. S. A. 108, 1308–1313. doi:10.1073/pnas.1017085108

Kufel, J., Tollervey, D., 2003. 3'-processing of yeast tRNATrp precedes 5'-processing. RNA 9, 202–8. doi:10.1261/rna.2145103

Kuhn, C.-D., Wilusz, J.E., Zheng, Y., Beal, P.A., Joshua-Tor, L., 2015. On-enzyme refolding permits small RNA and tRNA surveillance by the CCA-adding enzyme. Cell 160, 644–58. doi:10.1016/j.cell.2015.01.005

Kuhn, R.M., Clarke, L., Carbon, J., 1991. Clustered tRNA genes in Schizosaccharomyces pombe centromeric DNA sequence repeats. Proc. Natl. Acad. Sci. U. S. A. 88, 1306–

10.

Kumar, M.S., Pester, R.E., Chen, C.Y., Lane, K., Chin, C., Lu, J., Kirsch, D.G., Golub, T.R., Jacks, T., 2009. Dicer1 functions as a haploinsufficient tumor suppressor. Genes Dev. 23, 2700–2704. doi:10.1101/gad.1848209

Kumar, P., Anaya, J., Mudunuri, S.B., Dutta, A., 2014. Meta-analysis of tRNA derived RNA fragments reveals that they are evolutionarily conserved and associate with AGO proteins to recognize specific RNA targets. BMC Biol. 12, 78. doi:10.1186/s12915-014-0078-0

Kumar, P., Mudunuri, S.B., Anaya, J., Dutta, A., 2015. tRFdb: a database for transfer RNA fragments. Nucleic Acids Res. 43, D141-5. doi:10.1093/nar/gku1138

Küppers, R., 2003. B cells under influence: transformation of B cells by Epstein–Barr virus. Nat. Rev. Immunol. 3, 801–812. doi:10.1038/nri1201

Kutay, U., Lipowsky, G., Izaurralde, E., Bischoff, F.R., Schwarzmaier, P., Hartmann, E., Görlich, D., 1998. Identification of a tRNA-specific nuclear export receptor. Mol. Cell 1, 359–69.

Kwak, P.B., Tomari, Y., 2012. The N domain of Argonaute drives duplex unwinding during RISC assembly. Nat. Struct. Mol. Biol. 19, 145–51. doi:10.1038/nsmb.2232

Kwon, S.C., Nguyen, T.A., Choi, Y.-G., Jo, M.H., Hohng, S., Kim, V.N., Woo, J.-S., 2016. Structure of Human DROSHA. Cell 164, 81–90. doi:10.1016/j.cell.2015.12.019

Kyriacou, S. V, Deutscher, M.P., 2008. An important role for the multienzyme aminoacyl-tRNA synthetase complex in mammalian translation and cell growth. Mol. Cell 29, 419–27. doi:10.1016/j.molcel.2007.11.038

Ladewig, E., Okamura, K., Flynt, A.S., Westholm, J.O., Lai, E.C., 2012. Discovery of hundreds of mirtrons in mouse and human small RNA data. Genome Res. 22, 1634–1645. doi:10.1101/gr.133553.111

Lai, L.B., Vioque, A., Kirsebom, L. a, Gopalan, V., 2010. Unexpected diversity of RNase P, an ancient tRNA processing enzyme: challenges and prospects. FEBS Lett. 584, 287–96. doi:10.1016/j.febslet.2009.11.048

Laski, F.A., Fire, A.Z., RajBhandary, U.L., Sharp, P.A., 1983. Characterization of tRNA precursor splicing in mammalian extracts. J. Biol. Chem. 258, 11974–80.

Lau, P.-W., Guiley, K.Z., De, N., Potter, C.S., Carragher, B., MacRae, I.J., 2012. The molecular architecture of human Dicer. Nat. Struct. Mol. Biol. 19, 436–440. doi:10.1038/nsmb.2268

Lau, P.-W., Potter, C.S., Carragher, B., MacRae, I.J., 2009. Structure of the Human Dicer-TRBP Complex by Electron Microscopy. Structure 17, 1326–1332. doi:10.1016/j.str.2009.08.013

Lawrence, M., Huber, W., Pagès, H., Aboyoun, P., Carlson, M., Gentleman, R., Morgan, M.T., Carey, V.J., 2013. Software for Computing and Annotating Genomic Ranges. PLoS Comput. Biol. 9, e1003118. doi:10.1371/journal.pcbi.1003118

Lazzaretti, D., Tournier, I., Izaurralde, E., 2009. The C-terminal domains of human TNRC6A, TNRC6B, and TNRC6C silence bound transcripts independently of Argonaute proteins. RNA 15, 1059–66. doi:10.1261/rna.1606309

Lee, M.C., Knapp, G., 1985. Transfer RNA splicing in Saccharomyces cerevisiae. Secondary and tertiary structures of the substrates. J. Biol. Chem. 260, 3108–15.

Lee, N., Moss, W.N., Yario, T.A., Steitz, J.A., 2015. EBV noncoding RNA binds nascent RNA to drive host PAX5 to viral DNA. Cell 160, 607–18. doi:10.1016/j.cell.2015.01.015

Lee, S.R., Collins, K., 2005. Starvation-induced Cleavage of the tRNA Anticodon Loop in Tetrahymena thermophila. J. Biol. Chem. 280, 42744–42749. doi:10.1074/jbc.M510356200

Lee, Y., Hur, I., Park, S.-Y., Kim, Y.-K., Suh, M.R., Kim, V.N., 2006. The role of PACT in the RNA silencing pathway. EMBO J. 25, 522–532. doi:10.1038/sj.emboj.7600942

Lee, Y., Kim, M., Han, J., Yeom, K.-H., Lee, S., Baek, S.H., Kim, V.N., 2004. MicroRNA genes are transcribed by RNA polymerase II. EMBO J. 23, 4051–4060. doi:10.1038/sj.emboj.7600385

Lee, Y.S., Shibata, Y., Malhotra, A., Dutta, A., 2009. A novel class of small RNAs: tRNA-derived RNA fragments (tRFs). Genes Dev. 23, 2639–49. doi:10.1101/gad.1837609

Lerner, M.R., Andrews, N.C., Miller, G., Steitz, J.A., 1981. Two small RNAs encoded by Epstein-Barr virus and complexed with protein are precipitated by antibodies from patients with systemic lupus erythematosus. Proc. Natl. Acad. Sci. 78, 805–9.

Levitz, R., Chapman, D., Amitsur, M., Green, R., Snyder, L., Kaufmann, G., 1990. The optional E. coli prr locus encodes a latent form of phage T4-induced anticodon nuclease. EMBO J. 9, 1383–9.

Li, F., Xiong, Y., Wang, J., Cho, H.D., Tomita, K., Weiner, A.M., Steitz, T.A., 2002. Crystal structures of the Bacillus stearothermophilus CCA-adding enzyme and its complexes with ATP or CTP. Cell 111, 815–24.

Li, H., Durbin, R., 2010. Fast and accurate long-read alignment with Burrows–Wheeler transform. Bioinformatics 26, 589–595. doi:10.1093/bioinformatics/btp698

Li, H., Trotta, C.R., Abelson, J., 1998. Crystal structure and evolution of a transfer RNA splicing enzyme. Science 280, 279–84.

Li, H., Wu, C., Aramayo, R., Sachs, M.S., Harlow, M.L., 2015. Synaptic vesicles contain small ribonucleic acids (sRNAs) including transfer RNA fragments (trfRNA) and microRNAs (miRNA). Sci. Rep. 5, 14918. doi:10.1038/srep14918

Li, Z., Ender, C., Meister, G., Moore, P.S., Chang, Y., John, B., 2012. Extensive terminal and asymmetric processing of small RNAs from rRNAs, snoRNAs, snRNAs, and tRNAs. Nucleic Acids Res. 40, 6787–99. doi:10.1093/nar/gks307

Liang, C., Xiong, K., Szulwach, K.E., Zhang, Y., Wang, Z., Peng, J., Fu, M., Jin, P., Suzuki, H.I., Liu, Q., 2013. Sjogren syndrome antigen B (SSB)/La promotes global microRNA expression by binding microRNA precursors through stem-loop recognition. J. Biol. Chem. 288, 723–36. doi:10.1074/jbc.M112.401323

Lin, S., Gregory, R.I., 2015. MicroRNA biogenesis pathways in cancer. Nat. Rev. Cancer 15, 321–333. doi:10.1038/nrc3932

Liu, J., Carmell, M.A., Rivas, F. V, Marsden, C.G., Thomson, J.M., Song, J.-J.,

Hammond, S.M., Joshua-Tor, L., Hannon, G.J., 2004. Argonaute2 is the catalytic engine of mammalian RNAi. Science (80-.). 305, 1437–41. doi:10.1126/science.1102513

Liu, Y., Tan, H., Tian, H., Liang, C., Chen, S., Liu, Q., 2011. Autoantigen La promotes efficient RNAi, antiviral response, and transposon silencing by facilitating multiple-turnover RISC catalysis. Mol. Cell 44, 502–8. doi:10.1016/j.molcel.2011.09.011

Love, M.I., Huber, W., Anders, S., 2014. Moderated estimation of fold change and dispersion for RNA-seq data with DESeq2. Genome Biol. 15, 550. doi:10.1186/s13059-014-0550-8

Lu, J., Huang, B., Esberg, A., Johansson, M.J.O., Byström, A.S., 2005. The Kluyveromyces lactis gamma-toxin targets tRNA anticodons. RNA 11, 1648–54. doi:10.1261/rna.2172105

Lu, Y., Liang, F.-X., Wang, X., 2014. A synthetic biology approach identifies the mammalian UPR RNA ligase RtcB. Mol. Cell 55, 758–70. doi:10.1016/j.molcel.2014.06.032

Lu, Z., Filonov, G.S., Noto, J.J., Schmidt, C. a, Hatkevich, T.L., Wen, Y., Jaffrey, S.R., Matera, a G., 2015. Metazoan tRNA introns generate stable circular RNAs in vivo. RNA 21, 1554–65. doi:10.1261/rna.052944.115

Lund, E., Dahlberg, J.E., 1998. Proofreading and aminoacylation of tRNAs before export from the nucleus. Science 282, 2082–5. doi:10.1126/science.282.5396.2082

Lund, E., Güttinger, S., Calado, A., Dahlberg, J.E., Kutay, U., 2004. Nuclear export of microRNA precursors. Science 303, 95–8. doi:10.1126/science.1090599

Lung, R., Tong, J., To, K.-F., 2013. Emerging Roles of Small Epstein-Barr Virus Derived Non-Coding RNAs in Epithelial Malignancy. Int. J. Mol. Sci. 14, 17378–17409. doi:10.3390/ijms140917378

Lung, R.W.-M., Tong, J.H.-M., Sung, Y.-M., Leung, P.-S., Ng, D.C.-H., Chau, S.-L., Chan, A.W.-H., Ng, E.K.-O., Lo, K.-W., To, K.-F., 2009. Modulation of LMP2A Expression by a Newly Identified Epstein-Barr Virus-Encoded MicroRNA miR-BART22. Neoplasia 11, 1174–IN17. doi:10.1593/neo.09888

Lygerou, Z., Mitchell, P., Petfalski, E., Séraphin, B., Tollervey, D., 1994. The POP1 gene encodes a protein component common to the RNase MRP and RNase P ribonucleoproteins. Genes Dev. 8, 1423–33.

Lyons, S.M., Achorn, C., Kedersha, N.L., Anderson, P.J., Ivanov, P., 2016. YB-1 regulates tiRNA-induced Stress Granule formation but not translational repression. Nucleic Acids Res. 44, 6949–6960. doi:10.1093/nar/gkw418

Ma, H., Wu, Y., Choi, J.-G., Wu, H., 2013. Lower and upper stem-single-stranded RNA junctions together determine the Drosha cleavage site. Proc. Natl. Acad. Sci. 110, 20687–20692. doi:10.1073/pnas.1311639110

Ma, M., Li de la Sierra-Gallay, I., Lazar, N., Pellegrini, O., Durand, D., Marchfelder, A., Condon, C., van Tilbeurgh, H., 2017. The crystal structure of Trz1, the long form RNase Z from yeast. Nucleic Acids Res. 45, 6209–6216. doi:10.1093/nar/gkx216

Ma, Z., Swede, H., Cassarino, D., Fleming, E., Fire, A., Dadras, S.S., 2011. Up-Regulated Dicer Expression in Patients with Cutaneous Melanoma. PLoS One 6, e20494. doi:10.1371/journal.pone.0020494

Macfarlan, T.S., Gifford, W.D., Driscoll, S., Lettieri, K., Rowe, H.M., Bonanomi, D., Firth, A., Singer, O., Trono, D., Pfaff, S.L., 2012. Embryonic stem cell potency fluctuates with endogenous retrovirus activity. Nature 487, 57–63. doi:10.1038/nature11244

Mahony, R., Broadbent, L., Maier-Moore, J.S., Power, U.F., Jefferies, C.A., 2017. The RNA binding protein La/SS-B promotes RIG-I-mediated type I and type III IFN responses following Sendai viral infection. Sci. Rep. 7, 14537. doi:10.1038/s41598-017-15197-9

Mak, J., Kleiman, L., 1997. Primer tRNAs for reverse transcription. J. Virol. 71, 8087–8095.

Mandel, C.R., Kaneko, S., Zhang, H., Gebauer, D., Vethantham, V., Manley, J.L., Tong, L., 2006. Polyadenylation factor CPSF-73 is the pre-mRNA 3'-end-processing endonuclease. Nature 444, 953–6. doi:10.1038/nature05363

Maniataki, E., Mourelatos, Z., 2005. Human mitochondrial tRNAMet is exported to the cytoplasm and associates with the Argonaute 2 protein. RNA 11, 849–52. doi:10.1261/rna.2210805

Maraia, R.J., Arimbasseri, A.G., 2017. Factors That Shape Eukaryotic tRNAomes: Processing, Modification and Anticodon-Codon Use. Biomolecules 7. doi:10.3390/biom7010026

Maraia, R.J., Lamichhane, T.N., 2011. 3' processing of eukaryotic precursor tRNAs. Wiley Interdiscip. Rev. RNA 2, 362–75. doi:10.1002/wrna.64

Maraia, R.J., Mattijssen, S., Cruz-Gallardo, I., Conte, M.R., 2017. The La and related RNA-binding proteins (LARPs): structures, functions, and evolving perspectives. Wiley Interdiscip. Rev. RNA 8, e1430. doi:10.1002/wrna.1430

Marck, C., Grosjean, H., 2003. Identification of BHB splicing motifs in intron-containing tRNAs from 18 archaea: evolutionary implications. RNA 9, 1516–31.

Martin, N.C., Rabinowitz, M., Fukuhara, H., 1977. Yeast mitochondrial DNA specifies tRNA for 19 amino acids. Deletion mapping of the tRNA genes. Biochemistry 16, 4672–7.

Martino, L., Pennell, S., Kelly, G., Bui, T.T.T., Kotik-Kogan, O., Smerdon, S.J., Drake, A.F., Curry, S., Conte, M.R., 2012. Analysis of the interaction with the hepatitis C virus mRNA reveals an alternative mode of RNA recognition by the human La protein. Nucleic Acids Res. 40, 1381–1394. doi:10.1093/nar/gkr890

Mathews, M.B., Shenk, T., 1991. Adenovirus virus-associated RNA and translation control. J. Virol. 65, 5657–62.

Mathys, H., Basquin, J., Ozgur, S., Czarnocki-Cieciura, M., Bonneau, F., Aartse, A., Dziembowski, A., Nowotny, M., Conti, E., Filipowicz, W., 2014. Structural and Biochemical Insights to the Role of the CCR4-NOT Complex and DDX6 ATPase in MicroRNA Repression. Mol. Cell 54, 751–765. doi:10.1016/j.molcel.2014.03.036

Mattoccia, E., Baldi, I.M., Gandini-Attardi, D., Ciafrè, S., Tocchini-Valentini, G.P., 1988. Site selection by the tRNA splicing endonuclease of Xenopus laevis. Cell 55, 731–8.

Maute, R.L., Schneider, C., Sumazin, P., Holmes, A., Califano, A., Basso, K., Dalla-Favera, R., 2013. tRNA-derived microRNA modulates proliferation and the DNA damage response and is down-regulated in B cell lymphoma. Proc. Natl. Acad. Sci.

U. S. A. 2–7. doi:10.1073/pnas.1206761110

Mazabraud, a, Scherly, D., Müller, F., Rungger, D., Clarkson, S.G., 1987. Structure and transcription termination of a lysine tRNA gene from Xenopus laevis. J. Mol. Biol. 195, 835–45. doi:0022-2836(87)90488-8 [pii]

McCraith, S.M., Phizicky, E.M., 1991. An enzyme from Saccharomyces cerevisiae uses NAD+ to transfer the splice junction 2'-phosphate from ligated tRNA to an acceptor molecule. J. Biol. Chem. 266, 11986–92.

McCraith, S.M., Phizicky, E.M., 1990. A highly specific phosphatase from Saccharomyces cerevisiae implicated in tRNA splicing. Mol. Cell. Biol. 10, 1049–55.

Meerovitch, K., Pelletier, J., Sonenberg, N., 1989. A cellular protein that binds to the 5'-noncoding region of poliovirus RNA: implications for internal translation initiation. Genes Dev. 3, 1026–1034. doi:10.1101/gad.3.7.1026

Meerovitch, K., Svitkin, Y. V, Lee, H.S., Lejbkowicz, F., Kenan, D.J., Chan, E.K., Agol, V.I., Keene, J.D., Sonenberg, N., 1993. La autoantigen enhances and corrects aberrant translation of poliovirus RNA in reticulocyte lysate. J. Virol. 67, 3798–807.

Megel, C., Morelle, G., Lalande, S., Duchêne, A.-M., Small, I., Maréchal-Drouard, L., 2015. Surveillance and cleavage of eukaryotic tRNAs. Int. J. Mol. Sci. 16, 1873–93. doi:10.3390/ijms16011873

Mei, Y., Yong, J., Liu, H., Shi, Y., Meinkoth, J., Dreyfuss, G., Yang, X., 2010. tRNA Binds to Cytochrome c and Inhibits Caspase Activation. Mol. Cell 37, 668–678. doi:10.1016/j.molcel.2010.01.023

Meiri, E., Levy, A., Benjamin, H., Ben-David, M., Cohen, L., Dov, A., Dromi, N., Elyakim, E., Yerushalmi, N., Zion, O., Lithwick-Yanai, G., Sitbon, E., 2010. Discovery of microRNAs and other small RNAs in solid tumors. Nucleic Acids Res. 38, 6234–6246. doi:10.1093/nar/gkq376

Meister, G., Landthaler, M., Patkaniowska, A., Dorsett, Y., Teng, G., Tuschl, T., 2004. Human Argonaute2 Mediates RNA Cleavage Targeted by miRNAs and siRNAs. Mol. Cell 15, 185–197. doi:10.1016/j.molcel.2004.07.007

Meister, G., Landthaler, M., Peters, L., Chen, P.Y., Urlaub, H., Lührmann, R., Tuschl, T., 2005. Identification of Novel Argonaute-Associated Proteins. Curr. Biol. 15, 2149–2155. doi:10.1016/j.cub.2005.10.048

Melo, S.A., Moutinho, C., Ropero, S., Calin, G. a, Rossi, S., Spizzo, R., Fernandez, A.F., Davalos, V., Villanueva, A., Montoya, G., Yamamoto, H., Schwartz, S., Esteller, M., 2010. A Genetic Defect in Exportin-5 Traps Precursor MicroRNAs in the Nucleus of Cancer Cells. Cancer Cell 18, 303–315. doi:10.1016/j.ccr.2010.09.007

Melton, D.A., De Robertis, E.M., Cortese, R., 1980. Order and intracellular location of the events involved in the maturation of a spliced tRNA. Nature 284, 143–8.

Milek, M., Wyler, E., Landthaler, M., 2012. Transcriptome-wide analysis of protein–RNA interactions using high-throughput sequencing. Semin. Cell Dev. Biol. 23, 206–212. doi:10.1016/j.semcdb.2011.12.001

Mingot, J.M., Vega, S., Cano, A., Portillo, F., Nieto, M.A., 2013. eEF1A Mediates the Nuclear Export of SNAG-Containing Proteins via the Exportin5-Aminoacyl-tRNA Complex. Cell Rep. 5, 727–737. doi:10.1016/j.celrep.2013.09.030

Mishima, E., Inoue, C., Saigusa, D., Inoue, R., Ito, K., Suzuki, Y., Jinno, D., Tsukui, Y., Akamatsu, Y., Araki, M., Araki, K., Shimizu, R., Shinke, H., Suzuki, T., Takeuchi, Y., Shima, H., Akiyama, Y., Toyohara, T., Suzuki, C., Saiki, Y., Tominaga, T., Miyagi, S., Kawagisihi, N., Soga, T., Ohkubo, T., Yamamura, K., Imai, Y., Masuda, S., Sabbisetti, V., Ichimura, T., Mount, D.B., Bonventre, J. V., Ito, S., Tomioka, Y., Itoh, K., Abe, T., 2014. Conformational Change in Transfer RNA Is an Early Indicator of Acute Cellular Damage. J. Am. Soc. Nephrol. 25, 2316–2326. doi:10.1681/ASN.2013091001

Miyagawa, R., Mizuno, R., Watanabe, K., Ijiri, K., 2012. Formation of tRNA granules in the nucleus of heat-induced human cells. Biochem. Biophys. Res. Commun. 418, 149–155. doi:10.1016/j.bbrc.2011.12.150

Mohan, A., Whyte, S., Wang, X., Nashimoto, M., Levinger, L., 1999. The 3’ end CCA of mature tRNA is an antideterminant for eukaryotic 3’-tRNase. RNA 5, 245–56.

Mukerji, S.K., Deutscher, M.P., 1972. Reactions at the 3’ terminus of transfer ribonucleic acid. V. Subcellular localization and evidence for a mitochondrial transfer ribonucleic acid nucleotidyltransferase. J. Biol. Chem. 247, 481–8.

Murthi, A., Shaheen, H.H., Huang, H.-Y., Preston, M.A., Lai, T.-P., Phizicky, E.M., Hopper, A.K., 2010. Regulation of tRNA bidirectional nuclear-cytoplasmic trafficking in Saccharomyces cerevisiae. Mol. Biol. Cell 21, 639–49. doi:10.1091/mbc.E09-07-0551

Muto, A., Tashiro, S., Nakajima, O., Hoshino, H., Takahashi, S., Sakoda, E., Ikebe, D., Yamamoto, M., Igarashi, K., 2004. The transcriptional programme of antibody class switching involves the repressor Bach2. Nature 429, 566–571. doi:10.1038/nature02596

Naeeni, A.R., Conte, M.R., Bayfield, M. a, 2012. RNA chaperone activity of human La protein is mediated by variant RNA recognition motif. J. Biol. Chem. 287, 5472–82. doi:10.1074/jbc.M111.276071

Nagao, A., Suzuki, T., Katoh, T., Sakaguchi, Y., Suzuki, T., 2009. Biogenesis of glutaminyl-mt tRNAGln in human mitochondria. Proc. Natl. Acad. Sci. U. S. A. 106, 16209–14. doi:10.1073/pnas.0907602106

Nakanishi, K., Ascano, M., Gogakos, T., Ishibe-Murakami, S., Serganov, A.A., Briskin, D., Morozov, P., Tuschl, T., Patel, D.J., 2013. Eukaryote-Specific Insertion Elements Control Human ARGONAUTE Slicer Activity. Cell Rep. 3, 1893–1900. doi:10.1016/j.celrep.2013.06.010

Nakanishi, K., Weinberg, D.E., Bartel, D.P., Patel, D.J., 2012. Structure of yeast Argonaute with guide RNA. Nature 486, 368–74. doi:10.1038/nature11211

Nanbo, A., Inoue, K., Adachi-Takasawa, K., Takada, K., 2002. Epstein-Barr virus RNA confers resistance to interferon-alpha-induced apoptosis in Burkitt’s lymphoma. EMBO J. 21, 954–65. doi:10.1093/emboj/21.5.954

Nashimoto, M., 1997. Distribution of both lengths and 5’ terminal nucleotides of mammalian pre-tRNA 3’ trailers reflects properties of 3’ processing endoribonuclease. Nucleic Acids Res. 25, 1148–54.

Nedialkova, D.D., Leidel, S.A., 2015. Optimization of Codon Translation Rates via tRNA Modifications Maintains Proteome Integrity. Cell 161, 1606–18. doi:10.1016/j.cell.2015.05.022

Negrutskii, B.S., Deutscher, M.P., 1992. A sequestered pool of aminoacyl-tRNA in mammalian cells. Proc. Natl. Acad. Sci. U. S. A. 89, 3601–4.

Negrutskii, B.S., Deutscher, M.P., 1991. Channeling of aminoacyl-tRNA for protein synthesis in vivo. Proc. Natl. Acad. Sci. U. S. A. 88, 4991–5.

Németh, A., Conesa, A., Santoyo-Lopez, J., Medina, I., Montaner, D., Péterfia, B., Solovei, I., Cremer, T., Dopazo, J., Längst, G., 2010. Initial Genomics of the Human Nucleolus. PLoS Genet. 6, e1000889. doi:10.1371/journal.pgen.1000889

Nguyen, T.A., Jo, M.H., Choi, Y.-G., Park, J., Kwon, S.C., Hohng, S., Kim, V.N., Woo, J.-S., 2015. Functional Anatomy of the Human Microprocessor. Cell 161, 1374–1387. doi:10.1016/j.cell.2015.05.010

Nielsen, S., Yuzenkova, Y., Zenkin, N., 2013. Mechanism of Eukaryotic RNA Polymerase III Transcription Termination. Science (80-.). 340, 1577–1580. doi:10.1126/science.1237934

Nielsen, S., Zenkin, N., 2014. Response to Comment on "Mechanism of eukaryotic RNA polymerase III transcription termination." Science (80-.). 345, 524–524. doi:10.1126/science.1254246

Nissen, P., Kjeldgaard, M., Thirup, S. r., Polekhina, G., Reshetnikova, L., Clark, B.F.C., Nyborg, J., 1995. Crystal Structure of the Ternary Complex of Phe-tRNAPhe, EF-Tu, and a GTP Analog. Science (80-.). 270, 1464–1472. doi:10.1126/science.270.5241.1464

Noland, C.L., Ma, E., Doudna, J.A., 2011. siRNA Repositioning for Guide Strand Selection by Human Dicer Complexes. Mol. Cell 43, 110–121. doi:10.1016/j.molcel.2011.05.028

Noon, K.R., Guymon, R., Crain, P.F., McCloskey, J.A., Thomm, M., Lim, J., Cavicchioli, R., 2003. Influence of Temperature on tRNA Modification in Archaea: Methanococcoides burtonii (Optimum Growth Temperature [Topt], 23 C) and Stetteria hydrogenophila (Topt, 95 C). J. Bacteriol. 185, 5483–5490. doi:10.1128/JB.185.18.5483-5490.2003

O'Connor, J.P., Peebles, C.L., 1991. In vivo pre-tRNA processing in Saccharomyces cerevisiae. Mol. Cell. Biol. 11, 425–439. doi:10.1128/MCB.11.1.425

Ogawa, T., Tomita, K., Ueda, T., Watanabe, K., Uozumi, T., Masaki, H., 1999. A cytotoxic ribonuclease targeting specific transfer RNA anticodons. Science (80-.). 283, 2097–100.

Ohndorf, U.-M., Steegborn, C., Knijff, R., Sondermann, P., 2001. Contributions of the Individual Domains in Human La Protein to Its RNA 3′-End Binding Activity. J. Biol. Chem. 276, 27188–27196. doi:10.1074/jbc.M102891200

Okada, C., Yamashita, E., Lee, S.J., Shibata, S., Katahira, J., Nakagawa, A., Yoneda, Y., Tsukihara, T., 2009. A high-resolution structure of the pre-microRNA nuclear export machinery. Science 326, 1275–9. doi:10.1126/science.1178705

Okamura, K., Hagen, J.W., Duan, H., Tyler, D.M., Lai, E.C., 2007. The Mirtron Pathway Generates microRNA-Class Regulatory RNAs in Drosophila. Cell 130, 89–100. doi:10.1016/j.cell.2007.06.028

Okamura, K., Lai, E.C., 2008. Endogenous small interfering RNAs in animals. Nat. Rev. Mol. Cell Biol. 9, 673–678. doi:10.1038/nrm2479

Oler, A.J., Alla, R.K., Roberts, D.N., Wong, A., Hollenhorst, P.C., Chandler, K.J., Cassiday, P. a, Nelson, C. a, Hagedorn, C.H., Graves, B.J., Cairns, B.R., 2010. Human RNA polymerase III transcriptomes and relationships to Pol II promoter chromatin and enhancer-binding factors. Nat. Struct. Mol. Biol. 17, 620–8. doi:10.1038/nsmb.1801

Orioli, A., 2017. tRNA biology in the omics era: Stress signalling dynamics and cancer progression. BioEssays 39, 1600158. doi:10.1002/bies.201600158

Orioli, A., Pascali, C., Quartararo, J., Diebel, K.W., Praz, V., Romascano, D., Percudani, R., van Dyk, L.F., Hernandez, N., Teichmann, M., Dieci, G., 2011. Widespread occurrence of non-canonical transcription termination by human RNA polymerase III. Nucleic Acids Res. 39, 5499–512. doi:10.1093/nar/gkr074

Ott, C.A., Linck, L., Kremmer, E., Meister, G., Bosserhoff, A.K., 2016. Induction of exportin-5 expression during melanoma development supports the cellular behavior of human malignant melanoma cells. Oncotarget 7, 62292–62304. doi:10.18632/oncotarget.11410

Oyake, T., Itoh, K., Motohashi, H., Hayashi, N., Hoshino, H., Nishizawa, M., Yamamoto, M., Igarashi, K., 1996. Bach proteins belong to a novel family of BTB-basic leucine zipper transcription factors that interact with MafK and regulate transcription through the NF-E2 site. Mol. Cell. Biol. 16, 6083–6095. doi:10.1128/MCB.16.11.6083

Ozanick, S.G., Wang, X., Costanzo, M., Brost, R.L., Boone, C., Anderson, J.T., 2009. Rex1p deficiency leads to accumulation of precursor initiator tRNAMet and polyadenylation of substrate RNAs in Saccharomyces cerevisiae. Nucleic Acids Res. 37, 298–308. doi:10.1093/nar/gkn925

Pall, G.S., Hamilton, A.J., 2008. Improved northern blot method for enhanced detection of small RNA. Nat. Protoc. 3, 1077–1084. doi:10.1038/nprot.2008.67

Pang, Y.L.J., Abo, R., Levine, S.S., Dedon, P.C., 2014. Diverse cell stresses induce unique patterns of tRNA up- and down-regulation: tRNA-seq for quantifying changes in tRNA copy number. Nucleic Acids Res. 42, e170. doi:10.1093/nar/gku945

Pannone, B.K., Xue, D., Wolin, S.L., 1998. A role for the yeast La protein in U6 snRNP assembly: Evidence that the La protein is a molecular chaperone for RNA polymerase III transcripts. EMBO J. 17, 7442–7453. doi:10.1093/emboj/17.24.7442

Park, B.-J., Kang, J.W., Lee, S.W., Choi, S.-J., Shin, Y.K., Ahn, Y.H., Choi, Y.H., Choi, D., Lee, K.S., Kim, S., 2005. The haploinsufficient tumor suppressor p18 upregulates p53 via interactions with ATM/ATR. Cell 120, 209–21. doi:10.1016/j.cell.2004.11.054

Park, J.-E., Heo, I., Tian, Y., Simanshu, D.K., Chang, H., Jee, D., Patel, D.J., Kim, V.N., 2011. Dicer recognizes the 5′ end of RNA for efficient and accurate processing. Nature 475, 201–205. doi:10.1038/nature10198

Parrott, A.M., Mathews, M.B., 2007. Novel rapidly evolving hominid RNAs bind nuclear factor 90 and display tissue-restricted distribution. Nucleic Acids Res. 35, 6249–6258. doi:10.1093/nar/gkm668

Paushkin, S. V, Patel, M., Furia, B.S., Peltz, S.W., Trotta, C.R., 2004. Identification of a human endonuclease complex reveals a link between tRNA splicing and pre-mRNA

3’ end formation. Cell 117, 311–21.

Peebles, C.L., Gegenheimer, P., Abelson, J., 1983. Precise excision of intervening sequences from precursor tRNAs by a membrane-associated yeast endonuclease. Cell 32, 525–36.

Pekarsky, Y., Balatti, V., Palamarchuk, A., Rizzotto, L., Veneziano, D., Nigita, G., Rassenti, L.Z., Pass, H.I., Kipps, T.J., Liu, C., Croce, C.M., 2016. Dysregulation of a family of short noncoding RNAs, tsRNAs, in human cancer. Proc. Natl. Acad. Sci. 113, 5071–5076. doi:10.1073/pnas.1604266113

Pellegrini, O., Nezzar, J., Marchfelder, A., Putzer, H., Condon, C., 2003. Endonucleolytic processing of CCA-less tRNA precursors by RNase Z in Bacillus subtilis. EMBO J. 22, 4534–43. doi:10.1093/emboj/cdg435

Perkins, K.K., Furneaux, H., Hurwitz, J., 1985. Isolation and characterization of an RNA ligase from HeLa cells. Proc. Natl. Acad. Sci. U. S. A. 82, 684–8.

Persson, H., Kvist, A., Vallon-Christersson, J., Medstrand, P., Borg, A., Rovira, C., 2009. The non-coding RNA of the multidrug resistance-linked vault particle encodes multiple regulatory small RNAs. Nat. Cell Biol. 11, 1268–71. doi:10.1038/ncb1972

Perwez, T., Kushner, S.R., 2006. RNase Z in Escherichia coli plays a significant role in mRNA decay. Mol. Microbiol. 60, 723–37. doi:10.1111/j.1365-2958.2006.05124.x

Petz, M., Them, N., Huber, H., Beug, H., Mikulits, W., 2012. La enhances IRES-mediated translation of laminin B1 during malignant epithelial to mesenchymal transition. Nucleic Acids Res. 40, 290–302. doi:10.1093/nar/gkr717

Pfaff, J., Hennig, J., Herzog, F., Aebersold, R., Sattler, M., Niessing, D., Meister, G., 2013. Structural features of Argonaute-GW182 protein interactions. Proc. Natl. Acad. Sci. 110, E3770–E3779. doi:10.1073/pnas.1308510110

Popow, J., Englert, M., Weitzer, S., Schleiffer, A., Mierzwa, B., Mechtler, K., Trowitzsch, S., Will, C.L., Lührmann, R., Söll, D., Martinez, J., 2011. HSPC117 is the essential subunit of a human tRNA splicing ligase complex. Science 331, 760–4. doi:10.1126/science.1197847

Popow, J., Jurkin, J., Schleiffer, A., Martinez, J., 2014. Analysis of orthologous groups reveals archease and DDX1 as tRNA splicing factors. Nature 511, 104–7. doi:10.1038/nature13284

Quax, T.E.F., Claassens, N.J., Söll, D., van der Oost, J., 2015. Codon Bias as a Means to Fine-Tune Gene Expression. Mol. Cell 59, 149–161. doi:10.1016/j.molcel.2015.05.035

Quevillon, S., Agou, F., Robinson, J.C., Mirande, M., 1997. The p43 component of the mammalian multi-synthetase complex is likely to be the precursor of the endothelial monocyte-activating polypeptide II cytokine. J. Biol. Chem. 272, 32573–9.

Quevillon, S., Mirande, M., 1996. The p18 component of the multisynthetase complex shares a protein motif with the beta and gamma subunits of eukaryotic elongation factor 1. FEBS Lett. 395, 63–7.

Quevillon, S., Robinson, J.C., Berthonneau, E., Siatecka, M., Mirande, M., 1999. Macromolecular assemblage of aminoacyl-tRNA synthetases: identification of protein-protein interactions and characterization of a core protein. J. Mol. Biol. 285, 183–95. doi:10.1006/jmbi.1998.2316

Raab, J.R., Chiu, J., Zhu, J., Katzman, S., Kurukuti, S., Wade, P. a, Haussler, D., Kamakaka, R.T., 2012. Human tRNA genes function as chromatin insulators. EMBO J. 31, 330–350. doi:10.1038/emboj.2011.406

Raabe, C.A., Tang, T.-H., Brosius, J., Rozhdestvensky, T.S., 2014. Biases in small RNA deep sequencing data. Nucleic Acids Res. 42, 1414–1426. doi:10.1093/nar/gkt1021

Randau, L., Calvin, K., Hall, M., Yuan, J., Podar, M., Li, H., Söll, D., 2005a. The heteromeric Nanoarchaeum equitans splicing endonuclease cleaves noncanonical bulge-helix-bulge motifs of joined tRNA halves. Proc. Natl. Acad. Sci. U. S. A. 102, 17934–9. doi:10.1073/pnas.0509197102

Randau, L., Münch, R., Hohn, M.J., Jahn, D., Söll, D., 2005b. Nanoarchaeum equitans creates functional tRNAs from separate genes for their 5'- and 3'-halves. Nature 433, 537–41. doi:10.1038/nature03233

Rauhut, R., Green, P.R., Abelson, J., 1990. Yeast tRNA-splicing endonuclease is a heterotrimeric enzyme. J. Biol. Chem. 265, 18180–4.

Reese, C.B., Trentham, D.R., 1965. 2'-O-acyl ribonucleoside derivatives. Tetrahedron Lett. 6, 2459–65. doi:10.1016/S0040-4039(01)84007-7

Reich, P.R., Forget, B.G., Weissman, S.M., Rose, J.A., 1966. RNA of low molecular weight in KB cells infected with adenovirus type 2. J. Mol. Biol. 17, 428–439. doi:10.1016/S0022-2836(66)80153-5

Reiner, R., Ben-Asouli, Y., Krilovetzky, I., Jarrous, N., 2006. A role for the catalytic ribonucleoprotein RNase P in RNA polymerase III transcription. Genes Dev. 20, 1621–35. doi:10.1101/gad.386706

Reinhard, L., Sridhara, S., Hällberg, B.M., 2017. The MRPP1/MRPP2 complex is a tRNA-maturation platform in human mitochondria. Nucleic Acids Res. 45, 12469–12480. doi:10.1093/nar/gkx902

Reyes, V.M., Abelson, J., 1988. Substrate recognition and splice site determination in yeast tRNA splicing. Cell 55, 719–30.

Rijal, K., Maraia, R.J., Arimbasseri, A.G., 2015. A methods review on use of nonsense suppression to study 3' end formation and other aspects of tRNA biogenesis. Gene 556, 35–50. doi:10.1016/j.gene.2014.11.034

Rosa, M.D., Gottlieb, E., Lerner, M.R., Steitz, J.A., 1981. Striking similarities are exhibited by two small Epstein-Barr virus-encoded ribonucleic acids and the adenovirus-associated ribonucleic acids VAI and VAII. Mol. Cell. Biol. 1, 785–796. doi:10.1128/MCB.1.9.785

Rosenthal, L.J., Zamecnik, P.C., 1973. Amino-Acid Acceptor Activity of the "70S-Associated" 4S RNA from Avian Myeloblastosis Virus. Proc. Natl. Acad. Sci. 70, 1184–1185. doi:10.1073/pnas.70.4.1184

Rosewick, N., Momont, M., Durkin, K., Takeda, H., Caiment, F., Cleuter, Y., Vernin, C., Mortreux, F., Wattel, E., Burny, A., Georges, M., Van den Broeke, A., 2013. Deep sequencing reveals abundant noncanonical retroviral microRNAs in B-cell leukemia/lymphoma. Proc. Natl. Acad. Sci. 110, 2306–2311. doi:10.1073/pnas.1213842110

Rossmanith, W., 2011. Localization of human RNase Z isoforms: dual nuclear/mitochondrial targeting of the ELAC2 gene product by alternative

translation initiation. PLoS One 6, e19152. doi:10.1371/journal.pone.0019152

Roy, A., Zhang, M., Saad, Y., Kolattukudy, P.E., 2013. Antidicer RNAse activity of monocyte chemotactic protein-induced protein-1 is critical for inducing angiogenesis. Am. J. Physiol. Physiol. 305, C1021–C1032. doi:10.1152/ajpcell.00203.2013

Roychoudhuri, R., Hirahara, K., Mousavi, K., Clever, D., Klebanoff, C.A., Bonelli, M., Sciumè, G., Zare, H., Vahedi, G., Dema, B., Yu, Z., Liu, H., Takahashi, H., Rao, M., Muranski, P., Crompton, J.G., Punkosdy, G., Bedognetti, D., Wang, E., Hoffmann, V., Rivera, J., Marincola, F.M., Nakamura, A., Sartorelli, V., Kanno, Y., Gattinoni, L., Muto, A., Igarashi, K., O'Shea, J.J., Restifo, N.P., 2013. BACH2 represses effector programs to stabilize Treg-mediated immune homeostasis. Nature 498, 506–510. doi:10.1038/nature12199

Ruby, J.G., Jan, C.H., Bartel, D.P., 2007. Intronic microRNA precursors that bypass Drosha processing. Nature 448, 83–86. doi:10.1038/nature05983

Rüdel, S., Flatley, A., Weinmann, L., Kremmer, E., Meister, G., 2008. A multifunctional human Argonaute2-specific monoclonal antibody. RNA 14, 1244–1253. doi:10.1261/rna.973808

Russo, N., Acharya, K.R., Vallee, B.L., Shapiro, R., 1996. A combined kinetic and modeling study of the catalytic center subsites of human angiogenin. Proc. Natl. Acad. Sci. 93, 804–8.

Rybak-Wolf, A., Jens, M., Murakawa, Y., Herzog, M., Landthaler, M., Rajewsky, N., 2014. A Variety of Dicer Substrates in Human and C. elegans. Cell 159, 1153–1167. doi:10.1016/j.cell.2014.10.040

Safro, M., Klipcan, L., 2013. The mechanistic and evolutionary aspects of the 2'- and 3'-OH paradigm in biosynthetic machinery. Biol. Direct 8, 17. doi:10.1186/1745-6150-8-17

Saikia, M., Jobava, R., Parisien, M., Putnam, A., Krokowski, D., Gao, X.-H., Guan, B.-J., Yuan, Y., Jankowsky, E., Feng, Z., Hu, G. -f., Pusztai-Carey, M., Gorla, M., Sepuri, N.B. V., Pan, T., Hatzoglou, M., 2014. Angiogenin-Cleaved tRNA Halves Interact with Cytochrome c, Protecting Cells from Apoptosis during Osmotic Stress. Mol. Cell. Biol. 34, 2450–2463. doi:10.1128/MCB.00136-14

Samanta, M., Iwakiri, D., Kanda, T., Imaizumi, T., Takada, K., 2006. EB virus-encoded RNAs are recognized by RIG-I and activate signaling to induce type I IFN. EMBO J. 25, 4207–4214. doi:10.1038/sj.emboj.7601314

Sarkar, S., Azad, A.K., Hopper, A.K., 1999. Nuclear tRNA aminoacylation and its role in nuclear export of endogenous tRNAs in Saccharomyces cerevisiae. Proc. Natl. Acad. Sci. U. S. A. 96, 14366–71.

Saxena, S.K., Rybak, S.M., Davey, R.T., Youle, R.J., Ackerman, E.J., 1992. Angiogenin is a cytotoxic, tRNA-specific ribonuclease in the RNase A superfamily. J. Biol. Chem. 267, 21982–6.

Schaefer, M., Pollex, T., Hanna, K., Tuorto, F., Meusburger, M., Helm, M., Lyko, F., 2010. RNA methylation by Dnmt2 protects transfer RNAs against stress-induced cleavage. Genes Dev. 24, 1590–1595. doi:10.1101/gad.586710

Schaffer, A.E., Eggens, V.R.C., Caglayan, A.O., Reuter, M.S., Scott, E., Coufal, N.G.,

Silhavy, J.L., Xue, Y., Kayserili, H., Yasuno, K., Rosti, R.O., Abdellateef, M., Caglar, C., Kasher, P.R., Cazemier, J.L., Weterman, M.A., Cantagrel, V., Cai, N., Zweier, C., Altunoglu, U., Satkin, N.B., Aktar, F., Tuysuz, B., Yalcinkaya, C., Caksen, H., Bilguvar, K., Fu, X.-D., Trotta, C.R., Gabriel, S., Reis, A., Gunel, M., Baas, F., Gleeson, J.G., 2014. CLP1 Founder Mutation Links tRNA Splicing and Maturation to Cerebellar Development and Neurodegeneration. Cell 157, 651–663. doi:10.1016/j.cell.2014.03.049

Schimmel, P., 2017. The emerging complexity of the tRNA world: mammalian tRNAs beyond protein synthesis. Nat. Rev. Mol. Cell Biol. 19, 45–58. doi:10.1038/nrm.2017.77

Schirle, N.T., MacRae, I.J., 2012. The Crystal Structure of Human Argonaute2. Science (80-.). 336, 1037–1040. doi:10.1126/science.1221551

Schirle, N.T., Sheu-Gruttadauria, J., MacRae, I.J., 2014. Structural basis for microRNA targeting. Science (80-.). 346, 608–613. doi:10.1126/science.1258040

Schneider, C., Kudla, G., Wlotzka, W., Tuck, A., Tollervey, D., 2012. Transcriptome-wide Analysis of Exosome Targets. Mol. Cell 48, 422–433. doi:10.1016/j.molcel.2012.08.013

Schön, A., Kannangara, C.G., Gough, S., Söll, D., 1988. Protein biosynthesis in organelles requires misaminoacylation of tRNA. Nature 331, 187–90. doi:10.1038/331187a0

Schön, A., Krupp, G., Gough, S., Berry-Lowe, S., Kannangara, C.G., Söll, D., 1986. The RNA required in the first step of chlorophyll biosynthesis is a chloroplast glutamate tRNA. Nature 322, 281–284. doi:10.1038/322281a0

Schopman, N.C.T., Heynen, S., Haasnoot, J., Berkhout, B., 2010. A miRNA-tRNA mix-up: tRNA origin of proposed miRNA. RNA Biol. 7, 573–6. doi:10.4161/rna.7.4.13141

Schorn, A.J., Gutbrod, M.J., LeBlanc, C., Martienssen, R., 2017. LTR-Retrotransposon Control by tRNA-Derived Small RNAs. Cell 170, 61–71.e11. doi:10.1016/j.cell.2017.06.013

Schraivogel, D., Schindler, S.G., Danner, J., Kremmer, E., Pfaff, J., Hannus, S., Depping, R., Meister, G., 2015. Importin-β facilitates nuclear import of human GW proteins and balances cytoplasmic gene silencing protein levels. Nucleic Acids Res. 43, 7447–7461. doi:10.1093/nar/gkv705

Schramm, L., Hernandez, N., 2002. Recruitment of RNA polymerase III to its target promoters. Genes Dev. 16, 2593–620. doi:10.1101/gad.1018902

Schwarz, D.S., Hutvágner, G., Du, T., Xu, Z., Aronin, N., Zamore, P.D., 2003. Asymmetry in the Assembly of the RNAi Enzyme Complex. Cell 115, 199–208. doi:10.1016/S0092-8674(03)00759-1

Selitsky, S.R., Baran-Gale, J., Honda, M., Yamane, D., Masaki, T., Fannin, E.E., Guerra, B., Shirasaki, T., Shimakami, T., Kaneko, S., Lanford, R.E., Lemon, S.M., Sethupathy, P., 2015. Small tRNA-derived RNAs are increased and more abundant than microRNAs in chronic hepatitis B and C. Sci. Rep. 5, 7675. doi:10.1038/srep07675

Shaheen, H.H., Hopper, A.K., 2005. Retrograde movement of tRNAs from the cytoplasm

to the nucleus in Saccharomyces cerevisiae. Proc. Natl. Acad. Sci. 102, 11290–11295. doi:10.1073/pnas.0503836102

Shaheen, H.H., Horetsky, R.L., Kimball, S.R., Murthi, A., Jefferson, L.S., Hopper, A.K., 2007. Retrograde nuclear accumulation of cytoplasmic tRNA in rat hepatoma cells in response to amino acid deprivation. Proc. Natl. Acad. Sci. U. S. A. 104, 8845–50. doi:10.1073/pnas.0700765104

Sharma, K., Fabre, E., Tekotte, H., Hurt, E.C., Tollervey, D., 1996. Yeast nucleoporin mutants are defective in pre-tRNA splicing. Mol. Cell. Biol. 16, 294–301.

Sharma, U., Conine, C.C., Shea, J.M., Boskovic, A., Derr, A.G., Bing, X.Y., Belleannee, C., Kucukural, A., Serra, R.W., Sun, F., Song, L., Carone, B.R., Ricci, E.P., Li, X.Z., Fauquier, L., Moore, M.J., Sullivan, R., Mello, C.C., Garber, M., Rando, O.J., 2016. Biogenesis and function of tRNA fragments during sperm maturation and fertilization in mammals. Science (80-.). 351, 391–396. doi:10.1126/science.aad6780

Sheng, J., Xu, Z., 2016. Three decades of research on angiogenin: a review and perspective. Acta Biochim. Biophys. Sin. (Shanghai). 48, 399–410. doi:10.1093/abbs/gmv131

Shi, P.Y., Maizels, N., Weiner, A.M., 1998a. CCA addition by tRNA nucleotidyltransferase: polymerization without translocation? EMBO J. 17, 3197–206. doi:10.1093/emboj/17.11.3197

Shi, P.Y., Weiner, A.M., Maizels, N., 1998b. A top-half tDNA minihelix is a good substrate for the eubacterial CCA-adding enzyme. RNA 4, 276–84.

Shiba, K., Schimmel, P., Motegi, H., Noda, T., 1994. Human glycyl-tRNA synthetase. Wide divergence of primary structure from bacterial counterpart and species-specific aminoacylation. J. Biol. Chem. 269, 30049–55.

Shigematsu, M., Kirino, Y., 2015. tRNA-Derived Short Non-coding RNA as Interacting Partners of Argonaute Proteins. Gene Regul. Syst. Bio. 9, 27–33. doi:10.4137/GRSB.S29411

Shin, C., Nam, J.-W., Farh, K.K.-H., Chiang, H.R., Shkumatava, A., Bartel, D.P., 2010. Expanding the MicroRNA Targeting Code: Functional Sites with Centered Pairing. Mol. Cell 38, 789–802. doi:10.1016/j.molcel.2010.06.005

Sidrauski, C., Cox, J.S., Walter, P., 1996. tRNA ligase is required for regulated mRNA splicing in the unfolded protein response. Cell 87, 405–13. doi:10.1016/S0092-8674(00)81361-6

Simos, G., Tekotte, H., Grosjean, H., Segref, A., Sharma, K., Tollervey, D., Hurt, E.C., 1996. Nuclear pore proteins are involved in the biogenesis of functional tRNA. EMBO J. 15, 2270–84.

Sinha, N.K., Iwasa, J., Shen, P.S., Bass, B.L., 2018. Dicer uses distinct modules for recognizing dsRNA termini. Science (80-.). 359, 329–334. doi:10.1126/science.aaq0921

Sinha, N.K., Trettin, K.D., Aruscavage, P.J., Bass, B.L., 2015. Drosophila Dicer-2 Cleavage Is Mediated by Helicase- and dsRNA Termini-Dependent States that Are Modulated by Loquacious-PD. Mol. Cell 58, 406–417. doi:10.1016/j.molcel.2015.03.012

Skowronek, E., Grzechnik, P., Späth, B., Marchfelder, A., Kufel, J., 2014. tRNA 3' processing in yeast involves tRNase Z, Rex1, and Rrp6. RNA 20, 115–30. doi:10.1261/rna.041467.113

Smith, D.W., 1975. Reticulocyte transfer RNA and hemoglobin synthesis. Science 190, 529–35.

Sobala, A., Hutvagner, G., 2013. Small RNAs derived from the 5′ end of tRNA can inhibit protein translation in human cells. RNA Biol. 10, 553–563. doi:10.4161/rna.24285

Söderlund, H., Pettersson, U., Vennström, B., Philipson, L., Mathews, M.B., 1976. A new species of virus-coded low molecular weight RNA from cells infected with adenovirus type 2. Cell 7, 585–593. doi:10.1016/0092-8674(76)90209-9

Soifer, H.S., Sano, M., Sakurai, K., Chomchan, P., Sætrom, P., Sherman, M.A., Collingwood, M.A., Behlke, M.A., Rossi, J.J., 2008. A role for the Dicer helicase domain in the processing of thermodynamically unstable hairpin RNAs. Nucleic Acids Res. 36, 6511–6522. doi:10.1093/nar/gkn687

Solari, A., Deutscher, M.P., 1982. Subcellular localization of the tRNA processing enzyme, tRNA nucleotidyltransferase, in Xenopus laevis oocytes and in somatic cells. Nucleic Acids Res. 10, 4397–407.

Sommer, G., Dittmann, J., Kuehnert, J., Reumann, K., Schwartz, P.E., Will, H., Coulter, B.L., Smith, M.T., Heise, T., 2011. The RNA-binding protein La contributes to cell proliferation and CCND1 expression. Oncogene 30, 434–444. doi:10.1038/onc.2010.425

Song, J.-J., Smith, S.K., Hannon, G.J., Joshua-Tor, L., 2004. Crystal structure of Argonaute and its implications for RISC slicer activity. Science (80-.). 305, 1434–7. doi:10.1126/science.1102514

Späth, B., Canino, G., Marchfelder, A., 2007. tRNase Z: the end is not in sight. Cell. Mol. Life Sci. 64, 2404–12. doi:10.1007/s00018-007-7160-5

Speer, J., Gehrke, C.W., Kuo, K.C., Waalkes, T.P., Borek, E., 1979. tRNA breakdown products as markers for cancer. Cancer 44, 2120–3.

Sprinzl, M., 2006. Chemistry of aminoacylation and peptide bond formation on the 3'terminus of tRNA. J. Biosci. 31, 489–96.

Stade, K., Ford, C.S., Guthrie, C., Weis, K., 1997. Exportin 1 (Crm1p) is an essential nuclear export factor. Cell 90, 1041–50.

Stagsted, L.V.W., Daugaard, I., Hansen, T.B., 2017. The agotrons: Gene regulators or Argonaute protectors? BioEssays 39, 1600239. doi:10.1002/bies.201600239

Stapulionis, R., Deutscher, M.P., 1995. A channeled tRNA cycle during mammalian protein synthesis. Proc. Natl. Acad. Sci. U. S. A. 92, 7158–61. doi:10.1073/pnas.92.16.7158

Stolc, V., Altman, S., 1997. Rpp1, an essential protein subunit of nuclear RNase P required for processing of precursor tRNA and 35S precursor rRNA in Saccharomyces cerevisiae. Genes Dev. 11, 2926–37.

Sullivan, R., 2015. Epididymosomes: a heterogeneous population of microvesicles with multiple functions in sperm maturation and storage. Asian J. Androl. 17, 726–9.

doi:10.4103/1008-682X.155255

Suzuki, H.I., Arase, M., Matsuyama, H., Choi, Y.L., Ueno, T., Mano, H., Sugimoto, K., Miyazono, K., 2011. MCPIP1 Ribonuclease Antagonizes Dicer and Terminates MicroRNA Biogenesis through Precursor MicroRNA Degradation. Mol. Cell 44, 424–436. doi:10.1016/j.molcel.2011.09.012

Suzuki, H.I., Katsura, A., Yasuda, T., Ueno, T., Mano, H., Sugimoto, K., Miyazono, K., 2015. Small-RNA asymmetry is directly driven by mammalian Argonautes. Nat. Struct. Mol. Biol. 22, 512–521. doi:10.1038/nsmb.3050

Svitkin, Y. V, Pause, A., Sonenberg, N., 1994. La autoantigen alleviates translational repression by the 5' leader sequence of the human immunodeficiency virus type 1 mRNA. J. Virol. 68, 7001–7.

Swaminathan, S., Huang, C., Geng, H., Chen, Z., Harvey, R., Kang, H., Ng, C., Titz, B., Hurtz, C., Sadiyah, M.F., Nowak, D., Thoennissen, G.B., Rand, V., Graeber, T.G., Koeffler, H.P., Carroll, W.L., Willman, C.L., Hall, A.G., Igarashi, K., Melnick, A., Müschen, M., 2013. BACH2 mediates negative selection and p53-dependent tumor suppression at the pre-B cell receptor checkpoint. Nat. Med. 19, 1014–1022. doi:10.1038/nm.3247

Swerdlow, H., Guthrie, C., 1984. Structure of intron-containing tRNA precursors. Analysis of solution conformation using chemical and enzymatic probes. J. Biol. Chem. 259, 5197–207.

Taft, R.J., Glazov, E. a, Lassmann, T., Hayashizaki, Y., Carninci, P., Mattick, J.S., 2009. Small RNAs derived from snoRNAs. RNA 15, 1233–1240. doi:10.1261/rna.1528909

Taiji, M., Yokoyama, S., Miyazawa, T., 1985. Aminoacyl-tRNA exclusively in the 3'-isomeric form is bound to polypeptide chain elongation factor Tu. J. Biochem. 98, 1447–53.

Taiji, M., Yokoyama, S., Miyazawa, T., 1983. Transacylation rates of (aminoacyl)adenosine moiety at the 3'-terminus of aminoacyl transfer ribonucleic acid. Biochemistry 22, 3220–5.

Takaku, H., Minagawa, A., Takagi, M., Nashimoto, M., 2004. The N-terminal half-domain of the long form of tRNase Z is required for the RNase 65 activity. Nucleic Acids Res. 32, 4429–38. doi:10.1093/nar/gkh774

Takaku, H., Minagawa, A., Takagi, M., Nashimoto, M., 2003. A candidate prostate cancer susceptibility gene encodes tRNA 3' processing endoribonuclease. Nucleic Acids Res. 31, 2272–8.

Takano, A., Endo, T., Yoshihisa, T., 2005. tRNA actively shuttles between the nucleus and cytosol in yeast. Science (80-.). 309, 140–2. doi:10.1126/science.1113346

Tam, O.H., Aravin, A. a, Stein, P., Girard, A., Murchison, E.P., Cheloufi, S., Hodges, E., Anger, M., Sachidanandam, R., Schultz, R.M., Hannon, G.J., 2008. Pseudogene-derived small interfering RNAs regulate gene expression in mouse oocytes. Nature 453, 534–8. doi:10.1038/nature06904

Tamura, K., 2015. Origins and Early Evolution of the tRNA Molecule. Life 5, 1687–1699. doi:10.3390/life5041687

Tavtigian, S. V, Simard, J., Teng, D.H., Abtin, V., Baumgard, M., Beck, A., Camp, N.J., Carillo, A.R., Chen, Y., Dayananth, P., Desrochers, M., Dumont, M., Farnham, J.M.,

Frank, D., Frye, C., Ghaffari, S., Gupte, J.S., Hu, R., Iliev, D., Janecki, T., Kort, E.N., Laity, K.E., Leavitt, A., Leblanc, G., McArthur-Morrison, J., Pederson, A., Penn, B., Peterson, K.T., Reid, J.E., Richards, S., Schroeder, M., Smith, R., Snyder, S.C., Swedlund, B., Swensen, J., Thomas, A., Tranchant, M., Woodland, A.M., Labrie, F., Skolnick, M.H., Neuhausen, S., Rommens, J., Cannon-Albright, L.A., 2001. A candidate prostate cancer susceptibility gene at chromosome 17p. Nat. Genet. 27, 172–80. doi:10.1038/84808

Taylor, D.W., Ma, E., Shigematsu, H., Cianfrocco, M.A., Noland, C.L., Nagayama, K., Nogales, E., Doudna, J.A., Wang, H.-W., 2013. Substrate-specific structural rearrangements of human Dicer. Nat. Struct. Mol. Biol. 20, 662–670. doi:10.1038/nsmb.2564

Telonis, A.G., Loher, P., Honda, S., Jing, Y., Palazzo, J., Kirino, Y., Rigoutsos, I., 2015. Dissecting tRNA-derived fragment complexities using personalized transcriptomes reveals novel fragment classes and unexpected dependencies. Oncotarget 6, 24797–24822. doi:10.18632/oncotarget.4695

Telonis, A.G., Loher, P., Kirino, Y., Rigoutsos, I., 2014. Nuclear and mitochondrial tRNA-lookalikes in the human genome. Front. Genet. 5, 1–11. doi:10.3389/fgene.2014.00344

Teplova, M., Yuan, Y.-R., Phan, A.T., Malinina, L., Ilin, S., Teplov, A., Patel, D.J., 2006. Structural basis for recognition and sequestration of UUU(OH) 3’ temini of nascent RNA polymerase III transcripts by La, a rheumatic disease autoantigen. Mol. Cell 21, 75–85. doi:10.1016/j.molcel.2005.10.027

Thompson, D.M., Lu, C., Green, P.J., Parker, R., 2008. tRNA cleavage is a conserved response to oxidative stress in eukaryotes. RNA 14, 2095–2103. doi:10.1261/rna.1232808

Thompson, D.M., Parker, R., 2009. The RNase Rny1p cleaves tRNAs and promotes cell death during oxidative stress in Saccharomyces cerevisiae. J. Cell Biol. 185, 43–50. doi:10.1083/jcb.200811119

Thompson, L.D., Daniels, C.J., 1990. Recognition of exon-intron boundaries by the Halobacterium volcanii tRNA intron endonuclease. J. Biol. Chem. 265, 18104–11.

Thompson, M., Haeusler, R.A., Good, P.D., Engelke, D.R., 2003. Nucleolar Clustering of Dispersed tRNA Genes. Science (80-.). 302, 1399–1401. doi:10.1126/science.1089814

Thomson, D.W., Pillman, K. a., Anderson, M.L., Lawrence, D.M., Toubia, J., Goodall, G.J., Bracken, C.P., 2014. Assessing the gene regulatory properties of Argonaute-bound small RNAs of diverse genomic origin. Nucleic Acids Res. 43, 470–481. doi:10.1093/nar/gku1242

Tian, Y., Simanshu, D.K., Ma, J.-B., Park, J.-E., Heo, I., Kim, V.N., Patel, D.J., 2014. A Phosphate-Binding Pocket within the Platform-PAZ-Connector Helix Cassette of Human Dicer. Mol. Cell 53, 606–616. doi:10.1016/j.molcel.2014.01.003

Till, S., Lejeune, E., Thermann, R., Bortfeld, M., Hothorn, M., Enderle, D., Heinrich, C., Hentze, M.W., Ladurner, A.G., 2007. A conserved motif in Argonaute-interacting proteins mediates functional interactions through the Argonaute PIWI domain. Nat. Struct. Mol. Biol. 14, 897–903. doi:10.1038/nsmb1302

Tolkunova, E., Park, H., Xia, J., King, M.P., Davidson, E., 2000. The Human Lysyl-

tRNA Synthetase Gene Encodes Both the Cytoplasmic and Mitochondrial Enzymes by Means of an Unusual Alternative Splicing of the Primary Transcript. J. Biol. Chem. 275, 35063–35069. doi:10.1074/jbc.M006265200

Tomita, K., Fukai, S., Ishitani, R., Ueda, T., Takeuchi, N., Vassylyev, D.G., Nureki, O., 2004. Structural basis for template-independent RNA polymerization. Nature 430, 700–4. doi:10.1038/nature02712

Tomita, K., Ogawa, T., Uozumi, T., Watanabe, K., Masaki, H., 2000. A cytotoxic ribonuclease which specifically cleaves four isoaccepting arginine tRNAs at their anticodon loops. Proc. Natl. Acad. Sci. 97, 8278–8283. doi:10.1073/pnas.140213797

Torres, A.G., Batlle, E., Ribas de Pouplana, L., 2014. Role of tRNA modifications in human diseases. Trends Mol. Med. 20, 306–14. doi:10.1016/j.molmed.2014.01.008

Trotta, C.R., Miao, F., Arn, E.A., Stevens, S.W., Ho, C.K., Rauhut, R., Abelson, J.N., 1997. The yeast tRNA splicing endonuclease: a tetrameric enzyme with two active site subunits homologous to the archaeal tRNA endonucleases. Cell 89, 849–58.

Trotta, C.R., Paushkin, S. V, Patel, M., Li, H., Peltz, S.W., 2006. Cleavage of pre-tRNAs by the splicing endonuclease requires a composite active site. Nature 441, 375–7. doi:10.1038/nature04741

Trotta, R., Vignudelli, T., Candini, O., Intine, R. V, Pecorari, L., Guerzoni, C., Santilli, G., Byrom, M.W., Goldoni, S., Ford, L.P., Caligiuri, M.A., Maraia, R.J., Perrotti, D., Calabretta, B., 2003. BCR/ABL activates mdm2 mRNA translation via the La antigen. Cancer Cell 3, 145–60.

Tsuboi, T., Yamazaki, R., Nobuta, R., Ikeuchi, K., Makino, S., Ohtaki, A., Suzuki, Y., Yoshihisa, T., Trotta, C., Inada, T., 2015. The tRNA Splicing Endonuclease Complex Cleaves the Mitochondria-localized CBP1 mRNA. J. Biol. Chem. 290, 16021–30. doi:10.1074/jbc.M114.634592

Tsukumo, S. -i., Unno, M., Muto, A., Takeuchi, A., Kometani, K., Kurosaki, T., Igarashi, K., Saito, T., 2013. Bach2 maintains T cells in a naive state by suppressing effector memory-related genes. Proc. Natl. Acad. Sci. 110, 10735–10740. doi:10.1073/pnas.1306691110

Tumbula, D., Vothknecht, U.C., Kim, H.S., Ibba, M., Min, B., Li, T., Pelaschier, J., Stathopoulos, C., Becker, H., Söll, D., 1999. Archaeal aminoacyl-tRNA synthesis: diversity replaces dogma. Genetics 152, 1269–76.

Turowski, T.W., Karkusiewicz, I., Kowal, J., Boguta, M., 2012. Maf1-mediated repression of RNA polymerase III transcription inhibits tRNA degradation via RTD pathway. RNA 18, 1823–1832. doi:10.1261/rna.033597.112

Tycowski, K.T., Guo, Y.E., Lee, N., Moss, W.N., Vallery, T.K., Xie, M., Steitz, J.A., 2015. Viral noncoding RNAs: more surprises. Genes Dev. 29, 567–84. doi:10.1101/gad.259077.115

Ussery, M.A., Tanaka, W.K., Hardesty, B., 1977. Subcellular distribution of aminoacyl-tRNA synthetases in various eukaryotic cells. Eur. J. Biochem. 72, 491–500.

van Hoof, A., Lennertz, P., Parker, R., 2000. Three conserved members of the RNase D family have unique and overlapping functions in the processing of 5S, 5.8S, U4, U5, RNase MRP and RNase P RNAs in yeast. EMBO J. 19, 1357–65. doi:10.1093/emboj/19.6.1357

Volta, V., Ceci, M., Emery, B., Bachi, A., Petfalski, E., Tollervey, D., Linder, P., Marchisio, P.C., Piatti, S., Biffo, S., 2005. Sen34p depletion blocks tRNA splicing in vivo and delays rRNA processing. Biochem. Biophys. Res. Commun. 337, 89–94. doi:10.1016/j.bbrc.2005.09.012

Waldron, C., Lacroute, F., 1975. Effect of growth rate on the amounts of ribosomal and transfer ribonucleic acids in yeast. J. Bacteriol. 122, 855–65.

Wang, H.-W., Noland, C., Siridechadilok, B., Taylor, D.W., Ma, E., Felderer, K., Doudna, J.A., Nogales, E., 2009. Structural insights into RNA processing by the human RISC-loading complex. Nat. Struct. Mol. Biol. 16, 1148–1153. doi:10.1038/nsmb.1673

Wang, Q., Lee, I., Ren, J., Ajay, S.S., Lee, Y.S., Bao, X., 2013. Identification and functional characterization of tRNA-derived RNA fragments (tRFs) in respiratory syncytial virus infection. Mol. Ther. 21, 368–79. doi:10.1038/mt.2012.237

Watanabe, K., Miyagawa, R., Tomikawa, C., Mizuno, R., Takahashi, A., Hori, H., Ijiri, K., 2013. Degradation of initiator tRNA Met by Xrn1/2 via its accumulation in the nucleus of heat-treated HeLa cells. Nucleic Acids Res. 41, 4671–4685. doi:10.1093/nar/gkt153

Watanabe, T., Totoki, Y., Toyoda, A., Kaneda, M., Kuramochi-Miyagawa, S., Obata, Y., Chiba, H., Kohara, Y., Kono, T., Nakano, T., Surani, M.A., Sakaki, Y., Sasaki, H., 2008. Endogenous siRNAs from naturally formed dsRNAs regulate transcripts in mouse oocytes. Nature 453, 539–43. doi:10.1038/nature06908

Weber, M.J., 1972. Ribosomal RNA turnover in contact inhibited cells. Nat. New Biol. 235, 58–61.

Wei, F.-Y., Suzuki, T., Watanabe, S., Kimura, S., Kaitsuka, T., Fujimura, A., Matsui, H., Atta, M., Michiue, H., Fontecave, M., Yamagata, K., Suzuki, T., Tomizawa, K., 2011. Deficit of tRNA(Lys) modification by Cdkal1 causes the development of type 2 diabetes in mice. J. Clin. Invest. 121, 3598–608. doi:10.1172/JCI58056

Weinger, J.S., Parnell, K.M., Dorner, S., Green, R., Strobel, S.A., 2004. Substrate-assisted catalysis of peptide bond formation by the ribosome. Nat. Struct. Mol. Biol. 11, 1101–6. doi:10.1038/nsmb841

Weitzer, S., Martinez, J., 2007. The human RNA kinase hClp1 is active on 3' transfer RNA exons and short interfering RNAs. Nature 447, 222–6. doi:10.1038/nature05777

Welker, N.C., Maity, T.S., Ye, X., Aruscavage, P.J., Krauchuk, A.A., Liu, Q., Bass, B.L., 2011. Dicer's Helicase Domain Discriminates dsRNA Termini to Promote an Altered Reaction Mode. Mol. Cell 41, 589–599. doi:10.1016/j.molcel.2011.02.005

Whipple, J.M., Lane, E.A., Chernyakov, I., D'Silva, S., Phizicky, E.M., 2011. The yeast rapid tRNA decay pathway primarily monitors the structural integrity of the acceptor and T-stems of mature tRNA. Genes Dev. 25, 1173–1184. doi:10.1101/gad.2050711

Wichtowska, D., Turowski, T.W., Boguta, M., 2013. An interplay between transcription, processing, and degradation determines tRNA levels in yeast. Wiley Interdiscip. Rev. RNA 4, 709–722. doi:10.1002/wrna.1190

Wilcox, M., Nirenberg, M., 1968. Transfer RNA as a cofactor coupling amino acid synthesis with that of protein. Proc. Natl. Acad. Sci. U. S. A. 61, 229–36.

Wilson, R.C., Tambe, A., Kidwell, M.A., Noland, C.L., Schneider, C.P., Doudna, J.A., 2015. Dicer-TRBP complex formation ensures accurate mammalian microRNA biogenesis. Mol. Cell 57, 397–407. doi:10.1016/j.molcel.2014.11.030

Wilusz, J.E., Whipple, J.M., Phizicky, E.M., Sharp, P. a, 2011. tRNAs marked with CCACCA are targeted for degradation. Science 334, 817–21. doi:10.1126/science.1213671

Woese, C.R., Olsen, G.J., Ibba, M., Söll, D., 2000. Aminoacyl-tRNA synthetases, the genetic code, and the evolutionary process. Microbiol. Mol. Biol. Rev. 64, 202–36.

Wolf, J., Gerber, A.P., Keller, W., 2002. tadA, an essential tRNA-specific adenosine deaminase from Escherichia coli. EMBO J. 21, 3841–51. doi:10.1093/emboj/cdf362

Wolin, S.L., Sim, S., Chen, X., 2012. Nuclear noncoding RNA surveillance: is the end in sight? Trends Genet. 28, 306–13. doi:10.1016/j.tig.2012.03.005

Woolnough, J.L., Atwood, B.L., Giles, K.E., 2015. Argonaute 2 Binds Directly to tRNA Genes and Promotes Gene Repression in cis. Mol. Cell. Biol. 35, 2278–94. doi:10.1128/MCB.00076-15

Wu, J., Bao, A., Chatterjee, K., Wan, Y., Hopper, A.K., 2015. Genome-wide screen uncovers novel pathways for tRNA processing and nuclear-cytoplasmic dynamics. Genes Dev. 29, 2633–44. doi:10.1101/gad.269803.115

Xie, M., Li, M., Vilborg, A., Lee, N., Shu, M.-D., Yartseva, V., Šestan, N., Steitz, J. a, 2013. Mammalian 5'-capped microRNA precursors that generate a single microRNA. Cell 155, 1568–80. doi:10.1016/j.cell.2013.11.027

Xie, X., Dubrovsky, E.B., 2015. Knockout of Drosophila RNase Z L impairs mitochondrial transcript processing, respiration and cell cycle progression. Nucleic Acids Res. gkv1149. doi:10.1093/nar/gkv1149

Xiong, Y., Steitz, T.A., 2004. Mechanism of transfer RNA maturation by CCA-adding enzyme without using an oligonucleotide template. Nature 430, 640–5. doi:10.1038/nature02711

Xiong, Y., Steitz, T. a, 2006. A story with a good ending: tRNA 3'-end maturation by CCA-adding enzymes. Curr. Opin. Struct. Biol. 16, 12–7. doi:10.1016/j.sbi.2005.12.001

Xu, Q., Teplow, D., Lee, T.D., Abelson, J., 1990. Domain structure in yeast tRNA ligase. Biochemistry 29, 6132–8.

Xue, S., Calvin, K., Li, H., 2006. RNA recognition and cleavage by a splicing endonuclease. Science 312, 906–10. doi:10.1126/science.1126629

Yamasaki, S., Ivanov, P., Hu, G.-F., Anderson, P., 2009. Angiogenin cleaves tRNA and promotes stress-induced translational repression. J. Cell Biol. 185, 35–42. doi:10.1083/jcb.200811106

Yang, J.-S., Maurin, T., Robine, N., Rasmussen, K.D., Jeffrey, K.L., Chandwani, R., Papapetrou, E.P., Sadelain, M., O'Carroll, D., Lai, E.C., 2010. Conserved vertebrate mir-451 provides a platform for Dicer-independent, Ago2-mediated microRNA biogenesis. Proc. Natl. Acad. Sci. 107, 15163–15168. doi:10.1073/pnas.1006432107

Ye, X., Paroo, Z., Liu, Q., 2007. Functional Anatomy of the Drosophila MicroRNA-generating Enzyme. J. Biol. Chem. 282, 28373–28378.

doi:10.1074/jbc.M705208200

Yekta, S., Shih, I.-H., Bartel, D.P., 2004. MicroRNA-directed cleavage of HOXB8 mRNA. Science 304, 594–6. doi:10.1126/science.1097434

Yi, C., Pan, T., 2011. Cellular dynamics of RNA modification. Acc. Chem. Res. 44, 1380–8. doi:10.1021/ar200057m

Yi, R., Qin, Y., Macara, I.G., Cullen, B.R., 2003. Exportin-5 mediates the nuclear export of pre-microRNAs and short hairpin RNAs. Genes Dev. 17, 3011–6. doi:10.1101/gad.1158803

Yoda, M., Cifuentes, D., Izumi, N., Sakaguchi, Y., Suzuki, T., Giraldez, A.J., Tomari, Y., 2013. Poly(A)-Specific Ribonuclease Mediates 3′-End Trimming of Argonaute2-Cleaved Precursor MicroRNAs. Cell Rep. 5, 715–726. doi:10.1016/j.celrep.2013.09.029

Yoo, C.J., Wolin, S.L., 1997. The yeast La protein is required for the 3' endonucleolytic cleavage that matures tRNA precursors. Cell 89, 393–402. doi:10.1016/S0092-8674(00)80220-2

Yoshihisa, T., 2014. Handling tRNA introns, archaeal way and eukaryotic way. Front. Genet. 5, 213. doi:10.3389/fgene.2014.00213

Yudelevich, A., 1971. Specific cleavage of an Escherichia coli leucine transfer RNA following bacteriophage T4 infection. J. Mol. Biol. 60, 21–29. doi:10.1016/0022-2836(71)90444-X

Zaborske, J.M., Narasimhan, J., Jiang, L., Wek, S.A., Dittmar, K. a., Freimoser, F., Pan, T., Wek, R.C., 2009. Genome-wide Analysis of tRNA Charging and Activation of the eIF2 Kinase Gcn2p. J. Biol. Chem. 284, 25254–25267. doi:10.1074/jbc.M109.000877

Zasloff, M., 1983. tRNA transport from the nucleus in a eukaryotic cell: carrier-mediated translocation process. Proc. Natl. Acad. Sci. U. S. A. 80, 6436–40.

Zeng, Y., Yi, R., Cullen, B.R., 2005. Recognition and cleavage of primary microRNA precursors by the nuclear processing enzyme Drosha. EMBO J. 24, 138–48. doi:10.1038/sj.emboj.7600491

Zhang, H., Kolb, F.A., Jaskiewicz, L., Westhof, E., Filipowicz, W., 2004. Single Processing Center Models for Human Dicer and Bacterial RNase III. Cell 118, 57–68. doi:10.1016/j.cell.2004.06.017

Zhang, H., Kolb, F. a, Brondani, V., Billy, E., Filipowicz, W., 2002. Human Dicer preferentially cleaves dsRNAs at their termini without a requirement for ATP. EMBO J. 21, 5875–85.

Zhang, J., Ferré-D'Amaré, A., 2016. The tRNA Elbow in Structure, Recognition and Evolution. Life 6, 3. doi:10.3390/life6010003

Zhao, H., Bojanowski, K., Ingber, D.E., Panigrahy, D., Pepper, M.S., Montesano, R., Shing, Y., 1999. New role for tRNA and its fragment purified from human urinary bladder carcinoma conditioned medium: inhibition of endothelial cell growth. J. Cell. Biochem. 76, 109–17.

Zheng, G., Qin, Y., Clark, W.C., Dai, Q., Yi, C., He, C., Lambowitz, A.M., Pan, T., 2015. Efficient and quantitative high-throughput tRNA sequencing. Nat. Methods 12, 835–

837. doi:10.1038/nmeth.3478

Zheng, Q., Yang, H.-J., Yuan, Y.A., 2017. Autoantigen La Regulates MicroRNA Processing from Stem–Loop Precursors by Association with DGCR8. Biochemistry 56, 6098–6110. doi:10.1021/acs.biochem.7b00693

Zhu, J.Y., Pfuhl, T., Motsch, N., Barth, S., Nicholls, J., Grasser, F., Meister, G., 2009. Identification of Novel Epstein-Barr Virus MicroRNA Genes from Nasopharyngeal Carcinomas. J. Virol. 83, 3333–3341. doi:10.1128/JVI.01689-08

Zhu, L., Deutscher, M.P., 1987. tRNA nucleotidyltransferase is not essential for Escherichia coli viability. EMBO J. 6, 2473–7.

Zuker, M., 2003. Mfold web server for nucleic acid folding and hybridization prediction. Nucleic Acids Res. 31, 3406–3415. doi:10.1093/nar/gkg595

12. Acknowledgments

Mein erster, großer Dank geht an Prof. Dr. Gunter Meister, der diese Arbeit nicht nur auf wissenschaftlicher Ebene während der vielen Gespräche angeleitet hat. Vielmehr hat er es immer geschafft, meine Motivation aufrecht zu erhalten, und letztendlich einen Pessimisten von etwas Besserem zu überzeugen. Danke auch für die Geduld im Umgang mit meinen besonderen Charaktereigenschaften. Auch möchte ich mich für das Vertrauen bedanken, das mir ermöglicht hat, mich über diese Jahre weiterzuentwickeln und von dir und von den Kollegen zu lernen. Danke auch für das Ermöglichen von Forschungsaufenthalten und für die vielen Kongresse, die ich in dieser Zeit besuchen durfte.

Des Weiteren möchte ich mich ganz herzlich bei allen Mitgliedern meines Prüfungsausschusses bedanken: Prof. Dr. Klaus Grasser, PD Dr. Jan Medenbach und apl. Prof. Dr. Joachim Griesenbeck. Insbesondere möchte ich mich bei Prof. Dr. Inga Neumann und Prof. Dr. Stephan Schneuwly bedanken, die auch schon während meiner Studienzeit stets hilfsbereit waren.

Noch ein Mal möchte ich mich bei PD Dr. Jan Medenbach und bei PD Dr. Markus Kretz für die wissenschaftlichen Diskussionen und Anregungen bedanken. Euer Mitwirken ist zweifelsohne eine große Bereicherung für den ganzen Lehrstuhl!

Ein besonderer Dank geht an alle Kollegen, die über diese Jahre als Vorbilder gewirkt haben. An erster Stelle möchte ich mich bei Dr. Anne Dueck bedanken, die Person, die mit Sicherheit immer eine hilfreiche Antwort auf meine Fragen hatte und mit guten Vorschlägen und Ideen für ständig neue Anregungen gesorgt hat. Manchmal zauberte sie sogar spannende Northern Blot Membranen aus dem Nichts!

Ebenso sind Dr. Nora Treiber und Dr. Thomas Treiber eine unerschöpfliche und erfahrene Quelle an Ideen gewesen. Die gemeinsamen Gespräche ermöglichten mir einen anderen Blick auf meine Fragestellungen. Danke auch für die ganze Unterstützung mit Materialien verschiedenster Art, die so oft zum Erfolg der Experimente verholfen haben.

Ebenso wichtige Stützen für das Gelingen der Arbeit des ganzen Lehrstuhls sind Sigrun Ammon, Corinna Friederich, Gerhard Lehmann, Norbert Eichner und Robert Hett. Insbesondere möchte ich mich nochmals bei Gerhard für seine tatkräftige Unterstützung bei der Auswertung der Deep-Sequencing Datensätze bedanken. Ebenso stand mir Norbert stets zuverlässig und aufopferungsvoll zur Seite bei der Behebung jeglicher technischen Probleme.

Ein besonderer Dank geht auch an Birgit Clemens, die mit ihrer strahlenden Persönlichkeit und Hilfsbereitschaft für eine angenehme und reibungslose Arbeitsatmosphäre sorgt. Außerdem, Dank deiner Kenntnisse über unser gemeinsames Hobby konnten Becki und ich Vieles dazulernen!

Für die schöne gemeinsame Zeit im Labor und außerhalb, möchte ich mich bei Eva Schöller, Tiana Hanelt, Philipp Neumann, Daniela Strauß und Dr. Sébastien Ferreira-Cerca mit Emma, Lilly und Mathilda bedanken.

Un caro ringraziamento va anche a Claudia Latini. Seppure di calcio non capisca un fico secco, la sua presenza ha portato in laboratorio una ventata di vitalità e simpatia!

Ich wüsste nicht, wie ich diese Doktorarbeit überstanden hätte, ohne meine zwei Kollegen und besondere Freunde Dr. Ludwig Wankerl und dem Schachtelhuber, Dr. Leonhard Jakob, zusammen mit Nadja, Sophia und Valentin. Es bleiben mir viele lustige Erinnerungen an dem ganzen Blödsinn, den wir zusammen angestellt haben und ich bin froh, dass unsere Freundschaft (hoffentlich bald) drei Doktortitel überdauert hat. Zuletzt möchte ich mich in diesem offiziellen Rahmen bei Ludwig nochmals entschuldigen, dass ich damals bei meinem Vorstellungsgespräch am Lehrstuhl versäumt habe, mit dir zu reden. Es bleibt selbstverständlich unverzeihlich!

I also would like to acknowledge Rev. Prof. Dr. Dr. Robert Dodaro, O.S.A., for correcting parts of this manuscript. Furthermore, I am grateful for the support he constantly expressed towards my family in times of need. He demonstrated true moral integrity, which is far different from the simulated mercy of certain hypocrites.

Ein großer Dank gebührt auch Reinhold Bübl. Sein offenes Ohr und seine Unterstützung haben mich insbesondere durch die ersten schwierigen Jahre fern von der Heimat verholfen und ich freue mich über die nun vielen Jahre Freundschaft, die mich mit dir und mit deiner Familie verbinden.

Grazie anche a Silvia Felli, Daniele Giusto e Caterina Purini. La vostra amicizia mi ha sempre accompagnato durante questi anni lontano da casa. Ogni volta che ci rincontriamo, è come se il tempo non fosse mai passato.

Di tutto cuore ringrazio la mia famiglia. Mia madre e mio padre che con i loro sacrifici mi hanno permesso di intraprendere questo percorso, e mio fratello Eugenio che mi ha sempre sostenuto con grande generosità durante questi anni. Si è riversata su di noi una folle e crudele ingiustizia che ci ha messo a dura prova durante l´anno passato. Sono grato e fiero di avere voi come esempi di vita, che in un mondo corrotto da falsità e sotterfugi, hanno sempre mantenuto la loro integrità e dignità. Grazie di tutto, vi voglio bene!

Liebe Becki, die letzen Worte dieser Arbeit sind dir gewidmet. Mein größtes Glück war, dass sich unsere Wege hier gekreuzt haben. Danke für alles was du für mich getan hast, für die Unterstützung im Labor und beim Schreiben dieser Arbeit. Aber vor allem Danke für deine Nähe in den schwierigen Momenten des Lebens und für die vielen schönen Erlebnisse, die wir miteinander teilen. Bevor ich dich kennengelernt habe, war ich ein unruhiger und unzufriedener Mensch. Du hast immer die richtigen Worte und Gesten gefunden, um aus mir einen glücklichen Menschen zu machen. Ich liebe dich.